

**INVESTIGATION ON THE PHYSICAL PROPERTIES OF  
GLOW DISCHARGE AND ARC PLASMA**

THESIS SUBMITTED FOR THE DEGREE OF DOCTOR OF  
PHILOSOPHY ( SCIENCE ) OF THE  
UNIVERSITY OF NORTH BENGAL.

1991

UNIVERSITY OF NORTH BENGAL  
LIBRARY  
RAJA RAMMOHUNPUR, DARJEELING

*By*

*Mukul Nath*

DEPARTMENT OF PHYSICS  
**UNIVERSITY OF NORTH BENGAL**  
RAJA RAMMOHUNPUR, DARJEELING.  
WEST BENGAL, INDIA.

INVESTIGATION OF THE PHYSICAL PROPERTIES OF  
GLASS CARBON AND CARBON FIBERS

L

**ST - VERP**

**STOCK TAKING - 2011**

TO BE USED TO RECORD THE RESULTS OF THE  
PHYSICAL PROPERTIES INVESTIGATION OF THE  
GLASS CARBON AND CARBON FIBERS

1991

Ref.

530.44

N274L

108464

24 SEP 1992

RAM JRM

PROPERTY OF THE NATIONAL BUREAU OF STANDARDS  
PHYSICAL PROPERTIES INVESTIGATION OF THE  
GLASS CARBON AND CARBON FIBERS  
JAMES J. JACOBSON

## A C K N O W L E D G E M E N T

To work under the guidance of Prof. S.N.Sen, Senior Professor of the Department of Physics of North Bengal University, is a subject of great pleasure and pride. Particularly because, to any of his student he never acted like a prison, rather all of his students always enjoyed a right to breathe with freedom such that the student can really grow in the light of his wisdom and blessing. I express my whole hearted gratitude to the great teacher whose blessing and guidance made this compilation in the form of thesis possible for me.

I am thankful to the University of North Bengal for providing me with the laboratory, library and other facilities.

I express my thanks to all the teachers and technical staff of the department of physics and USIC for their co-operation.

All the library staff of the University of North Bengal has extended their hands of co-operation as and when required by me. I extend my thanks to all of them.

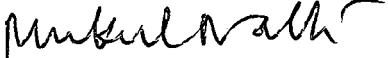
During the period of my research the authority and all my colleagues of the department of physics of Siliguri College allowed me to have their co-operation. I would like to express my thanks to all of them.

I also recall my thanks to M. Chakraborty and B. Bagchi for their help in the final stage of this compilation.

I must, also, remember and be thankful to Sajal Sarkar for his many invaluable suggestion and help throughout the period of my research.

Finally, I am indebted to my wife for her sacrifice and co-operation during the period of my research.

Dated 12.12.1991  
Department of Physics,  
North Bengal University

  
(Mukul Nath)

DEDICATED TO MY FATHER

# C O N T E N T S

	Page
CHAPTER I    Review of the previous work Bibliography Scope of the work	1-70
CHAPTER II    Experimental set up	71-89
CHAPTER III    Energy loss mechanism in a collision dominated plasma	90-115
CHAPTER IVA    Measurement of plasma current and capacitative current in a radio frequency gas discharge.	116-122
CHAPTER IVB    Radio frequency conductivity of an ionised gas in a transversed magnetic field.	123-131
CHAPTER IVC    Propagation of microwaves through a plasma filled wave-guide - a possible diagnostic method.	132-142
CHAPTER IVD    Critical frequency for microwave propagation in a rarefied magnetised plasma.	143-162
CHAPTER V     Low density plasma in a magnetic field	163-186
CHAPTER VI    Current generation process, high current density and cathode phenomena in an arc plasma.	187-215
CHAPTER VII    Low frequency oscillation in arc plasma	216-235
CHAPTER VIIIA    Evaluation of plasma magnetisation coefficient.	236-243
CHAPTER VIIIB    Study of magnetic field dependence of traditionally used plasma magnetisation coefficient and of cross sectional area of an arc.	244-255
CHAPTER IX    Summary and Conclusion	256-261

CHAPTER I

REVIEW OF THE PREVIOUS WORK

BIBLIOGRAPHY

SCOPE OF THE WORK

## CHAPTER - I

### Review of the Previous work

A precise review on the phenomena related to the proposed work is, hereby, presented below with the object to work further and introduce new lines of investigation. Work is proposed to be carried out along the following lines.

- A. Electron Collision loss factor in Collision dominated plasma
  - B. Theory on the radio frequency real and imaginary currents through a plasma
  - I. Measurement of radio frequency real current and imaginary current.
- II. Radio frequency conductivity of a magnetised plasma.
- C. Low frequency self excited oscillation in a plasma.
  - D. Cathode phenomena in an arc.
  - E. Diffusion and Hall voltage in a magnetised plasma.
  - F. Plasma Magnetisation Coefficient and Effective Arc Cross-Section.
    - A. Collision loss in a plasma

Energy loss in a plasma may be either due to elastic collisions or due to inelastic collisions. Inelastic collisions result in vibrational excitation, rotational excitation, recombination, capture, attachment, dissociation, ionization and collision of the second kind (Kleins and Rosseland). In case of inelastic collisions electrons lose their kinetic energy resulting in a decrease in the kinetic energy of plasma

and hence potential energy of plasma increases.

This problem of determining the collision loss of electrons may be handled with the knowledge of electron energy distribution function and energy transfer cross-section. Defining drift velocity as the ratio of flow density of electrons to electron concentration, Von Engel (1965) obtained in the steady state,

$$\frac{v_d}{C} = \left(\frac{1}{2} K\right)^{1/2} \quad (1.1)$$

where  $v_d$  and  $C$  are drift and random velocities and  $K$  is the collision loss factor. For Maxwellian electron energy distribution with small values of  $(E/P)$ , Compton and Langmuir (1930) obtained an expression for collision loss factor for electrons as

$$K = 2.66 \frac{m_e M}{(m_e + M)^2} \times \left(1 - \frac{\frac{1}{2} M C^2}{\frac{1}{2} m_e C_e^2}\right) \quad (1.2)$$

Thus for electron energy much higher than molecular energy,

$$K = \frac{8 m_e}{3 M}$$

Thus in case of  $N_2$ ,  $K = \frac{8 \times 9 \times 10^{-28}}{3 \times 28 \times 1.67 \times 10^{-24}} = 5.1 \times 10^{-5}$

when the collision is purely elastic.

But  $K$  for  $N_2$  as measured by Demitriades (1967) for slow electrons lies within  $2.3 \times 10^{-4}$  to  $4.9 \times 10^{-4}$ . Also in case of  $H_2$ , elastic collision loss factor is found to be

$$K = \frac{8 \times 9 \times 10^{-28}}{3 \times 2 \times 1.67 \times 10^{-24}} = 7.19 \times 10^{-4}$$

But  $K$  for  $H_2$  as experimentally measured by Bekefi and Brown (1958) for slow electrons (0.039 eV to 1.6 eV) is found to be

$$K = (3.5 \pm .5) \times 10^{-3}$$

Thus even for slowest electrons, inelastic collision losses in molecular gases is quite appreciable. This is because the energy required for vibrational excitation does not exceed 0.5 eV for majority of cases of diatomic molecules.

Bashmin and Demitriev (1976) found for reduced electric field from 20 to 60 V/cm in plasma that 10% of the electron energy goes to excitation of rotational and translational degrees of freedom and 50% goes to excitation of vibrational degrees of freedom.

Since collision is elastic only when electron energy is extremely small, so the study of slow electrons has drawn the attention of many investigators [Bekefi and Brown (1958), Demitriades (1967), Brood (1925), Rusch (1925), Bruche (1927) Bamsaauer and Kollah (1929), Normand (1930), Gilardini (1972)].

Measurement was also performed for non-slow or fast electrons by Medies (1958), Bowe (1960), Afrosimov et al (1972), Janaca (1967), Biberman et al (1966).

Again characteristics of slow electrons (25 eV) are highly different from that of the fast electrons because of Ramsauer effect [Ramsauer (1921)]. In this range of energy, momentum transfer cross-section shows minima and maxima [Harnwell (1929)] and thus collision loss factor becomes highly dependent on electron energy. Though for higher energies there is a steady change in the collision loss factor. Morse (1935) obtained an expression for fraction of energy lost by an electron in one collision

$$\frac{\Delta \epsilon}{\epsilon} = \frac{2 \Delta v}{v} = \frac{2m}{M} (1 - \cos \theta) \quad (1.3)$$

And that lost per sec by an electron is,

$$dW = \frac{16 \pi N Q}{M} m \epsilon^2 f d\epsilon \quad (1.4)$$

for electrons lying within an energy  $\epsilon$  to  $\epsilon + d\epsilon$ .  $Q$  is the momentum transfer cross-section,  $f$  is the energy distribution function for the electrons. Thus average collision loss factor requires the knowledge of momentum transfer cross section [Houston, (1928)]. Cross-section for energy transfer was measured by Normard (1930), Morse et al (1935) Crompton and Sutton (1952), Townsend and Baily (1921), Bowe (1960) and many others.

To raise the electron temperature much above the gas temperature ohmic heating was employed by Shingarkina (1972).

He measured the actual Hall parameter and thus the actual mean free time which is a function of electron temperature. The inelastic loss factor is evaluated for  $N_2$  through comparison of results with computer calculation of electron energy balance.

With micro wave heating technique Gould (1954), Gilardini (1957), Bekefi and Brown (1958), Phelps et al (1957) performed their investigation.

Bekefi and Brown carried their measurement, for electron energy from 0.03 eV to 1.6 eV, and obtained an expression

$$T_e = T_g + \frac{2e^2 E^2}{3mK\omega^2 k} \quad (1.5)$$

Where  $E$  is the r.m.s. value of electric field at the centre of the cavity and is to be replaced by  $0.758E$  for the average field inside the cavity.  $K$  is the collision loss factor and is obtained by comparison of results.

$$K = (3.5 \pm 0.5) \times 10^{-3} \text{ for hydrogen.}$$

Demetriads (1967) also obtained with micro wave heating technique, the collision loss factor of electrons for gas temperature  $1700^\circ\text{K}$  to  $6100^\circ\text{K}$  and electron temperature raised to  $4127^\circ\text{K}$  to  $7540^\circ\text{K}$  and is given by

$$K = \frac{2e^2}{3km\omega^2} \left( \frac{Z}{A_r} \right) \left( \frac{dT_e}{dp} \right)^{-1} \quad (1.6)$$

and they obtained  $K$  from  $2.9 \times 10^{-4}$  to  $4.9 \times 10^{-4}$  for  $N_2$  plasma.

Adiabatic trap method was used by Pastukhov (1974) for the determination of collision loss factor. The expression is obtained on the basis of approximate solution of Fokker-Planck equation, which is found to yield good results.

Another method of precision analysis of the spectra of inelastic energy losses on atomic collision was adopted by Afrosimov et al (1972) which can be used for the determination of collision loss factor.

Bowe (1960) obtained expressions which can cover both elastic collision and inelastic collision for the determination of collision loss factor. They analysed the expression on the basis of the data obtained for  $H_e$ ,  $N_e$ , Ar, Kr and  $X_e$ . They used

$$K = \lambda(\epsilon) \frac{2m}{M} \quad (1.7)$$

$$\text{and} \quad \lambda(\epsilon) = \alpha \epsilon^{-j} \quad (1.8)$$

Thus knowing  $\alpha$ ,  $j$  the collision loss factor can be calculated for various value of energy  $\epsilon$ .

A theoretical work done by Dote and Shimoda (1980) describes individual loss factor for elastic collision, excitation, ionisation and for mean collision loss factor and they compared the relations on the basis of published data for  $H_e$ ,  $N_e$  and Ar and was found to yield good results.

Sen and Jana (1978) measured the momentum transfer collision cross-section for slow electrons in magnetic field from radio-frequency conductivity measurements.

### B. Measurement of Real and Imaginary Current through plasma

The passage of a.c discharge current through an ionized medium has been considered for a long time. For low frequency and high pressure, the current density set up by an ac electric field is given by Langavín (1905) mobility formula. The current remains in phase with the impressed electric field.

On the other hand, if rf voltage, not sufficient to cause breakdown for the gas be applied, the rf current flowing through the gas is given by Vandar Pol (1919)

$$j_{rf} = \frac{e^2 n E_0}{m} \left[ \frac{\nu}{\nu^2 + \omega^2} - i \frac{\omega}{\nu^2 + \omega^2} \right] \quad (1.9)$$

where  $E = E_0 \exp.(i\omega t)$  is the applied rf field and  $\nu$  is the collision frequency of electrons with neutral atoms,  $e$  and  $m$  are charge and mass of electrons and  $n$  is the electron density. Thus current is represented by formula involving characteristics of electrons and a part of the current is in phase quadrature with the ac field.

Assuming the energy distribution to be Maxwellian Margenau (1946) obtained for current density which has two components

$$i_{\text{real}} = \frac{4e^2 E \lambda n}{(2\pi m k T)^{1/2}} \cos \omega t \quad (1.10)$$

$$i_{\text{imaginary}} = \frac{e^2 E n}{m \omega} \sin \omega t \quad (1.11)$$

where,  $i_{\text{real}}$  is in phase with applied electric field.

Everhart and Brown (1949) measured the admittance in the micro wave region by measuring the discharge current for applied hf field of sufficient amplitude in helium which filled the cavity of a magnetron.

Sodha (1960) obtained an expression for the current density which has two components, one in phase and the other out of phase with the applied field. He has shown that for constant mean free path and energy loss factor and for low frequency, the distribution is Druyvesteyn. The conductivity obtained by Sodha (1960) was obviously a complex one.

The electrical conductivity of the conducting medium was determined by Koritz and Keck (1964) from measurement of Joule losses produced by alternating magnetic field in a coil surrounding the discharge tube. In addition, there are number of authors, who [Tanaka and Usami (1962), Gourdin (1963), Khvashchetevaski (1962)] made conductor approximation for

plasma which means, when an ac is imposed upon a plasma, the plasma acts just like a resistance and ac conductivity essentially becomes a dc conductivity.

$$\sigma_{ac} = \frac{ne^2}{m\delta} \left[ \frac{\delta^2}{\delta^2 + \omega^2} - i \frac{\omega\delta}{\delta^2 + \omega^2} \right] \quad (1.12)$$

A general theory regarding the variation of rf conductivity of ionized gases and its variation with pressure and magnetic field has been worked out by Gilardini (1959) who derived the expression for the conductivity of ionized gases,

$$\sigma_{rf} = \frac{e^2 n}{m} \cdot \frac{1}{\delta + i\omega} \quad (1.13)$$

and in presence of magnetic field he defined two conductivities, one for right-handed polarisation and other for the left-handed polarization,

$$\text{(rt. handed polarisation)} \quad \sigma_c = \frac{e^2 n}{m} \left[ \frac{1}{\delta + i(\omega - \omega_b)} \right] \quad (1.14)$$

$$\text{(left handed polarization)} \quad \sigma_o = \frac{e^2 n}{m} \left[ \frac{1}{\delta + i(\omega + \omega_b)} \right] \quad (1.15)$$

$\omega_b$  is the electron cyclotron frequency.

And conductivity in the direction of the magnetic field, H, is given by

$$\sigma_H = \frac{1}{2} (\sigma_c + \sigma_o) \quad (1.16)$$

The complex conductivity is, in general, related to plasma parameters by the following expression of Heald and Wharton (1965)

$$\sigma_r + i\sigma_i = -\frac{4\pi}{3} \epsilon_0 \omega_p^2 \int_0^{\infty} \frac{1}{\nu(v) + i\omega} \cdot \frac{d}{dv} [f_0(v)] v^3 dv \quad (1.17)$$

$v$  is the electron velocity and  $f_0(v)$  is the distribution function in the steady state,  $\nu$  is the electron atom collision frequency and  $\omega$  is the angular frequency of the applied r.f. electric field.

Thus it is evident that a plasma, under the action of impressed r.f. electric field, carries real current, as well as imaginary current through it. Francis and Von Engel (1953) have pointed out that the capacitative current is much greater than the discharge current. The current flowing through the discharge can be estimated by loading the circuit with a resistance or a capacity which induce the same voltage drop as the discharge. In order to measure the current, it is necessary to discriminate one part of the gas discharge current from the capacitative current. A differential method is, therefore necessary to balance out the capacitative current flowing across the electrodes. Francis and Von Engel (1953) considered the total current and no mention, however, was made about the individual part of the discharge current. In order to reduce the capacitative current, they considered the electrode as small as possible. The capacitative current flowing across

the electrodes was then balanced out by a bridge method. The bridge became unbalanced when the current was allowed to flow through the gas. The unbalanced component was proportional to the discharge current, and was then amplified, rectified and displayed on a CRO Screen. The calibration of the circuit was made by replacing the gas discharge by a known impedance and then observing the displacement of the trace on the CRO screen.

Penfold and Warder (Jr.) (1967) reviewed a number of methods commonly used for the measurement of rf plasma discharge current. A common method of current measurement is to monitor the voltage across a capacitor or an inductor element. A capacitor tends to suppress the harmonics, while the inductance emphasizes them. The voltage can be determined by the use of a high voltage probe with an oscilloscope read out. Penfold and Warder (Jr) (1967) measured the current by measuring the voltage drop across a specially constructed centre tapped inductor.

Clark, Earl and New (1970) measured the gas discharge current separating out the capacitative components by a bridge method similar in principle to that employed by Francis and Von Engel (1953). They also measured the maintenance voltage and phase relation between the gas discharge current and maintenance voltage from which the discharge characteristics and complex impedance were obtained.

The real part of the r.f. conductivity of ionised gases such as air and nitrogen was measured by Sen and Ghosh (1966);

from the variation of r.f. conductivity with pressure it was possible to calculate the electron density, collision frequency and electron temperature. The work was extended to rare gases by Sen and Gupta (1969) and in addition to electron density, collision frequency and electron temperature, dielectric constant and Debye shielding distance were also measured and their variation with pressure was also investigated.

Ghosal, Nandi and Sen (1976) measured the azimuthal radio frequency conductivity of an arc plasma by measuring the reflected resistance of a primary coil wound around a mercury arc tube. A linear relationship between the azimuthal conductivity and discharge current has been obtained. The nonlinearity and existence of maxima observed by the previous authors in the change of band width versus axial conductivity curve have been explained theoretically by considering a generalised equivalent circuit. It has been pointed out that the conductivity measurement by this method is only possible where the conductivity of the plasma is fairly high. Radio frequency conductivity of a magnetised plasma:

(A) Rf conductivity of an ionized gas without magnetic field:

Radio frequency conductivity as suggested by Vandarpol (1919) is given by

$$\sigma = \frac{e^2 n}{m} \left[ \frac{\nu}{\nu^2 + \omega^2} - i \frac{\omega}{\nu^2 + \omega^2} \right] \quad (1.18)$$

$n$  is the electron concentration,  $\nu$  is the electron atom collision frequency and  $\omega$  is the frequency of the impressed field. The above equation shows that rf conductivity is complex and its real part tends towards maximum when  $\omega$  approaches  $\nu$  [Sen and Ghosh (1966)].

Conductivity of ionized air was measured by Child (1932) at 1 MC/S. Appleton and Chapman (1932) studied the rf conductivity of air plasma at 1000 MC/S. Appleton and Chapman found a maximum in the conductivity with pressure. Similar studies were made by Imam and Khastgir (1937) for pressure 10 to 120 cm at wave length 481 cm. Margenau (1946) considering velocity distribution and Boltzman transport equation obtained

$$\sigma_r = \frac{4}{3} \cdot \frac{ne^2 \lambda}{\sqrt{2\pi} mkT_e} \cos \omega t \quad (1.19)$$

$$\sigma_i = \frac{ne^2 \lambda \omega}{3kT_e} \sin \omega t \quad (1.20)$$

Dawson and Oberman (1962, 1963) calculated hf conductivity of ionized gas and Berk (1964) showed how Dawson and Oberman model can be extended to yield kinetic description of the electrical process, which is uniformly valid for high and low frequency theories. Sen and Ghosh (1966) observed maxima, as observed by Appleton and Chapman. But they found the maximum conductivity to decrease with decrease of discharge current. The real part of the conductivity of the ionized air and nitrogen was measured

for various values of pressure and discharge current. The frequency of the rf current in their measurement lies within 2 to 3 MC/S. Johnson (1967) calculated the electrical conductivity for a variety of assumed electron molecule collision frequencies. Nagata (1966) presented a simple technique for the measurement of plasma conductivity and discharge current was within 5 to 100 mA and various gas pressures were used. Experimental value of  $\sigma$  were in good agreement with the theoretical values of  $\sigma$ .

Ghosal, Nandi and Sen (1976 & 1978) measured azimuthal radio frequency conductivity and its change with radial distance for a mercury arc plasma.

~~(B) Magnetic field effects on the rf conductivity of an ionized gas:~~

Since the effect of magnetic field changes the electron and ion distribution in a plasma, the transport properties obviously undergo certain changes with change of magnetic field. Conductivity of ionized gases (air,  $N_2$  and  $H_2$ ) in a magnetic field was measured by Ionescu and Mihul (1932) above a pressure of  $10^{-3}$  torr. With very intense magnetic field only electron vibration remains and maxima in conductivity with pressure undergoes changes with change in magnetic field.

An improved probe method for the measurement of electrical conductivity of low temperature plasma was derived by Khozhalev and Yasin (1966). Ciampi and Talini (1967) measured the average plasma conductivity by a rf probe for a

cylindrical plasma which is assumed radially homogeneous. They obtained the average conductivity values from 75 to 100 mho/s with a Q factor measurement between 0.5 to 1.5 MHz. The probe used was calibrated with electrolyte ( $H_2SO_4$ ) solution of standard conductivity.

From a study of the complex conductivity of Hg vapour at microwave frequencies Adler (1949) has shown plots of  $\sigma_r$  and  $\sigma_i$  with pressure or current when the other remains unaltered. Adler found that the theoretical and experimental value agree closely and  $\sigma$  varies linearly with discharge current.

Aleksandrov and Yalsenko (1965) studied the complex conductivity of neon plasma by the Q-meter method. The frequency range used was 0.5 to 25 MC/S. A theory of rf conductivity of a magnetised plasma was proposed by Appleton and Boohariwala (1935) who found that the real part of rf conductivity is given by

$$\sigma_{rH} = \frac{ne^2}{m} \times \frac{\gamma(\omega^2 + \omega_b^2 + \gamma^2)}{(\omega^2 + \omega_b^2 + \gamma^2)^2 - 4\omega^2\omega_b^2} \quad (1.21)$$

where  $\omega_b = eH/m$  - - - - - (1.22)

A general theory of rf conductivity as a function of magnetic field and pressure was obtained by Gilardini (1959). The complex conductivity is given by

108464

24 SEP 1992

 195971 200005  
 UNIVERSITY LIBRARY  
 101A W. 42ND STREET

$$\sigma = \frac{e^2 n}{m} \cdot \frac{1}{\delta + i\omega} \quad (1.13)$$

in absence of magnetic field and in presence of magnetic field he defined two conductivities, one due to right hand polarization and other due to left hand polarization

$$\sigma_{LH} = \frac{e^2 n}{m} \left[ \frac{1}{\delta + i(\omega - \omega_b)} \right] \quad (1.24)$$

for left hand polarization and

$$\sigma_{RH} = \frac{e^2 n}{m} \left[ \frac{1}{\delta + i(\omega + \omega_b)} \right] \quad (1.25)$$

for right hand polarisation.

And rf conductivity in the direction of the field is given by

$$\sigma_H = \frac{1}{2} (\sigma_{LH} + \sigma_{RH}) \quad (1.26)$$

Hence real part of the rf conductivity of a magnetised plasma is given by

$$\sigma_{rH} = \frac{e^2 n}{m} \left[ \frac{1}{\delta^2 + (\omega - \omega_b)^2} + \frac{1}{\delta^2 + (\omega + \omega_b)^2} \right] \quad (1.17)$$

which on simplification reduces to the expression obtained by Appleton and Boohariwala. This relation was experimentally studied by Gupta and Mandal (1967) for air and carbon dioxide with magnetic field upto 680 Gauss. They found that maximum conductivity decreases and corresponding pressure at which conductivity attained the maximum value, gradually shifted towards higher pressure with the increase of magnetic field.

Sen and Gupta (1969) measured rf conductivity with and without magnetic field for Ne, He and Ar and found to follow the relation approximately

$$\frac{\sigma_{rH}}{\sigma_r} = \frac{P_{max}}{P_{Hmax}} \quad (1.18)$$

Blackman (1959), Wu (1965), Oberman and Shure (1963), Nedospasov and Shipuk (1966), Schweitzir and Milchner (1967), Green et al (1965), Pradhan and Das Gupta (1967), Maiti and Basu (1968), Gupta, Mandal and Sen (1968) studied rf conductivity and its variation with pressure, current and magnetic field.

Ram, Chandra and Sarkar (1972) studied rf conductivity of a magnetized plasma both for transverse and longitudinal magnetic fields. They found large variation of  $\sigma_{rH}$  in case of longitudinal magnetic field while variation of  $\sigma_{rH}$  in case of transverse magnetic field was considerably small in their experiment.

Sen and Jana (1978) showed that

$$\frac{H}{P_{\max}} = \text{Constant} \quad (1.29)$$

corresponding to the maximum rf conductivity at a pressure  $P_{\max}$ , when the plasma was treated with a transverse magnetic field  $H$ . They performed experiment at 2.45 MHz with Hydrogen and oxygen for transverse magnetic field 1150G to 1850G and obtained excellent agreement with theory and experiment.

C. Oscillation in a plasma, particularly in connection with low frequency oscillation:

The oscillation in a plasma is either longitudinal oscillation where no magnetic field component is associated with the wave generated, or "magnetohydrodynamic" or "hydromagnetic" waves in which case the frequency is low and velocity of propagation is many order less than that of light. This later category may be sub divided in two groups in which time varying magnetic field component is either parallel or perpendicular to the static magnetic field. Though in both cases time varying magnetic field component is small compared to the static magnetic field. Hydromagnetic waves are small amplitude plane waves.

The plasma oscillation was initially discovered by Penning (1926) and a detailed theory was put forward by Langmuir and Tonk (1929) according to which the natural frequency of electron plasma oscillation is given by

$$\omega_e = \left( \frac{n_e e^2}{\pi m_e} \right)^{1/2} = 8980 n_e^{1/2} \quad (1.30)$$

where  $n_e$ ,  $e$  and  $m_e$  are concentration, charge and mass of the electron. And the ion plasma frequency is given by

$$\omega_p = \omega_e \left( \frac{m_e}{m_p} \right)^{1/2} \quad (1.31)$$

$m_p$  is the mass of the ions. The oscillation of larger wave lengths are similar to sound and its velocity of propagation approaches a value given by

$$v = \left( \frac{kT_e}{m_p} \right)^{1/2} \quad (1.32)$$

The frequency 300 to 1000 MC/S agrees well with the predicted frequency of electron oscillation in a plasma. Another observed frequency of 50 to 60 MC/S may correspond to the beam electrons, while the frequency 1.5 MC/S and below may be attributed to + Ve ion oscillation. Penning (1926) observed the radio frequency oscillation in a low pressure Hg vapour under same condition as those lead to electron scattering [Langmuir (1926)]. The frequency of the corresponding plane wave associated with the electron plasma oscillation is given by

$$\omega^2 = \frac{n_e e^2}{\pi m_e} + \frac{c^2}{\lambda^2} \quad (1.33)$$

where  $c$  is the velocity of the wave and  $\lambda$  is the wave length. The frequency of the ion plasma oscillation is given by

$$\omega_p = \left[ \frac{n_e e^2}{\pi m_p + \frac{n_e e^2 m_p \lambda^2}{kT_e}} \right]^{1/2} \quad (1.34)$$

The efficiency of power conversion to the oscillatory power may hardly attain a value more than one percent for a well-designed experimental set up. This was observed by Emeleus and his co-workers in their work (1949, 1951).

However, in this review of the previous works on oscillation in a plasma, we shall confine our discussion in general to the plasma oscillations and waves whose frequency is said to be low.

Wehner (1950) described a plasma oscillator where he succeeded in producing an uniform parallel beam of electrons which reflected to and fro several times between the grid and the repeller, and oscillation of 1-4000 MC/S could be picked up at the repeller, and the frequency could be regulated by the anode current or voltage and it was claimed by author that the frequency of oscillation was stable. This is probably the most successful plasma oscillator of practical importance.

Gabor (1951) gave a new mathematical formalism for oscillation in a plasma irrotational stream and showed that if the electrons are originated outside the magnetic field or if they issued from a cathode where there was no normal component of magnetic field, the curl of the total or Schwarzschild momentum would be zero every where.

Rohner (1955) described an experimental tube for studying the plasma oscillation and discussed them in terms of Tonk-Langmuir (1929) formula for ion oscillation.

Konyukov (1957) worked on low frequency oscillation inside a plasma formed of electronegative gases, where electrons, positive ions and negative ions were assumed to exist as different individual components of the plasma. Two bunches of low frequency oscillation were established whose frequency was found to depend on respective concentration in different ways.

Stix (1957) considered the natural mode of oscillation of a cylindrical plasma of finite density at zero pressure in presence of longitudinal magnetic field. They found the lower limit of frequency of the hydromagnetic wave to be close to the frequency of ion cyclotron frequency.

Bernstein and Kulsrud (1960) derived a dispersion relation for electrostatic oscillation in a magnetic field on the basis of Boltzman equation for arbitrary velocity distribution and for propagation in an arbitrary direction for five specified boundary conditions. The growth rate and frequencies of this oscillation are also determined and ion wave instabilities are discussed.

Fried and Gould (1961) explored the properties of ion plasma oscillation using Vlasov's equation for  $T_e = T_i$  and it was found that there were discrete sequences of ion-plasma oscillation but all were strongly damped, i.e.,  $-I_m \omega / R_e \omega \geq 0.5$  and hence were likely not to be observed. The ratio  $-I_m \omega / R_e \omega$  can be made zero either by increasing  $T_e / T_i$  or by producing current through the plasma. In the later case  $I_m \omega$

can even be made positive. The current flow required is smaller the greater is the ratio  $T_e/T_i$ . This growing wave is seen to be an unstable oscillation.

D'Angelo and Motley (1963) observed low frequency oscillation in an inhomogeneous plasma. These oscillation seem to propagate across the magnetic field with the same velocity as the pressure gradient drift. And that this oscillation should follow from the macroscopic equation of collisionless plasma was noted by D'Angelo (1963). In addition to the experiment of D'Angelo and Motley (1963), the experiment of Lashinsky (1964) and Buchelnikova (1964) have established that the excitation of low frequency oscillation in a low pressure plasma depends in an important way on effects at the boundaries perpendicular to the magnetic field. The primary evidence for this is the fact that oscillation ordinarily develops when plasma is positively charged with respect to the end electrodes.

Chen (1964) studied the propagation of low frequency electrostatic oscillation through a low density fully ionised plasma in a strong magnetic field  $B$ . Two sets of waves were obtained by him. The wave either travels along  $B$  or transverse to  $B$ . They travel at the electron or ion diamagnetic drift velocities. Chen (1965) showed that when there is an electron sheath at the ends, the drift oscillation is short circuited and the instability leading to oscillation cannot develop. But an ion sheath in contrast particularly insulates the plasma from the connecting end plates and permits the growth of oscillation with wave lengths appreciably longer than the system.

In this connection one must mention that Langmuir and Mott-Smith (1924) divided the discharge space into "sheaths" and "plasmas". The sheath is a thin layer of charge surrounding the electrodes or probes or wall with strong gradient of electrostatic potential.

Vladimirov (1965) showed that the acceleration of ions in their escape to the ends may also lead to the excitation of low frequency oscillation which is said to be longitudinal ambipolar sound by the author.

Tanaka (1966, 1969), Kato et al (1967), Shut'ko (1968), Noon et al (1970), Tauth et al (1970), Duncan (1970), Krolikowsky (1969), Basannikov (1979), Agashi (1983), Penkratov (1971) and many others have investigated low frequency oscillations in plasmas under different conditions.

Rosa et al (1969) investigated low frequency uniform oscillation of the positive column of a low pressure arc. The oscillation is found not to be determined by the discharge circuit impedance and are not generated at either the cathode or the anode region. Both the electron density and electron temperature were found to be coherently oscillating. This phenomenon was interpreted as the ion-acoustic resonance mode of the plasma column oscillation.

Pasechnik and Popovich (1970) showed that the condition of oscillation and the frequency of oscillation is critically dependent on the potential difference between the plasma and

the end of the electrodes. They studied the excitation of low frequency oscillation in a bounded plasma under controlled variation of conditions at the ends and obtained an expression for frequency

$$f = \frac{p}{\pi L} \sqrt{\frac{2e \cdot \Delta U}{M}} \quad (1.35)$$

where  $p$  is the mode of longitudinal oscillation,  $L$  is the length of the discharge,  $M$  is the mass of an ion,  $e$  is the charge of an ion and  $\Delta U$  is the ambipolar diffusion potential between the end plates and plasma column. The intensity of oscillation increases rapidly as the potential  $U$  of the end plates with respect to the plasma is decreased below -10 volts. The frequency of oscillation is about 10 to 20 KHz. The oscillation does not occur below  $10^{-2}$  torr. The oscillation is found to be practically independent of magnetic field, gas pressure and plasma density but is strongly dependent on  $U$ .

Gabovich et al (1973) studied the excitation of ion Langmuir oscillation by a fast ion beam and typical spectra by excited oscillation is shown in good agreement with the theoretical prediction. It was also found that the oscillation growth rate decreased with increasing magnetic field. Thus increase of magnetic field lead to the reduction of amplitude of oscillation and hence suppression of instabilities leading to oscillation. The oscillation propagated nearly right angle to the beam.

Zvereva et al (1977) investigated the radial distribution of intensity of the spontaneous low frequency oscillation and noise in the frequency range of  $10^4$  to  $2 \times 10^5$  Hz in a mercury vapour discharge under a pressure between 0.18 to 1.2 torr. The conformity of the axial and radial distribution of the intensity was shown. The velocity of ion-sound wave ( $1.7 \times 10^5$  cm/sec) and lower bound frequency (21 KHz) were calculated using the results of measurement of the radial distribution of intensity and phase. A comparison with theory was given and the resonance character of the radial modes of oscillation excited by the electron stream was pointed out.

In case of a discharge tube operating in its negative resistance region of its VI characteristics, the negative glow as pointed out by Sanduloviciu (1968) is a source of self excited oscillation. The frequency of oscillation may be represented with L,R,C where L is the discharge inductance, R is the resistance between anode and the wall of the negative glow region and C is the capacitance of this region including the wall with respect to the surroundings. The LRC of the circuit representing oscillation in a discharge tube differ with LRC in an ordinary circuit. Because in case of ordinary circuit LRC is independent of current flowing through the circuit but in case of discharge tube LRC and hence the frequency of oscillation is strongly dependent on discharge current [Sanduloviciu (1971)].

Mitra (1975) explained the increase in frequency of oscillation with decrease in discharge current on the basis of an inequality obtained by him by applying the observation of Sanduloviciu (1968, 1969, 1971).

#### D. Cathode phenomena in an arc

In spite of extensive research the cathode phenomena in an arc is poorly understood because of formidable complexities prevailing in this region. The most useful factor to know regarding the cathode of an arc is the mechanism underlying the emission of current from the cathode.

The expression for thermal current density first obtained by Richardson (1912) and latter modified by Dushman (1923, 1930) is represented as

$$j_c = AT_c^2 e^{-b/T_c} \quad (1.36)$$

where  $j_c$  is the current density,  $T_c$  is the surface temperature and A, b are constants.

But this equation, in general, cannot cope with the requirement of current density in an arc. This is particularly true for all low melting point cathode materials operating in the vapour mode. But in case of refractory materials like C, W, rare earth metals, the current density experimentally measured by Froom (1948, 1949), Somerville (1952), Von Engel (1965) was found to be in reasonable agreement with the value of current density calculated from Richardson-Dushman equation with cathode temperature not more than the boiling point of the cathode material.

Seeliger and Schmick (1927), Cobine and Gallegher (1948), Wroe (1958), Newman (1936), Ruthstein (1948), Arnold and Von Engel (1961), Holmes (1976) found that the transition of thermionic arc mode of the refractory metals to vapour mode takes place when pressure is brought down below a critical pressure at a constant current; they also observed that when current is raised above a critical current for a particular value of pressure similar transition is observed. Though no such transition was ever observed in case of low melting point vapour mode cathodes, for any pressure and current. The current density on the cathode of a vapour mode arc was found to be of the order of  $10^6 \text{ A/cm}^2$  and hence too high to be explained on the basis of thermionic emission. Richardson equation was modified by Schottky (1923) on the assumption of electrostatic image force on the cathode, thus

$$j_c = AT_c^2 e^{-b/T_c} \exp \left[ \frac{e^{3/2} E^{1/2}}{k T_c \sqrt{4\pi\epsilon_r}} \right] \quad (1.37)$$

where  $j_c$  and  $T_c$  have the same significance as before, and  $e$ ,  $E$  and  $\epsilon_r$  are respectively electronic charge, electric field and permittivity of the emitting space.

Jones and Nicholas (1961) experimentally studied this relation for field ranging from  $10^3 \text{ V/cm}$  to  $10^6 \text{ V/cm}$  for two temperatures  $197^\circ \text{K}$  and  $298^\circ \text{K}$  and found the relation to hold good only for high field in terms of the nature of curve expected from the equation. And out of the three unknown

constants, *vide*, emitting area, work function and field intensification factor, if any two correspond to any set of realistic values, the third one is definitely unrealistic. So such facts raise serious questions regarding the applicability of thermionic emission theory to the cathode of an arc. It is true, the energy released by the +Ve ions maintains the high temperature of the cathode. If these ions come from +Ve column, the ions must land on a large area of the cathode reducing current density on the cathode to a low value. So it is usually presumed that the +Ve ions are produced in the cathode fall region. In this case, high electron current density relative to the +Ve ion current density will be required to produce sufficient +Ve ions essential for maintaining the high temperature of the cathode [Cobine (1958)]. And due to high velocity of electrons, there will be only +Ve space charge in the cathode fall region. The fraction of +Ve ion current to the cathode may be obtained from the work of Shih and Pfender (1970). From the energy balance at the cathode fall space including heat lost by radiation, conduction and convection, they obtained

$$\frac{i_p}{i} = \frac{\phi_c}{V_c + V_i + \frac{k T_e}{e}} \quad (1.38)$$

where  $i_p$  and  $i$  are the ion current and total current density.  $\phi_c$ ,  $V_c$ ,  $V_i$ ,  $T_p$ ,  $e$  and  $k$  are respectively the work function, cathode fall, ionisation potential, ion temperature, ionic charge and Boltzman constant.

This gives an ion current density at the cathode of an arc ranging from 15 to 50% of the total current density. Compton from heat balance at the cathode of an arc obtained.

$$\frac{i_p}{i_c} = \frac{\phi_c}{V_c + V_i - \phi_c} \quad (1.39)$$

Von Engel and Steenbeck estimated for a carbon arc in air; taking  $V_c = V_i = 15.8$  Volt and  $\phi_c = 4.5$  eV and obtained  $\left[ \frac{i_p}{(i_e + i_p)} \right] = 1/7$ . Thus ion current was 15% of the total current. Also Daalder (1978) found ion current fraction at the cathode of an arc to be within 10 to 20%.

In a refined model Lee and Greenwood (1963) and Lee et al. (1964) were able to calculate the fraction of ion current over the entire thickness of the cathode fall space and cathode transition space and found for a 200A carbon arc that this fraction varies from 15% at the cathode surface to zero at the column end.

This increase in the ion current density towards the cathode of an arc is consistent with the formation of net +ve space charge forming the cathode sheath close to the cathode surface. The existence of +ve space charge close to the cathode

surface can produce an electric field [Malter (1936)] strong enough to produce enhanced current emission from the cathode. Due to high velocity of electrons than that of the ions, only +ve space charge [Hsu and Pfender (1983)] may be considered in the cathode fall region and the space charge equation of Child (1911) gives

$$j_p = \frac{1}{9\pi} \sqrt{\frac{2e}{m_p}} \cdot \frac{V_c^{3/2}}{d_c^2} \quad (1.40)$$

where  $j_p$ ,  $e$ ,  $m_p$ ,  $V_c$  and  $d_c$  are respectively the ion current density, ionic charge, ionic mass, cathode fall voltage and span of the cathode fall space.

Von Engel and Steenbeck (1934) obtained the expression for field  $E_c$  at the cathode from the space charge equation and is given by,

$$E_c = \frac{4}{3} \left[ \frac{9\pi j_p}{\sqrt{2e/m_p}} \right]^{2/3} \cdot d_c^{1/3} \quad (1.41)$$

which give  $E_c = \frac{4V_c}{3d_c}$  [Cobine (1958)] (1.42)

Now for low intensity arcs,  $V_c$  is of the order of ionization potential and  $d_c$  is of the order of a mean free path near the cathode. So the field at the cathode for a nitrogen arc between refractory electrode is of the order of  $3.5 \times 10^5$  V/cm and may be of the order of  $10^6$  V/cm for Cu-arc where dense cathode vapour may reduce the mean free path resulting in increase in the field.

The high field at the cathode led many investigators to favour the theory of field emission and investigation was done by Compton (1923), Langmuir (1923), Dyke and Trolan (1953), Doucet (1960), Von Engel and Steenbeck (1934), Bauer (1961, 1966), Rakhovskii (1965), Guozdetskii (1970), Porotnikov et al (1976), Litvinov (1982).

Another expression for electric field  $E_c$  at the cathode is obtained by Mackeown (1929) in which the effect of both +ve ion current density and electron current density at the cathode is considered, where

$$E_c^2 = 7.57 \times 10^5 V_c^{1/2} [j_p (1845 W_p)^{1/2} - j_e] \quad (1.43)$$

where  $j_e$ ,  $j_p$  and  $W_p$  are respectively the electronic current density, ionic current density and ionic mass.

Now taking  $V_c$  to be 10 volts for low intensity arcs,  $j_e + j_p = 400 \text{ amp/cm}^2$ , the equation gives,

$$E_c > 5 \times 10^5 \text{ V/cm for } j_p = 0.05 j_e$$

$$\text{and } E_c > 1.3 \times 10^6 \text{ V/cm for } j_p = 0.30 j_e$$

Thus it appears that such fields may lead to field emission.

Fowler-Nordheim's (1928) theory of field emission, which was later modified by Murphy and Good (1956) was applied to the emission from an arc cathode,

$$I_c = 38.5 \times 10^{12} S E_c^2 \frac{\epsilon_F^{1/2}}{(\epsilon_F + \phi) \phi^{1/2}} \cdot \frac{\pi kT/d}{\sin(\pi kT/d)} \cdot \exp \left[ - \frac{6.8 \times 10^7 \phi^{3/2}}{E_c} \right] \quad (1.44)$$

$I_c$  is the cathode current,  $S$  is the emitting area and  $E_c$  is the field at the cathode. The equation may be written as

$$j_c(T) = j_c(0) \frac{\pi kT/d}{\sin(\pi kT/d)} = j_c(0) K_T \quad (1.45)$$

$$\text{so } \frac{j_c(T_1)}{j_c(T_2)} = \frac{K_{T_1}}{K_{T_2}} = \frac{I_c(T_1)}{I_c(T_2)} \quad (1.46)$$

Jones and Nicholas (1961) obtained experimental verification of this relation, though absolute value of emission current is of the order of  $10^{-6}$  to  $10^{-7}$  amp/cm<sup>2</sup> which is far lower than the actual current density on the cathode of any arc.

Since logarithmic of field current is experimentally a decreasing function of the reciprocal of the field strength, the field current increases extremely as the field strength is increased beyond the minimum field required to produce the first perceptible current [Eyring et al (1928)]. The presence of low work function impurity would greatly increase the current density in the local region of the cathode. Any point of increased emission will result in increase in the field strength at the cathode and hence further increase in current and hence a cumulative process will set in. And such impurities are believed to be necessary for the cold cathode tungsten arc observed by Newman (1932). In the experiment of Eyring et al (1928), Chamber (1934) and Beams (1933) measurable emission begins at fields of the order of  $10^6$  V/cm for pure surfaces and  $10^5$  V/cm for impure surfaces.

If current density from an arc cathode is plotted against pressure for constant discharge current as done by Seeliger and Schmick (1927), there is a sudden increase in current density with lowering of pressure at about 10 cm of Hg for a pure carbon arc in air. The transition is believed by the author to be due to change of thermionic mode to vapour mode of emission. Similar transition is also observed by Beckman and Somermeyer (1936) and Cobine et al (1939) under continuous arcing condition. The transition observed by Seeliger and Schmick and others for pure carbon and tungsten in air is a sudden transition of wandering arc spot to fixed arc spot, with the rise of pressure, showing also a sudden rise in arc burning voltage with the transition; while wandering cathode spot is an inevitable criteria of field type cold low boiling point cathodes only. Also during lowering of pressure at the point of transition from thermionic to vapour spot on the cathode, arc spots contract and start moving violently and arc burning voltage drops with the appearance of vapour mode and the whole process is reversed on reversing the mode of change of pressure, which indicates that the whole nature of change is reversible. The transition pressure is lowered for higher discharge current. Moreover it was found by Arnold and Von Engel (1961) that the transition pressure depends on electrode separation. The appearance of luminous intensity, violent motion of the spot, low arc burning voltage for carbon in air corresponds in every way to the spot

on copper. Also it was noticed by Arnold and Von Engel (1961) that the wall of the arc container which remains clear during thermionic arc mode starts becoming black on transition to vapour mode, indicating absence and presence of carbon vapour in the thermionic mode and vapour mode respectively. The lower arc drop in the vapour mode suggests that smaller energy is consumed in the vapour mode spot than in the thermionic mode spot.

The excitation theory of arcs with evaporating low boiling point cathodes assumes the emission of electrons from the excited vapour atoms evaporated from the cathode of an arc [Von Engel and Robson (1957)].

Also the work of Kimblin (1971) is worth mentioning where he found, assuming single ionization, 55% of the vapour leaving the cathode fall space went through ionization.

Beilis (1988), Mentel (1977) and Blackburn (1978) also observed the effect of vapourization on the mechanism of emission in an arc.

From the theory of stepwise ablation Von Engel and Arnold (1960) found the excited vapour atoms to vapourise cathode material by transferring their energy to the individual atoms rather than heating the lattice as a whole. Thus in this condition simultaneous emission of electrons and vapour are possible without a high lattice temperature. Since the area of a spot is small, this is possible that the true heat influx to the lattice is small and hence lattice attains only a

moderate temperature [Somerville (1952)] and most of the energy is spent against emission of vapour and electron. To maintain the temperature of the overall cathode, the kinetic energy is brought by the back scattered and fast neutral atoms resulting from the charge transfer and thus the temperature of the overall cathode is maintained.

Leycuras (1975), instead of considering emission of electrons from metal surface to vacuum, assumes the electrons to be emitted from metal surface to a dense vapour space which is usually formed around a vapour spot and finds that the work function is greatly lowered. Hence, as soon as, current density in the needles grown on the cathode surface [Alpert (1967), Jomaschke and Alper (1967)] and Mitterauer et al (1973) exceeds a critical value, heat generated becomes sufficient to raise the temperature of the needles above the boiling point of the cathode material and dense vapour is formed around the needles. And thus due to reduction of work function in presence of vapour, there is a tremendous increase in current density, Leycuras also obtained the vapour density in case of Hg and other eight metals, the results show consistency with the experiment made by Kimblin (1973).

It has also been observed by Seeliger and Smick (1927) that carbon arc in argon and neon has highly mobile cathode spot over a wide range of pressure. Thus neon and argon apparently support vapour mode with carbon electrodes while the same in molecular gases like nitrogen and air supports

both vapour mode and thermionic mode depending on the pressure, discharge current and cathode geometry and electrode separation.

It has also been observed by Von Engel and Arnold that during thermionic emission, the cathode appears dull red while it becomes black as soon as stationary spot is transformed to vapour spot.

In case of addition of impurity gas to a carbon arc operating in the vapour mode, either the arc extinguishes or is transformed to a thermionic arc. In case of addition of nitrogen as impurity, this conversion is due to quenching of excited carbon atom ( $C^*$ ) by nitrogen molecule [Von Engel and Arnold (1961) and Holmes (1976)]. Holmes found that the transition from thermionic to vapour arc is initiated by excessive particle loss from the arc spot, whereas the reverse transition to the thermionic arc is caused by the nitrogen molecule quenching of excited carbon  $C^*$  atoms.

The way in which  $C^*$  is quenched by  $N_2$  is described by Arnold and Von Engel (1961). The energy level diagram of  $N_2$  shows that the first triplet state is about 6.2 eV [Hertzberg (1953)] above ground state giving rise to Vegard-Kaplan bands, while  $C^*$  has about 6.5 eV excitation (resonance) energy. Thus the triplet levels are very close for the  $C^*$  to lose its excitation energy to a  $N_2$  molecule [Mitchell and Zemansky (1934)]. Hence quenching cross-section in this case is very high because of nearness of complete energy

resonance. But  $C^*$  cannot be quenched by  $N_e$  atoms whose lowest resonance level is about 16.5 eV [Von Engel and Arnold (1962)].

Another fact obtained by Zhu and Von Engel (1981) is that the cathode fall of Cu in air is the same as that in argon, indicating that the Cu-vapour atmosphere around cathode spot is the dominant medium. Though thermionic mode cathode fall sharply depends on the working fluid in the arc container. The gas condition, however, has an important role towards the nature of cathode surface due to adsorbed gases which can exist as an impurity on the cathode surface resulting in decrease in work function as is done by the presence of oxygen [Suits et al (1938), Cobine (1938), Doan et al (1932)] as an adsorbed gas on the cathode surface.

Due to continuous arcing such adsorbed gases are gradually removed with increase in work function of the cathode surface. This explains why duration of field phase is gradually reduced when the arc operates at a current close to the critical transition current and transforms the arc to a thermionic arc after certain time of operation [Beckmen et al (1936) and Cobine et al (1939)]. So at the on set of thermionic emission, cathode consumption will rise and hence there should be a rise in arc burning voltage. Owing to low current density obtained from Fowler-Nordheim theory and its particular failure to cold cathode emission, Rieder (1967) obtained an expression for field emission cathode current density from cold cathodes, which is valid for low cathode temperature and high field  $> 10^7$  v/cm

$$j_c = 1.54 \frac{E_c^2}{e\phi_c} \exp\left[\frac{-6.83 \times 10^9 (e\phi_c)^{3/2}}{E_c} f\left(\frac{3.79 E_c^{1/2}}{e\phi_c} \times 10^{-5}\right)\right] \quad (1.47)$$

where  $j_c$ ,  $E_c$ ,  $\phi_c$  etc have same significance as before.

From the relation of Mackeown (1929) and Rieder (1967), it follows that the field emission is possible only when  $j_c > 10^7 \text{ V/cm}^2$ , even if unrealistically low work function is assumed.

A modification of field emission theory was suggested by Druyvesteyn (1936) on the basis of observation of Guntherschulze and Frick (1933), where they presumed the field to be produced in an extremely thin layer of high resistance material with +ve ions on the outer surface. Such layers may be due to oxide coating. Ramberg (1932) found that the cathodes of Ca, C, W, Mg are thermionic in nature and that of Cu, Ag, Au and Hg are field emission type. But cathodes of Pt, Sn, Pb, Ni, Zn, Al, Fe, Cd lie truly in neither of the above groups and for metals with high boiling point in this group may combine the effect of thermionic and field emission and such emission is commonly known as TF-emission [Lee (1957), Lee (1958), Lee (1959), Ecker (1961), Bauer (1966) and Hantzsche (1982)].

Finally another work must be mentioned; Thomson and Loeb believe that the current of all arcs arises due to thermionic emission for which they presented the following arguments. If the current density at the cathode of an Cu arc is taken to be  $3000 \text{ amp/cm}^2$  and 3.33% of this is carried by

+Ve ions, the +Ve ion current entering per square cm of cathode will be  $100 \text{ amp/cm}^2$ . If the cathode fall is of the order 20 volt, which is usually the order of cathode fall of an arc [Sen et al (1988)], the power consumed per sq. cm on the cathode surface will be 2000 jule or 480 cal/sec. If the specific heat of Cu is taken to be 0.10, 1 gm of Cu will undergo a rise of temperature of  $4800^\circ\text{C}$  in one sec. If the heat flow is low and such high temperature can exist on the cathode surface, the temperature of a layer of 500 atoms thickness (about  $10^{-5} \text{ cm}$ ) and 1 sq. cm area should undergo a rise of temperature of  $4000^\circ\text{C}$  in only  $7.5 \times 10^{-5} \text{ sec}$ . So even from a low boiling point metal surface, the necessary emission of electrons will be possible. And such a high rate of change of temperature can explain the experiment of Stolt (1924) where he moved an arc cathode at a high speed over a metal surface and found no trace leaving on the metal surface. Holmes (1976) presented a theoretical comparison between the thermionic and vapour mode arcs, which illustrates the essential similarity of the two arcs. Using carbon arc in nitrogen, the arc spot parameters are derived for both arc modes and are in good agreement with the theoretical predictions.

### E. Diffusion phenomena in a magnetised plasma and Hall effect.

Owing to the highly mobile nature of electrons, and comparatively smaller velocity of ions there develops an electron concentration gradient in a direction transverse to the electric field which sets up a potential difference in a direction perpendicular to the applied electric field resulting in a change in ionic velocity in those directions. This results in the formation of space charge in the positive column of the plasma. Nature of the fluid, its pressure, thermal state and other factors like energy loss etc come into play for the final equilibrium to be established.

When in addition to electric field in a discharge plasma, there is a magnetic field in a direction either parallel or perpendicular to the electric field, there is again redistribution in the velocity space of plasma due to Lorentz force which acts on the random motion and drift motion of the charged particles and the plasma becomes anisotropic in many respects.

Townsend (1912) obtained a theoretical expression for diffusion co-efficient under the action of transverse magnetic field, given by

$$D_H = \frac{1}{1 + \omega_B^2 \tau^2} \quad (1.48)$$

where  $\omega_B$  is the gyrofrequency and  $\tau$  is the mean time of collision. In an attempt to formulate a quantitative theory of diffusion in presence of magnetic field, Tonk and Langmuir (1929) used theoretical results of Townsend (1912). These results were latter confirmed by Baily (1930) in experiments with electron swarm for photo electric currents and was found to hold for larger currents when allowance was made for space charge. Davis (1953) used a spectroscopic method to investigate the influence of magnetic field on electron temperature which was latter shown to be connected to diffusion voltage by the relation derived by Sen, Ghosh and Ghosh (1983)

$$\frac{k T_{eB}}{e} = \frac{V_{RB}}{\log \left[ J_0(2.405 r/R) \exp. (-\alpha B) \right]} \quad (1.49)$$

where  $V_{RB}$  is the diffusion voltage and  $T_{eB}$  is the electron temperature both in presence of transverse magnetic field applied to a cylindrical plasma column.

Davis (1953) observed small increase in the electron temperature which is in accordance with the observation of Sadhya and Sen (1980) where they verified the relation derived by Sen, Das and Gupta (1972)

$$T_{eB} = T_e \left( 1 + C_1 \frac{B^2}{p^2} \right)^{1/2} \quad (1.50)$$

Tonk (1941) found for uniform longitudinal magnetic field that the Boltzman equation is to be replaced by

$$n_e = n_0 \exp.(- ev/kTl) \quad (1.51)$$

where

$$l = \frac{\alpha D_e - \mu D_p}{\alpha D_e + \mu \frac{D_p T_e}{T_p}} \quad (1.52)$$

$\mu$  is the ratio of radial drift velocity of electrons and ions, and he found that for longitudinal magnetic field,

$$D_e = D_{eB} \quad \text{and} \quad D_p = D_{pB}$$

Diffusion process of a plasma column in a longitudinal magnetic field was studied by Hoh and Lehnert (1960) which confirmed the earlier results of Lehnert (1958). Experiment with He, Ne, Ar, Kr, N<sub>2</sub>, H<sub>2</sub> are described. In the case of He good agreement was obtained between the collision diffusion theory and experiment upto a certain critical magnetic field. For stronger magnetic field potential drop across the column indicated a much higher diffusion rate across the magnetic field than expected by binary collision theory. He also observed that for tube length more than fifty times the radius of the column, the transition from normal to abnormal diffusion does not depend on the tube length and magnetic field length.

The positive column in a longitudinal magnetic field was studied by Bickerton and Von Engel (1956). They concluded

that in a zero magnetic field the Langmuir theory of free fall of ions describes best the properties of discharge plasma whereas in a magnetic field of sufficient strength Schottky theory of ambipolar diffusion works well in the discharge plasma. They also concluded that when the gas becomes highly ionized, the partial pressure of electron gas may become so effective that longitudinal component of electric field and electron temperature should become independent of magnetic field. Their previous observation on low pressure positive column in Cesium at high current density was cited as an evidence behind their conclusion.

Bohm (1949) theoretically derived a new diffusion co-efficient in a magnetised plasma according to which the transverse diffusion co-efficient is given by

$$D_{\perp} = \frac{1}{3} \omega_r \tau_b \alpha \quad (1.53)$$

where

$$\frac{4\alpha}{\pi} = \frac{(n - n_0)_{av}^2}{n_0^2} \quad (1.54)$$

is the mean square deviation of density fluctuation and  $\tau_b$  is the Larmour radius of electrons and  $\omega_r$  is the mean thermal velocity. Bohm (1949) also gave new expression for ambipolar diffusion co-efficient in a direction transverse to magnetic field according to which

$$D_{\perp} = 2D_{-1} \quad (1.55)$$

in place of

$$D_{\perp} = 2D_{+1} \quad (1.56)$$

and obtained large discrepancy in the theory and experiment and suggested this to be owing to plasma oscillation.

Later Simon (1955) pointed out that due to highly anisotropic conductivity of a magnetised plasma, the ambipolar diffusion no longer exists, and ions and electrons diffuse across the magnetic field at their own intrinsic rate and space charge neutralization is maintained by slight adjustment of current in the direction of magnetic field. Their results were confirmed by Goswami (1957). Langmuir and Rosenbluth (1956) investigated like and unlike particle collision in a magnetised plasma where they found that the unlike particle collision diffusion predominated over that due to like particle collision. Kaufman (1958) extended the theory of diffusion to include the effect of transverse temperature gradient in a magnetised plasma and a closed set of equations is derived by an expansion in two small parameters " $a$ " (radius of gyration) and  $\nabla n/n$  (characteristic macroscopic distance). It is found that to the first order of  $\mathcal{L} [= a/(\nabla n/n)]$ , the ions and electrons diffuse at the same velocity but to the higher order in  $\mathcal{L}$ , the diffusion velocity are different and charge separation may occur in a magnetised plasma. Thus Hall effect following the charge separation may arise. In their paper the relevant transport co-efficient like electrical resistivity, thermal conductivity and thermo-electric co-efficient are derived.

But Simon (1955) and Langmuir and Rosenbluth (1956) assumed no charge separation could occur as a result of ion-ion collision because of charge neutralization by electron flow along the magnetic lines of force. It was found that the ratio of flux from ion-ion collision to that due to ion-electron collision is of the order of

$$\left(\frac{m_i}{m_e}\right)^{1/2} \left(\frac{R_i}{D}\right)^2$$

where  $R_i$  is the ionic radius of gyration and  $D$  is the characteristic distance of the density variation.

But Spitzer (1956) and Chapman and Cowling (1953) and Kaufman (1958) found that a low density fully ionized plasma confined by a strong magnetic field diffused across the magnetic field primarily by ion-electron collision, the flux being proportional to the density gradient and Kaufman (1958) showed that the effect like particle collision on density gradient cannot be enough considerable because the ratio of flux due to like-like collision and like unlike collision is only

$$\left(\frac{R_e}{D}\right)^2$$

instead of that stated by Langmuir and Rosenbluth (1956). And the ratio  $(R_e/D)^2$  is negligibly small.

Simon (1955) also showed that diffusion rate across a magnetic field did not obey Fick's law, i.e., the diffusion is proportional to  $H^{-2}$ , instead it was stated that the diffusion

was proportional to the inverse fourth power of magnetic field strength and diffusion rate due to like particle collision was usually smaller than that due to unlike particle collision but may some time dominate.

Now there exists two theories to account for diffusion of a plasma across a magnetic field  $B$ . The first theory is essentially based on the Boltzman equation with collision terms and can be derived by Chapman-Enskog method. This theory is known as classical diffusion theory or  $1/B^2$  diffusion theory and was extensively investigated and put to confirmation by D'Angelo and Rynn (1961), Simon (1958), Langmuir and Rosenbluth (1956), Demirkhanov (1961) and others. According to the theory,

$$\text{transverse diffusions co-eff. } D_{\perp} = \frac{1}{3} \nu_c \gamma_b^2$$

$$\text{and parallel diffusion co-eff. } D_{\parallel} = \frac{1}{3} \nu_c \lambda^2 = D_{H=0}$$

where  $\lambda$  is the m.f.p. and  $\nu_c$  is the electron-ion collision frequency and  $\gamma_b$  is the Larmor radius of electrons at the mean thermal velocity  $\omega$ , given by

$$\frac{1}{2} m \omega^2 = \frac{3}{2} k T_e \quad (1.57)$$

And another theory is the Bohm's  $1/B$  diffusion theory which was later derived by Spitzer (1960) and also by Petschek (1960) by entirely different assumptions. This  $1/B$  diffusion was experimentally confirmed by Hoh and Lehnert (1960), Bonnal et al (1961), Chen and Bingham (1961) and Yoshikawa and Rose (1962).

Takayana et al (1954) used probe technique to measure Hall voltage in a hot cathode discharge plasma. They obtained Hall voltage in argon upto 400 mV at a pressure of one torr for magnetic field varying upto 14 Gauss.

Sanduloviciu and Toma (1970) investigated Hall voltage in plasma and cautioned about superficial processes by the fast electrons in a dc glow discharge when working with Hall probes. They also studied the optimum working condition when working with Hall probes in a dc glow discharge.

Kunkel (1981) described a simple experimental arrangement for the measurement of Hall voltage in a low density plasma column. And they obtained an expression for Hall voltage,

$$V_H = \frac{x_2 - x_1}{2} E_H - \frac{kT_e}{e} \log \frac{\sin \frac{\pi x_2}{L}}{\sin \frac{\pi x_1}{L}} \quad (1.58)$$

$E_H$  is the Hall field. This expression shows if  $x_1$  and  $x_2$  are selected at equal distance from  $L/2$ , the last term in the expression for Hall voltage vanishes, giving

$$V_H = \frac{1}{2} (x_2 - x_1) E_H \quad (1.59)$$

This shows that the Hall voltage between the opposite sides of such a positive column measures only half of that expected ideally in a conductor with the same carrier density. They supposed the reduction was caused by the ambipolar diffusion

of the carrier whose density distribution is distorted in the presence of transverse magnetic field. They studied Hall voltage across a helium discharge column as a function of magnetic field, discharge current and gas pressure.

Sen and Ghosh (1985) deduced an expression for Hall field given by

$$E_y = \frac{iH}{n_0 e \left[ 1 + \gamma \log \left( 1 + C_1 \frac{H^2}{p^2} \right)^{-1/2} \right]^{1/2}} \quad (1.60)$$

$$\gamma = \frac{2T_e}{T_e + 2eV_i} \quad (1.61)$$

They reported results of their measurements for a Hg-arc carrying a current of 3 amp and placed in a transverse magnetic field ranging from 64G to 526G and the results were in excellent agreement with that theoretically predicted.

Utilizing the expression given by Sen, Ghosh and Ghosh (1983), the open circuited diffusion voltage in an arc plasma (arc current varying from 2 to 5A and for three background pressures of .075, 0.1 and 0.13 torr) has been measured by Sen, Gantait and Acharyya (1989). Utilizing the radial distribution function of conductivity as introduced by Ghosal, Nandi and Sen (1978), an analytical expression for diffusion voltage has been calculated which can satisfactorily explain the observed results.

The diffusion voltage in a mercury arc plasma has been measured for arc currents from 2.5 to 5A in transverse and axial magnetic field from 380 to 1.1 KG by Sen et al (1990). Assuming the radial distribution of charged particles proposed by Ghosal et al (1978) and utilizing the method of Sen et al (1983) the ratio of electron temperature with and without a magnetic field has been evaluated. It becomes a maximum in an axial magnetic field and then decreases whereas it shows a minimum in a transverse field and then increases. An expression for the ratio of electron temperature with and without a field has been deduced that explains the results. Quantitative agreement between experiment and theory is quite satisfactory.

Sen, Acharyya and Gantait (1981) measured the diffusion current and the corresponding diffusion voltage in an arc plasma (arc current 2 to 5A and three pressures 0.075, 0.1, 0.13 torr) and utilizing the radial distribution function of conductivity as introduced by Ghosal et al (1983) the values of diffusion coefficient of mercury vapour have been evaluated. The diffusion coefficient of electrons in mercury vapour has been found to be of the order of  $10^3 \text{ cm}^2/\text{sec}$  which increases with the increase of arc current and decreases with the increase of pressure. A qualitative explanation of the observed results has been presented.

## SCOPE AND OBJECT OF THE PRESENT WORK

Though a large amount of work has been carried out regarding the breakdown of gases and consequent production of plasma, measurement of plasma parameters, waves and oscillations in a plasma and other allied problems, still the nature of some of the physical processes occurring in a plasma during the period of its formation and maintenance have not been adequately investigated. The physical processes occurring in the initiation and maintenance of an arc plasma are still not properly understood. Further it is evident that the cathode phenomena in an arc discharge needs thorough investigation. The process of phase transition from glow to arc should be investigated in order to develop a theoretical basis for the occurrence of an arc plasma. Hence it is proposed to take up investigations in the following lines in the present work.

## A. Energy loss mechanism in a collision dominated plasma

In case of collision dominated plasma, an electron suffers energy loss on account of its various interactions with other charged and uncharged particles. Such interactions are known as collision which, in turn, falls in two categories, *vide*, elastic collision and inelastic collision. A collision is said to be elastic when the total kinetic energy and momentum for the particles undergoing collision remains conserved but one of the particles with higher kinetic energy transfers a part of its kinetic energy to the other one during the collision.

Such a loss of kinetic energy, in case of plasma, frequently occurs with electrons whose kinetic energy is usually much higher than that of other constituent particles of the plasma. To account for the fraction of energy lost in one collision, a factor, known as average collision loss factor has been associated with the electron. An expression for such a factor ( $K$ ) associated only with elastic collision has been given by Compton and Langmuir (1930), which was expected to be valid for low values of  $E/P$ . But experimental measurements for slow electrons undertaken by Bekfi and Brown (1958), Demitriades (1967), Brood (1925), Rusch (1925), Bruche (1927), Ramsauer and Kollah (1929), Normand (1930), Gilardini (1957, 1972), Bushmin and Demitriev (1976) show that even for very low values of  $E/P$ , the value of  $K$  was found to be much higher than the theoretically expected value of  $K$  for elastic collision. Thus even the slowest electrons do not suffer pure elastic collision. Moreover the value of  $K$  was found to depend on  $E/P$  and the characteristic of the working fluid and also on other factors like gas temperature, external magnetic field etc. An inelastic collision loss may arise due to either of the processes like vibrational excitation, recombination, attachment, dissociation, ionization and collision of the 2nd kind. For fast electrons, when inelastic collision has frequent occurrence, the collision loss factor has been measured by Shingaripina and Vasilev (1972), Bowe (1960), Medis (1958), Afrosinov et al (1972), Janca (1967), Biberman et al (1966).

All the above measurements were performed either for different range of  $E/P$  or for different range of electron energy.

But a general theory for the mechanism of collision loss of energy of the electrons was still to be developed. Such a theory is expected to relate the collision loss factor with reduced electric field, electron temperature and a constant which bears the characteristic of the working fluid. Also it was expected that the Joule heating in a discharge plasma is due to the collision loss of energy of the electrons which has almost the sole contribution to the discharge current. So, a relation between the discharge current and the collision loss factor which depends on the said parameters, was naturally expected. Collision loss factor is a function of the ratio of drift and random velocities (Von Engel 1965); and discharge current, collision loss factor and electron temperature - all depend on  $E/p$ , so such a theory was expected to have considerable impact on the understanding of the subject of discharge plasma. So it is proposed to undertake a detailed theoretical investigation regarding the energy loss in a collision dominated plasma and also provide experimental data to verify the theoretical results in case of low density discharge plasma with hydrogen, air and nitrogen as working fluid.

## (B) Radio frequency conductivity of Ionised Gases

Vandarpol (1919) obtained an expression for rf current through a discharge plasma, which is found to be the composition of real and imaginary parts of the gas discharge current. Appleton and Chapman (1932), Margenau (1946), Adler (1949), Sen and Ghosh (1966), Gilardini (1959), Sen and Jana (1978) and many others showed that the rf conductivity through a gas discharge plasma is a complex quantity which points out that the current through a gas discharge plasma is a complex current.

Francis and Von Engel (1953) measured the real current by separating out the capacitative current by balancing a bridge. Penfield and Warder (Jr.) (1967) measured the r.f. real current by measuring the voltage drop across a specially constructed centre tapped inductor. Clark, Earl and New (1970) measured the gas discharge rf current by separating out the capacitative component of the current by a bridge method similar in principle to the method employed by Francis and Von Engel (1953).

Thus it is evident that to separate out the real and imaginary parts of the gas discharge rf current by the bridge balancing method is a difficult task. A lot of adjustment and screening is necessary throughout the measurement at different ranges of applied voltage. So it was felt that a convenient method might be developed in this respect. Thus we propose a resonance method following a theoretical support which will enable one to measure the real as well as the imaginary parts of the gas discharge rf current with the help of only two rf current meters connected in the circuit.

(C) Radio frequency conductivity in presence of transverse magnetic field

Radio frequency conductivity of a gas discharge plasma was found to be a complex quantity [Vandarpol (1919), Margenau (1946), Berk (1964), Sen and Ghosh (1966), Ciampi and Talini (1967), Adler (1949)], Adler (1949) has shown plots for  $\sigma_r$  and  $\sigma_i$  with pressure and current when the other parameters remain constant.

The rf conductivity in presence of transverse magnetic field was calculated by Gilardini (1959) which was found to be a complex conductivity. Later Sen and Ghosh (1966) modified this theory to explain the experimental results of the rf conductivity measurement in presence of transverse magnetic field. Gupta and Mandal (1967), Sen and Gupta (1969), Sen and Jana (1978) measured the rf conductivity of a gas discharge plasma in presence of transverse magnetic field. Ram, Chandra and Sarkar (1972) measured the rf conductivity in presence of both transverse as well as longitudinal magnetic field.

But almost all of the measurement is related to the measurement of real part of the rf conductivity of the gas discharge plasma. But it is presumed that the imaginary part of the rf conductivity in presence of transverse magnetic field still requires some attention for the clear insight of the physical process occurring in a r.f. discharge through gas discharge plasma, so the theoretical analysis regarding the r.f. conductivity of ionised gas (its imaginary part) in a

transverse magnetic field has thus been undertaken. It will be of interest to see how the r.f. conductivity varies with the variation of magnetic field.

#### D. Plasma Parameters diagnostic

Though there are a number of methods for the determination of plasma parameters such as single and double probe method, Radio frequency conductivity method, Microwave transmission and reflection method, spectroscopic method and Laser diagnostic technique, still a simple and alternative method has been proposed to be developed which can act as a supplementary method to the above. A microwave beam of variable frequency is proposed to be sent through a rectangular wave guide filled with plasma and with the help of a microwave interferometer the attenuation and phase change can be measured ( $\alpha$  and  $\beta$  where  $\alpha$  is the attenuation per unit length and  $\beta$  is the phase constant per unit length). The cut off frequency for the wave guide when filled with air and also when filled with plasma can be experimentally measured. A detailed mathematical analysis has been carried out where  $\sigma_r$  the conductivity (real part) and  $\sigma_i$  the conductivity (imaginary part),  $\epsilon'$  the dielectric constant (real part) and  $\epsilon''$  the dielectric constant (imaginary part) can be related with the experimentally measured quantities,  $\alpha$ ,  $\beta$ ,  $\omega_c$ ,  $\omega_{cp}$  where  $\omega_c$  and  $\omega_{cp}$  are the cut off frequencies of the wave guide without and with the plasma respectively. From these relations it has been shown how the electron density and collision frequencies can be evaluated.

### E. Effect of magnetic field on the cut off frequency of Microwaves in a plasma

The microwave reflection method is a well known plasma diagnostic method for determining the electron density in a plasma. It utilizes the same principle as is used in determining electron and ion density in the Ionosphere. But the essential criteria for the successful operation of a thermonuclear reactor is that magnetic field is used for the confinement of the plasma and in wave propagation in the ionosphere the effect of earth's magnetic field has to be taken into consideration. Hence it has been thought worthwhile to consider the effect of magnetic field on the value of cut off frequency when a microwave beam is propagated through the plasma column. A detailed mathematical analysis has been presented and variation of cut off frequency with magnetic field has been investigated. The calculations are useful when determining the electron and ion density in a magnetically confined plasma as in a thermo nuclear reactor.

### F. Investigation of low density plasma in a magnetic field

In presence of transverse magnetic field, the diffusion inside a discharge plasma undergoes certain changes resulting in change in diffusion voltage. But due to Lorentz force there appears a Hall voltage too. Many investigators measured diffusion

voltage in presence of transverse magnetic field. The work of Sen and Ghosh (1983), Tonk (1941), Bohm (1949), Simon (1955), Goswami (1957), Langmuir and Rosenbluth (1956), Kaufman (1958), and Spitzer (1956) may be mentioned. Many investigators have measured the diffusion voltage in a transverse magnetic field.

Some of the investigators like Sanduloviciu and Toma (1970), Kunkel (1981), Sen and Ghosh (1985) measured Hall voltage in case of a plasma.

But Hall voltage and diffusion voltage appear in the same plasma space so it is difficult to measure these two voltages separately. Thus it was felt necessary to have a detailed theoretical investigation to calculate the combination of the diffusion and that of Hall effect separately which will enable us to find a theoretical expression for the total voltage developed. So we have proposed a theory which gives an expression for the composition of two voltages, viz., diffusion voltage and Hall voltage. Experimental results for such a measurement as obtained here in case of a low density plasma shows excellent agreement for moderately transverse magnetic field. In the low field intensity region, there is, however, certain discrepancy. Separation of the two effects will enable one to find the relative importance of each effect in the different regions of the applied magnetic field.

### G. Cathode Phenomena in an arc plasma

From the early part of the 20th century, the physical processes occurring on the surface and neighbourhood of cathode of an arc have drawn attention of many investigators because of its high current density, high current and low cathode fall unlike the cathode of a glow discharge.

The early attempt to explain the cathode phenomena was on the basis of thermionic emission and later field emission was also considered by many investigators and then in some cases it was thought that both thermionic and field emission have simultaneous role on the emission mechanism from the cathode of an arc. Thus cathode of Cu, Ag, Au etc. fall in one category where field emission plays the dominant role, while, C, W, rare earth metals fall in another category where thermionic emission is prominent. But the latter shows field emission below certain pressure in certain gases. Again Fe, Zn, Al etc are found to have combined effect of thermionic and field emission. Thus no general theory and origin of cathode phenomena of an arc has been proposed.

In this present investigation we undertake the problem to put forward a general theory which can cover all category of above said cathodes and thereby reducing the complexities prevailing towards the understanding of the cathode phenomena of an arc.

In the present work we have proposed a general theory with adequate mathematical background and selected three different electrode materials in such a way, which were earlier observed to fall into three different categories, *vide*, thermionic emission category, field emission category and TF emission category, for consideration of testing the theory proposed by us. The experimental results with the said electrodes show excellent agreement with the present theory. As the occurrence and maintenance of a high current arc is not yet properly understood the proposed work may help in providing a generalised theory specially with regard to cathode processes in the arc.

#### H. Low frequency oscillation in an arc plasma

A plasma can support oscillations under different conditions all of which are longitudinal because the electric field and line of oscillation are parallel to the direction of propagation of oscillation. In one category of oscillation, there is no component of magnetic field associated with the oscillation while in some other cases small time varying magnetic field may be associated either along the direction or transverse to the direction of propagation of oscillation. These later oscillations are associated with the wave known as "magnetohydrodynamic" or hydromagnetic wave which propagates with velocities much lower than the velocity of light and the frequency, too, in this case, is many order less than in the

case of electron plasma oscillation and may even be smaller than ion plasma oscillation.

But all of these processes usually transform power into the oscillation, which is no more than a little percentage of the total power associated with the discharge. But in the early time gas discharge tube with negative resistance characteristics were used for the generation of radio waves which had much higher percentage of total power conversion to the oscillation, as in the case of dynatron oscillator. In case of mercury arc which has a negative resistance characteristics and whose design is simple and inexpensive, a negative resistance oscillator may be designed which can handle and produce larger oscillatory power. A simple theory for such an oscillator was proposed by Cobine (1958). Thus we undertake this work with the aim of designing a high power oscillator whose design is simple and frequency will be easily adjusted with the help of L and C. Though in our Hg arc,  $\frac{dv}{di}$  is negative for the portion of the v-i characteristics, we have utilised, the oscillation is never like dynatron oscillation whose frequency depends entirely on the tank circuit parameters. In the present case frequency and amplitude of oscillation detected is entirely controlled by the inner characteristics of arc. These low frequency oscillations depend on the properties of mercury arc tube. We have investigated the mechanism of

generation of such oscillations and advanced an analytical theory showing their variation with pressure, arc current and magnetic field. The experimental results are in conformity with the theoretical derivation. The source of these low frequency oscillations has also been suggested.

B I B L I O G R A P H Y

1. Adler, P., J. Appl. Phys. 20, 1125, 1949.
2. Afrosimov, V.V., et al, Zh. Tekh. Fiz. (USSR) 142,  
125, 1972.
3. Agashi, V.V., IEEE, p 47, 1983.
4. Aleksandrov, A.F. and Yalsenko, I.M., High Temp.  
3, 321, 1965.
5. Alpert, D.J., J. Appl. Phys., 38, 880, 1967.
6. Appleton, E.V. and Chapman, E.W., Proc. Phys. Soc.  
(Lond), 44, 246, 1932.
7. Appleton, E.V. and Bohariwalla, D.B., Proc. Phys. Soc.,  
47, 1074, 1935.
8. Armstrong, B.G. and Emeleus, K.G., Proc. Instr. Elect.  
Engrs. III, 96, 390, 1949.
9. Arnold, K.W. and Von Engel A, Vth Int. Conf. Ioniz.  
Phen. gases, I, 859, 1961.
10. Baily, V.A., Phil. Mag., 9, 560, 1930.
11. Basannikov, A.L. et al, Fiz. Plazmy (USSR), 5, 391,  
1979.
12. Bauer, A, Z. Phys. (Germany) 164, 563, 1961.
13. Ibid, 165, 34, 1961.
14. Ibid, Beitr. Plasma Physik (Germany), 6, 281, 1966.
15. Beams, J.W., Phys. Rev., 44, 803, 1933.
16. Beilis, I. I., Akad. Nauk. SSSR (USSR), 298, 1108, 1988.
17. Bekefi, G and Brown, S.C., Phys. Rev., 112, 159, 1958.
18. Berk, H.L., Phys. of Fluids, 7, 257, 1964.
19. Bernstein, I.B. and Kulsrud, R.M., Phys. Fluids, 3,  
837, 1960.
20. Biberman, L.M. and Muatsakanyan, A.K.,  
Teplofix. Vysokikh Temp. (USSR), 4, 491, 1966.
21. Bickerton, R.J. and Von Engel, A., Proc. Phys. Soc.  
(Lond.), 69B, 468, 1956.
22. Blackburn, T.R., Elect. Energy Conf. p 156 (1978)

23. Blackman, V.H., ARS report No. 1001-59, 1959.
24. Bohm, D., "The Ch. of Elect. discharge in Mag. fld.",  
Edited by A. Gunthrie & R.K. Wakerling,  
McGraw Hill Book Co., 1949.
25. Bowe, J.C., Phys. Rev., 117, 1411, 1960.
26. Brood, R.B., Phys. Rev., 25, 636, 1925.
27. Bruche, E., Ann. Physik, 82, 912, 1927.
28. Buchelnikova, N.S., Zh. Eksp. Teor. Fiz.,  
46, 1147, 1964.
29. Bushmin, A. S. and Demitriev, L.M.  
Teplofiz. Vys. Temp. (USSR), 14, 266, 1976.
30. Chamber, C.C., J. Franklin Inst., 218, 463, 1934.
31. Chen, F.F. and Bingham, R., Bull. Am. Phys. Soc.,  
6, 189, 1961.
32. Chen F.F., Phys. of Fluids, 7, 949, 1964.
33. Ibid., 8, 752, 1965.
34. Chen, F.F., Plasma Phys., 7, 399, 1965.
35. Child, E.C., Phil Mag., 13, 873, 1932.
36. Child, C.D., Phys. Rev., 32, 492, 1911.
37. Ciampi, M. and Talini, N., J. Appl. Phys. (USA),  
38, 3771, 1967.
38. Clerk, J.L., Earl, R.G. and New, J., Int. Conf.  
Gas discharge (Lond.), IEEE, p 172, 1970.
39. Cobine, J.D. and Gallagher, C.J., Phys. Rev., 74,  
524, 1948.
40. Cobine, J.D., "Gaseous Conductors", p 303, 1958.
41. Cobine, J.D. et al, J. Appl. Phys., 10, 420, 1939.
42. Ibid, Phys. Rev., 53, 911, 1938.
43. Compton, K.T., Phys. Rev., 37, 1077, 1931.
44. Ibid, 21, 266, 1923.
45. Compton, K.T. and Langmuir, I. I., Rev. Mod. Phys.,  
2, 211, 1930.
46. Ibid, 3, 191, 1931.
47. Crompton, R.W. and Sutton, J.J., Proc. Roy. Soc. (Lond.)  
A215, 467, 1952.
48. Daalder, J.E., J. Phys. D (GB), 11, 1667, 1978.

49. Davis, L.W., Proc. Phys. Soc., B66, 33, 1953.
50. Dawson, J and Oberman, C., Phys. of Fluids, 5,  
517, 1962.
51. Ibid, 6, 394, 1963.
52. D'Angelo, N. and Rynn, N., Phys. of Fluids, 4,  
1303, 1961.
53. D'Angelo, N., Phys. of Fluids, 6, 592, 1963.
54. D'Angelo, N and Motley, R.W., Phys. of Fluids,  
6, 422, 1963.
55. Demetriades, S.T., Phys. Rev., 158, 215, 1967.
56. Demirkhanov, R.A. et al (USSR), Proc. Vth Int. Conf.  
on "Ioniz. Phen. in Gases" II, 1344, 1961.
57. Doan, G.E. and Myer, J.L., Elect. Eng., 51, 624, 1932.
58. Dote, T. and Shimoda, M., J. Phys. Soc. (Japan),  
49, 1442, 1980.
59. Doucet, H., C.R. Acad. Sci (Paris), 250, 1007, 1960.
60. Druyvesteyn, M.J., Nature, 137, 580, 1936.
61. Dushman, S., Phys. Rev., 21, 623, 1923.
62. Ibid, Rev. Mod. Phys., 2, 458, 1930.
63. Ducan, A.J. and Forrest, J.R., Phys. Letter A  
(Netherlands), 32, 469, 1970.
64. Dyke, W.P. and Trolan, J.K., Phys. Rev., 89, 799, 1953.
65. Ecker, G., Ergebn. exakt. Naturw, 33, 1, 1961.
66. Everhart, E. and Brown, S.C., Phys. Rev., 78, 839, 1949.
67. Eyring, C.F., et al, Phys. Rev., 31, 900, 1928.
68. Fowler, R.H. and Nordheim, L.W., Proc. Roy. Soc. (Lond.),  
A119, 173, 1928.
69. Francis, G. and Von Engel, A., Phil. Trans. Royl.  
Soc. (Lond.), A246, 143, 1953.
70. Fried, B.D. and Gould, R.W., Phys. of Fluids, 4, 139,  
1961.
71. Froome, K.D., Proc. Phys. Soc. (Lond.), 60, 424, 1948.
72. Ibid, B62, 805, 1949.
73. Gabor, D., Brit. J. Appl. Phys., 2, 209 (1951)
74. Gabovich, M.D. et al., Zh. Eksp and Teor. Fiz (USSR)1973.

75. Ghosal, S.K., Nandi, G.P. and Sen, S.N., *Int. J. Electronics*, 44, 409, 1978.
76. *Ibid*, 41, 509, 1976.
77. Gilardini A.L., *Nuovo Cimento, Supp. Sec.* 10(1-2), 13, 1959.
78. Gilardini A.L., "Low energy electron collision in gases, Swarm and plasma methods applied to their study", 1972 (John Wiley).
79. Gilardini, A.L., and Brown S.C., *Phys. Rev.*, 105, 25, 1957.
80. *Ibid*, 105, 31, 1957.
81. Goswami, S.N., *Nuovo Cimento*, 5, 1969, 1957.
82. Gould L. and Brown S.C., *Phys. Rev.*, 95, 897, 1954.
83. Green H.S. and Leipnik, R.B., *Int. J. Eng. Sci. (GB)*, 3, 491, 1965.
84. Guntherschulze A and Fricke H., *Zeit. f. Physik*, 86, 451, 1933.
85. Guozodetskii, V.S., *Avtom Svarka (USSR)*, 3, 1970.
86. Gupta, R.N. and Mandal, S.K., *Ind. J. Phys.*, 41, 251, 1967.
87. Gupta, R.N., Mandal, S.K. and Sen, S.N., *Proc. Ind. Sci. Cong.*, 1968.
88. Hantzsche E., *Beitr. Plasma Phys.*, 22, 325, 1982.
89. Heald M.A. and Wharton C.B., "Plasma Diagnostics with Microwaves", (John Wiley & Sons).
90. Hertzberg G., "Spectra of diatomic molecules", 1953.
91. Hoh F.C. and Lenhart B., *Phys. of Fluids*, 3, 600, 1960.
92. Holmes A.J.T., *J. Phys. D (GB)*, 9, 537, 1976.
93. Hornwell G.P., *Phys. Rev.*, 33, 559, 1929.
94. Hsu K.C. and Pfender E., *J. Appl. Phys. (USA)*, 54, 3818, 1983.
95. Iman A. and Khastgir S.R., *Phil. Mag.*, 23, 858, 1937.
96. Ionescu V. and Mihul C., *J. Phys. Radium*, 6, 35, 1935.
97. Janca J., *Phys. Letters (Netherlands)*, 25A, 165, 1967.
98. Johnson R.R., *Phys. of Fluids*, 10, 108, 1967.

99. Jones F.L. and Nicholas D.J., Vth Int. Conf. on "Ioniz. Phen. in Gases", II, 1961.
100. Kato K and Yoseli M., J. Phys. Soc. (Japan), 23, 671, 1967.
101. Kaufman A.N., Phys. Rev., 109, 1, 1958.
102. Khozhalev M.B. and Yasin L.P., High. Temp (USA), 4, 576, 1966.
103. Khvashchtevaski S., Nukleonika, 7, 369, 1962.
104. Kimblin C.W., Proc. IEEE (USA), 59, 546, 1971.
105. Ibid, Proc. XIth Int. Conf. on "Phen Ioniz. Gases", 1973.
106. Konyukov M.V., Sov. Phys. JETP, 5, 429, 1957.
107. Koritz H.E. and Keck J.C., Rev. Sc. Instr., 35, 201, 1964.
108. Krolikowski C, Proc. 9th Int. Conf. on "Phen Ioniz. Gases", p358, 1969 (Rumania).
109. Kunkel W.B., Am. J. Phy., 49, 733, 1981.
110. Langavin P., Ann. Chem. Phys., 8, 238, 1905.
111. Langmuir I., Gen. Elect. Rev., 26, 735, 1923.
112. Langmuir C.L. and Rosenbluth M.N., Phys. Rev., 103, 507, 1956.
113. Langmuir I. and Mott-Smith H., Gen. Elect. Rev., Vol. 27 p(449, 538, 616, 762, 810), 1924.
114. Langmuir I., Proc. Nat. Acad. Sci., 14, 625, 1926.
115. Langmuir I. and Tonks L., Phys. Rev., 33, 195, 1929.
116. Lashinsky H., Phys. Rev. Lett., 12, 121, 1964.
117. Ibid, 13, 47, 1964.
118. Lee T.H. and Greenwood A., ARL Rep., 63, 163, 1963.
119. Lee T.H. et al, ARL Rep., 64, 152, 1964.
120. Lee T.H., J. Appl. Phys., 28, 920, 1957.
121. Ibid, 29, 734, 1958.
122. Ibid, 30, 166, 1959.
123. Lenhert B., Proc. 2nd Int. Conf. on Peaceful uses of atomic energy, 32, 349, 1958.
124. Leycuras A., Proc. XIIth Int. Conf. "Phen. Ioniz. Gases" I, 244, 1975.

125. Litvinov E.A. & Parfynov A.G., IEEE, p138, 1982.
126. Loeb L.B., "Fundamental Process of electrical discharge in Gases", p631.
127. Mackeown S.S., Phys. Rev., 34, 611, 1929.
128. Maiti J.N. and Basu J., Nucl. Phys. and Solid State Phys. Symp. digest, Powai, p58, 1968.
129. Malter L., Phys. Rev., 49, 478, 1936.
130. Margenau H., Phys. Rev., 69, 508, 1946.
131. Medies G., J. Appl. Phys., 29, 903, 1958.
132. Mentel J., Appl. Phys. (Germany), 14, 269, 1977.
133. Mitchell A.C.G. and Zemansky M.W., "Resonance Radiation and excited atoms", 1934.
134. Mitra D.P., Ind. J. Phys., 49, 161, 1975.
135. Miterauer J. et al, Proc. XIth Int. Conf. on "Phen. Ioniz. Gases", 1973.
136. Murphy E.L. and Good R.H., Phys. Rev., 102, 1464, 1956.
137. Nagata M., Elect. Enging. Japan (USA), 86, 40, 1966.
138. Nedospasov A.V. and Shipuk Ya., Teplofiz Vysokikh Temp. (USSR), 3, 186, 1965.
139. Neill, T.R. and Emeleus K.G., Proc. Roy. Irish Acad., A53, 197, 1951.
140. Newman, F.H., Phil. Mag. 22, 463, 1936.
141. Ibid, Phil. Mag., 14, 788, 1932.
142. Noon J.H. et al., Plasma Phys (GB), 12, 477, 1970.
143. Normand C.E., Phys. Rev. 35, 1217, 1930.
144. Oberman C. and Shure F., Phys. of Fluids, 6, 834, 1963.
145. Pasechnik L.L. and Popovich A.S., Dokl. Akad. Nauk (USSR), 191, 1263, 1970.
146. Pastukhov V.P., Nucl. Fission (Australia), 14, 3, 1974.
147. Penfold A.S. and Warder (Jr) R.C., Rev. Sc. Instr. (USA) 38, 1533, 1967.
148. Penkratov I.M. and Stepanov K.N., Ukr. Fiz. Zh (USSR) 16, 1979, 1971.
149. Penning F.M., Nature, Lond., 118, 301, 1926.
150. Ibid., Physica, 6, 241, 1926.

151. Petschek, H.E., Avco Research Lab, Everett, Massachusetts, Tech. report AFOSR 360, 1960.
152. Phelps A.V., et al, Phys. Rev., 84, 559, 1951.
153. Porotnikov A.A. et al, 17, 22, 1976.
154. Pradhan T and Das Gupta B., Phys. Rev., 160, 184, 1967.
155. Rakhovskii V.L., Zh. Tekh. Fiz. (USSR), 35, 2228, 1965.
156. Ram V, Chandra A and Sarkar D.C., Ind. J. Pure and Appl. Phys., 10, 850, 1972.
157. Ramberg W, Ann. d. Physik, 12, 319, 1932.
158. Ramsauer C and Kollah R., Ann. Physik, 4, 91, 1929.
159. Richardson O.W., Phil. Mag., 23, 594, 1912.
160. Rieder W., "Plasma and Lichtbogen" Friedr. Vieweg, Braunschweig, Germany, 1967.
161. Rohner, E., Appl. Sc. Res. B5, 90, 1955.
162. Rosa R and Allen J.E., 9th Int. Conf. on "Phen in ionized gases" (Rumania) 1969.
163. Rusch M, Physik. Z., 26, 748, 1925.
164. Ruthstein J., J. Appl. Phys., 19, 1181, 1948.
165. Sadhya S.K. and Sen S.N., J. Phys. D, Appl. Phys., 13, 2775, 1980.
166. Sanduloviciu M, Phys. Letter, 27A, 313, 1968.
167. Ibid, 9th Int. Conf. on "Phen. ionized gases" Bucherest p149, 1969.
168. Ibid, Le J. De Physique, 32, 157, 1971.
169. Sanduloviciu M. and Toma M., Z. Phys. 239, 300, 1970.
170. Schottky C.W., Z. Physik, 14, 63, 1923.
171. Schweitzer S. and Milchuer M., Phys. of Fluids, 10, 799, 1967.
172. Seeliger R and Schmick H., Phys. Zeits, 28, 605, 1927.
173. Sen S.N. and Ghosh A.K., Ind. J. Pure and Appl. Phys., 4, 70, 1966.
174. Ibid, Ind. J. Phys., 35, 101, 1961.
175. Sen S.N. and Gupta R.N., Ind. J. Pure and Appl. Phys., 7, 462, 1969.

176. Sen S.N. and Jana D.C., *Ind. J. Phys.*, 52B, 288, 1978.
177. Sen S.N., Gantait M and Jana D.C., *Ind. J. Phys.*, 62B, 78, 1988.
178. Sen S.N., Das R.P. and Gupta R.N., *J. Phys. D, Appl. Phys.*, 5, 1259, 1972.
179. Sen S.N. and Ghosh B., *Proc. Ind. Natn. Sci. Acad.*, 51A, 346, 1985.
180. Sen S.N., Ghosh S.K. and Ghosh B, *Ind. J. Pure & Appl. Phys.*, 21, 613, 1983.
181. Sen S.N., Gantait M and Acharyya C., *Ind. J. Pure and Appl. Phys.*, 27, 220, 1989.
182. Sen S.N., Acharyya C and Gantait M., *Ind. J. Pure and Appl. Phys.*, 29, 238, 1991.
183. Sen S.N., et al., *Int. J. Elect.*, 68, 621, 1990.
184. Shih K.T. and Pfender E., *AIAAJ*, 8, 211, 1970.
185. Shingerkina V.A., et al., *Zh. Tekh. Fiz. (USSR)* 17, 1043, 1972.
186. Shutko A.V., *Zh. Teph. Fiz.*, 38, 1431, 1968.
187. Simon A., *Phys. Rev.*, 98, 315, 1955.
188. *Ibid*, *Phys. Rev.*, 100, 557, 1955.
189. *Ibid*, *Proc. 2nd Int. Conf. on peaceful uses of atomic energy, UN, Geneva*, 32, 342, 1958.
190. Sodha M.S., *Phys. Rev.*, 118, 378, 1960.
191. Somerville J.M., et al, *Proc. Phys. Soc.*, B65, 963, 1952.
192. Spitzer L.S., *Phys. of fully ionized gases, Int. Sc. Pub. Inc., New York*, 1956.
193. Spitzer L.S. (Jr.), *Phys. of Fluids*, 3, 600, 1960.
194. Stix T.H., *Phys. Rev.*, 106, 1146, 1957.
195. Stolt H., *Ann. d. Physik*, 74, 80, 1924.
196. *Ibid*, *Zeit. f. Physik*, 26, 95, 1924.
197. Suit C.G. and Hocker J.P., *Zeit. f. Physik*, 86, 451, 1933.
198. Takamaya K., Suzuki T. and Yabumoto T., *Letters in Phys. Rev.* 96, 531, 1954.

199. Tanaka H and Usami S., Bull. Fac. Eng., Yokohama Nat. Univ., 11, 65, 1962.
200. Tanaka Y., J. Phys. Soc. (Japan), 27, 516, 1969.
201. Tanaka Y. and Yamamoto K., Elect. Engng. Japan (USA), 86, 01, 1966.
202. Tauth T. et al, Nucl. Instrum. Metal (Netherlands), 85, 245, 1970.
203. Thomson J.J. and Thomson G.P., "Conduction of Elect. through gases", Vol. II, p 596.
204. Tomaschke H. and Alpert D., J. Appl. Phys., 38, 881, 1967.
205. Tonks L. and Langmuir I., Phys. Rev., 34, 876, 1929.
206. Tonks L., Phys. Rev., 59, 514, 1941.
207. Townsend S.J. and Baily V.A., Phil. Mag., 42, 873, 1921.
208. Townsend J.S., Proc. Roy. Soc. (Lond), A86, 571, 1912.
209. Ibid, Phil. Mag., 25, 459, 1912.
210. Vandarpol B., Phil. Mag., 38, 352, 1919.
211. Valdiminov V.V., Zh. Eksp. Teor. Fiz., 48, 175, 1965.
212. Von Engel, A., Ionized gases, p 275, 1965.
213. Von Engel A. and Steenbeck M., Elektrisch Gasentladungen, ihre Physik u. Technik, 2, 132, 1934.
214. Von Engel A. and Robson A.E., Proc. Roy. Soc., A242, 217, 1957.
215. Von Engel A. and Arnold R.W., Nature, 187, 1101, 1960.
216. Ibid, Proc. Phys. Soc. (Lond.), 79, 1098, 1962.
217. Wehner G, J. Appl. Phys., 21, 62, 1950.
218. Wroe H, Brit. J. Appl. Phys., 9, 488, 1958.
219. Wu C.S., Phys. Rev., A51, 138, 1965.
220. Yoshikawa, S and Rose D.J., Phys. of Fluids, 5, 334, 1962.
221. Zhu S.L. and Von Engel A., J. Phys. D (GB), 14, 2225, 1981.
222. Zvereva F.G., et al., Izv. Vuz. Radiofiz., 20, 1232, 1977.

CHAPTER II

EXPERIMENTAL SET UP

## CHAPTER - II

## EXPERIMENTAL SET UP

## 2.1. Collision loss factor:

Apparatus and Accessories: (1) Glow discharge tube for diffusion voltage measurement (2) High voltage power supply (3) Constant current generator (4) Digital Voltmeter (Model No. Hill 205) (5) Ammeter (Sett & Dey) (6) R.C. filter (7) McLoyd Gauge (8) Pirani Gauge (9) Two stage Rotary Pump.

2.1.1. The discharge tube is cylindrical in shape and made of corning glass with two circular brass electrodes fitted symmetrically at two ends inside the tube and in such a way that they face parallel to each other. To stop any spurious discharge with the back side of the electrodes, the backside of the electrodes are tightly covered with teflon cap and the connecting tungsten rods are sealed with thin glass coating. So the chance of any spurious discharge resulting in sudden undesired fluctuation of discharge current was thus totally eliminated. In absence of such sealing, there is face to face discharge between the electrodes for low values of  $E/p$ , but when  $E/p$  is gradually made high, there is sudden rise of discharge current showing luminous glow behind the electrodes. Such a change in discharge current cannot occur when only the front surfaces of the electrodes are open to discharge.

2.1.2. The probes for the measurement of diffusion voltage were made of very thin tungsten wire of diameter 0.2 mm and placed

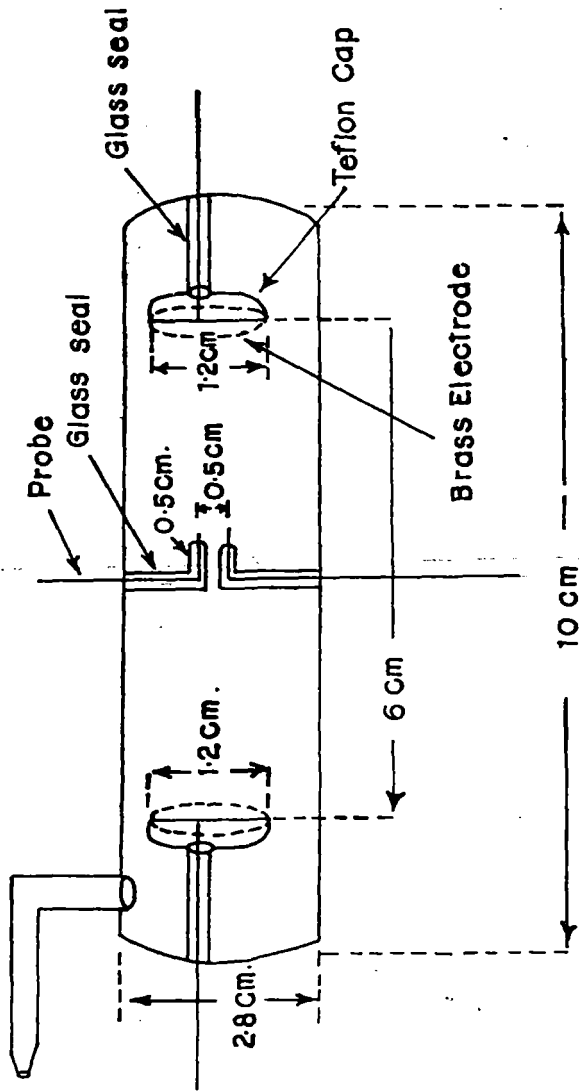


Fig. 2.1.

F 2.1

parallel to the electric field, of which one is placed along the symmetry axis of the plasma column while the other one is placed 5 mm away from the axis. The length of each probe is 5 mm and the electrodes are sealed with thin glass coating except at the ends of each. The length of the open portion of the probes are no more than 0.2 mm each. Both of the electrodes point towards the same direction in the discharge tube. The Schematic diagram of the complete discharge tube is shown in Fig. 2.1.

2.1.3. The gases used in the experiment were at least analytically pure. Three gases are used in this experiment, vide, air, hydrogen and nitrogen. Air was made pure by passing first through caustic potash solution removing carbon dioxide and then through distilled water and finally through highly concentrated sulphuric acid followed by several U tubes filled up with caustic potash pellet. The rate of flow through the purification system was kept extremely small to ensure the purification process to be complete. Finally pure air is stored in a five litre vessel connected with the purification system.

Pure hydrogen is produced by electrolysis of dilute barium hydroxide solution. To remove any trace of impurity present in the hydrogen, the prepared gas is allowed to pass through heated platinum net followed by caustic potash pellet and phosphorus pentoxide.

Nitrogen is produced by controlled heating of sodium chloride and ammonium nitrite solution mixed in a round bottom flask. This nitrogen contains little chlorine, ammonia, nitric oxide and water vapour. To remove these impurities from the nitrogen, the gas is allowed to pass through concentrated solution of caustic potash and then through concentrated sulphuric acid. Finally the gas is made to pass through highly heated copper turnings to remove nitric oxide by reducing it into nitrogen. This is pure nitrogen and has been used in the present experiment.

2.1.4. Pressure during discharge is measured with the help of a McLoyd gauge and a Pirani gauge simultaneously so that correctness of the pressure measured is assured. The calibration curves for the Pirani gauge in air, hydrogen and nitrogen were supplied by the manufacturer.

2.1.5. High voltage power supply is designed to have a supply of voltage maximum upto 2.5 KV and a current maximum upto 10 mA (HV 4800D).

2.1.6. To ensure the discharge current to be constant in a particular set of experiment a series current controller is designed and connected in series with the discharge tube in addition to a high watt resistance (51.3 K. Ohm) in series. After fixing the current in the discharge circuit, the current controller and the high voltage power supply is gradually adjusted in such a way that the drop across the current controller is within the specified limit. Under this condition

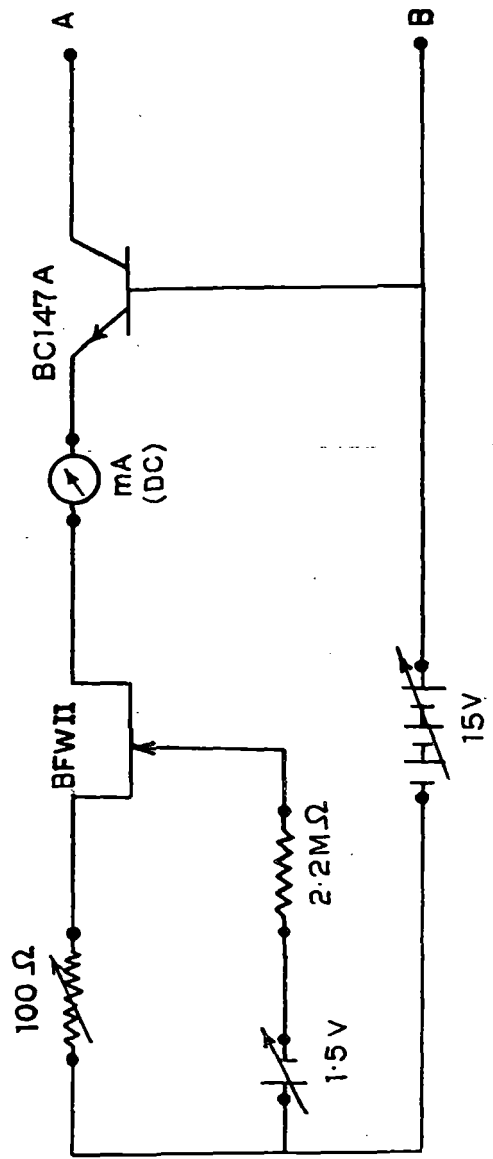


Fig. 2-2. Ckt - Current Controller

the current through the discharge tube remains fairly constant against any spurious fluctuation in the system. Circuit diagram is shown in Fig. 2.2.

2.1.7. The probes are connected with the input of a  $\pi$ -type RC filter whose time constant is 2.4 sec. The value of R is 100 kilo ohm and that of the two condensers are  $24 \mu\text{F}$ . The aim of such filter is to stop any spurious ac voltage to appear at the output of the filter. Particularly the low frequencies which are frequently present in such glow discharge tubes, disturb the measurement of diffusion voltage. Because the probes in addition to dc diffusion voltage also pick up such spurious ac voltages present during the discharge. The impedance between the probes is high because of extremely small surface area open to the discharge and comparatively high distance between the open tips of the probes and also due to low conductivity in case of low density plasma formed in a glow discharge tube.

Also because of small surface area open, the power picked up by the probes against diffusion voltage is quite small. So it has to be assured that the circuit measuring diffusion voltage does not consume any appreciable power which may result in faulty measurement of diffusion voltage.

Thus the condensers in the R-C filter are selected in such a way that leakage current does not exceed nano-Ampere and to ensure that any change in voltage between the probes can

immediately effect the output of the filter in a linear way, high quality rapid discharge condensers are used in this construction.

Use of L-C filter in such cases has been tested in the laboratory, which shows that such use is inconvenient because of large size of the filter required to prevent any low frequency to appear at the output of the filter.

2.1.8. The voltmeter connected at the output of the filter for the measurement of the diffusion voltage under the stated condition, as described, needs to have high input impedance.

Also since the diffusion voltage is a floating voltage in a discharge tube where both probes are immersed in high voltages, the voltmeter must be isolated with respect to the main discharge voltage source, otherwise erratic and impossible voltages may be shown by the voltmeter. To prevent such problem, it is convenient to use battery operated digital voltmeter whose input impedance is also high in addition to the ability to measure any such floating voltage. In this experiment the digital voltmeter Hill 205 has been used whose input impedance is more than 10 Meg ohm.

2.1.9. The pressure inside the discharge tube is maintained with the help of a double stage rotary pump and one needle valve. The needle valve which has adjustable microleak allows

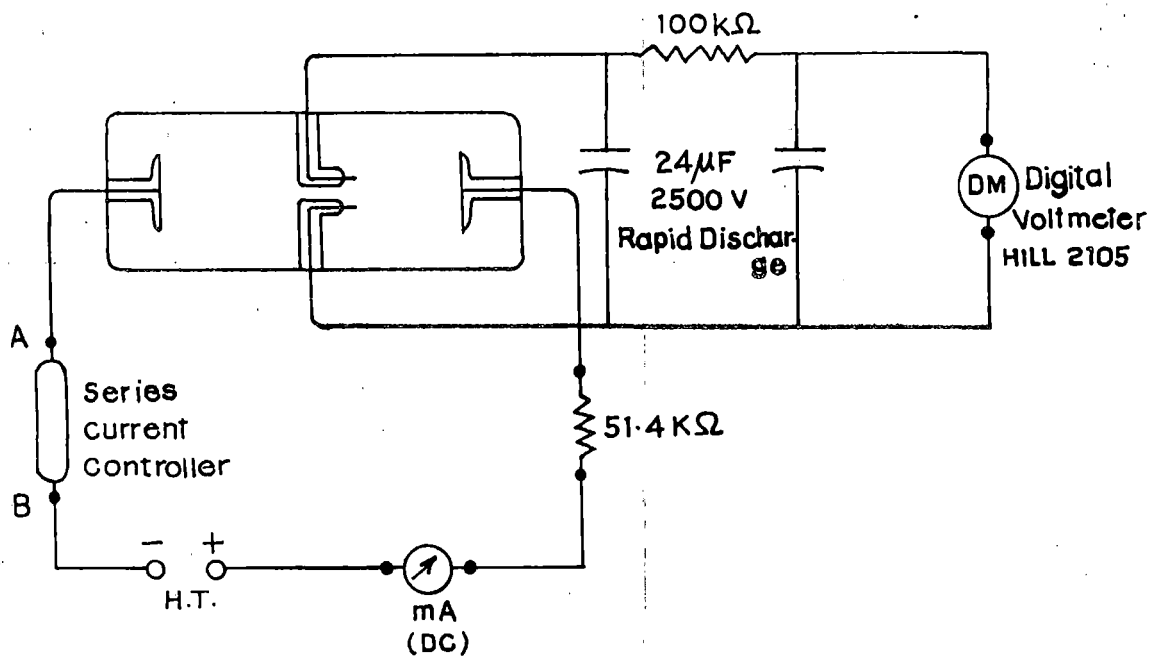


Fig. 2. CKT. Diffusion voltage Measurement

Fig. 2-3

one to control the flow of experimental gas into the discharge tube. When pressure and temperature of the system come to equilibrium after some time of operation of the discharge, the reading can be recorded. The complete block diagram of the discharge system is shown in Fig. 2.3.

2.1.10. The diffusion voltage is related to the electron temperature (Sen, Ghosh and Ghosh, 1983) by relation

$$\frac{k T_e}{e} = \frac{V_R}{\log \left[ J_0 \left( 2.405 \frac{r}{R} \right) \right]} \quad (2.1)$$

where  $V_R$  is the diffusion voltage, and  $T_e$  is the electron temperature,  $r$  is the distance between the probes,  $R$  is the tube radius,  $J_0$  is the zeroth order Bessel's function,  $k$  is the Boltzman constant and  $e$  is the electronic charge.

Thus in this system we are able to measure electron temperature from the measurement of diffusion voltage with different pressure and discharge current ( $i_D$ ). Since  $T_e$ ,  $i_D$  and collision loss factor  $K$  is related with  $E/p$  as shown in the theory developed in the present work, we can measure mean collision loss factor for the electrons.

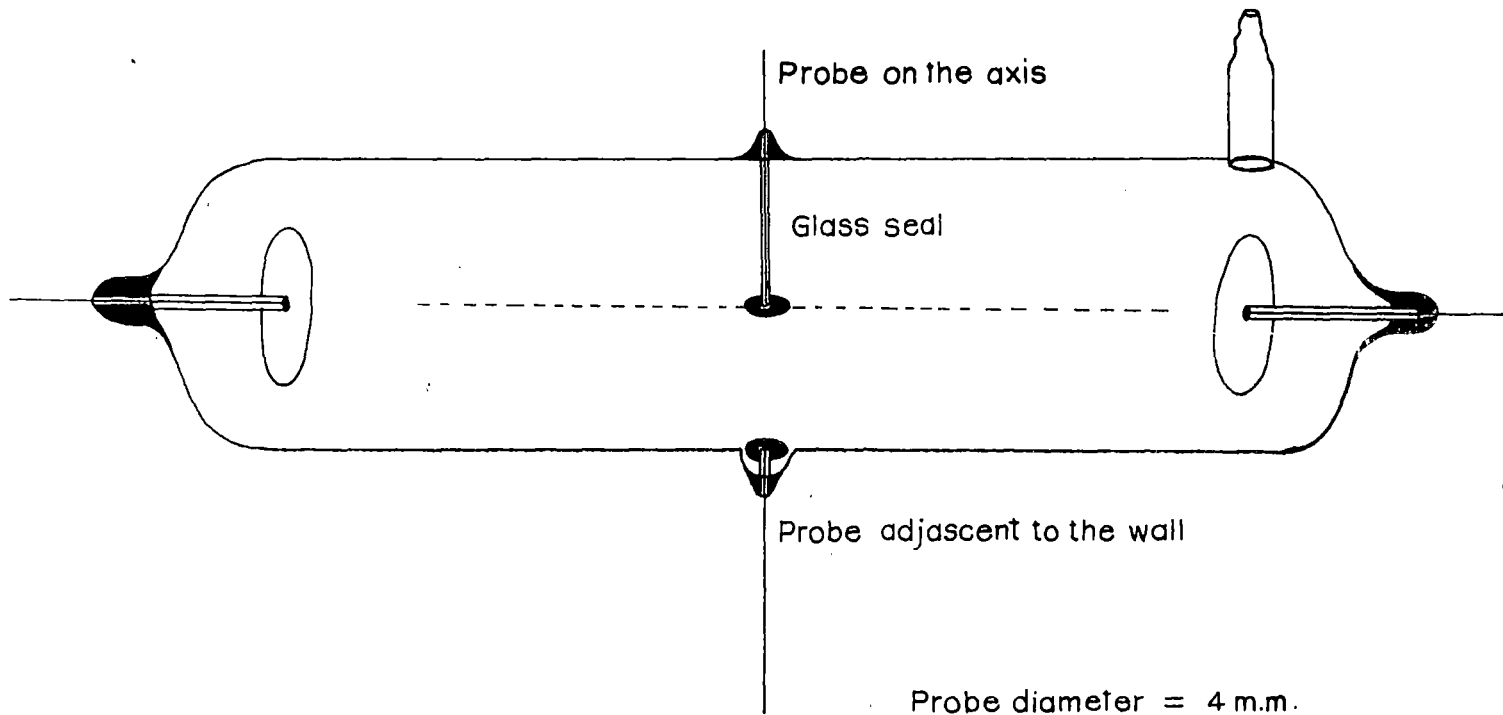
2.2. Hall voltage and diffusion voltage in transverse magnetic field in case of a low density discharge plasma.

Apparatus and Accessories: (1) Glow discharge tube for the measurement diffusion voltage as well as Hall voltage with the same pair of probes. (2) Voltmeter (3) Magnet power supply

(4) Electromagnet (5) High voltage power supply (6) Current meter (7) McLoyd Gauge (8) Pirani Gauge. (9) R-C filter (10) Needle valve (11) Double stage Rotary Pump (12) Air Purification arrangement.

2.2.1. The discharge tube in this case has the same design except for the probes which, in this discharge tube, are two thin circular brass plates connected face to face parallel to each other, one along the axis while the other at the periphery of the discharge tube. The connecting tungsten rods are sealed with thin glass coating. Thus the electrodes form the same configuration as the circular parallel plate condenser, besides the fact that the medium inside is a partially conducting medium. Thus the probes including the partially conducting medium inside forms a semi-metal and hence under the influence of magnetic field in a direction transverse to the direction of discharge current through the space between the probes must result in the appearance of Hall voltage, which means the separation of charges in the plasma which has a strong tendency against the formation of any such charge separation. So there must be strong diffusion under this circumstances which will try to resist the Hall voltage. So these two voltages should act opposit to each other under such arrangement and condition.

Also it has been shown in the theory that under the placement of the probes as stated, i.e., one on the axis and other at the periphery of the discharge tube, there will be no initial diffusion voltage between the probes. Thus such a design of the



Probe diameter = 4 m.m.  
 Electrode diameter = 2.0 c.m.  
 Discharge tube diameter = 2.4 c.m.  
 Probes' separation = 1.2 c.m.  
 Electrodes' separations = 6 c.m.  
 Tube length = 12 c.m.

Fig. 2.4.

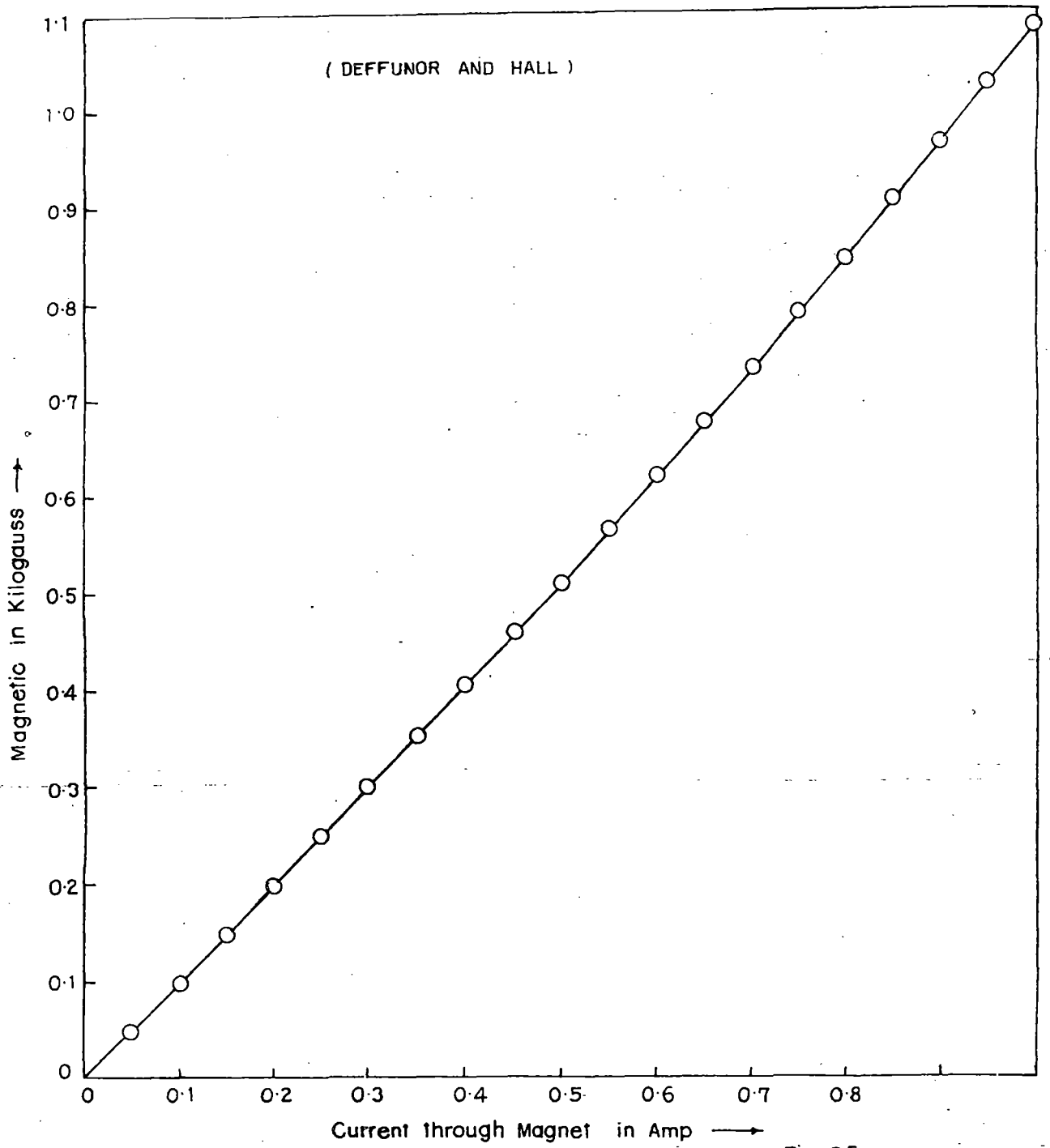


Fig. 25

discharge tube will enable one to measure Hall voltage in combination with the diffusion voltage in presence of transverse magnetic field. The diagram of the discharge tube is shown in Fig. 2-4.

2.2.2. The electromagnet is calibrated with the help of a Hall probe electronic gauss meter. The result of calibration is shown in the table 2a and Fig. 2.5 .

Table 2a

Current through the magnet in Amp	Magnetic field in K.Gauss		Mean Magnetic field in Kilo Gauss
	When current in one direction	When current in reversed direction	
0	0	0	0
0.05	0.05	0.05	0.05
0.10	0.10	0.10	0.10
0.15	0.15	0.15	0.15
0.20	0.20	0.20	0.20
0.25	0.25	0.25	0.25
0.30	0.30	0.30	0.30
0.35	0.36	0.35	0.355
0.40	0.41	0.40	0.405
0.45	0.46	0.46	0.46
0.50	0.51	0.51	0.51
0.55	0.56	0.57	0.565
0.60	0.62	0.62	0.62
0.65	0.67	0.68	0.675
0.70	0.73	0.73	0.73
0.75	0.79	0.79	0.79
0.80	0.85	0.84	0.845
0.85	0.90	0.91	0.905
0.90	0.97	0.96	0.965
0.95	1.02	1.03	1.025
1.00	1.08	1.09	1.085

### 2.2.3. Magnet power supply is a constant current power source.

This enables one to keep the current through the magnet at a constant value and hence the magnetic field across the discharge tube for the time until the system comes to thermal equilibrium with new arrangement of distribution of current.

The voltmeter is a digital voltmeter which can measure floating voltage without interaction with the main discharge system.

The current meter in this case is required to be sensitive since there is a change in discharge current with magnetic field even if the supply voltage and other impedences in the circuit remain same. In this experiment, "Sett & Dey" current meter has been used.

McLloyd gauge, Pirani gauge, R-C filter and High voltage power supply are same as described in 2.1.

### 2.3. Cathode fall measurement in a metal arc for different pressure and discharge current.

Apparatus and Accessories: (1) Discharge tube with movable electrode arrangement (2) Water cooling system for discharge tube (3) 350 volt power supply (4) Series current controller (5) Ammeter (6) Voltmeter (7) Two needle valves (8) Mercury Manometer for measurement of pressure from a few mm of Hg to 76 cm of Hg pressure (9) Double stage rotary Pump.

2.3.1 The discharge tube for the measurement of cathode fall at various pressure needs to have arrangement for the adjustment of electrode separation from outside the discharge tube. So at the two ends of the discharge tube there are two B34 standard joint socket. B34 inner counterpart forms the lid of the discharge tube. A pair of tungsten rods are sealed with each of the lids. The tungsten rods help electrical connection from out to within the tube. In addition, each pair of tungsten rods on each lid can support an electrode holder. The electrode holder each on the other open end has inside thread which allows the fitting of the experimental electrodes tightly and which at their one end has outer thread which fits well into the thread of the electrode holder. One of the electrode holder is formed of two parts connected by screw system. One part is fixed with a pair of tungsten fused on one lid while the other part passes through a socket which allows the electrode pass through it but prevents any rotation of the electrode. As a result, when the corresponding lid of the discharge tube is manually rotated from outside the electrode moves forward or backward. To record the amount of displacement of the electrode, the lid is connected with a large "protractor" which has 360 degree uniform graduation. The "protractor" is again connected with another screw through gear system, such that the screw moves parallel to a linear scale when the circular scale is rotated. Screw pitch for the electrode screw and the outer screw are same. So just like screw gauge one can read the displacement of the electrode

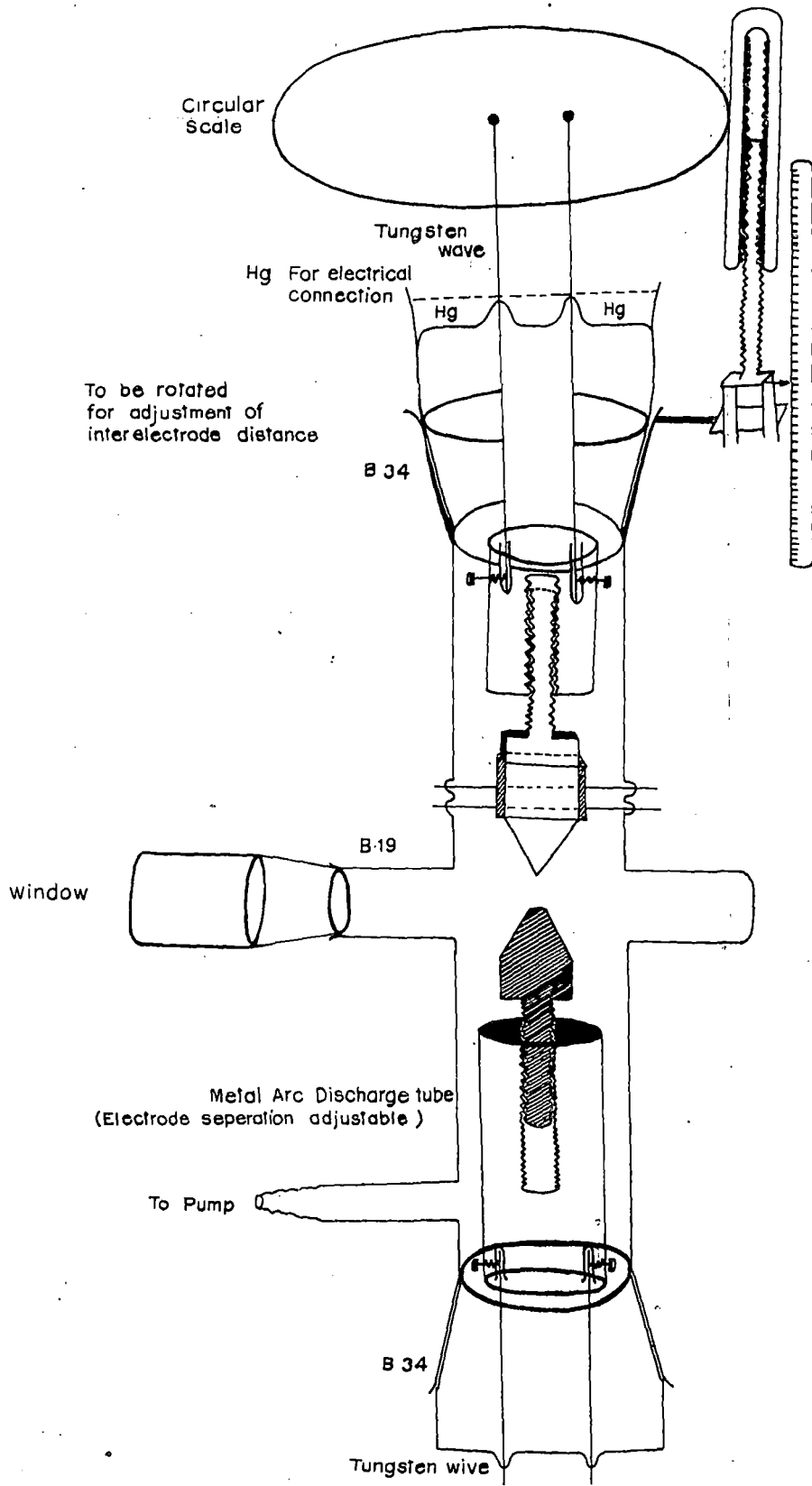
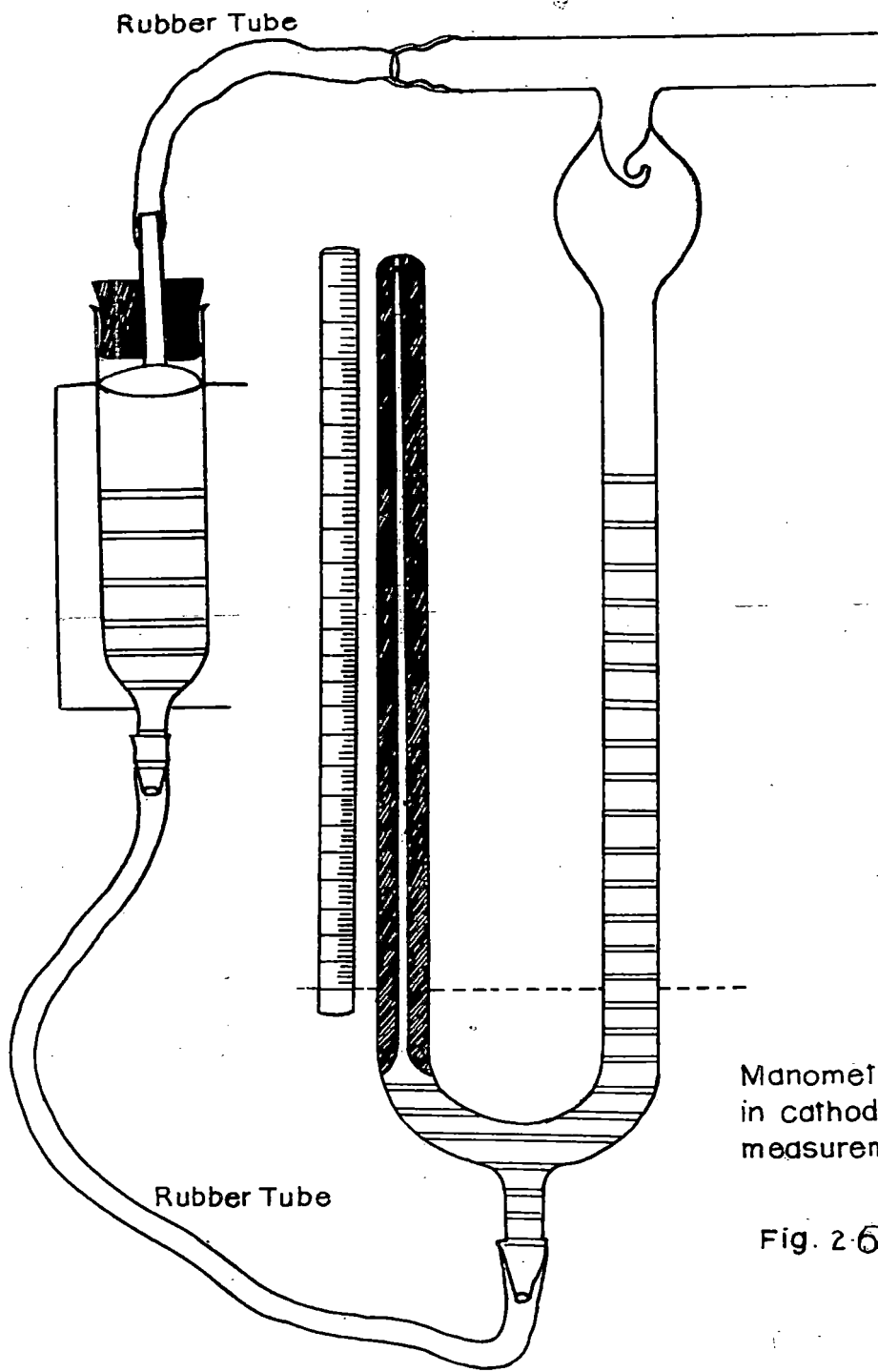


Fig. 2-7.



Manometer used  
in cathod Fall  
measurement

Fig. 2.6.

by taking the circular scale reading and linear scale reading. The discharge tube is shown in Fig. 2.7.

2.3.2 The manometer is about 80 cm long and made of capillary tube of 1.5 mm diameter. Its one end is sealed and space above mercury is perfectly vacuum. The inside of the manometer is cleaned with chromic acid and then with caustic soda and finally with distilled water. Then highly distilled mercury is poured inside the manometer. The bottom of the manometer has opening which is connected with the lower end of a large container by a rubber tube. The upper end of the container is connected to the open limb of the manometer with another rubber tube. The container can be moved up and down so that the mercury level inside the open limb, which is in the same level as in the container, can be adjusted. A linear scale is fitted parallel to the closed limb. The scale reads gradually higher from the bottom to the top. Thus when the mercury level in the open limb is brought to a particular mark, the mercury level in the closed limb directly reads the pressure inside the discharge tube which is also connected with the open limb of the manometer. The Manometer is shown in the Fig. 2.6.

2.3.3 Constant current controller is designed with several power transistors in parallel such that the current capacity reaches the desired current level. The voltage tolerance of the controller is 90 volt. So it is set at 45 volt at the required

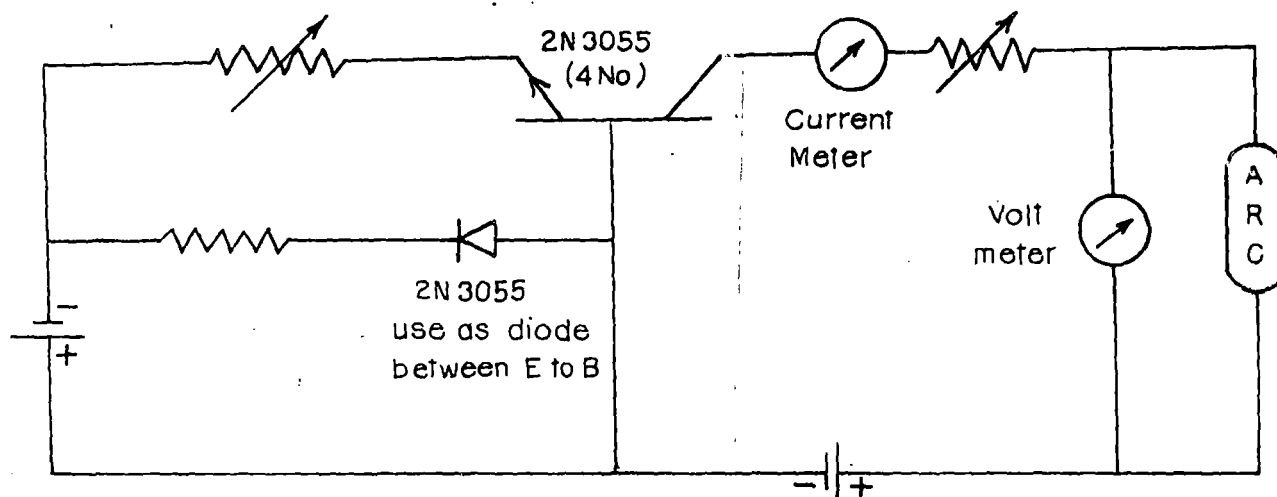


Fig. 2-8. : Series current controller used in arc circuit

discharge current. So, any voltage fluctuation or impedance fluctuation in the arc will be compensated upto  $\pm 45$  volt at the same discharge current level. The circuit diagram is shown in Fig. 2.8.

2.3.4 Digital voltmeter is used to record the burning voltage of the arc for electrode separation varying from 0 to several mm.

2.3.5 Due to intense heating in the arc in addition to the electrodes, the glass container may undergo some cracks unless some efficient cooling is provided. So the discharge tube is dipped upto its neck in water which runs through another container. Thus the life of the discharge tube is much lengthened.

2.3.6 The experiment is performed upto a pressure of one atmosphere, so to maintain the pressure inside the discharge tube with a double stage rotary pump two needle valves are required. One needle valve is connected just after the pump, so that the pump cannot draw much gas from the system and another needle valve is connected with the discharge tube which allows the desired gas to enter the system through its leak. Thus the pressure inside the system can be increased either by increasing the leak of the needle valve with the discharge tube or by decreasing the leak size of the needle valve close to the pump. And the pressure inside the discharge tube can be reduced by decreasing the leak size of the needle valve which allows

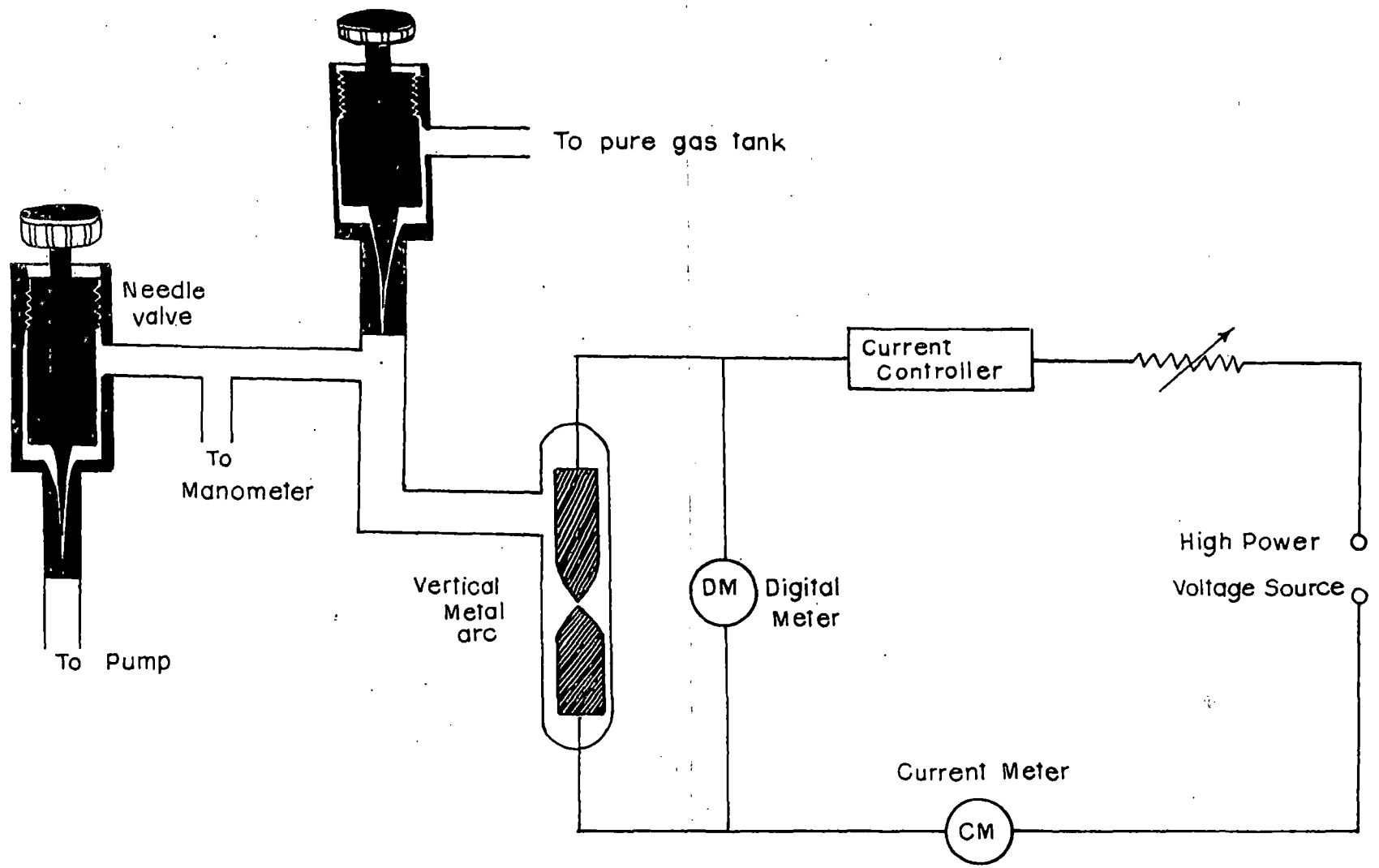
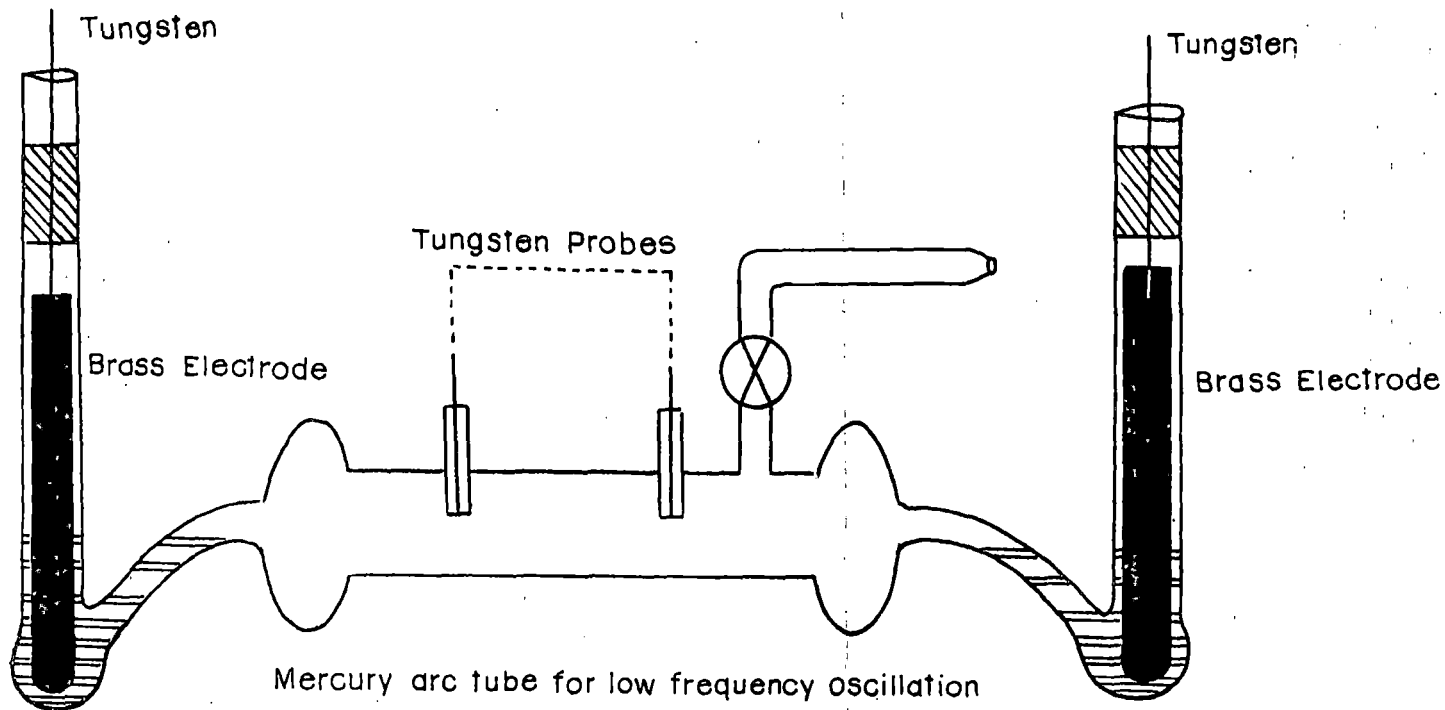


Fig. 2-9 : Fall voltage measurement (Metal Arc)

gas into the discharge tube system and also by increasing the leak size of the needle valve close to the pump. Thus with the help of two needle valves and a rotary suction pump any desired pressure not exceeding atmospheric pressure can be maintained inside the discharge tube. The needle valves are adjusted in such a way that the rate at which the experimental gas enters the system is extremely low irrespective of the pressure inside the system. If this condition is not achieved, there may be a shortage of purified gas in the supply gas tank. The arrangement is shown in Fig. 2.9.

2.3.7 The cathode fall in an arc is determined by plotting the graph of arc burning voltage with electrode separation. [Sen, Gantait and Jana (1988)] Because of corrosion of the electrode surface, the measurement of the correct inter-electrode separation is difficult. So every time the electrode surface is to be rubbed to have a plane surface. And the reading has to be taken repeatedly and at a considerable swiftness. Particularly when the interelectrode distance becomes less than a millimeter, the arc is suddenly shorted because of the dense vapour and high temperature close to the cathode. Thus every set of experiment is required to be repeated to check the correct and repeatable results. Block diagram for the whole circuit and accessories is shown in Fig. 2.9.



Tube length 30 cm.  
 Tube Diameter 1.8 cm.  
 Brass electrode diameter 0.8 cm.  
 Brass electrode length 0.5 cm.

Fig. 2.10.

## 2.4 Low frequency oscillation in a Mercury arc Plasma.

Apparatus and Accessories: (1) Mercury arc discharge tube (2) CRO (3) Digital frequency meter (4) Variable inductance tank circuit (5) Voltmeter (6) Current meter (7) One needle valve (8) McLoyd Gauge (9) Pirani gauge (10) Power supply (11) Double stage rotary pump (12) Cooling arrangement (13) Thermometer (14) Magnet Power Supply (15) Electromagnet (16) Gas supply system (17) RF choke.

2.4.1 The arc tube is a conventional mercury arc tube of high length (about 30 cm, end to end) and 1.8 cm diameter with one difference that the electrical connection between the mercury inside and outside of discharge tube uses two thick (diameter 0.8 cm) and long brass electrodes in between the tungsten rod and the mercury at both ends of the discharge tube. If in place of such thick and long electrodes we use only tungsten rods (diameter 1 mm) for electrical connection, it appears in case of study of oscillation that the rod undergoes some physical change with time and after some hour of study of oscillation sometime a red spot starts forming frequently somewhere along the length of the tungsten rod and when such spot is formed the arc undergoes immediate extinction. And thus to remove such trouble we have introduced the above mentioned thick and long rods in between the tungsten and Mercury. The whole diagram is shown in Fig. 2.10

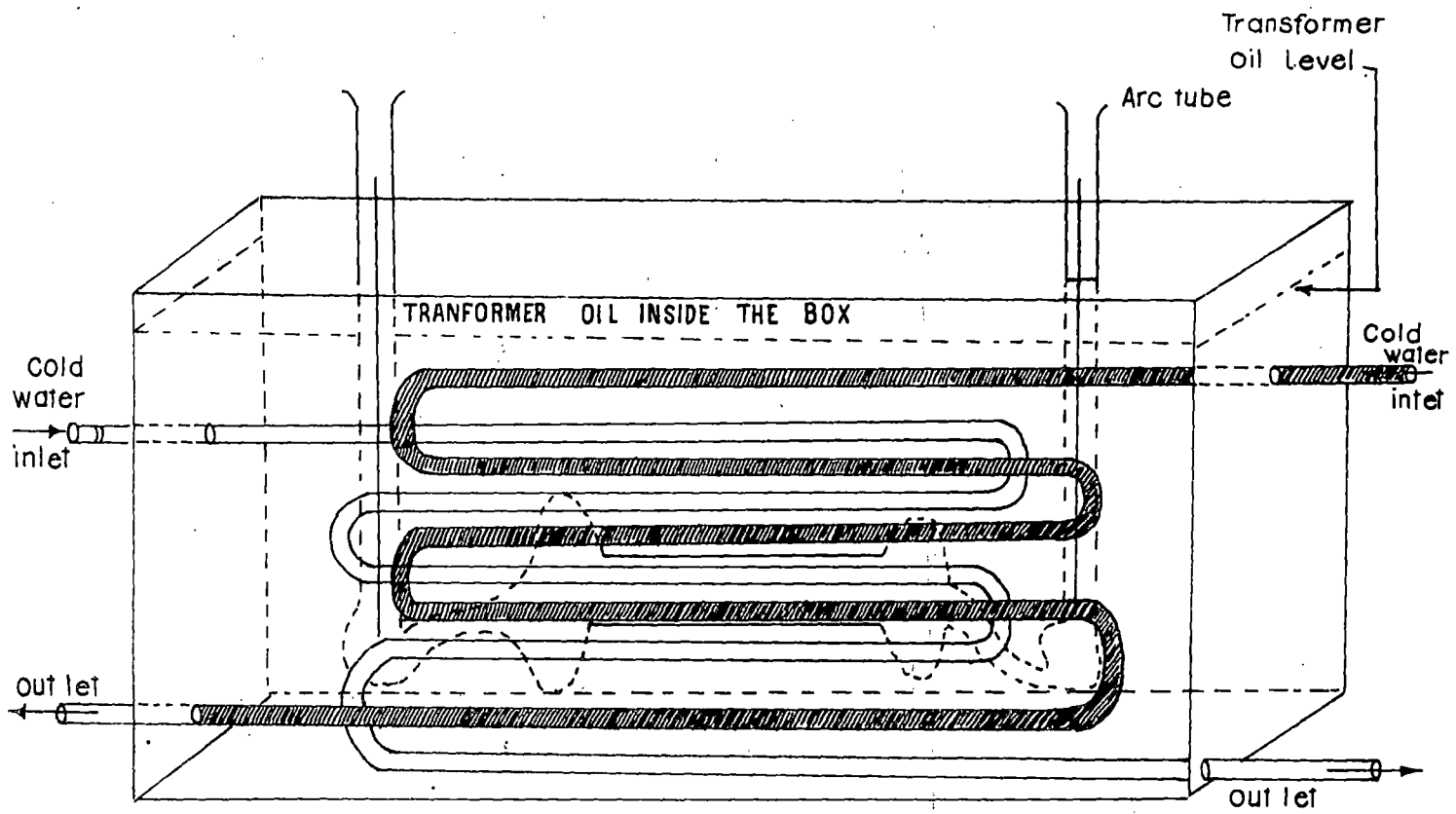


Fig. 2-11. Oil cooling box for Hg - Arc.

2.4.2 To study such a low frequency oscillation the arc tube is to be operated for large time until the tube is perfectly conditioned. This will make the characteristic of the arc to be stable and the tube will operate at a particular operating point on its characteristics curve and hence frequency and amplitude of oscillation will be stable, which is a fundamental utility of any oscillator. But such a long time operation with a perfect thermal equilibrium is very difficult for arcs which consumes high power resulting in either instability in thermal equilibrium or fracture of the tube. So an oil cooling arrangement is provided. This cooling system utilises transformer oil inside a metallic box which contains two array of thin walled copper tubes through which cold water is continuously allowed to pass. In between these two array of pipes inside the oil, the discharge tube is dipped. In this system the arc can be made to run for long time with perfect thermal equilibrium of the discharge tube with surrounding transformer oil. The temperature of the oil in the present case is about  $55^{\circ}\text{C}$ . The diagram of this cooler is shown in Fig. 2.11.

2.4.3 The tank circuit in parallel to the discharge tube utilises one variable air core choke and a  $4 \mu\text{F}$  condenser and a variable resistance. It was initially intended to construct a negative resistance oscillator, but it did not really occur as per the plan. Reason behind this is probably embedded in the discharge tube. The theory suggests, in this case, that the d.c.

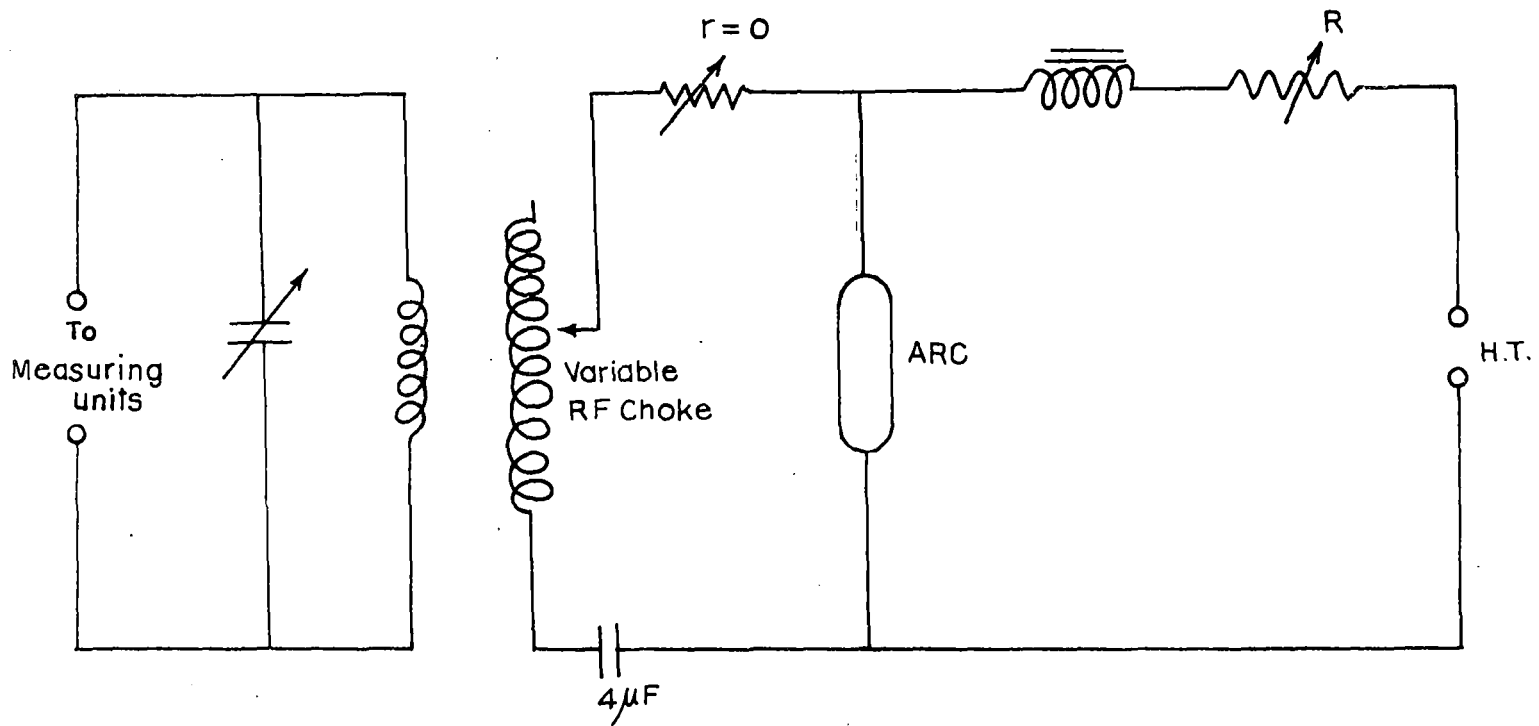


Fig.2-12. Circuit for study of oscillation .

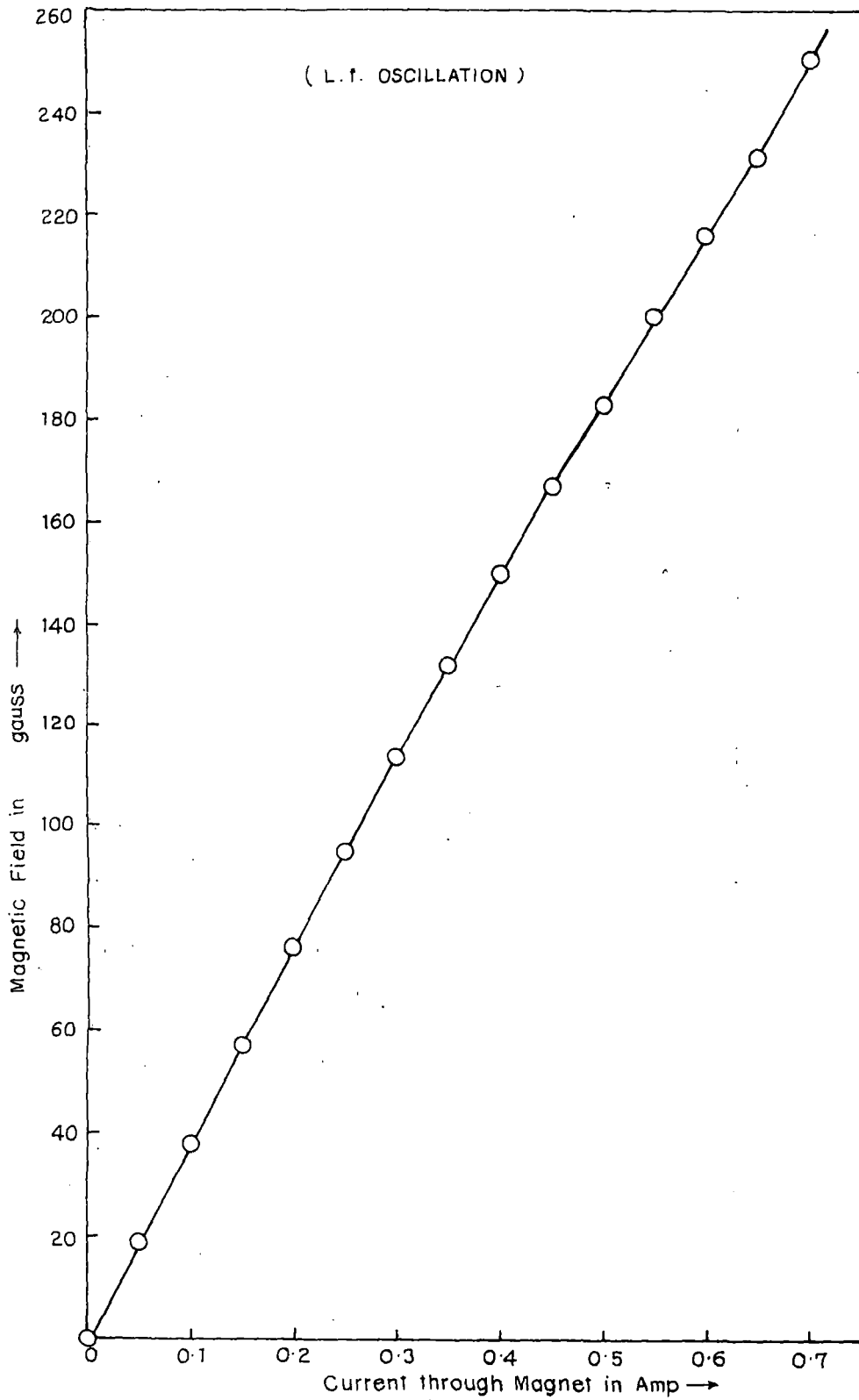


Fig. 2-13.

resistance and a.c. resistance both work in series in case of oscillation, unlike the case of the dynatron oscillator where only a.c. resistance works behind the oscillation. However, the resistance is found to be coupled and the sum of these two resistance for the present discharge tube is positive. So negative resistance oscillator could not be constructed.

On the other hand, it is found that a low frequency a.c. appears in the tank circuit whose frequency does not change with change in the value of inductance and the amplitude becomes maximum when the resistance that is inserted in the tank circuit is reduced to zero. The higher value of condenser increases the amplitude of the ac in the circuit without any change in frequency. These observation suggests that the ac is self generated inside the tube. Complete circuit diagram is shown in Fig. 2.12. The ac is picked up by loosely coupled secondary coil used in the measurement of amplitude and frequency.

2.4.4 The transverse magnetic field applied to mercury arc column is supplied by an electromagnet. The calibration data is shown in table "2b" and the curve in Fig. 2.13.

Table 2b

Magnet current in Amp	Magnetic field in Gauss		Mean Magnetic field in Gauss
	When current in one direction	When current in reversed direction	
0	0	0	0
0.05	19	19	19
0.10	38	38	38
0.15	57	57	57
0.20	76	76	76
0.25	95	95	95
0.30	114	114	114
0.35	132	132	132
0.40	150	150	150
0.45	167	167	167
0.50	183	182	182.5
0.55	200	200	200
0.60	216	216	216
0.65	332	231	231.5
0.70	250	251	250.5
0.75	265	265	265

2.4.5 The voltmeter in such experiment is required to be capable of measuring fraction of a volt correctly. Because the oscillation builds up only within a very small range of discharge current and to measure the correct value of ac resistance, within a small discharge current limit, the fraction of a voltage change in arc burning voltage must be recorded properly. The situation with change of magnetic field is more critical because the arc undergoes extinction for a magnetic

field of the order of 150 gauss only as soon as the oscillation is allowed to develop in the LCR circuit parallel to the arc. So to know the ac resistance for a magnetic field not exceeding 150 gauss for which arc burning voltage changes only a few volt which is only 4 to 5 percent of the total arc burning voltage. So we have used a digital voltmeter which is capable of recording change in voltage in the second decimal place.

2.4.6 The characteristic curve in presence of transverse magnetic field is to be drawn to know the value of ac resistance, for a particular value of initial discharge current and different value of magnetic field applied to the arc. By the initial discharge current we mean the discharge current in absence of magnetic field. For this initial discharge current we gradually change the value of transverse magnetic field and go on recording the value of discharge currents and arc burning voltages for different value of magnetic fields. Thus we get a new characteristic curve for the arc with various transverse magnetic field. The initial discharge current for this new characteristic curve becomes a parameter which should remain essentially constant when the data for the new curve with transverse magnetic field is recorded. Most interesting fact is that sum of the ac and dc resistances for  $H = 0$  and for  $H \rightarrow 0$  are found to have fairly different values.

2.4.7 Change in frequency with change in pressure of discharge current or magnetic field is not more than a few percent. So a digital frequency meter will enable one to record such a small change in frequency. Such a record of frequency is essential to verify the theory which predicts that,

$$f = \frac{1}{\pi(r_{ac} + r_{dc})C}$$

i.e., the frequency is directly proportional to the inverse of the sum of the ac and dc resistances, which change a little for change in either of the factors like pressure, discharge current and magnetic field.

2.4.8 A CRO is used for visual observation and record of the amplitude of the ac developed. Photograph is also taken from the CRO screen for analysis and measurement of ac amplitude.

2.4.9 Pure air is prepared as described in 2.1 and allowed to enter the system through the needle valve. The pressure is measured with McLoyd Gauge and Pirani Gauge as described in 2.1.

CHAPTER III

ENERGY LOSS MECHANISM IN A COLLISION  
DOMINATED PLASMA

## CHAPTER - III

## ENERGY LOSS MECHANISM IN A COLLISION DOMINATED PLASMA

INTRODUCTION

The loss of energy by electrons when moving through an ionised gas has been investigated by Von Engel (1964) and also by Massy, Burhop and Gilbody (1971). It can be shown that when only elastic losses are taken into consideration the loss factor,  $K = \frac{4m}{M}$ , where  $m$  is the mass of the electron and  $M$  is the mass of the atom or molecule with which the electron is colliding. The loss of energy by electrons is mainly due to collision in an ionised gas and we can neglect the energy lost by ions as they are less mobile. It has further been shown that  $K$ , the loss factor, increases (not always linearly) with  $(E/P)$  where  $E$  is the electric field and  $P$  is the pressure and at higher  $(E/P)$  values inelastic losses set in. The purpose of the present investigation is to present a generalised theory regarding the loss of energy by electrons in an ionised gas taking into consideration the variation of  $K$  with  $(E/P)$  and thereby deduce an expression for the main discharge current in a collision dominated plasma. In the course of our deduction some plasma parameters have naturally been introduced and it is also the object to verify the theory from experimental results. Besides other parameters, experimental determination of  $T_e$  the electron temperature is necessary for a wide range of  $(E/P)$  values.

### EXPERIMENTAL ARRANGEMENT

The detailed experimental technique for the evaluation of electron temperature by measurement of diffusion voltage has been provided in earlier papers (Sen, Ghosh and Ghosh, 1983; Sen, Acharyya, Gantait and Bhattacharjee, 1989) where it is shown that

$$\frac{kT_e}{e} = \frac{V_R}{\log J_0 \left( 2.405 \frac{r}{R} \right)} \quad (3.1)$$

where  $V_R$  is the diffusion voltage,  $R$  is the radius of the discharge tube and  $r$  is the distance of the probe from the axis of the discharge tube. The discharge tube having inner diameter 2.8 cm and length 10 cm is fitted with two parallel circular brass electrodes (diameter 1.2 cm) and separated by a distance of 6 cm. The back sides of the electrodes were perfectly sealed with glass and teflon caps. Two probes one along the axis and the other away from the axis were placed parallel to each other and were separated by a distance of 5 mm. Both the probes made of the tungsten wire (0.2 mm diameter) were sealed within glass except at the ends, the schematic diagram is shown in Fig. (2.1). Fig. (2.3) represents the circuit diagram which consists of a high voltage power supply with a limiter resistance (51.4 k $\Omega$ ) and one current controller (Fig. 2.2) in series with the discharge tube. The diffusion voltage at the probes was measured by means of a digital voltmeter (HILL 205) whose input impedance is greater

than 10 M $\Omega$ . An R-C filter circuit (RC = 2.4 sec.) was placed parallel to the probes to prevent any fluctuating voltage to appear across the digital voltmeter.

Pressure was measured by a Pirani gauge and adjusted with a needle valve to maintain a constant pressure throughout the experiment. The results are reported here for air ( $T_e$  for E/P upto 800 volts/cm. torr) for hydrogen ( $T_e$  for E/P upto 240 volts/cm. torr) and for nitrogen ( $T_e$  for E/P upto 320 volts/cm. torr). The discharge current has been measured for three pressures  $P = 0.4, 0.3$  and  $0.2$  torr for the corresponding values of (E/P) for the three gases. Pure gas was allowed to enter the discharge tube through the needle valve. Hydrogen and nitrogen were purified and dried with concentrated  $H_2SO_4$  and KOH pellets in succession.

#### THEORETICAL ANALYSIS AND DISCUSSION

The drift velocity of the electron,  $v_d = \frac{eL_e}{m v_r} \left( \frac{E}{P} \right)$  and so the energy gained between successive collisions by a single electron due to drift =  $\frac{1}{2} \cdot \frac{e^2 L_e^2}{m v_r^2} \cdot \frac{E^2}{P^2}$  and as the frequency of collision =  $\frac{v_r P}{L_e}$  the energy gained by the electron per sec. =  $\frac{e^2 L_e}{2 m v_r} \cdot \frac{E^2}{P}$  where  $v_r$  is the random velocity of the electron and  $L_e$  is the mean free path of the electron at a pressure of 1 torr. We consider that the electron starts with zero velocity after collision and reaches the maximum velocity just before collision. When we consider the loss of power by an electron due to collision, we have to

introduce the mean free path of the electron as deduced by Von Engel (1964) which is given by

$$L_e = \frac{12 T_e K^{1/2} k}{\sqrt{2} e (E/p)}$$

So the power lost by one electron per sec. is

$$\frac{e^2}{2 m v_r} \cdot \frac{E^2}{p} \cdot \frac{12 K^{1/2} k T_e}{\sqrt{2} e (E/p)}$$

and as  $\frac{1}{2} m v_r^2 = \frac{3}{2} k T_e$

the power lost by one electron per sec. is  $e E \left[ \frac{6 k T_e K}{m} \right]^{1/2}$

Hence the excess power lost by one electron per sec. due to an increase in  $E$  by  $dE$  is  $e \left[ \frac{6 k T_e K}{m} \right]^{1/2} dE$ . Number of electrons which constitute the current is  $(n_e v_d A)$  each of which spends a time  $d_0/v_d$  in the electric field where  $d_0$  and  $A$  are the inter electrode distance and cross sectional area of the plasma respectively. So the total time spent by these electrons in the electric field is  $n_e d_0 A$ . So the extra loss of energy by  $n_e v_d A$  electrons flowing per sec. is that lost by one electron by collision in time  $n_e d_0 A$  and hence total energy lost by  $n_e v_d A$  electrons flowing per sec. is

$$dW_1 = e \left[ \frac{6 k T_e K}{m} \right]^{1/2} n_e A d_0 dE$$

Again electrical energy lost by  $n_e v_d A$  electrons is  $i E d_0$  where  $i$  is the discharge current and  $E d_0$  is the voltage drop. When  $E$  increases to  $E + dE$  and current changes from  $i$  to  $i + di$  the electrical energy lost by electrons is  $(i + di) (E + dE)$

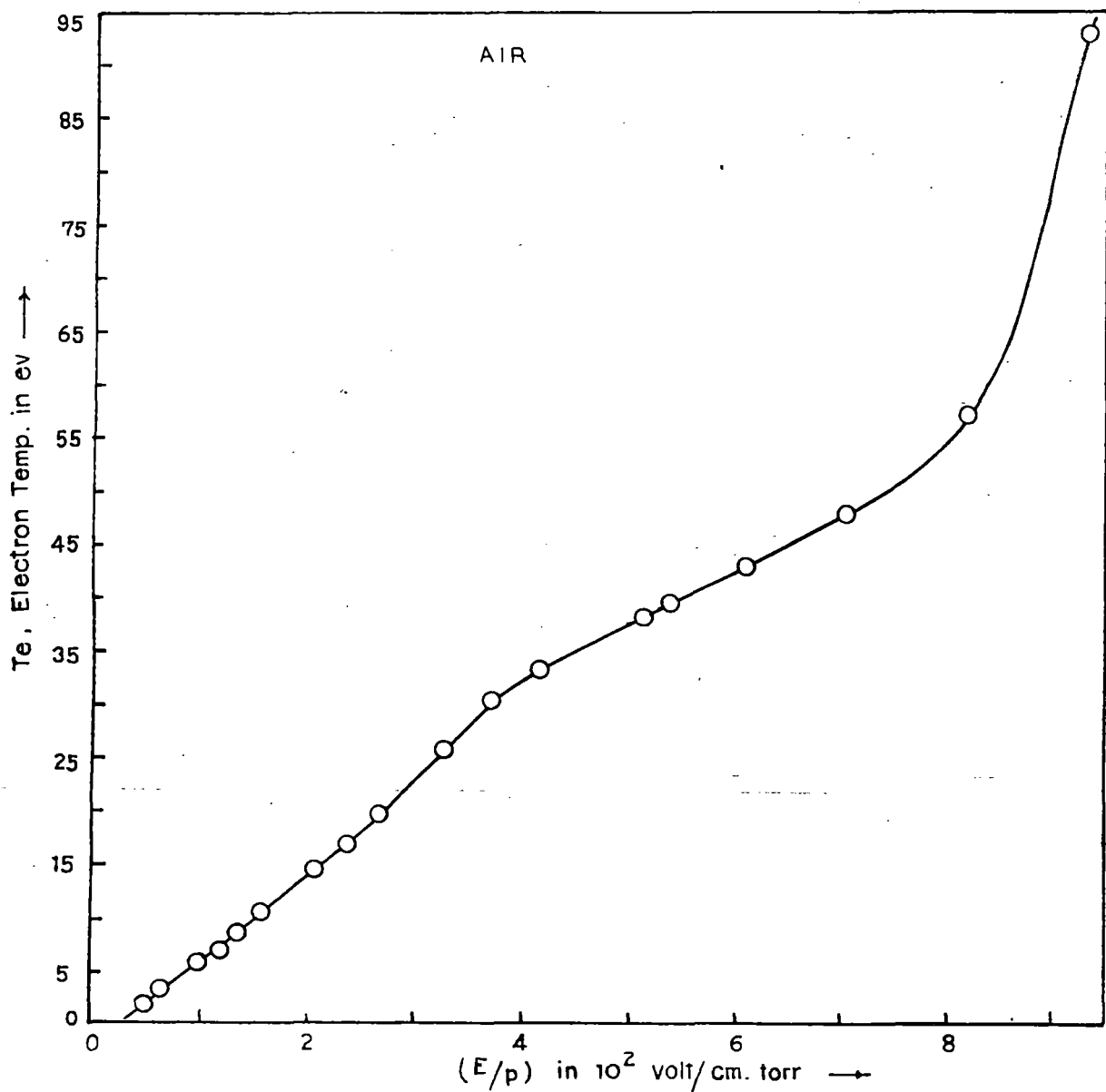


Fig. 3-1.

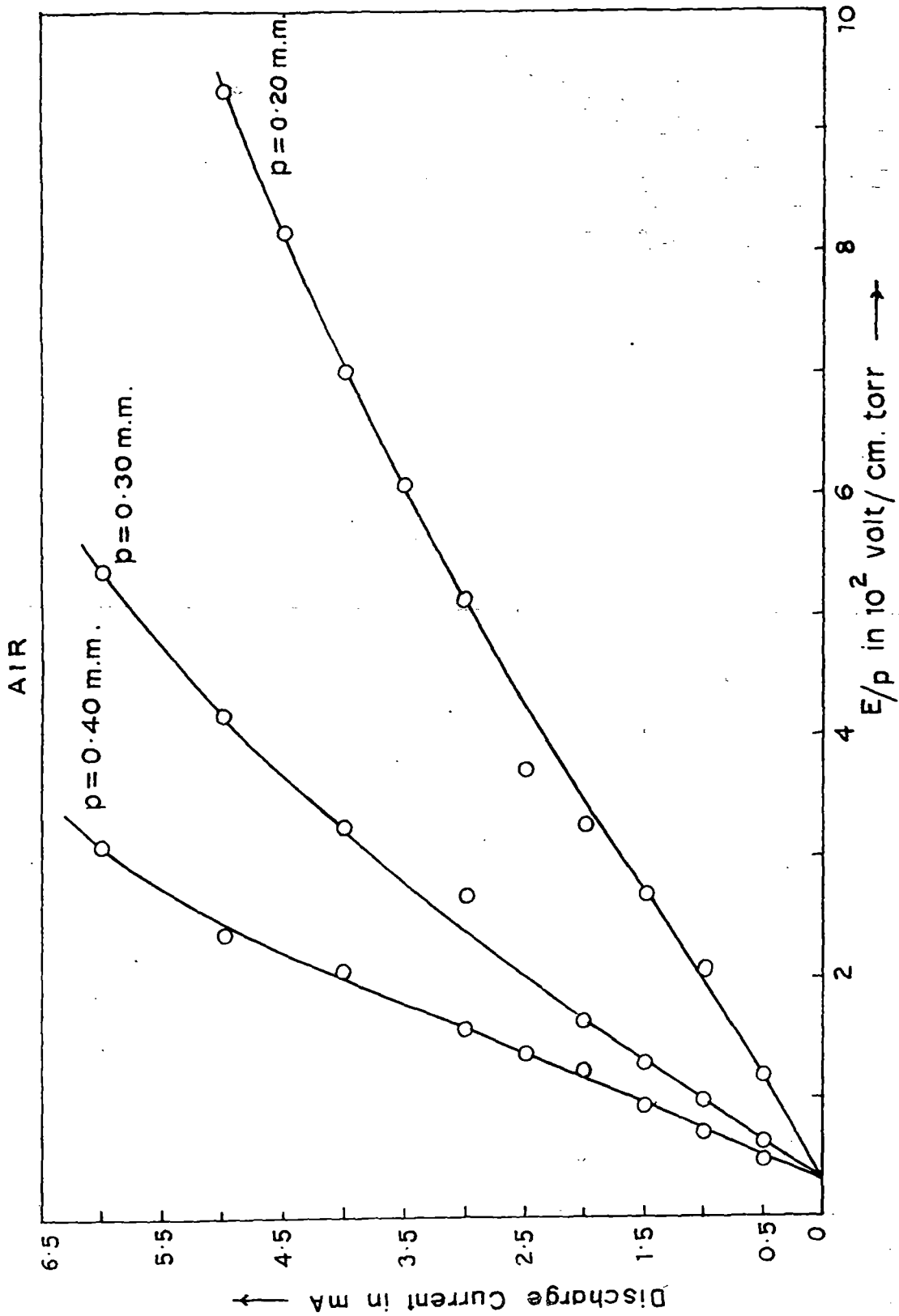


Fig. 3.2.

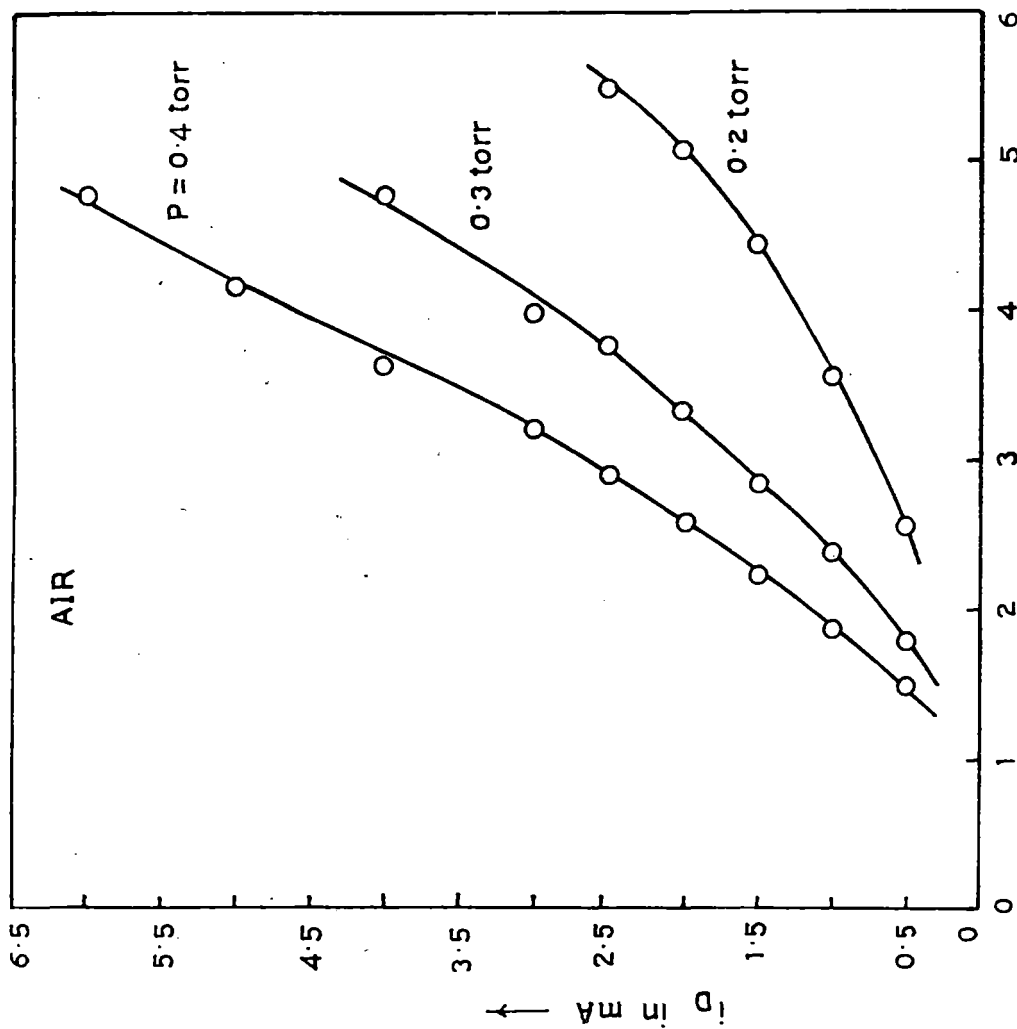


Fig.3.3.

100 200

So the extra power lost by electrons due to increase in  $E$  by  $dE$  is given by

$$\begin{aligned} dW_2 &= (i + di)(E + dE)d_0 - iEd_0 \\ &= (idE + Edi)d_0 \end{aligned}$$

We can consider the energy lost by the electrons due to change of current by  $di$  is the same as the energy lost by the electrons due to collision so we get

$$en_e A d_0 \left[ \frac{6KkT_e}{m} \right]^{1/2} dE = dW_1 = dW_2 = (idE + Edi)d_0$$

For small change in  $E$ ,  $i = \sigma E$  where  $\sigma$  is the conductivity and  $di = \sigma dE$ ,

$$\text{then } idE + Edi = 2\sigma E dE$$

$$en_e A \left[ \frac{6KkT_e}{m} \right]^{1/2} = 2\sigma E$$

$$\text{then } i = \sigma E = en_e A \left[ \frac{3KkT_e}{2m} \right]^{1/2} = i_D \text{ (say)} \quad (3.2)$$

Experimental values of  $T_e$  for different  $(E/P)$  values have been plotted in Fig. (3.1) in case of air. The observed values of discharge current in air, for different  $(E/P)$  values have been plotted in Fig. (3.2). Taking the values of  $T_e$  for different  $(E/P)$  values from Fig. (3.1) the discharge current  $i_D$  has been plotted against  $\sqrt{T_e}$  for three different pressures in Fig. (3.3). According to equation (3.1) the curves should be straight lines but the linearity relation is not maintained between  $i_D$ , the discharge current, and  $\sqrt{T_e}$  as is evident from Fig. (3.3) in

case of air; the variation of  $T_e$  with  $(E/P)$  is shown in Fig. (3.4) for hydrogen, and that for nitrogen in Fig. (3.5). Plot of current  $i_D$  against  $\sqrt{T_e}$  shows that linearity relation between  $i_D$  and  $T_e^{1/2}$  is not maintained in case of hydrogen and nitrogen as well. This is due to the fact that the loss factor  $K$  increases with  $(E/P)$  (Von Engel, 1964) and hence with  $T_e$ ; as  $(E/P)$  increases inelastic collisions increase as is evident from the study of variation of collision cross section with  $(E/P)$ .

Next we proceed to calculate the value of the discharge current by taking into consideration the variation of  $K$  with  $(E/P)$ . We assume that the loss of energy by an electron due to drift when the displacement is  $\lambda_e$  is  $W_e$  and so for drift velocity  $v_d$  the loss per sec is  $W_e v_d / \lambda_e$  and as the frequency of collision is  $v_r / \lambda_e$  so the loss of energy due to drift by one electron per unit collision is  $W_e v_d / v_r$ . So the loss of energy per unit collision by one electron when  $E$  changes to  $(E + dE)$  is  $W_e \left[ \frac{v_d}{v_r} + d \left( \frac{v_d}{v_r} \right) \right]$ . Hence the extra loss of energy per unit collision due to increase in  $E$  by  $dE$  is  $W_e d \left( \frac{v_d}{v_r} \right)$ . But the extra loss of energy is different for plasma of different gases even if  $W_e d \left( \frac{v_d}{v_r} \right)$  is the same. So this must depend on the nature of the gas of the plasma, so the extra true loss is

$$\gamma W_e d \left( \frac{v_d}{v_r} \right) = \gamma W_e d \left\{ \frac{e L_e}{m v_r^2} \cdot \frac{E}{P} \right\}$$

where  $\gamma$  is a constant related to the characteristics of the nature of the gas of the plasma.

So the extra loss is

$$\gamma W_e \frac{eL_e}{3k} d\left(\frac{E}{pT_e}\right)$$

$$= a W_e d\bar{X}$$

$$\text{where } a = \frac{\gamma e L_e}{3k}$$

$$\text{and } \bar{X} = E/pT_e$$

We have further  $W_e = KW$  where  $K$  is the loss factor and  $W$  is the energy of the electron before collision, so the extra energy loss by the electron due to increase in  $E$  to  $E + dE$  is  $KdW - dW_e$  and hence

$$KdW - dW_e = a W_e d\bar{X} \quad (3.3)$$

but as  $K$  is not a constant,

$$dW_e = KdW + WdK \quad (3.4)$$

So from equations (3.3) and (3.4) we get

$$- \frac{WdK}{W_e} = a d\bar{X}$$

$$\text{or } - \frac{dK}{K} = a d\bar{X}$$

$$\text{or } K = e^{-a\bar{X}}$$

where  $l$  is a constant of integration and the above equation shows the variation of  $K$  with  $E/P$  and  $T_e$ .

Let  $K = K_0$  when  $\bar{X} = \bar{X}_0$  [where  $K_0 = \frac{8m}{3M}$ ]

and  $K = 1$  when  $\bar{X} = \bar{X}_m$

where  $\bar{X}_m$  is the minimum value of  $\bar{X}$  when plotted against  $(E/P)$  where  $K$  must be a maximum; since after  $\bar{X}_m$  there is an increase in the value of  $\bar{X}$  with the increase in  $(E/P)$ . Then

$$K_0 = l e^{-a\bar{X}_0}$$

$$l = K_0 e^{a\bar{X}_0}$$

$$\text{and } K = K_0 e^{a(\bar{X}_0 - \bar{X})} \quad \text{-----} \quad (3.5)$$

$$\text{also } 1 = l e^{-a\bar{X}_m} \quad \text{and } l = K_0 e^{a\bar{X}_0}$$

$$\text{so, } e^{a\bar{X}_m} = K_0 e^{a\bar{X}_0}$$

$$\bar{X}_0 = \bar{X}_m - \frac{\log K_0}{a}$$

So from equation (3.2) after putting the value of  $K$  from equation (3.5)

$$i_D = en_e A \sqrt{\frac{3kT_e K_0}{2m}} \cdot e^{\frac{a}{2}(\bar{X}_0 - \bar{X})}$$

$$= \beta n_e T_e^{1/2} e^{\frac{a}{2}(\bar{X}_0 - \bar{X})} \quad \text{-----} \quad (3.6)$$

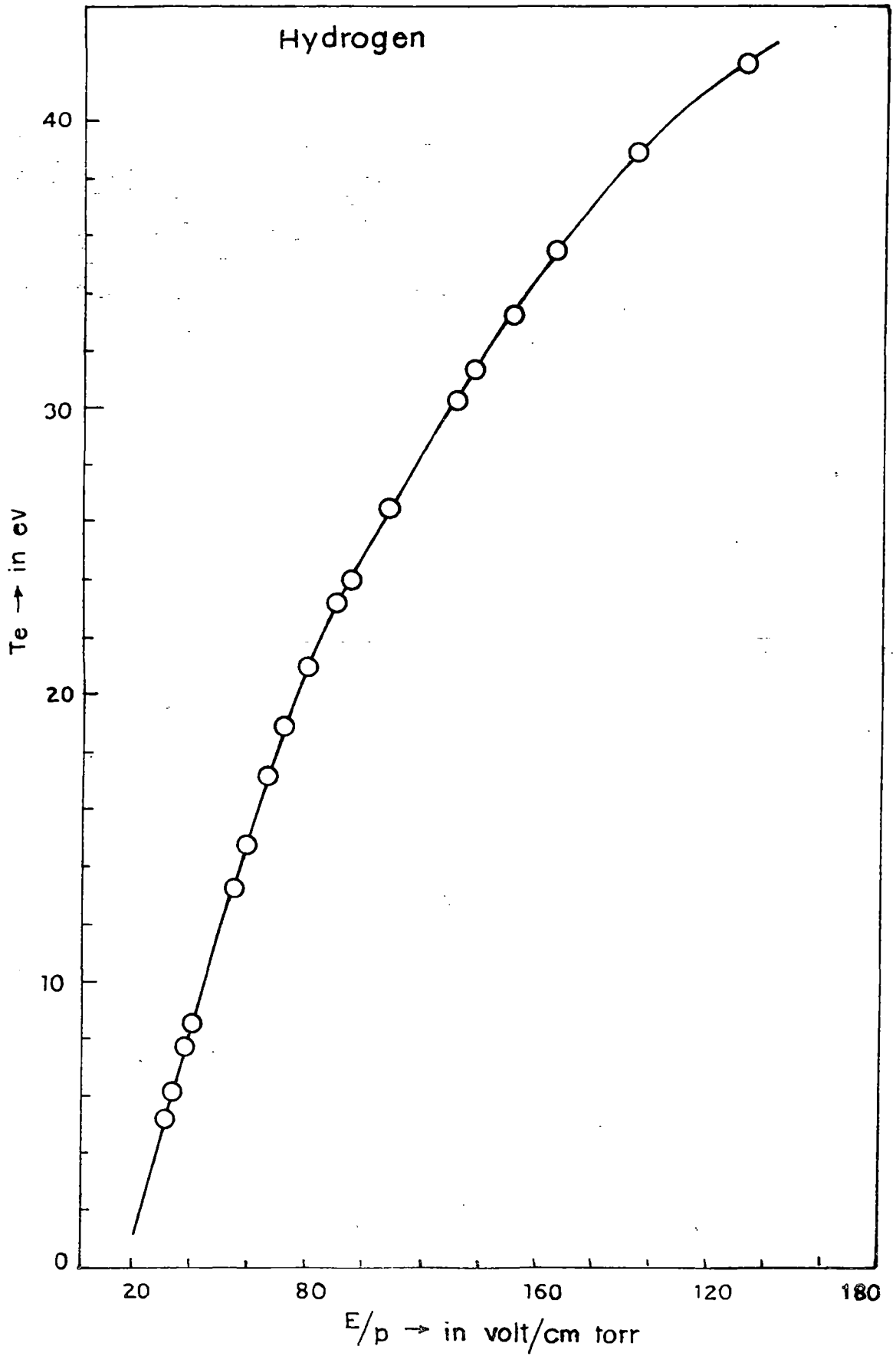


Fig. 3-4.

27 Fig. 3-4

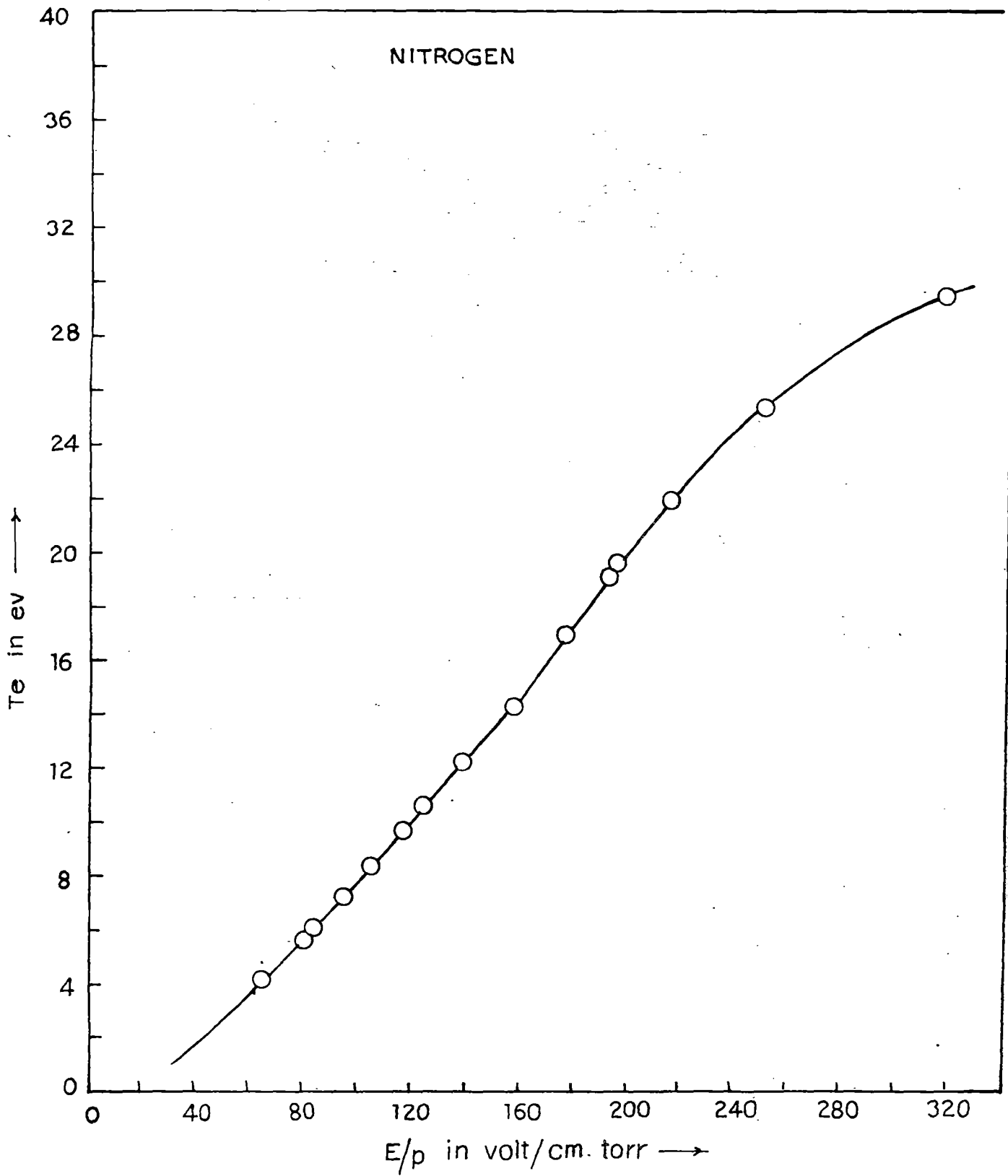


Fig. 3-5.

—  $E/p$  —

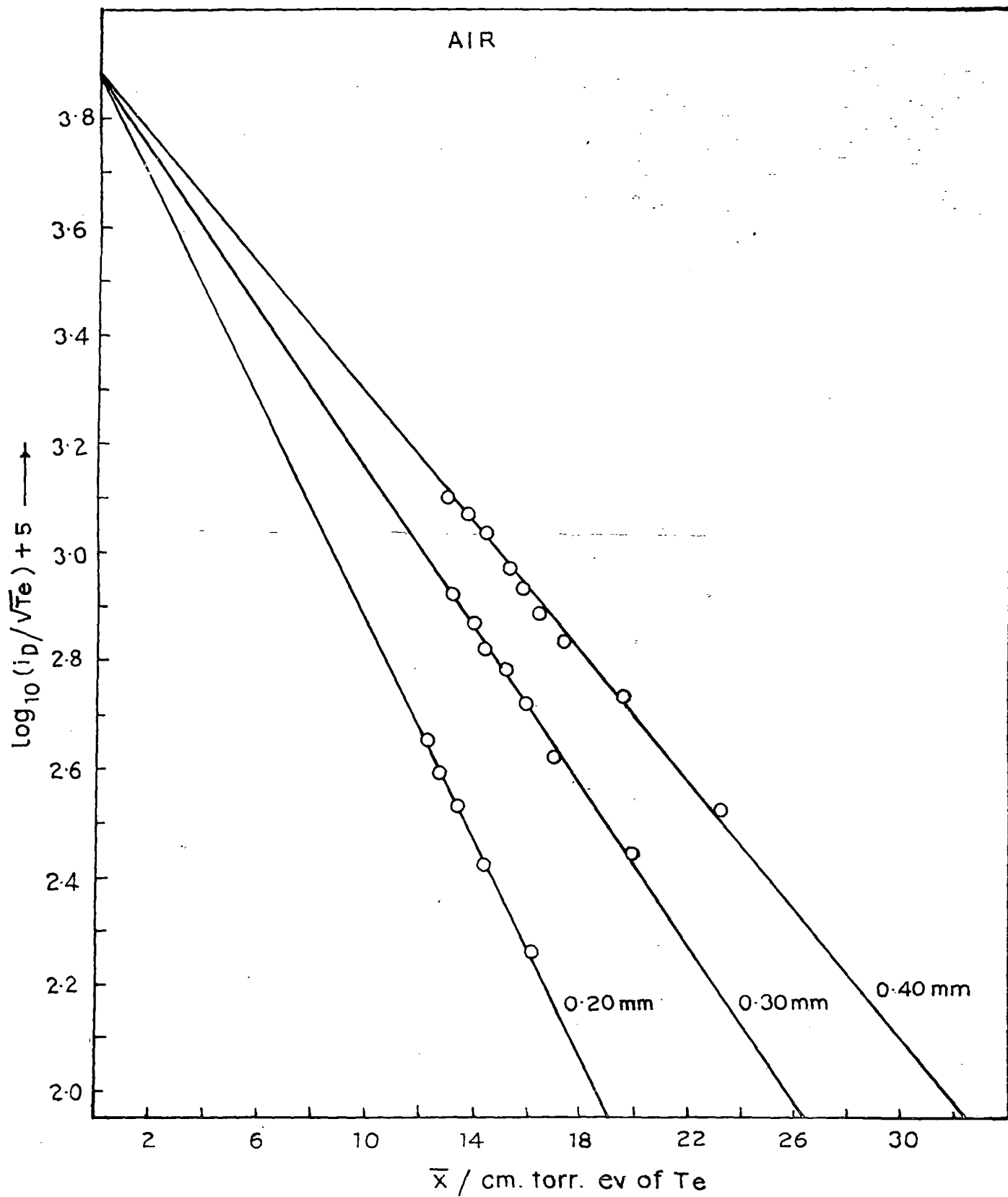


Fig. 3-6.

2-10-55

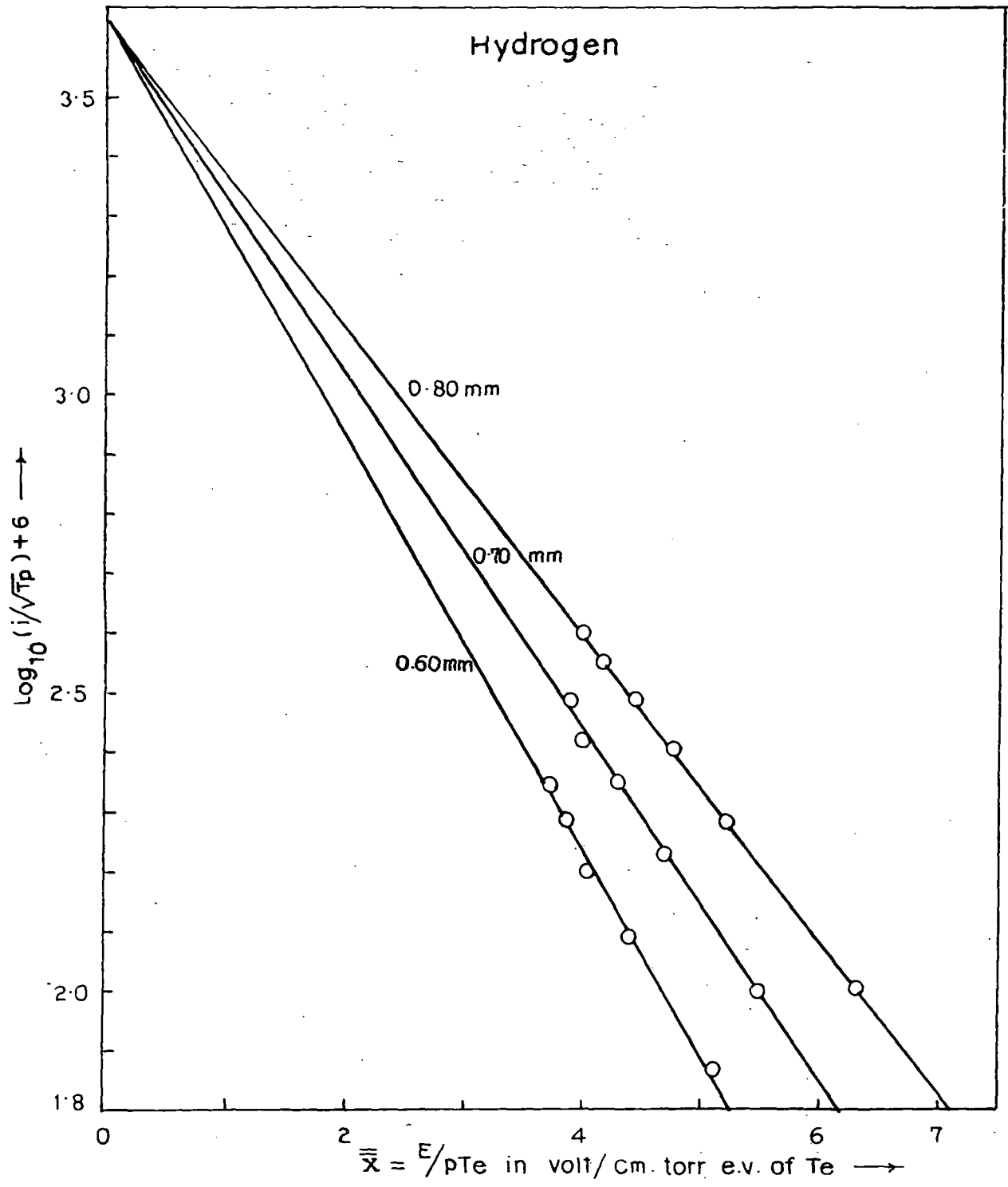


Fig. 3-7.

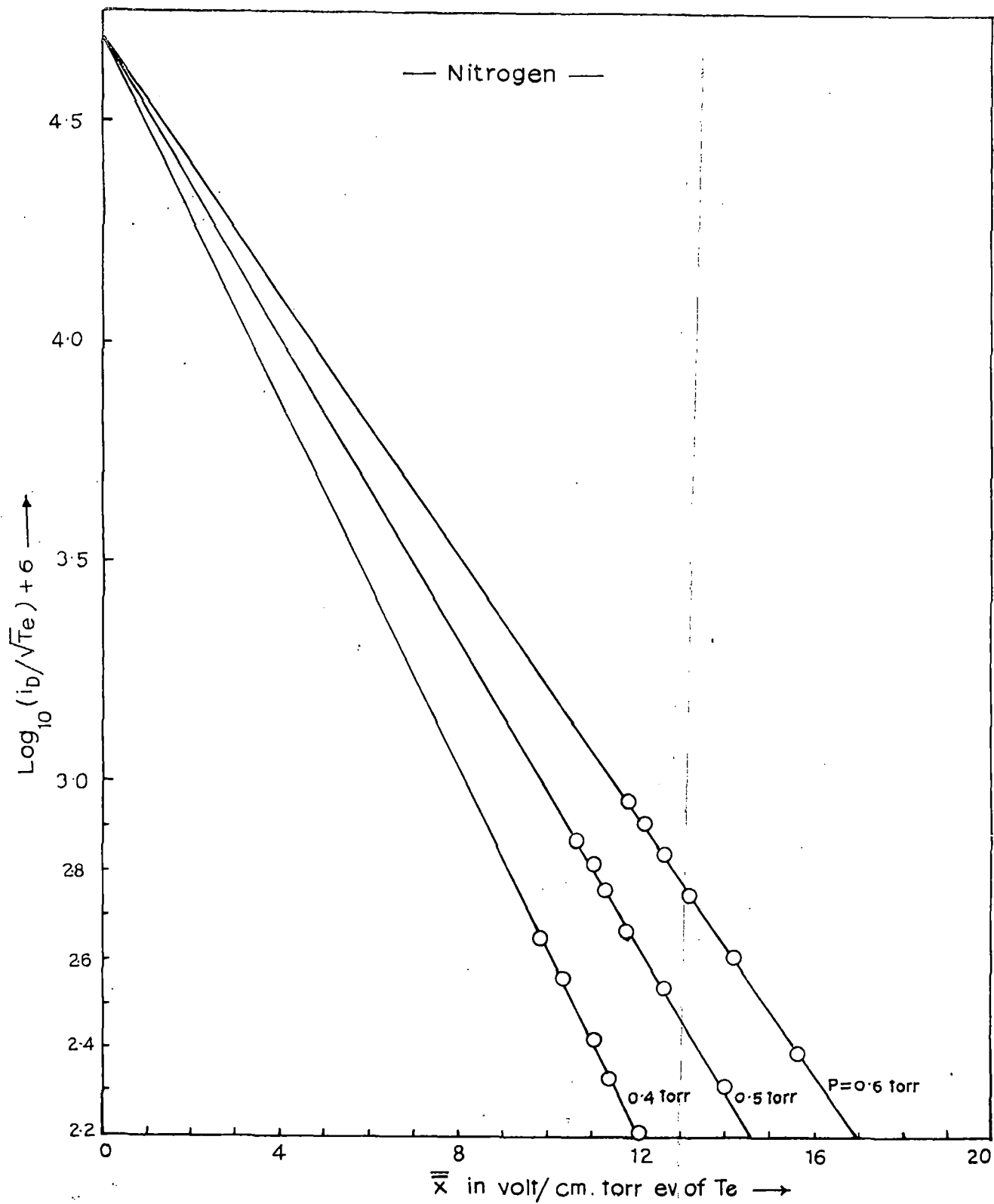


Fig. 3-8.

3.8

where  $\beta = eA \sqrt{\frac{3k K_0}{2m}}$

or  $\log \left[ \frac{i_D}{T_e^{1/2}} \right] = -\frac{1}{2} a\bar{X} + \log (\beta n_e e^{1/2} a\bar{X}_0) \dots \dots \dots (3.7)$

Thus when the variation of  $K$  with  $(E/P)$  is taken into consideration we get equation (3.7) and according to this equation the variation of  $\log (i_D/T_e^{1/2})$  with  $\bar{X} = \frac{E}{pT_e}$  should be a straight line. The results are plotted in Fig. (3.6) in case of air which shows that the relation (3.7) is well satisfied for all the three pressures investigated. The variation of  $T_e$  with  $(E/P)$  is shown in Fig. (3.4) in case of hydrogen and the variation of  $\log (i_D/T_e^{1/2})$  against  $\bar{X} = \frac{E}{pT_e}$  is plotted in Fig. (3.7) which is in conformity with equation (3.7). The variation of  $T_e$  with  $(E/P)$  for nitrogen is shown in Fig. (3.5) and the variation of  $\log [i_D/T_e^{1/2}]$  against  $\bar{X} = E/pT_e$  is plotted in Fig. (3.8) which is also in conformity with equation (3.7).

We can thus conclude that the energy loss of electrons is mainly due to collision with neutral atoms and molecules and a mathematical analysis shows that the variation of loss factor  $K$  with increasing  $(E/P)$  has to be taken into consideration to explain quantitatively the variation of discharge current.

In order to put the theory developed to a quantitative test the following parameters of the ionised gas (air, hydrogen and nitrogen) have been calculated utilising the results obtained. A detailed calculation for air at  $P = 0.2$  mm of mercury and  $E/P = 100$  volt/cm torr is shown.

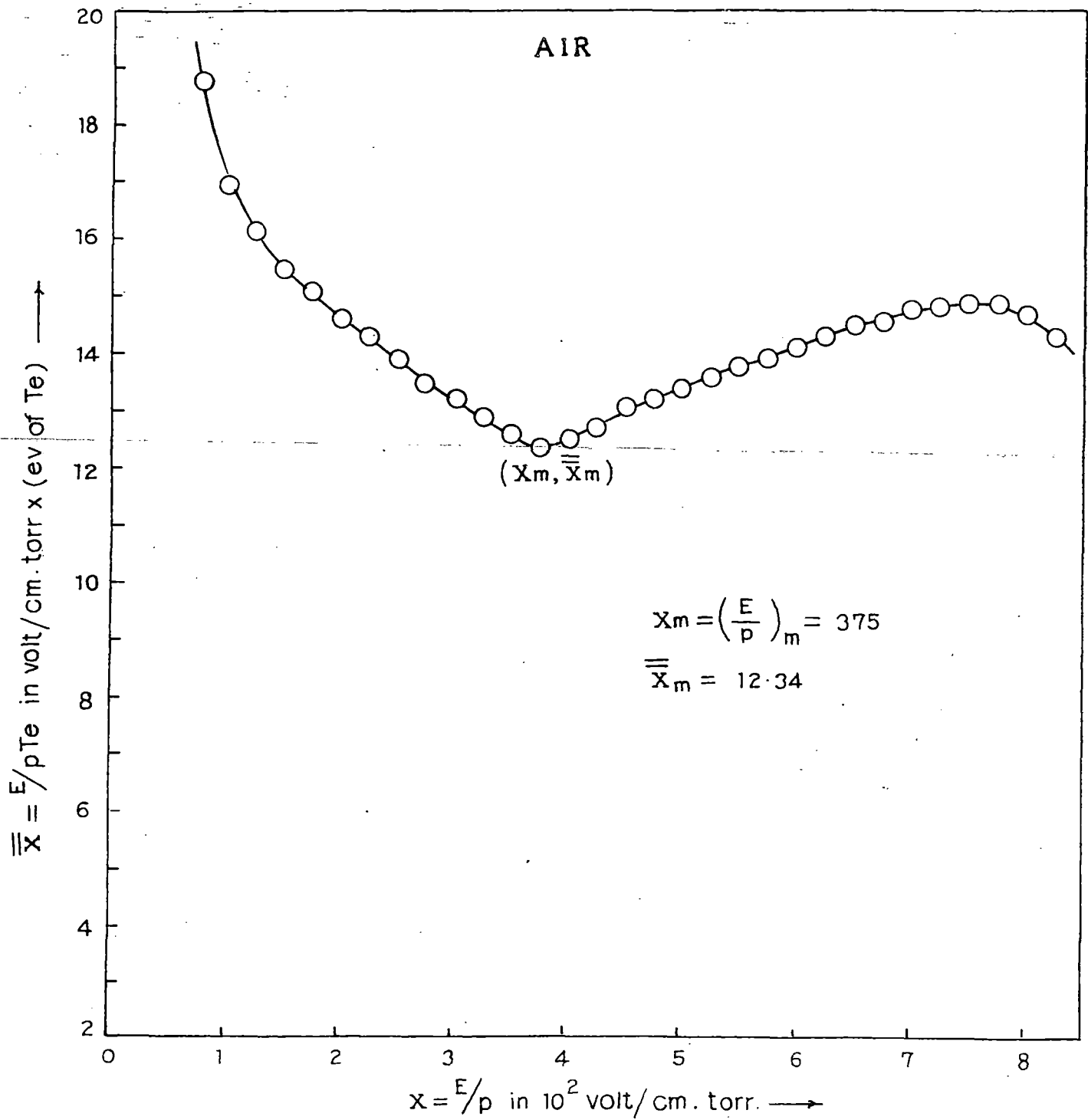


Fig. 3-9.

Fig. 3-9

From Fig. (3.6) the slope of the curve, "a" is given by

$$-\frac{1}{2} a \times 0.4343 = \frac{\left(\log \frac{i_p}{\sqrt{T_e}}\right)_2 - \left(\log \frac{i_p}{\sqrt{T_e}}\right)_1}{\bar{X}_2 - \bar{X}_1}$$

$$\text{or } a = 0.4667 / \left[ \frac{\text{volt/cm}}{\text{mm. of Hg.} \times \text{ev}} \right]$$

$$\text{and } \left[ \log \frac{i_p}{\sqrt{T_e}} + 5 \right]_{\bar{X}=0} = 3.95$$

$$\text{or } \left( \frac{i_p}{\sqrt{T_e}} \right)_{\bar{X}=0} = 8.913 \times 10^{-2} \text{ in mixed unit}$$

The variation of  $\bar{X} = E/pT_e$  against  $E/P$  is shown in Fig. (3.9) in case of air; from the relation

$$\bar{X}_0 = -\log \frac{K_0}{0.4343 a} + \bar{X}_m$$

$$\text{and } K_0 = 1.0003 \times 10^{-4}$$

and  $\bar{X}_m$  from the curve = 12.34 and  $\bar{X}_0 = 32.07$  in volt/cm.torr.ev.  
then  $e^{\frac{1}{2} a \bar{X}_0} = 1.778 \times 10^{-3}$ .

$$\left( \frac{i_p}{\sqrt{T_e}} \right)_{\bar{X}=0} = 8.913 \times 10^{-2} \text{ and } \left( \frac{i_p}{\sqrt{T_e}} \right)_{\bar{X}=0} = \beta n_e e^{\frac{1}{2} a \bar{X}_0}$$

$$\text{So, } \beta n_e = 5.01 \times 10^{-5} \text{ in mixed unit}$$

$$\beta n_e \text{ in e.s.u.} \equiv \left( i_p / \sqrt{T_e} \text{ in amp./}\sqrt{\text{ev}}, \text{ when converted to esu} \right. \\ \left. \text{gives, } \beta n_e \text{ in esu} = \frac{i_p \times 3 \times 10^9 \text{ e.s.u.}}{\sqrt{T_e} \times 7740^\circ \text{ ergs}} \right.$$

$$= \left[ \text{value of } i_p / \sqrt{T_e} \text{ in mixed unit} \times 3.41 \times 10^7 \right]$$

in e.s.u unit

$$\text{Hence } \beta n_e \text{ in e.s.u.} = 5.01 \times 10^{-5} \times 3.41 \times 10^7 \\ = 1.708 \times 10^3$$

$$\beta \text{ in e.s.u.} = eA \sqrt{\frac{3}{2} \cdot \frac{K_0}{m} \cdot k} = 1.408 \times 10^{-5}.$$

with  $A = 6.15 \text{ cm}^2$ .

$$n_e = \beta n_e / \beta = \frac{1.708 \times 10^3}{1.408 \times 10^{-5}} = 1.2 \times 10^8 / \text{c.c.}$$

$$v_d = \sqrt{\frac{3kT_e}{m} \cdot \frac{K}{2}} = 3.43 \times 10^7 \text{ cm/sec.}$$

$$v_r = \sqrt{\frac{3kT_e}{m}} = 1.423 \times 10^8 \text{ cm/sec.}$$

for  $T_e = 5.75 \text{ eV.}$        $K = 0.1164, L_1 = 11.1 \times 10^{-2} \text{ cm.}$

Similarly the following values have been obtained for hydrogen

for  $p = 0.70 \text{ mm of Hg}$  and  $E/P = 50 \text{ volt/cm torr}$  and  $T_e = 11.8 \text{ eV}$

$$n_e = 1.04 \times 10^7 / \text{c.c.} \quad v_r = 4.15 \times 10^9 \text{ cm/s}$$

$$v_d = 5.727 \times 10^8 \text{ cm/sec.} \quad L_1 = 9.9 \times 10^{-1} \text{ cm}$$

$K = 0.5513$  for  $P = 0.70 \text{ mm. of Hg}$ , and Nitrogen for

$P = 0.5 \text{ torr}$ , and  $E/P = 140 \text{ volt/cm torr}$ ,  $T_e = 12.3 \text{ eV.}$

$$L_1 = 0.1935 \text{ cm.} \quad n_e = 2.56 \times 10^7 / \text{cc}$$

$$v_d = 7.89 \times 10^7 \text{ cm/sec.}$$

$$v_r = 2.068 \times 10^8 \text{ cm/sec.}$$

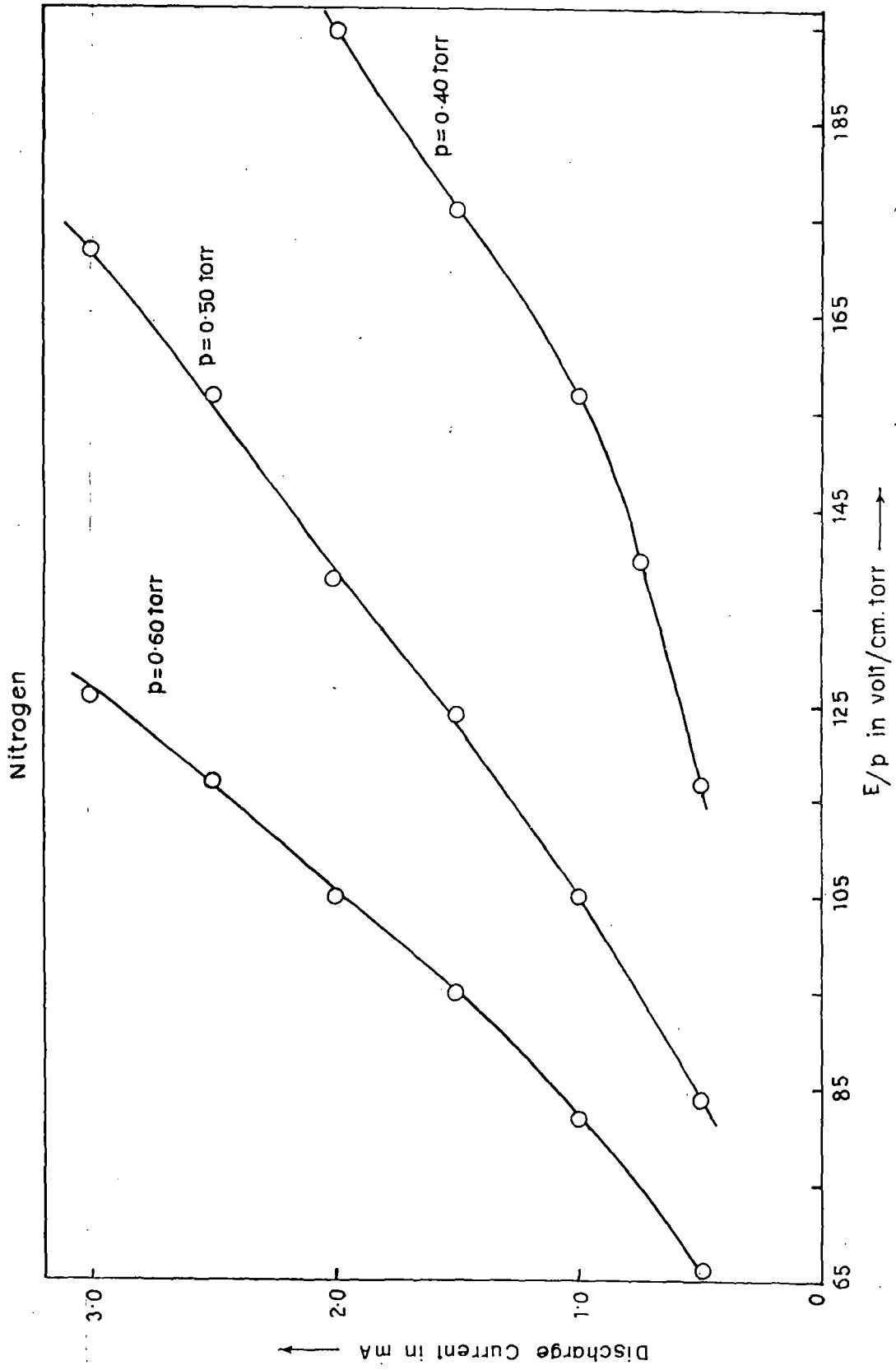


Fig. 3.10.

... ..

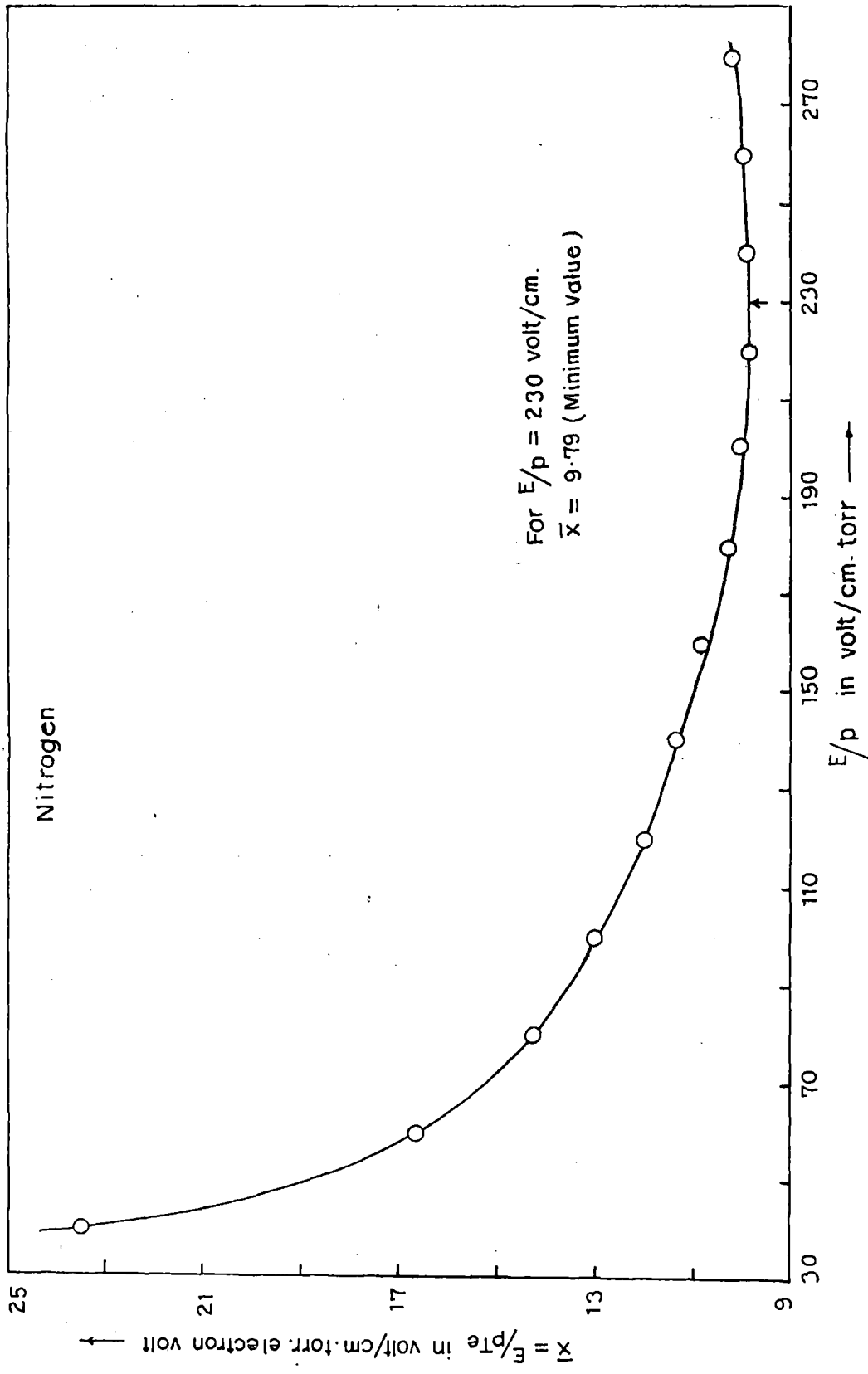


Fig. 3-11

Fig. 3-11

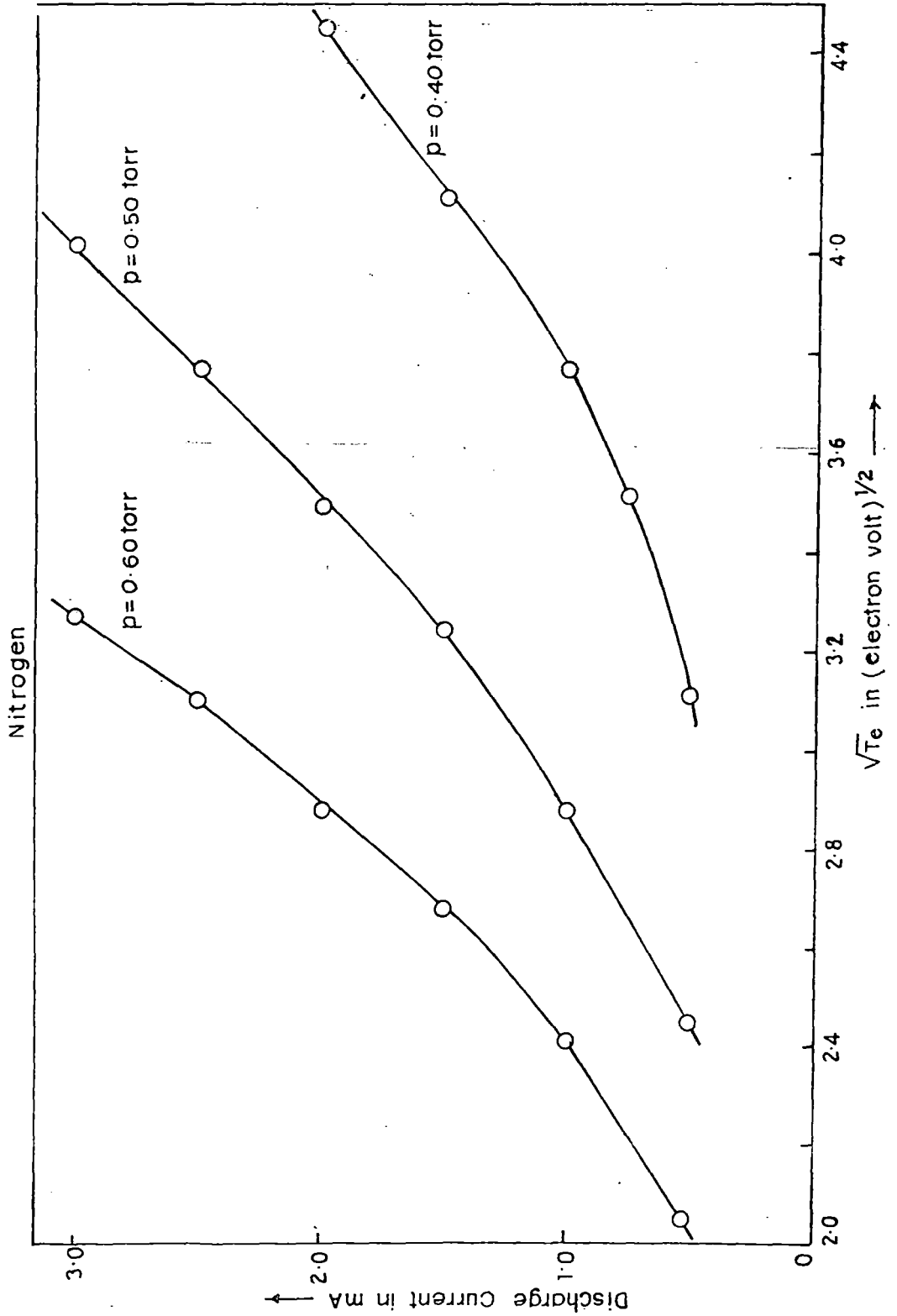


Fig. 3-12.

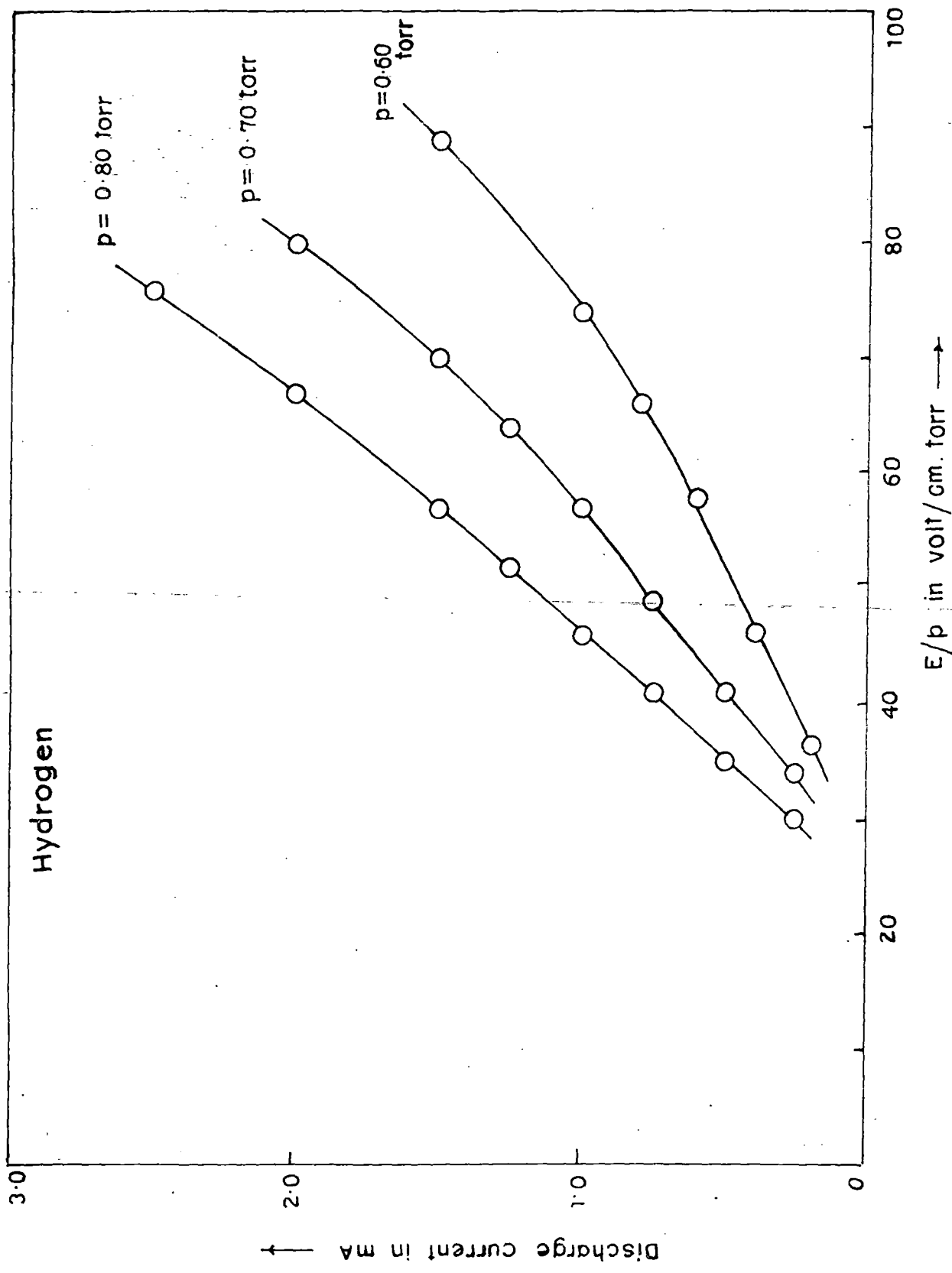


Fig. 3.13  
3/13

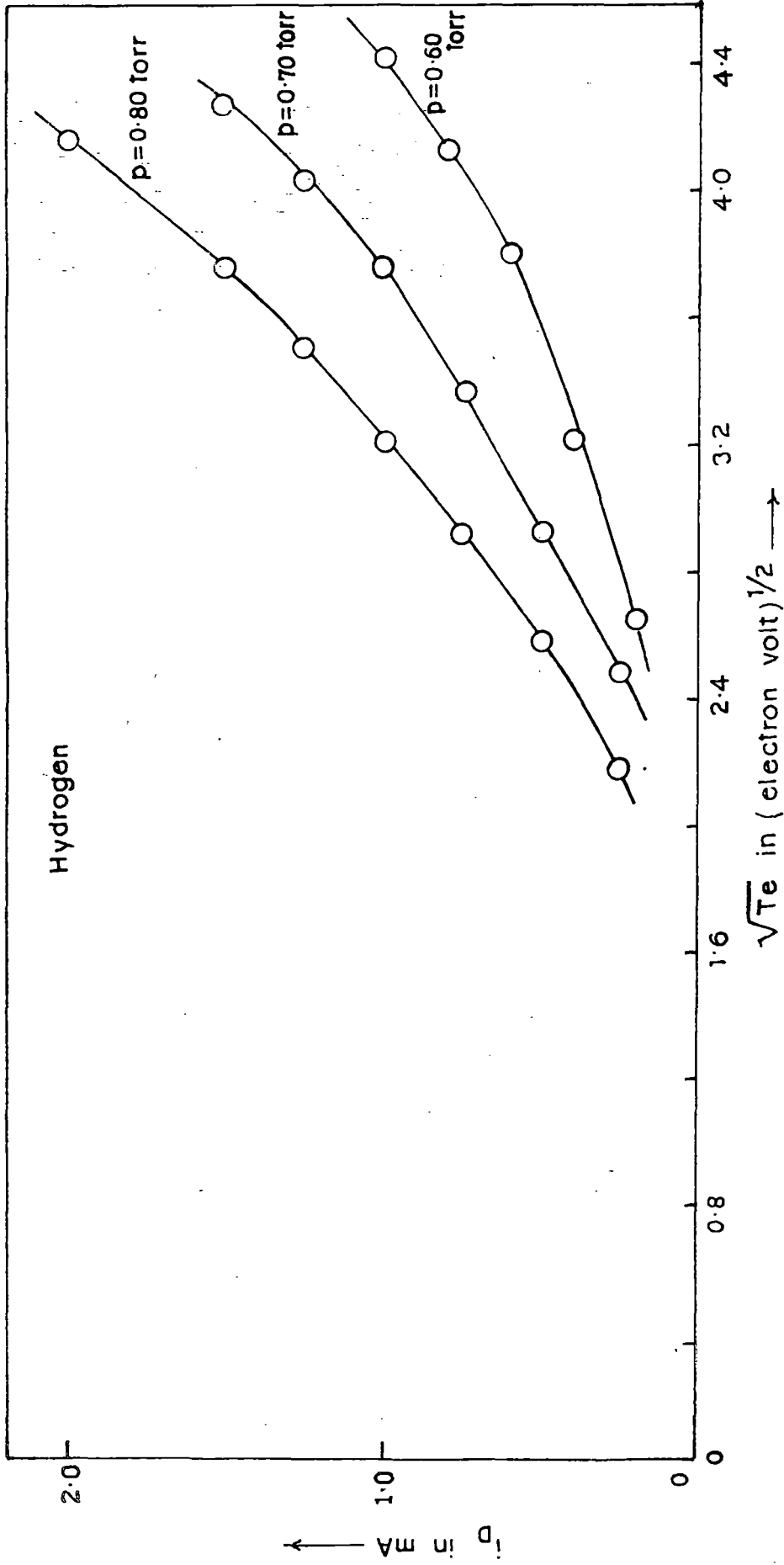


Fig. 3-14.

Fig 314

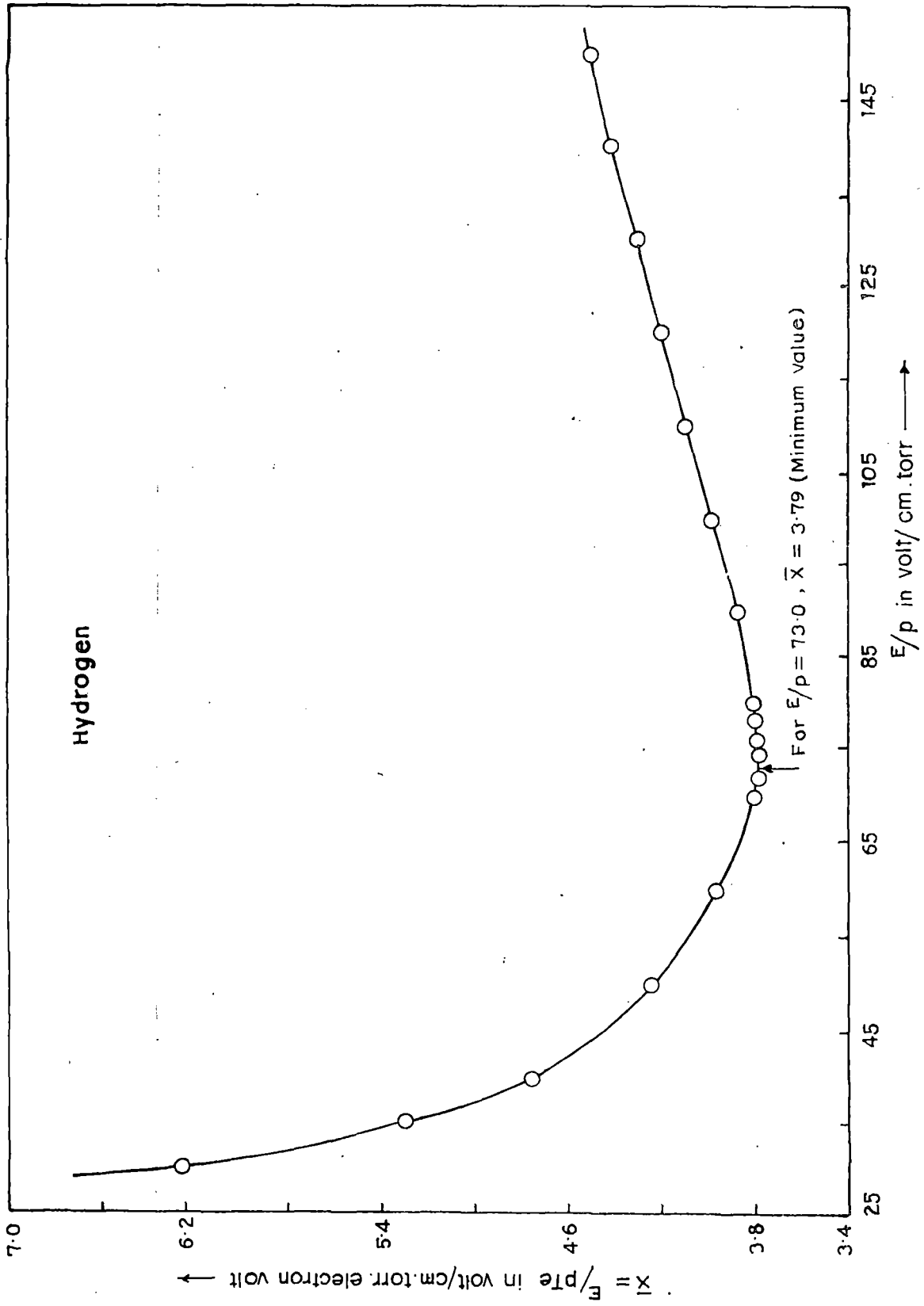


Fig. 3-15.

We can thus conclude that loss of energy in a plasma is due to collision of electrons with atoms and molecules and the variation of  $K$  with  $(E/P)$  has to be taken into account to explain the variation of plasma current with  $(E/P)$ . The theory developed can not only explain the experimentally observed variation of discharge current with  $(E/P)$  but the calculated values of the plasma parameters such as electron density, random velocity, electron temperature and electronic mean free path are in quite good agreement with standard literature values.

Detailed experimental data for air, hydrogen and nitrogen are provided in TABLE 3a, 3b, 3c, 3d, 3e, 3f and 3g.  $i_D$  vs  $E/P$  in Fig. 3.13,  $i_D$  vs  $\sqrt{T_e}$  in Fig. 3.14 and  $(E/P \cdot T_e)$  vs  $E/P$  in Fig. 3.15 are shown for hydrogen. And Fig. 3.10, 3.11 and 3.12 are the corresponding plots for Nitrogen.

TABLE 3a

Low density air plasma (dc glow discharge)  
 Brass electrodes, total fall voltage = 350 volt  
 Interelectrode distance,  $d = 6$  cm

Pressure in torr $p$	Discharge current in mA $i_D$	Total supply voltage $V_T$ in volt	Voltage across the discharge tube in volt $V_D = V_T - i_D R$	Reduced electric field $X = E/P$ $= \frac{V_D - 350}{pd}$ in V/cm torr	Diffusion voltage in volt $V_R$	Electron temperature in eV with $V_R$ in volt (1 eV = 7740°K) $T_e = 7.49 V_R$
0.20	0.50	520	494	120.0	0.95	7.12
	1.00	650	599	207.5	1.95	14.61
	1.50	750	673	269.2	2.63	19.70
	2.00	850	747	330.8	3.45	25.84
	2.50	925	796	371.7	4.04	30.26
	3.00	1120	966	513.3	5.10	38.20
	4.00	1400	1194	703.3	6.39	47.86
	5.00	1725	1468	931.7	12.40	92.88
0.30	0.5	495	469	66.1	0.47	3.52
	1.0	580	529	99.4	0.79	5.92
	1.5	660	583	129.4	1.03	7.71
	2.0	750	647	165.0	1.80	13.48
	2.5	855	727	209.4	2.02	15.13
	3.0	990	836	270.0	2.46	18.43
	4.0	1145	939	327.4	3.09	23.14
	5.0	1360	1103	418.3	4.45	33.33
	6.0	1625	1317	537.2	5.27	39.47

TABLE 3a (Contd..)

0.50	495	469	49.6	0.26	1.95
1.00	575	524	72.5	0.47	3.52
1.50	655	578	95.0	0.67	5.02
2.00	750	647	123.8	0.91	6.82
2.50	805	677	136.3	1.15	8.61
3.00	880	726	156.7	1.40	10.49
4.00	1050	844	205.8	1.91	14.31
5.00	1175	918	236.7	2.25	16.85
6.00	1400	1092	309.2	3.47	25.99

---

TABLE 3b  
Low density air plasma

Pressure in torr p	Discharge current in Amp $i_D$	E/P in volt/cm x torr X	$T_e^{1/2}$ in (eV) <sup>1/2</sup>	$i_D/\sqrt{T_e}$ in A/ $\sqrt{\text{eV}}$ $\times 10^6$	$\log_{10}(i_D/\sqrt{T_e})$ + 6	$\bar{X} = E/P T_e$ in volt/cm x torr x (eV)
0.20	$500 \times 10^{-6}$	120	2.72	183.8	2.2644	16.22
	$1000 \times 10^{-6}$	210	3.81	262.5	2.4191	14.48
	$1500 \times 10^{-6}$	270	4.47	335.6	2.5258	13.50
	$2000 \times 10^{-6}$	331	5.09	392.9	2.5943	12.78
	$2500 \times 10^{-6}$	375	5.51	453.7	2.6568	12.34
	$3000 \times 10^{-6}$	512	6.16	487.0	2.6875	13.50
	$4000 \times 10^{-6}$	703	6.92	578.0	2.7619	14.88
0.30	$500 \times 10^{-6}$	66	1.80	277.8	2.4438	20.0
	$1000 \times 10^{-6}$	100	2.40	416.7	2.6198	16.95
	$1500 \times 10^{-6}$	129	2.86	524.5	2.7197	16.00
	$2000 \times 10^{-6}$	165	3.35	597.0	2.7760	15.25
	$2500 \times 10^{-6}$	209	3.81	656.2	2.8170	14.50
	$3000 \times 10^{-6}$	239	4.10	737.7	2.8679	14.10
	$4000 \times 10^{-6}$	305	4.796	834.0	2.9212	13.15

Contd..

TABLE 3b (Contd..)

0.40	$500 \times 10^{-6}$	52	1.50	333.3	2.5228	23.2
	$1000 \times 10^{-6}$	70	1.87	534.8	2.7281	19.6
	$1500 \times 10^{-6}$	93	2.24	669.6	2.8258	17.35
	$2000 \times 10^{-6}$	115	2.61	766.3	2.8844	16.40
	$2500 \times 10^{-6}$	137.5	2.91	859.1	2.9341	15.80
	$3000 \times 10^{-6}$	157.5	3.24	925.9	2.9665	15.36
	$4000 \times 10^{-6}$	197.5	3.67	1089.9	3.0370	14.65
	$5000 \times 10^{-6}$	246.0	4.19	1193.3	3.0766	13.95
$6000 \times 10^{-6}$	307.5	4.82	1244.8	3.0952	13.10	

---

TABLE 3c  
Low density air plasma

E/P in volt/cm torr	$T_e$ in eV	E/P $T_e$ in volt/cm x torr x (eV)	E/P in volt/cm torr	$T_e$ in (eV)	E/P $T_e$ in volt/cm torr x (eV)	Minimum value of E/P $T_e$ and corresponding E/P
35	1.0	35.0	375	30.4	12.34	
50	2.0	25.0	380	30.7	12.38	E/P $T_e$ = 12.34
75	4.0	18.75	385	31.0	12.42	
100	5.9	16.95	390	31.3	12.46	for E/P = 375
125	7.75	16.13	395	31.65	12.48	
150	9.7	15.46	400	32.00	12.50	
175	11.6	15.09				
200	13.7	14.60				
225	15.75	14.29				
250	18.00	13.89				
275	20.4	13.48				
300	22.6	13.27				
325	25.2	12.90				
350	27.75	12.61				
375	30.4	12.34				
400	32.0	12.50				
425	33.5	12.69				
450	34.5	13.04				

Contd..

TABLE 3c (Contd..)

475	36.0	13.19
500	37.25	13.42
525	38.75	13.55
550	40.00	13.75
575	41.3	13.92
600	42.5	14.12
625	43.7	14.30
650	45.0	14.44
675	46.4	14.55
700	47.5	14.74
725	49.0	14.80
750	50.4	14.88
775	52.2	14.85
800	54.7	14.63

---

TABLE 3d  
(Hydrogen)

Pressure in torr	Discharge current in Amp x 10 <sup>6</sup> = $i_D \times 10^6$	Reduced electric field in volt/cm torr E/P	Electron Temperature in eV $T_e$	$\sqrt{T_e}$	$\frac{i_D \times 10^6}{\sqrt{T_e}}$	$\text{Log}_{10} (i_D / \sqrt{T_e}) + 6$	$X = E/P T_e$
.60	200	36.5	7.1	2.66	75.2	1.8761	5.12
	400	46.0	10.4	3.22	124.2	2.0941	4.41
	600	58.0	14.5	3.81	157.5	2.1973	4.00
	800	66.0	17.1	4.14	193.20	2.2860	3.86
	1000	74.0	19.5	4.42	226.2	2.3545	3.79
.70	250	34	6.2	2.49	100.4	2.0017	5.50
	500	41	8.6	2.93	170.7	2.2322	4.70
	750	49	11.4	3.38	221.9	2.3461	4.28
	1000	57	14.2	3.77	265.3	2.4237	4.02
	1250	64	16.4	4.05	308.6	2.4906	3.84
	1500	70	18.4	4.29	349.7	2.5437	3.80

Contd..

TABLE 3 d (Contd..)

109

	250	29.9	4.75	2.18	99.60	1.9983	6.30
0.80	500	35.0	6.70	2.59	193.05	2.2858	5.23
	750	41.0	8.60	2.93	255.97	2.4082	4.75
	1000	46.0	10.40	3.22	310.56	2.4922	4.42
	1250	52.0	12.40	3.52	355.11	2.5503	4.16
	1500	57.0	14.30	3.78	396.83	2.5986	3.99

---

TABLE 3e  
(Hydrogen)

Reduced electric field in volt/cm or E/P	Electron Temperature in eV $T_e$	X = E/P $T_e$ in volt per cm torr eV	Minimum value of X = $X_m$ (From graph)	Value of E/P corresponding to $X_m$ (From graph)
30	4.8	6.25		
35	6.6	5.30		
40	8.4	4.76		
50	11.8	4.24		
60	15.1	3.97		
70	18.4	3.80		
72	19.0	3.79		
74	19.5	3.79		
76	20.0	3.80	3.79	73.00
78	20.5	3.80		
80	21.0	3.81		
90	23.2	3.88		
100	25.1	3.98		
110	26.9	4.09		
120	28.6	4.20		
130	30.2	4.30		
140	31.75	4.41		

Contd..

TABLE 3e (Contd..)

150	33.30	4.50
160	34.75	4.60
170	36.10	4.71
180	37.40	4.81
190	38.60	4.92
200	39.65	5.04
210	40.50	5.19
220	41.30	5.33
230	42.10	5.46
240	42.80	5.61

---

TABLE 3f  
(Nitrogen)

Pressure in torr p	Discharge current in Amp $\times 10^6$ $= i_D \times 10^6$	Reduced electric field E/P in volt/cm $\times$ torr	Electron temperature in eV $T_e$	$\sqrt{T_e}$	$\frac{i_D \times 10^6}{\sqrt{T_e}}$	$\log_{10}(i_D/\sqrt{T_e})$ + 6	$\bar{X} = E/P T_e$
0.40	500	117	9.7	3.11	160.8	2.2063	12.06
	750	140	12.35	3.51	213.7	2.3298	11.34
	1000	157	14.2	3.77	265.3	2.4237	11.06
	1500	176	16.9	4.11	365.0	2.5625	10.40
	2000	195	19.9	4.45	449.4	2.6526	9.85
0.50	500	84	6.0	2.45	204.1	2.3098	14.0
	1000	105	8.3	2.88	347.2	2.5406	12.65
	1500	124	10.5	3.24	463.0	2.6656	11.81
	2000	138	12.2	3.49	573.0	2.7582	11.31
	2500	157	14.2	3.77	663.1	2.8215	11.06
	3000	172	16.2	4.02	746.3	2.8729	10.62

Contd..

TABLE 3f (Contd..)

0.60	500	66	4.2	2.05	243.9	2.3872	15.71
	1000	82	5.8	2.41	414.9	2.6179	14.14
	1500	95	7.2	2.68	559.7	2.7479	13.19
	2000	105	8.3	2.88	694.4	2.8416	12.65
	2500	117	9.6	3.10	806.5	2.9066	12.19
	3000	126	10.7	3.27	917.4	2.9626	11.78

---

TABLE 3g  
(Nitrogen)

Reduced electric field in volt/cm torr E/P	Electron temperature in eV $T_e$	$\bar{X} = E/P T_e$ in V/cm x torr x eV	Minimum value of X $= X_m$ (From graph)	Value of E/P corresponding to $X_m$ (From graph)
40	1.7	23.53		
60	3.6	16.67		
80	5.6	14.29		
100	7.7	12.99		
120	10.0	12.00		
140	12.3	11.38	9.79	230
160	14.7	10.88		
180	17.5	10.29		
200	20.1	9.95		
220	22.4	9.82		
240	24.4	9.84		
260	26.1	9.96		
280	27.5	10.18		
300	28.7	10.45		

R E F E R E N C E S

Massey H.S.W. Burhop, E.H.S. and Gilbody, H.B. 1971,  
Electrons and Ion Impact Phenomena, Vol. III,  
2nd Edition (Oxford Clarendon Press).

Von Engel, A., 1964, Ionised gases, Second Edition,  
Oxford University Press.

Sen, S.N., Ghosh, S.K. and Ghosh, B, Ind. Jour.  
Pure & Appl. Phys., 21, 613, 1983.

Sen, S.N., Acharyya, C., Gantait, M. and Bhattacharjee, B.,  
International Jour. Electronics (G.B.) 66, 1989.

## ENERGY LOSS MECHANISM IN A COLLISION DOMINATED PLASMA

S N SEN AND M NATH

*Department of Physics, North Bengal University, Siliguri-734430, India*

*(Received 26 April 1990; Revised 20 July 1990; Accepted 25  
September 1990)*

The loss of energy of the electron due to collision with neutral atoms and molecules in a collision dominated plasma has been theoretically investigated. It is shown that as the loss factor  $R$  is dependent upon  $(E/P)$ , where  $E$  is the electric field and  $P$  is the pressure it is essential to take into consideration the variation of  $R$  in calculating the current through the plasma. The theoretical expression for the plasma current thus deduced agrees very well with observed experimental results. Further the values of the plasma parameters such as electron density, drift and random velocity of the electron calculated from the theoretical expression combined with the data obtained from experimental results in case of air, nitrogen and hydrogen agree quite well with literature values.

**Key Words:** Energy Loss; Collision; Plasma Electron Density

### Introduction

The loss of energy by electrons when moving through an ionised gas has been investigated by von Engel<sup>1</sup> and also by Massy, Burhop and Gilbody<sup>2</sup>. It can be shown that when only elastic losses are taken into consideration the loss factor  $R=4m/M$ , where  $m$  is the mass of the electron and  $M$  is the mass of the atom or molecule with which the electron is colliding. The loss of energy by electrons is mainly due to collision in an ionised gas and we can neglect the energy lost by ions as they are less mobile. It has further been shown that  $R$  the loss factor increases (not always linearly) with  $(E/P)$ , where  $E$  is the electric field and  $P$  is the pressure and at higher  $(E/P)$  values inelastic losses set in. The purpose of the present investigation is to present a generalised theory regarding the loss of energy by electrons in an ionised gas taking into consideration the variation of  $R$  with  $(E/P)$  and thereby deduce an expression for the main discharge current in a collision dominated plasma. In the course of our deduction some plasma parameters have naturally been introduced and it is also the object to verify the theory from experimental results. Besides other parameters, experimental determination of  $T_e$  the electron temperature is necessary for a wide range of  $(E/P)$  values.

### Experimental Arrangement

The detailed experimental technique for the evaluation of electron temperature by measurement of diffusion voltage has been provided in two earlier papers<sup>3,4</sup> where it is shown that

$$KT_c = \frac{V_R}{\log J_0 \left( 2.405 \frac{r}{R} \right)},$$

where  $V_R$  is the diffusion voltage,  $R$  is the radius of the discharge tube and  $r$  is the distance of the probe from the axis of the discharge tube. The discharge tube having inner diameter 2.8 cm and length 10 cm is fitted with two parallel circular brass electrodes (diameter 1.2 cm) and separated by a distance of 6 cm. The backsides of the electrodes were perfectly sealed with glass and teflon caps. Two probes one along the axis and the other away from the axis were placed parallel to each other and were separated by a distance of 5 mm. Both the probes made of thin tungsten wire (0.2 mm diameter) were sealed within glass except at the ends. The schematic diagram is shown in Fig. 1. Fig. 2 represents the circuit diagram which consists of a high voltage power supply with a limiter resistance (51.4 k $\Omega$ ) and one current controller (Fig. 3) in series with the discharge tube. The diffusion voltage at the probes was measured by means of a digital voltmeter (HILL 205) whose input impedance is greater than 10 M $\Omega$ . An R-C filter circuit (RC=2.4 sec.) was placed parallel to the probes to prevent any fluctuating voltage to appear across the probes.

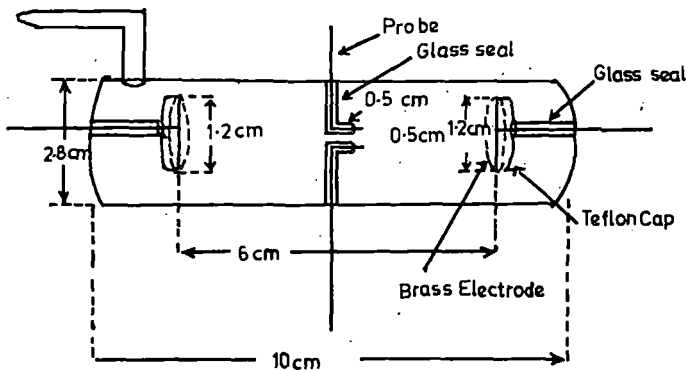


Fig. 1 The circuit diagram

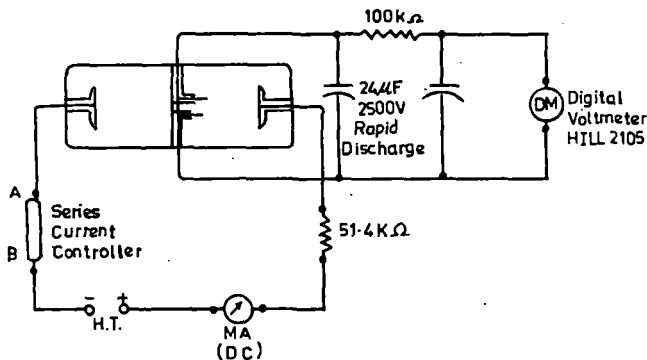


Fig. 2 Circuit for diffusion voltage measurement

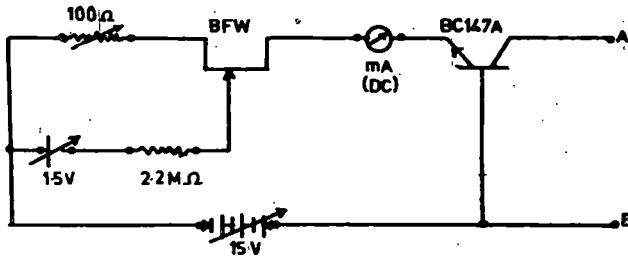


Fig. 3 Circuit for current controller

Pressure was measured by a Pirani gauge and adjusted with a needle valve to maintain a constant pressure throughout the experiment. The results are reported here for air ( $T_e$  for  $E/P$  upto 800 volts/cm torr) for hydrogen ( $T_e$  for  $E/P$  upto 240 volts/cm torr) and for nitrogen ( $T_e$  for  $E/P$  upto 320 volts/cm torr). The discharge current has been measured for three pressures  $P=0.4, 0.3$  and  $0.2$  torr for the corresponding values of  $(E/P)$  for the three gases. Pure gas was allowed to enter the discharge tube through the needle valve. Hydrogen and nitrogen were purified and dried with concentrated  $H_2SO_4$  and KOH pellets in succession.

### Theoretical Analysis and Discussion

The drift velocity of the electron  $v_d = (eL_e/mv_r)(E/P)$  and so the energy gained between successive collisions by a single electron due to drift  $= (1/2)(e^2L_e^2/mv_r^2)(E^2/\rho^2)$ , and as the frequency of collision  $= (v_r PL_e)$  the energy gained by the electron per sec.  $= (e^2L_e/2mv_r)(E^2/P)$ , where  $v_r$  is the random velocity of the electron and  $L_e$  is the mean freepath of the electron at a pressure of 1 torr. We consider that the electron starts with zero velocity after collision and reaches the maximum velocity just before collision. When we consider the loss of power by an electron due to collision we have to introduce the mean free path of the electron as deduced by von Engel<sup>1</sup> which is given by

$$L_e = \frac{12KT_e R^{1/2}}{\sqrt{2e(E/P)}}$$

So the power lost by one electron per sec. is

$$\frac{e^2}{2mv_r} \cdot \frac{E^2}{P} \cdot \frac{12KT_e R^{1/2}}{\sqrt{2e(E/P)}}$$

and as

$$1/2mv_r^2 = 3/2KT$$

the power lost by one electron is  $eE[6KT_eR/m]^{1/2}$ . Hence, the excess power lost by one electron due to an increase in  $E$  by  $dE$  is  $e[6KT_eR/m]^{1/2}dE$ . Number of electrons which constitute the current is  $n_e v_d A$  each of which spends a time  $d_0/v_d$  in the electric field where  $d_0$  and  $A$  are the inter electrode distance and cross sectional area of the plasma respectively. So the total time spent by  $n_e v_d A$  electrons in the electric field is  $n_e d_0 A$ . So the extra loss of energy by  $n_e v_d A$  electrons by collision per sec. is

$$dw_1 = e \left[ \frac{6KT_eR}{m} \right]^{1/2} n_e A v_d dE.$$

Again electrical energy lost by  $n_e v_d A$  electrons is  $iEd_0$ , where  $i$  is the discharge current and  $Ed_0$  is the voltage drop. When  $E$  increases to  $E+dE$  and current changes from  $i$  to  $i+di$  the electrical energy lost by electrons is  $(i+di)(E+dE)$ . So the extra power lost by electrons due to increase in  $E$  by  $dE$  is given by

$$\begin{aligned} dw_2 &= (i+di)(E+dE)d_0 - iEd_0 \\ &= (idE + Edi)d_0 \end{aligned}$$

We can consider that the energy lost by the electrons is the same as the energy lost by the electrons due to collision so we get

$$dw_1 = dw_2$$

$$en_e A d_0 \left[ \frac{6RKT_e}{m} \right]^{1/2} dE = (idE + Edi)d_0$$

For small changes in  $E$ ,  $i = \sigma E$  where  $\sigma$  is the conductivity and  $di = \sigma dE$ , then

$$\text{then } idE + Edi = 2\sigma EdE.$$

$$en_e A \left[ \frac{6RKT_e}{m} \right]^{1/2} = 2\sigma E$$

then

$$i = \sigma E = en_e A \left[ \frac{3RKT_e}{2m} \right]^{1/2} \dots (1)$$

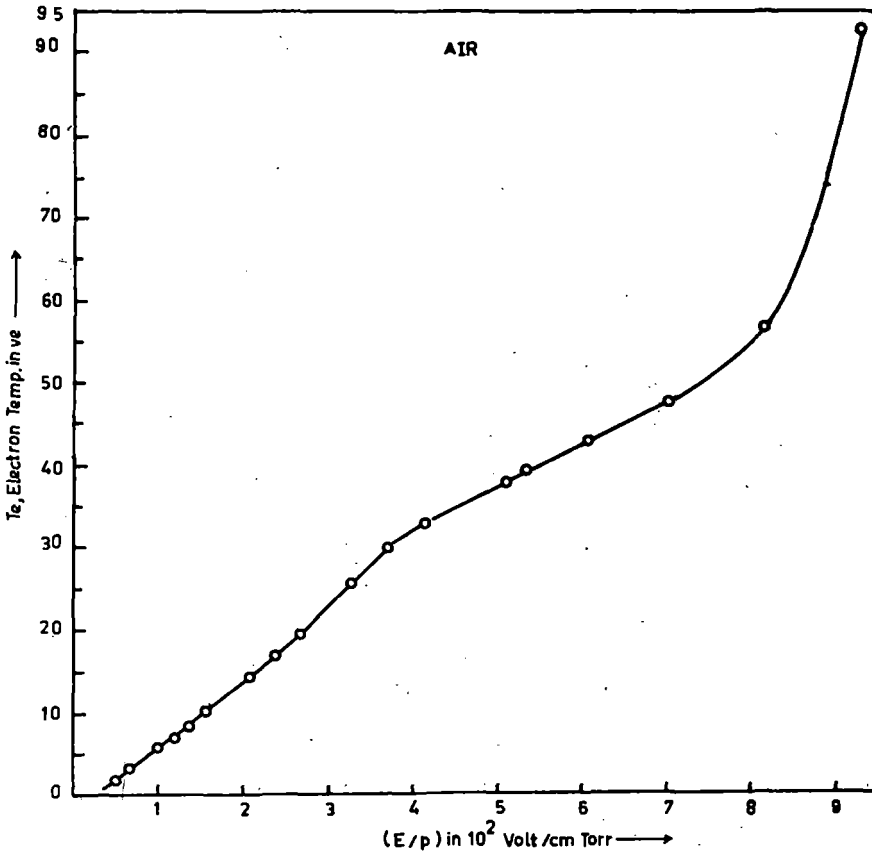


Fig 4 Variation of electron temperature against  $(E/P)$  (air)

Experimental values of  $T_e$  for different  $(E/P)$  values have been plotted in Fig. 4, in case of air. The observed values of discharge current in air, for different  $(E/P)$  values have been plotted in Fig. 5. Taking the values of  $T_e$  for different  $(E/P)$  values from Fig. 4 the discharge current  $i$  has been plotted against  $\sqrt{T_e}$  for three different pressures (Fig. 6). According to eq (1), the curves should be straight lines but the linearity relation is not maintained between  $i$  the discharge current and  $\sqrt{T_e}$  as is evident from Fig. 6, in case of air; the variation of  $T_e$  with  $(E/P)$  is shown in Fig. 7 for hydrogen, and that for nitrogen in Fig. 8. Plot of current  $i$  against  $\sqrt{T_e}$  shows that linearity relation between  $i$  and  $\sqrt{T_e}$  is not maintained in case of hydrogen and nitrogen as well. This is due to the fact that the loss factor  $R$  increases with  $(E/P)^1$  and hence with  $T_{ei}$  as  $(E/P)$  increases inelastic collisions increase as is evident from the study of variation of collision cross section with  $(E/P)$ .

Next we proceed to calculate the value of the discharge current by taking into consideration the variation of  $R$  with  $(E/P)$ . We assume that the loss of energy by an electron due to drift when the displacement is  $\lambda_e$  is  $w_e$  and so for

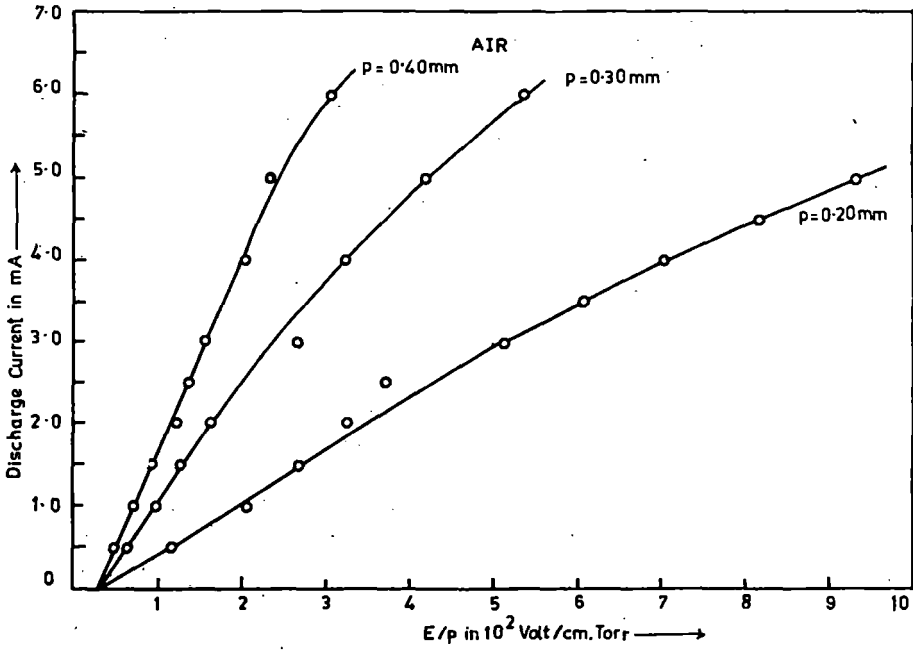


Fig 5 Variation of discharge current against  $(E/P)$  (air)

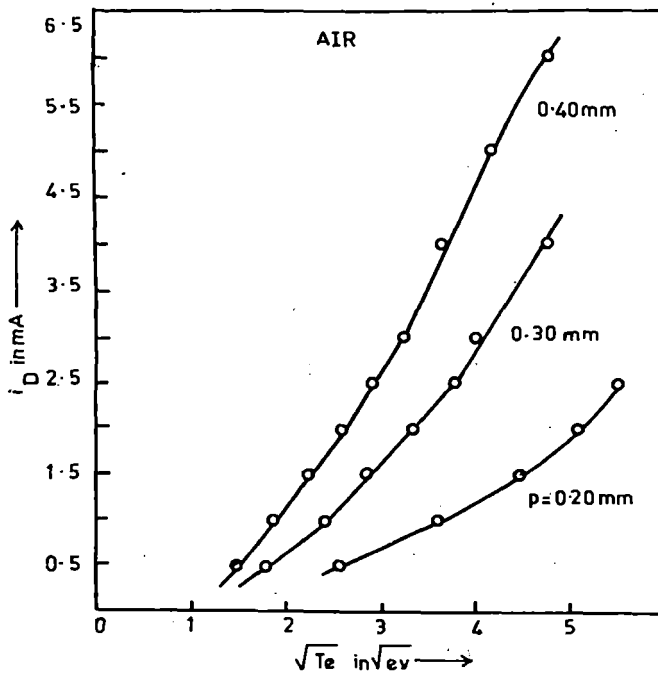
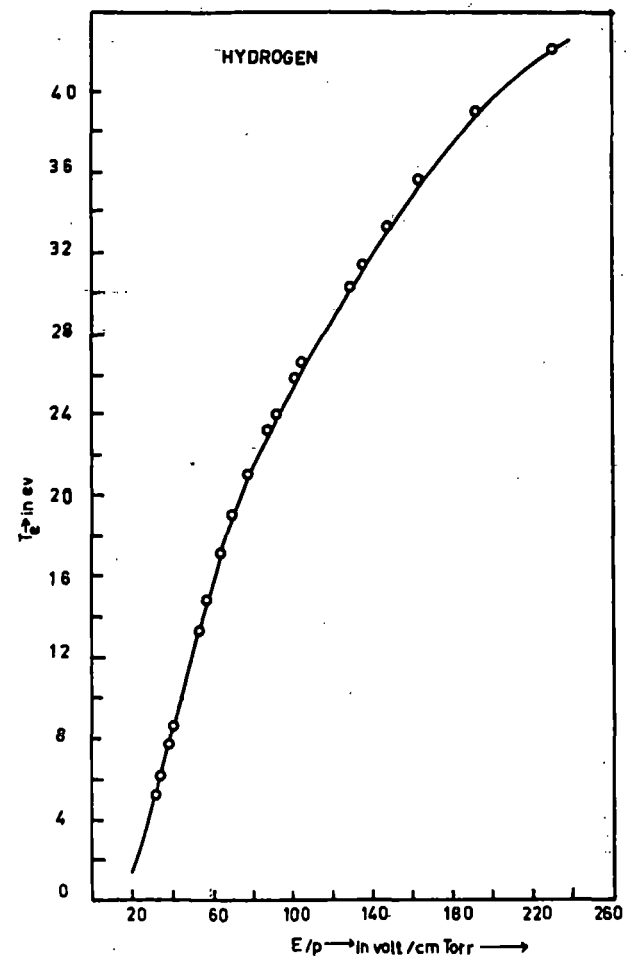
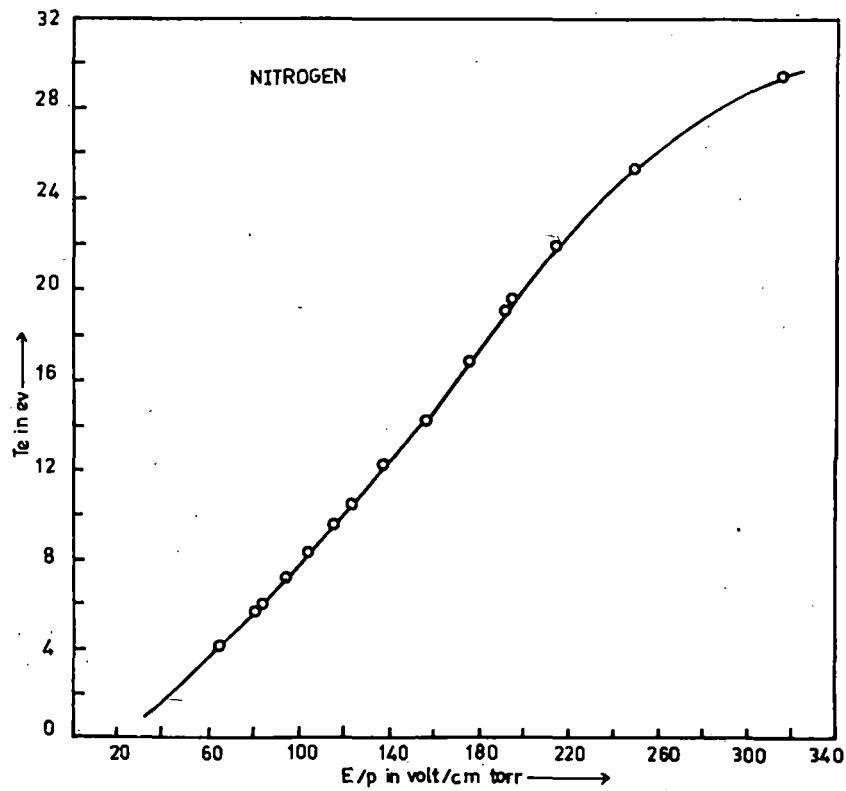


Fig 6 Variation of discharge current against  $\sqrt{T_e}$

Fig 7 Variation of  $T_e$  against  $(E/P)$  hydrogenFig 8 Variation of  $T_e$  against  $(E/P)$  nitrogen

drift velocity  $v_d$  the loss is  $w_e v_d / \lambda_e$  and as the frequency of collision is  $\nu_r / \lambda_e$  so the loss of energy due to drift by one electron per unit collision is  $W_e v_d / \nu_r$ . So the loss of energy per unit collision by one electron when  $E$  changes to  $(E + dE)$  is  $W_e d[(v_d / \nu_r) + d(v_d / \nu_r)]$ . Hence, the extra loss of energy per unit collision due to increase in  $E$  by  $E + dE$  is  $W_e d(v_d / \nu_r)$ . But the extra loss of energy is different for plasma of different gases even if  $W_e d(v_d / \nu_r)$  is the same. So this must depend on the nature of the gas of the plasma so the extra true loss is

$$r w_e d\left(\frac{v_d}{\nu_r}\right) = r W_e d\left\{\frac{e L_e}{m \nu_r^2} \frac{E}{P}\right\},$$

where  $r$  is a constant related to the characteristics of the nature of the gas of the plasma.

So the extra loss is

$$r w_e \frac{e L_e}{3K} d\left(\frac{E}{PT_e}\right)$$

$$= a w_e d\chi$$

$$\text{where } a = \frac{r e L_e}{3K}$$

$$\text{and } \chi = \frac{E}{PT_e}$$

We have further  $W_e = R w$ , where  $R$  is the loss factor and  $w$  is the energy of the electron before collision so the extra energy loss by the electron due to increase in  $E$  to  $E + dE$  is  $R d w - d w_e$  and hence

$$R d w - d w_e = a w_e d\chi \quad \dots (3)$$

but as  $R$  is not a constant,

$$d w_e = R d w + w d R \quad \dots (4)$$

So from equations (3) and (4) we get

$$\frac{-w d R}{w_e} = a d\chi$$

or

$$\frac{dR}{R} = -a d\chi$$

or

$$R = l e^{-a\chi},$$

where  $l$  is a constant of integration and the above equation shows the variation of  $R$  with  $E/P$  and  $T_e$ .

Let  $R = R_0$  when  $\chi = \chi_0$

and  $R = 1$  when  $\chi = \chi_m$ ,

where  $\chi_m$  is the minimum value of  $\chi$  when plotted against  $(E/P)$  where  $R$  must be a maximum; since after  $\chi_m$  there is a decrease in the value of  $\chi$  with the increase in  $(E/P)$ . Then

$$R_0 = l e^{-a\chi_0}$$

$$l = R_0 e^{a\chi_0}$$

and

$$R = R_0 e^{a(\chi_0 - \chi)} \tag{5}$$

also  $1 = l e^{-a\chi_m}$  and  $l = R_0 e^{a\chi_0}$

So  $e^{a\chi_m} = R_0 e^{a\chi_0}$

$$\chi_0 = \chi_m - \frac{\log R_0}{a}$$

So from eq. (1) after putting the value of  $R$  from eq. (5)

$$i = en_e A \sqrt{\frac{3KT_e R_0}{2m}} e^{a/2(\chi_0 - \chi)}$$

$$= \beta n_e T_e^{1/2} e^{a/2(\chi_0 - \chi)} \tag{6}$$

$$\text{where } \beta = eA \sqrt{\frac{3R_0K}{2m}}$$

$$\text{or } \log \left[ \frac{i}{T_e^{1/2}} \right] = -\frac{1}{2}a\chi + \log(\beta n_e e^{(1/2)a\chi_0}) \quad (7)$$

Thus when the variation of  $R$  with  $(E/P)$  is taken into consideration we get eq. (7) and according to this equation the variation of  $\log(i/T_e^{1/2})$  with  $\chi = E/PT_e$  should be a straight line. The results are plotted in Fig. 9 in case of air which shows that the relation (7) is well satisfied for all the three pressures investigated. The variation of  $T_e$  with  $(E/P)$  is shown in Fig. 7 in case of hydrogen and the variation of  $\log(i/T_e^{1/2})$  against  $\chi = E/PT_e$  is plotted in Fig. 10 which is in

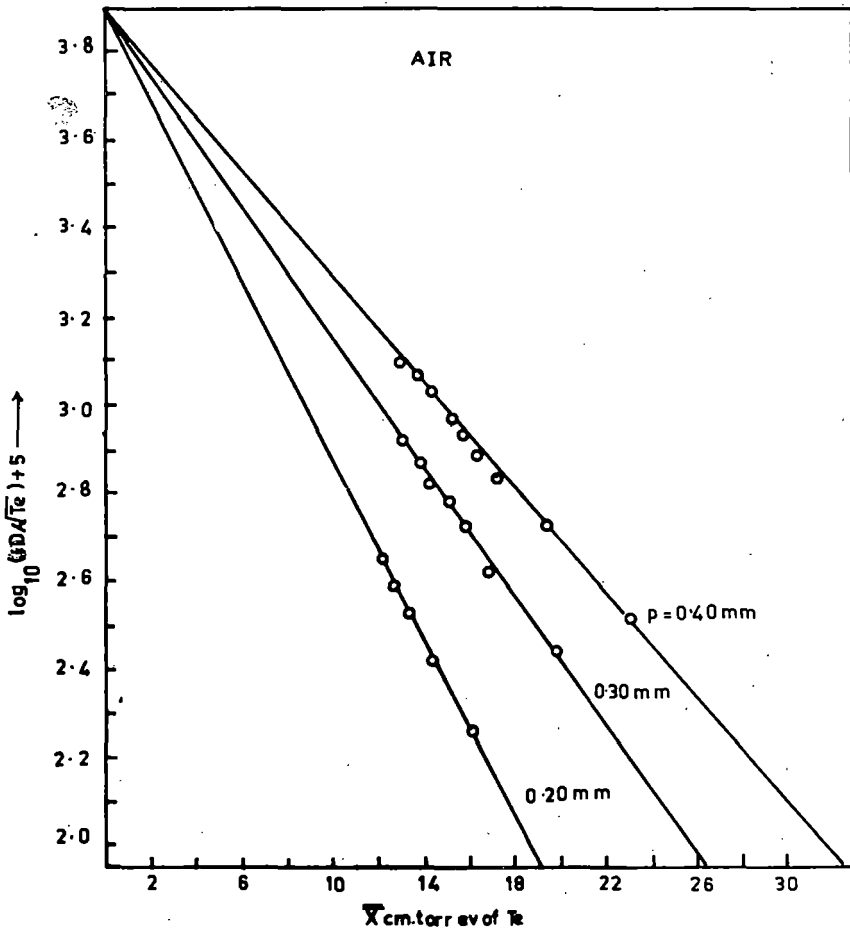


Fig 9 Variation of  $\log_{10}(i/\sqrt{T_e}) + 5$  against  $\chi$  (air)

conformity with equation (7). The variation of  $T_e$  with  $(E/P)$  for nitrogen is shown in Fig. 8 and the variation of  $\log[i/T_e^{1/2}]$  against  $\chi = E/PT_e$  is plotted in Fig. 11 which is also in conformity with Eq. (7).

We can thus conclude that the energy loss of electrons is mainly due to collision with neutral atoms and molecules and a mathematical analysis shows that the variation of loss factor  $R$  with increasing  $(E/P)$  has to be taken into consideration to explain quantitatively the variation of discharge current.

In order to put the theory developed to a quantitative test the following parameters of the ionised gas (air, hydrogen and nitrogen) have been calculated utilizing the results obtained. A detailed calculation for air at  $P=0.2\text{mm}$  of mercury is shown.

From Fig. 9 the slope of the curve "a" is given by

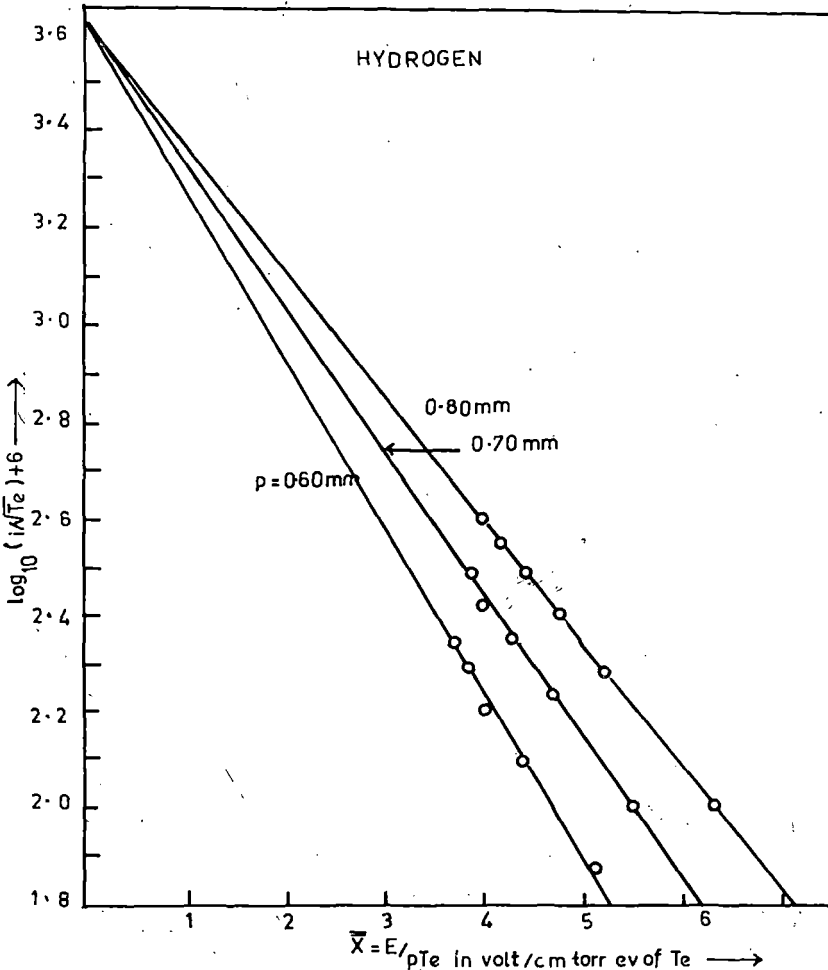


Fig 10 Variation of  $\log_{10}(i/T_e) + 5$  against  $\chi$  (hydrogen)

$$-\frac{1}{2}a \times 0.4343 = \frac{\left(\log \frac{i}{\sqrt{T_e}}\right)_{\chi_2} - \left(\log \frac{i}{\sqrt{T_e}}\right)_{\chi_1}}{\chi_2 - \chi_1}$$

or  $a = 0.4667/\text{volt/cm. mm. Hg. eV}$

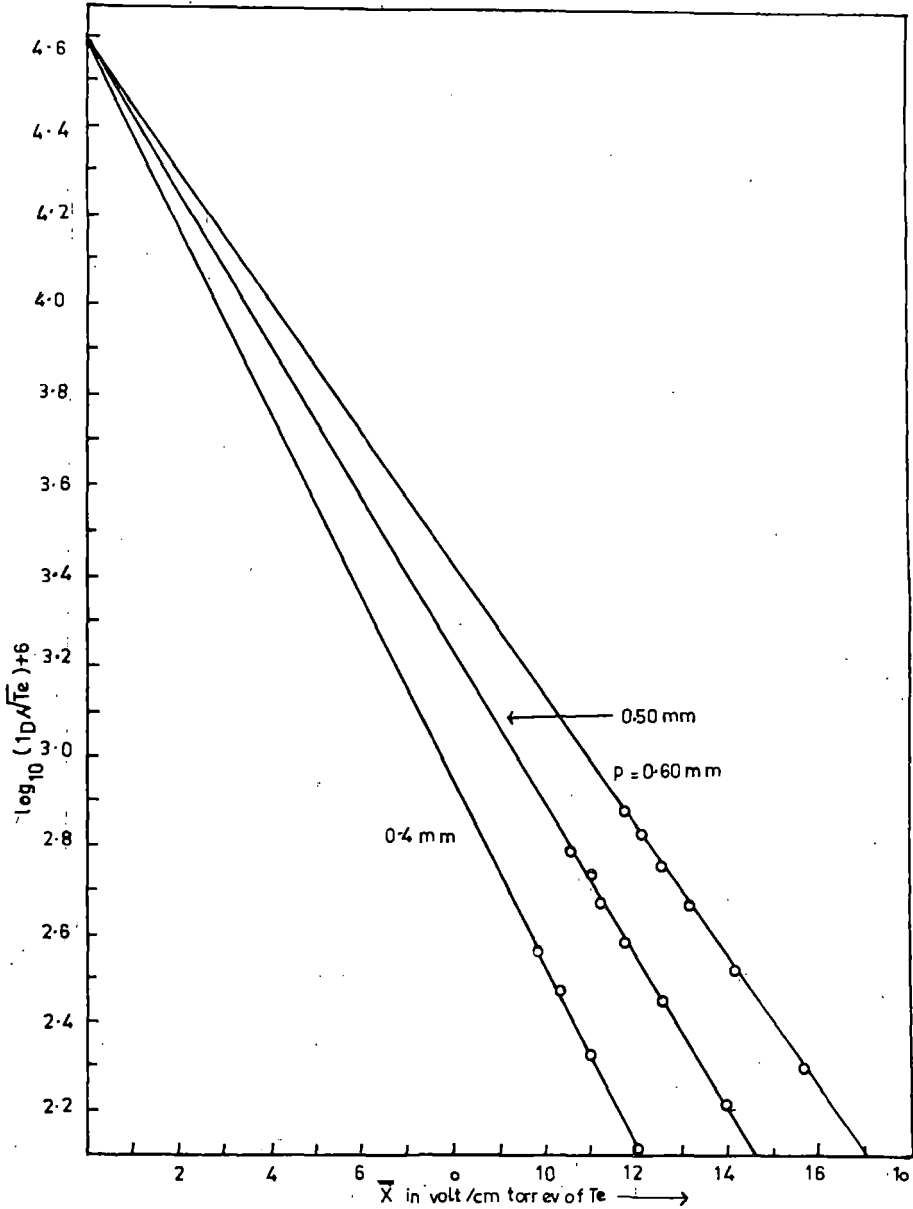


Fig 11 Variation of  $\log_{10}(i/\sqrt{T_e}) + 5$  against  $\chi$  (nitrogen)

and  $\left[ \log \frac{i}{\sqrt{T_e}} + 5 \right]_{x=0} = 3.95$

or  $\left( \frac{i}{T_e^{1/2}} \right)_{x=0} = 8.913 \times 10^{-2}$  in mixed unit.

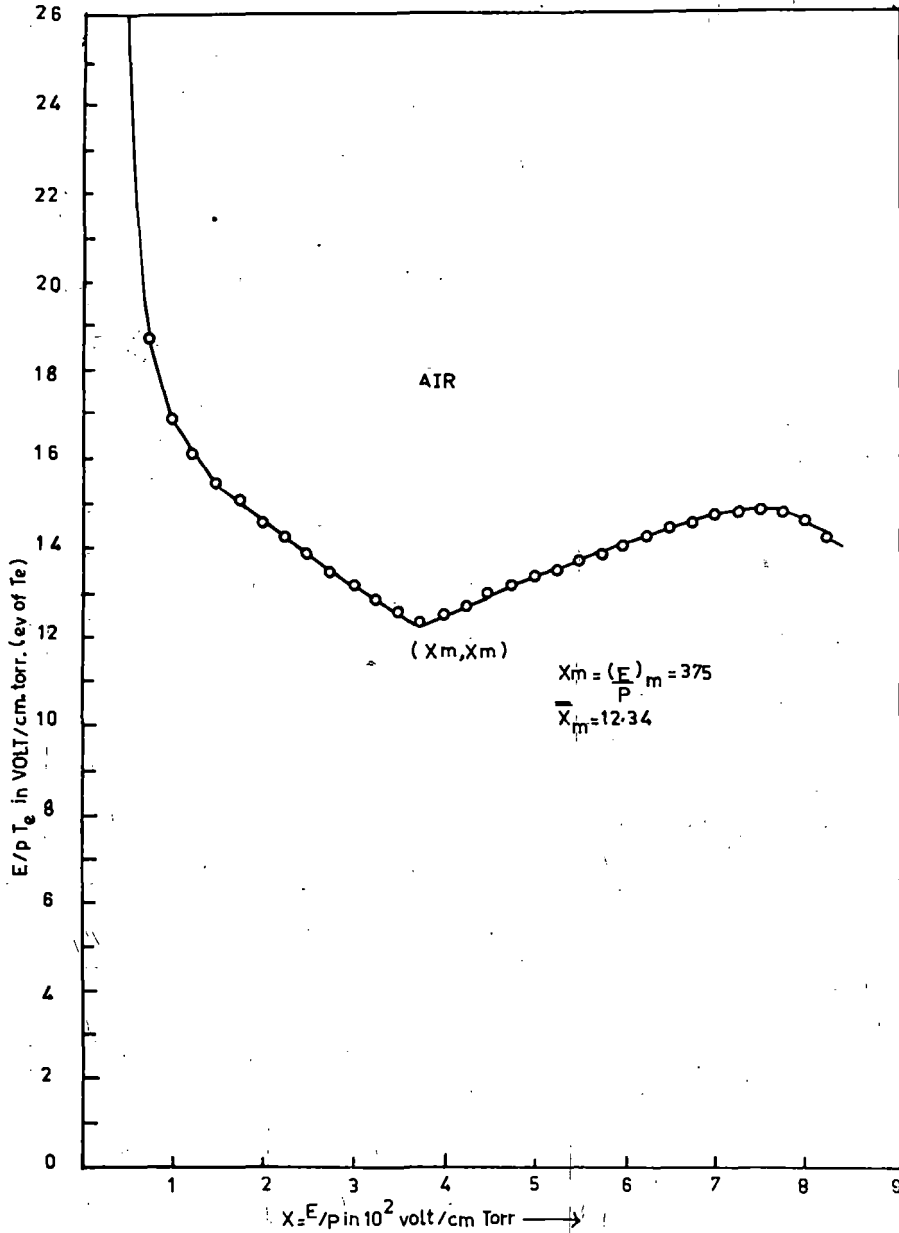


Fig 12 Variation of  $E/p T_e$  against  $E/p$  in case of air

The variation of  $\chi = E/PT_e$  against  $E/P$  is shown in Fig. 12 in case of air, from the relation

$$\chi_0 = -\log \frac{R_0}{0.4343 a} + \chi_m$$

$$\text{and } R_0 = 1.0033 \times 10^{-4}$$

$$\text{and } \chi_m \text{ from the curve} = 12.34 \text{ and } \chi_0 = 32.07$$

$$\text{then } e^{(1/2)\alpha\chi_0} = 1.778 \times 10^{-3}$$

$$\text{and } \left( \frac{i}{\sqrt{T_e}} \right)_{\chi=0} = 1.778 \times 10^{-3} = \beta n_e e^{(1/2)\alpha\chi_0}$$

$$\beta n_e = 5.01 \times 10^{-5} \text{ in mixed unit}$$

$$\beta n_e \text{ in e.s.u.} = \frac{i}{\sqrt{T_e}} \text{ in amp} \sqrt{\text{ev.}}$$

$$= \frac{i \times 3 \times 10^9}{\sqrt{T_e} \times 7740} \text{ e.s.u.}$$

$$= 3.41 \times 10^7$$

$$\text{Hence } \beta n_e \text{ in e.s.u.} = 5.01 \times 10^{-5} \times 3.41 \times 10^7 \text{ e.s.u.}$$

$$= 1.708 \times 10^3$$

$$\beta \text{ in e.s.u.} = eA \sqrt{\frac{3 R_0}{2 m}} K = 1.408 \times 10^{-5}$$

$$A = 6.15 \text{ cm}^2.$$

$$n_e = \frac{\beta n_e}{\beta} = \frac{1.708 \times 10^3}{1.408 \times 10^{-5}} = 1.2 \times 10^8 / \text{c.c.}$$

$$v_d = \sqrt{\frac{3KT_e R}{m 2}} = 3.43 \times 10^7 \text{ cm/sec.}$$

$$v_r = \sqrt{\frac{3KT_e}{m}} = 1.423 \times 10^8 \text{ cm/sec.}$$

for  $T_e = 5.75$  eV.  $R = 0.1164$ .  $L_1 = 11.1 \times 10^{-2}$  cm:

Similarly, the following values have been obtained for hydrogen and nitrogen

$$n_e = 1.04 \times 10^7 / \text{c.c.} \quad v_r = 4.15 \times 10^9 \text{ cm/s.}$$

$$v_d = 5.727 \times 10^8 \text{ cm/sec.} \quad L_1 = 9.9 \times 10^{-1} \text{ cm}$$

$R = 0.5513$  for  $P = 0.70$  mm of Hg and Nitrogen; for  $P = 0.5$  torr,  $T_e = 12.3$  eV.

$$L_1 = 0.1935 \text{ cm.} \quad n_e = 2.56 \times 10^7 / \text{cc}$$

$$v_d = 7.89 \times 10^7 \text{ cm/sec.}$$

$$v_r = 2.068 \times 10^8 \text{ cm/sec.}$$

We can thus conclude that loss of energy in a plasma is due to collision of electrons with atoms and molecules and the variation of  $R$  with  $(E/P)$  has to be taken into account to explain the variation of plasma current with  $(E/P)$ . The theory developed can not only explain the experimentally observed variation of discharge current with  $(E/P)$  but also the calculated values of the plasma parameters such as, electron density, random velocity, electron temperature and electronic mean free path are in quite good agreement with standard literature values.

### References

- 1 A von Engel *Ionised Gases* (Second Edn) Oxford University Press (1964)
- 2 H S W Massey, E H S Burhop and H B Gilbody *Electrons and Ion Impact Phenomena* Vol. III (2nd Edn) Oxford Clarendon Press (1971)
- 3 S N Sen, S K Ghosh and B Ghosh *Indian J pure & appl Phys* **21** (1983) 613.
- 4 S N Sen, C Acharyya, M Gantait and B Bhattacharjee *Int J Electron (GB)* **66** (1989)

## CHAPTER IVA

MEASUREMENT OF PLASMA CURRENT AND  
CAPACITATIVE CURRENT IN A RADIO FREQUENCY  
GAS DISCHARGE

## CHAPTER - IVA

## MEASUREMENT OF PLASMA CURRENT AND THE CAPACITATIVE CURRENT IN A RADIO FREQUENCY GAS DISCHARGE.

When a discharge occurs in a cylindrical glass tube, fitted with internal or external plane parallel electrodes and excited by a radio frequency source then in addition to the two components of discharge current whose phase difference with the applied radio frequency field depends upon the ratio of applied frequency and collision frequency of electrons with neutral atoms there will be a current due to capacitative effect of the electrodes fitted in the discharge tube. If the discharge current is measured by a radio frequency meter then the two currents one due to flow through the plasma and the other flowing due to capacitative effect of the discharge tube (vacuum displacement current) cannot be separated from one another.

Francis and Von Engel (1953) measured the actual current flowing through the discharge where the capacitative current flowing across the external electrodes is balanced by a bridge, the bridge becoming unbalanced when current flows through the gas; with the help of a similar procedure Penfield and Warder (1967) developed and tested an electronic circuit to measure the current in a high voltage radio frequency plasma; Clerk, Earl and New (1970) determined the complex impedance of a radio-frequency discharge excited in hydrogen by a similar

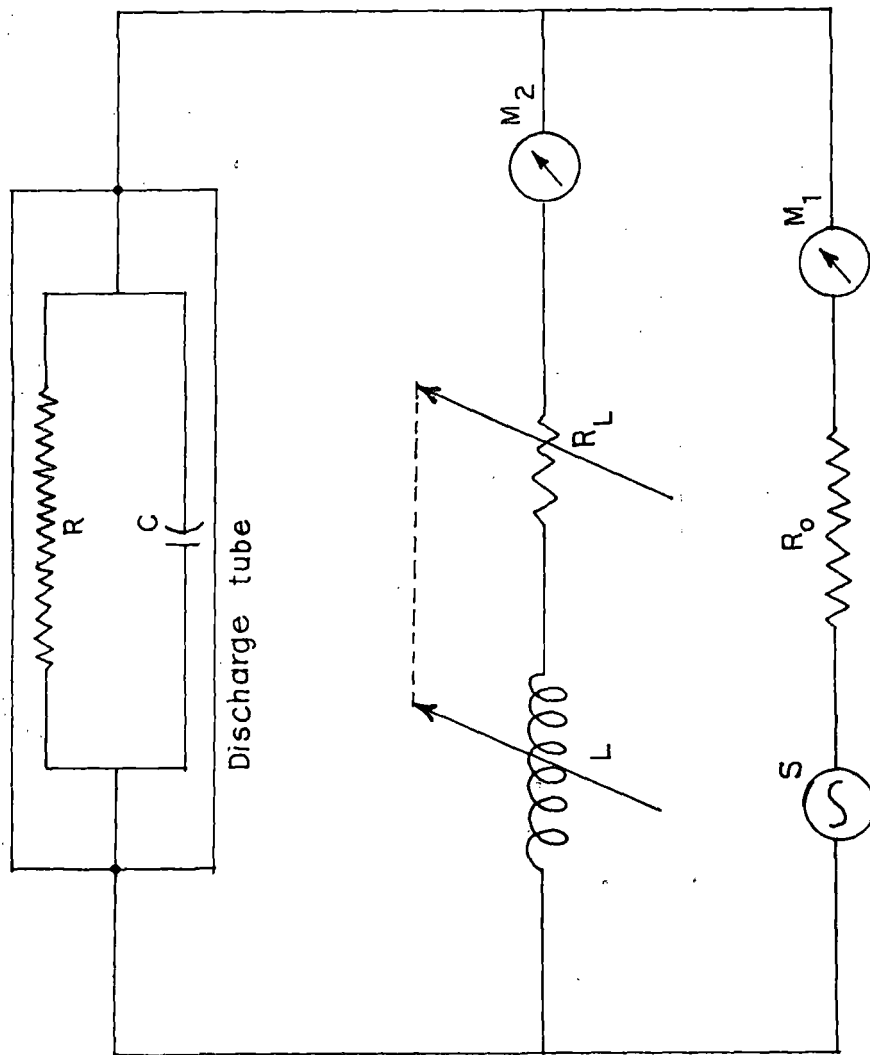


Fig. 4.1

technique. It is however, observed in practice that it is difficult to balance the bridge accurately and a lot of adjustment and screening is necessary throughout the measurements at different ranges of applied voltages. An alternative method of separating and measuring the plasma current and the capacitative current is suggested here.

We consider the circuit as shown in Fig. 4.1,  $R$  is the ohmic resistance of the plasma and  $C$  is the capacity of the discharge tube with two electrodes; in parallel with the discharge tube there is a variable inductance  $L$  in series with a radio frequency milliammeter  $M_2$  whereas  $M_1$  is the radio frequency milliammeter which indicates the main current in the discharge.  $R_L$  is the ohmic resistance of the inductance  $L$ . Hence the total current

$$I = I_R + I_{cp} + I_c + I_L \quad (4.1)$$

where  $I_R$  is the resistive part of the current through the plasma of resistance  $R$ ,  $I_{cp}$  is the capacitative current through the plasma due to capacity of the plasma of capacitance  $C_p$ ,  $I_c$  through the capacity  $C$  and  $I_L$  through the inductance  $L$

$$I = \frac{V}{R} + j\omega C_p V + \frac{V}{R_L + j\omega L} + j\omega C V$$

$$= \frac{V}{R} + \frac{VR_L}{R_L^2 + \omega^2 L^2} + j\omega V(C + C_p) - \frac{j\omega VL}{R_L^2 + \omega^2 L^2}$$

where  $V$  is the radio frequency voltage applied to excite the discharge,

at resonance,

$$I_0 = \frac{V}{R} + \frac{VR_L}{R_L^2 + \omega^2 L^2} \quad (4.2)$$

for resonance

$$C + C_p = \frac{L}{R_L^2 + \omega^2 L^2} \quad (4.3)$$

now  $C_p = \epsilon C$ , where  $\epsilon$  is the dielectric constant of the plasma, and

$$\epsilon = \left[ 1 - \frac{\omega_p^2}{\omega^2 + \gamma_c^2} \right]$$

where  $\omega_p$  is the electron plasma frequency and  $\gamma_c$  is the collision frequency of electrons with neutral molecules, for low density plasma,  $\epsilon$  is almost equal to unity and  $C + C_p = 2C$

So from eqn. (4.3) 
$$C = \frac{L}{2[R_L^2 + \omega^2 L^2]} \quad (4.4)$$

and 
$$I_0 = \frac{V}{R} + \frac{VR_L}{R_L^2 + \omega^2 L^2} = \frac{V}{R} + \frac{2VR_L C}{L} \quad (4.5)$$

In case of glow discharge tubes  $C = \frac{A}{4\pi d\epsilon_0}$ , where  $A$  is the area of the electrodes and  $d$  is the distance between them. If  $A/d$  is not much different from unity.

$$C = \frac{A}{4 \pi d \times 9 \times 10^{11}} \quad F \approx 10^{-12} F.$$

From equation (4.4)

$$\omega^2 L^2 - \frac{L}{2C} + R_L^2 = 0$$

$$L = \frac{\frac{1}{2C} \pm \sqrt{\frac{1}{4C^2} - 4\omega^2 L^2}}{2\omega^2} \quad (\text{at resonance})$$

So there are two values of L for resonance namely  $L_1$  and  $L_2$  and

$$L_1 + L_2 = \frac{1}{2\omega^2 C} = \frac{1}{2 \times 10^{12} \times 10^{-12}} = 0.5 \quad \text{if } \omega = 10^6 \text{ C/sec.}$$

$$\text{and } L_1 L_2 = \frac{R_L^2}{\omega^2}$$

If we design the coil L so that  $R_L$  is of the order of a few ohms then  $L_1 L_2 = 10^{-12} \text{ H}^2$  and as  $L_1 + L_2 = 0.5 \text{ H}$  then  $L_1$  is of the order of one Henry and  $L_2$  is of the order of  $10^{-12}$  Henry. If we use the higher value of L for resonance then the total current at resonance  $I_0$  from eqn. (4.5)

$$I_0 = \frac{V}{R} + \frac{2VR_L C}{L}$$

if it is assumed that the radio frequency voltage is of the order  $10^3$  volts

$$I_o = \frac{V}{R} + \frac{2 \times 10^3 \times 10^{-12}}{1}$$

but as the total discharge current is of the order of a few milliamperes then  $I_o$  the current at resonance is

$$I_o = V/R \quad (4.6)$$

and  $I_c = J\omega CV \approx 10^6 \times 10^{-12} \times 10^3 \approx 10^{-3}$

so the current through the condenser will also be of the order of a few milliamperes.

$$I_c = |2J\omega CV| = \left| - \frac{J\omega VL}{R_L^2 + \omega^2 L^2} \right| \quad (4.7)$$

which can approximately be written as

$$I_c \approx \left| \frac{R_L V}{R_L^2 + \omega^2 L^2} - \frac{J\omega LV}{R_L^2 + \omega^2 L^2} \right| \quad (4.8)$$

As  $R_L \approx 1 \Omega$  and  $L \approx 1$  Henry so the contribution of the 1st term is insignificant with that of the second term. So

$$I_c = \left| \frac{V(R_L - J\omega L)}{R_L^2 + \omega^2 L^2} \right| = \left| \frac{V}{R_L + J\omega L} \right| = I_L \quad (4.9)$$

Hence noting the current at resonance in meter  $M_1$  we can get  $I_R$  and noting the current in meter  $M_2$  we can get  $I_C$ .

So by inserting a variable choke in parallel to the discharge tube and attaining resonance by changing  $L$  we can directly measure the current through the plasma and the capacitative current through the discharge tube separately. It is thus evident that as the capacitative current is of the same order as the current through the plasma, its contribution to the main current should be taken into consideration in calculating the radio frequency conductivity of the ionised gas.

In the paper by Francis and Von Engel (1953) no data has been provided for capacitative current so actual comparison cannot be made. The capacitative effect of plasma has been taken into consideration and as it is a low density plasma the dielectric constant of the plasma is almost equal to unity.

This method is valid for applied radio frequency of the order of few megacycles, voltage of the order of  $10^3$  volts and radio frequency current of the order of a few milliamperes.

R E F E R E N C E S

Francis, G and Von Engel, A., Phil. Trans. Roy. Soc.  
(London) 246A, 1953, 143.

Penfold, A.S. and Warder, Jr. R.C., Rev. Sci. Instruments  
(USA), 38, 1967, 1533.

Clark, J.L., Earl, R.G. and New J., Proc. Int. Conf. Gas  
discharge (London), 1970, 172.

CHAPTER IV B

RADIO FREQUENCY CONDUCTIVITY OF AN IONISED  
GAS IN A TRANSVERSED MAGNETIC FIELD

## Measurement of plasma current and the capacitive current in a radiofrequency gas discharge

S N Sen, M Nath & R N Gupta

Department of Physics, North Bengal University,  
 Siliguri 734 430

Received 31 August 1990; revised received 4 April 1991

By introducing a variable choke in parallel with the discharge tube and noting the resonant current in the main circuit as well as in the parallel circuit the plasma current as well as the capacitive current can be separated and measured. A mathematical formulation of the theory of measurement has been presented.

When a discharge occurs in a cylindrical glass tube, fitted with internal or external plane parallel electrodes and excited by a radio frequency source then in addition to the two components of discharge current whose phase difference with the applied radio frequency field depends upon the ratio of applied frequency and collision frequency of electrons with neutral atoms, there will be a current due to capacitive effect of the electrodes fitted in the discharge tube. If the discharge current is measured by a radio frequency meter then the two currents one due to flow through the plasma and the other flowing due to capacitive effect of the discharge tube (vacuum displacement current) cannot be separated from one another.

Francis and von engel<sup>1</sup> measured the actual current flowing through the discharge where the capacitive current flowing across the external electrodes is balanced by a bridge, the bridge becoming unbalanced when current flows through the gas. By means of a similar procedure Penfield and Warder<sup>2</sup> developed and tested an electronic circuit to measure the current in a high voltage radio frequency plasma. Clark *et al.*<sup>3</sup> determined the complex impedance of a radio-frequency discharge excited in hydrogen by a similar technique. It is however, observed in practice that it is difficult to balance the bridge accurately and a lot of adjustment and screening is necessary throughout the measurements at different ranges of applied voltages. An alternative method of separating and measuring the plasma current and the capacitive current is suggested here.

We consider the circuit as shown in Fig. 1.  $R$  is the ohmic resistance of the plasma and  $C$  is the capacity of the discharge tube with two electrodes; in parallel

with the discharge tube there is a variable inductance  $L$  in series with a radio frequency milliammeter  $M_2$  whereas  $M_1$  is the radio frequency milliammeter which indicates the main current in the discharge.  $R_L$  is the ohmic resistance of the inductance  $L$ . Hence, the total current

$$I = I_R + I_{CP} + I_C + I_L \quad \dots (1)$$

where  $I_R$  is the resistive part of the current through the plasma of resistance  $R$ ,  $I_{CP}$  is the capacitive current through the plasma due to capacity of the plasma of capacitance  $C_p$ ,  $I_C$  through the capacitance  $C$  and  $I_L$  through the inductance  $L$ .

$$I = \frac{V}{R} + J\omega C_p V + \frac{V}{R_L + J\omega L} + J\omega C V$$

$$= \frac{V}{R} + \frac{VR_L}{R_L^2 + \omega^2 L^2} + J\omega V(C + C_p) - \frac{J\omega VL}{R_L^2 + \omega^2 L^2}$$

where  $V$  is the radio frequency voltage applied to excite the discharge.

At resonance

$$I_0 = \frac{V}{R} + \frac{VR_L}{R_L^2 + \omega^2 L^2} \quad \dots (2)$$

For resonance

$$C + C_p = \frac{L}{R_L^2 + \omega^2 L^2} \quad \dots (3)$$

now  $C_p = C\epsilon$ , where  $\epsilon$  is the dielectric constant of the plasma and  $\epsilon = [1 - \omega_p^2 / (\omega^2 + \nu_c^2)]$  where  $\omega_p$  is the electron plasma frequency,  $\omega_p = (4\pi n e^2 / m)^{1/2}$  and  $\nu_c$  is the collision frequency of electrons with neutral molecules. For low density plasma,  $\epsilon$  is almost equal to unity and  $C + C_p = 2C$ .

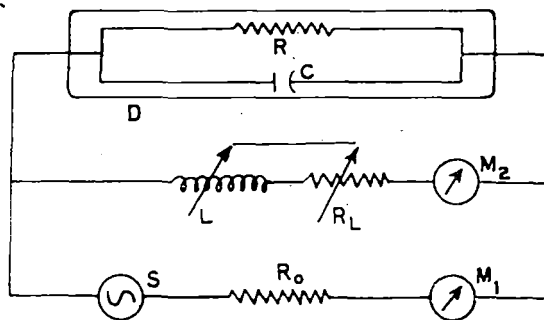


Fig. 1—Circuit for measurement of plasma and capacitive currents

So from Eq. (3)  $C = \frac{L}{2[R_L^2 + \omega^2 L^2]}$  ... (4)

and  $I_0 = \frac{V}{R} + \frac{VR_L}{R_L^2 + \omega^2 L^2} = \frac{V}{R} + \frac{2VR_L C}{L}$  ... (5)

In the case of glow discharge tubes  $C = A/(4\pi d)$ , where  $A$  is the area of the electrodes and  $d$  is the distance between them. If  $A/d$  is not much different from unity, then

$C = \frac{A}{4\pi d \times 9 \times 10^{11}} \text{ F} \approx 10^{-12} \text{ F}$ . From Eq. (4)

$\omega^2 L^2 - \frac{L}{2C} + R_L^2 = 0$

$L = \frac{\frac{1}{2C} \pm \sqrt{\frac{1}{4C^2} - 4\omega^2 L^2}}{2\omega^2}$  (at resonance)

So there are two values of  $L$  for resonance namely  $L_1$  and  $L_2$  and

$L_1 + L_2 = \frac{1}{2\omega^2 C} = \frac{1}{2 \times 10^{12} \times 10^{-12}} \approx 0.5$  if  $\omega = 10^6$

and  $L_1 L_2 = \frac{R_L^2}{\omega^2}$

If we design the coil  $L$  so that  $R_L$  is of the order of a few ohms then  $L_1 L_2 \approx 10^{-12}$  and as  $L_1 + L_2 \approx 0.5$  then  $L_1$  is of the order of one henry and  $L_2$  is of the order of  $10^{-12}$  H. If we use the higher value of  $L$  for resonance then the total current at resonance  $I_0$  from Eq. (5) is:

$I_0 = \frac{V}{R} + \frac{2VR_L C}{L}$

If it is assumed that the radio frequency voltage is of the order  $10^3 \text{ V}$

$I_0 = \frac{V}{R} + \frac{2 \times 10^3 \times 10^{-12}}{1}$

but as the total discharge current is of the order of a few milliamperes then  $I_0$ , the current at resonance is

$I_0 = V/R$  ... 6

and  $I_C = J\omega CV \approx 10^6 \times 10^{-12} \times 10^3 \approx 10^{-3} \text{ A}$

So the current through the condenser will also be of the order of a few milliamperes.

$I_C = J\omega CV = -\frac{J\omega VL}{R_L^2 + \omega^2 L^2}$  ... (7)

which can approximately be written as

$I_C = \frac{R_L V}{R_L^2 + \omega^2 L^2} - \frac{J\omega VL}{R_L^2 + \omega^2 L^2}$  ... (8)

As  $R_L \approx 1 \Omega$  and  $L \approx 1 \text{ H}$ , the contribution of the first term is insignificant compared to the second term

$I_C = \frac{V(R_L - J\omega L)}{R_L^2 + \omega^2 L^2} = \frac{V}{R_L + J\omega L} = I_L$  ... (9)

Hence noting the current at resonance in meter  $M_1$  we can get  $I_R$  and noting the current in meter  $M_2$  we can get  $I_C$ .

So by inserting a variable choke in parallel to the discharge tube and attaining resonance by changing  $L$  we can directly measure the current through the plasma and the capacitive current through the discharge tube separately. It is thus evident that as the capacitive current is of the same order as the current through the plasma, its contribution to the main current should be taken into consideration in calculating the radio frequency conductivity of the ionised gas.

In the paper by Francis and von Engel<sup>1</sup> no data were provided for capacitive current; so actual comparison cannot be made. We are taking measurements and the results will be reported in our future communication.

The capacitive effect of plasma has been taken into consideration and as it is a low density plasma, the dielectric constant of the plasma is almost equal to unity.

This method is valid for applied radiofrequency of the order of few megacycles, voltage of the order of  $10^3 \text{ V}$  and radio frequency current of the order of a few milliamperes.

**References**

- 1 Francis G & von Engel A. *Phil Trans Roy Soc A (London)*, 246 (1953) 143.
- 2 Penfield A S & Warder Jr R C. *Rev Sci Instrum (USA)*, 38 (1967) 1533.
- 3 Clark J L, Earl R G & New J. *Proceedings of the international conference on gas discharge, London, (1970) 172.*

## CHAPTER - IV

## PART B

RADIO FREQUENCY CONDUCTIVITY OF AN IONISED  
GAS IN A TRANSVERSE MAGNETIC FIELDINTRODUCTION

The real part of radio frequency conductivity  $\sigma_r$  of ionised gases (air and nitrogen) was measured by Sen and Ghosh (1966) at various pressures (5 to  $300\mu$ ) and also at values of discharge current (10, 20 and 30 m.a). It was observed that  $\sigma_r$  increases with pressure, becomes a maximum at a pressure of  $30\mu$  in case of air and at a pressure of  $84\mu$  in case of nitrogen. From theoretical analysis of the results the values of  $n$  (electron density)  $v_r$  the random velocity and  $T_e$  the electron temperature were obtained. The nature of variation of  $n$  and  $T_e$  were explained. A radio frequency probe was used for measurement, it was assumed that the ionised gas acts like a lossy dielectric and a mathematical analysis was presented for calculation of  $\sigma_r$  by representing the ionised column as an equivalent circuit of capacitance and a lossy resistance.

Gupta and Mandal (1967) also measured the real part of radio frequency conductivity in the case of air and carbon dioxide by the same method as adopted by Sen and Ghosh (1966) over a pressure range of a few microns to 0.3 torr but in presence of some fixed values of transverse magnetic field

( $H = 0, 275, 410, 550$  and  $680$  G). It was observed that conductivity decreases in presence of magnetic field for all values of pressure and the pressure at which the conductivity becomes a maximum increases with the increase of the magnetic field. The theory put forward by Gilardini (1959) was modified by the authors to explain the experimental results quantitatively.

Sen and Gupta (1969) measured the real part of r.f. conductivity in case of helium, neon and argon over the range of pressure from a few microns to  $700\mu$  and under an external magnetic field varying from zero to 550 gauss. From the data obtained the plasma parameters such as electron density, collision frequency and electron temperature and their variation with magnetic field has been obtained.

Ghosal, Nandi and Sen (1976) measured the azimuthal radio frequency conductivity of an arc plasma by measuring the reflected resistance of a primary coil wound around a mercury arc tube and studied its variation with increasing arc current. It was however, pointed out that the azimuthal conductivity measurement by this method is possible only when the conductivity of the plasma is fairly high.

Most of the measurements reported here refer to investigation of  $\sigma_r$  the real part of radio frequency conductivity and its variation with magnetic field and pressure. Little work has been reported regarding the variation of the r.f. current which is out of phase with the real part of the radio frequency

current by  $\pi/2$ . This current will also vary with pressure and magnetic field. The object of the present investigation is to study the variation of this current in presence of a variable transverse magnetic field at a constant pressure.

### THEORETICAL ANALYSIS

The radio frequency current  $I_{rf}$  in a transverse magnetic field is given by

$$\begin{aligned}
 I_{rf} &= \frac{ne^2}{m} \frac{\nu_c + J\omega}{(\nu_c + J\omega)^2 + \omega_B^2} E_0 e^{J\omega t} \\
 &= \frac{ne^2}{m} E_0 e^{J\omega t} \frac{\nu_c (\nu_c^2 + \omega_B^2 + \omega^2) + J\omega(\omega_B^2 - \omega^2 - \nu_c^2)}{(\nu_c^2 + \omega_B^2 - \omega^2)^2 + 4\nu_c^2 \omega^2} \\
 &= (I_{rf})_{H \text{ real}} + J(I_{rf})_{iH}
 \end{aligned}$$

So that

$$(I_{rf})_{iH} = \frac{ne^2}{m} E_0 e^{J\omega t} \frac{\omega(\omega_B^2 - \omega^2 - \nu_c^2)}{(\nu_c^2 + \omega_B^2 - \omega^2)^2 + 4\nu_c^2 \omega^2} \quad (4.10)$$

where  $(I_{rf})_{rH}$  and  $(I_{rf})_{iH}$  are the real and imaginary parts of the radio frequency current.

where  $\nu_c$  is the collision frequency,  $\omega$  the frequency of the applied r.f. field,  $\omega_B$  is the electron cyclotron frequency and  $n$  is the electron density. At this stage we make some assumptions

(a) the plasma is collision dominated so that  $\nu_c \gg \omega$  if the measurement is carried out at radio frequency.

(b) Due to the presence of the magnetic field the electric field is modified to  $E_H$  where  $E_H = E (1 + C_1 H^2 / P^2)^{1/2}$  (Beckman, 1948, Sen and Gupta (1971), where  $C_1 = (\frac{e}{m} \frac{L}{v_r})^2$  where  $L$  is the mean free path of the electron in the gas at 1 torr and  $v_r$  is the random velocity of the electron.

So replacing  $E_0$  by  $E_H$ ,

$$(I_{rf})_{iH} = \frac{ne^2}{m} E_H e^{J\omega t} \frac{\omega(\omega_B^2 - \nu_c^2)}{(\nu_c^2 + \omega_B^2)^2 + 4\nu_c^2 \omega^2} \quad (4.11)$$

and  $(I_{rf})_i$  in absence of magnetic field

$$(I_{rf})_i = \frac{ne^2}{m} E_0 e^{J\omega t} \frac{\omega}{\nu_c^2 + \omega^2} \quad (4.12)$$

Putting  $E_H = E_0 (1 + C_1 H^2 / P^2)^{1/2}$  we get from equations (4.11)

and (4.12)

$$\frac{(I_{rf})_{iH}}{(I_{rf})_i} = \left(1 + C_1 \frac{H^2}{P^2}\right)^{1/2} \frac{(\omega_B^2 - \nu_c^2) \nu_c^2}{(\nu_c^2 + \omega_B^2)^2 + 4\nu_c^2 \omega^2}$$

$$\text{now } w_B = \frac{eH}{m} \quad \text{so, } H^2 = \frac{w_B^2 m^2}{e^2}$$

$$\begin{aligned} \text{and } C_1 \frac{H^2}{p^2} &= \frac{e^2 L^2}{m^2 v_r^2} \cdot \frac{1}{p^2} \cdot \frac{w_B^2 m^2}{e^2} \\ &= \frac{L^2}{v_r^2 p^2} w_B^2 = \alpha w_B^2 \end{aligned}$$

where  $L$  is the mean free path of the electron at a pressure 1 torr.

where  $\alpha = L^2 / v_r^2 p^2$  is a constant at a constant pressure.

We can now find the variation of  $(I_{rf})_{iH} / (I_{rf})_i$  with  $w_B$ . After a detailed calculation it can be shown that

$$\begin{aligned} \frac{d}{dw_B} \left[ \frac{(I_{rf})_{iH}}{(I_{rf})_i} \right] &= \frac{7}{2} \alpha w_B^6 + \left( \frac{5}{2} \alpha \nu_C^2 + 3 \right) w_B^4 \\ &+ \left[ 6\alpha \nu_C^2 w^2 - \frac{3}{2} \alpha \nu_C^4 + 2\nu_C^2 \right] w_B^2 \\ &- \frac{\alpha}{2} \nu_C^6 - 2\alpha \nu_C^4 w^2 - \nu_C^4 + 4\nu_C^2 w \end{aligned} \quad (4.13)$$

To find whether  $(I_{rf})_{iH}$  shows any maximum or minimum value with the variation of  $w_B$ , i.e.,  $H$  we can put the equation (4.13) in the form

$$y^3 + py^2 + qy + r = 0 \quad (4.14)$$

$$\text{where } w_B^2 = y, \quad p = \frac{5\alpha \gamma_C^2 + 6}{7\alpha}$$

$$q = \frac{12\alpha \gamma_C^2 w^2 - 3\alpha \gamma_C^4 + 4\gamma_C^2}{7\alpha}$$

$$r = \frac{8\gamma_C^2 w^2 - \alpha \gamma_C^6 - 4\alpha \gamma_C^4 w^2 - 2\gamma_C^4}{7\alpha}$$

The equation can be reduced to the form  $x^3 + ax + b = 0$  by substituting for  $y$  the value of  $(x - \frac{p}{3})$

$$\text{where } a = \frac{1}{3} [3q - p^2]$$

$$b = \frac{1}{27} [2p^3 - 9pq + 27r]$$

and the solutions are

$$x = A+B, \quad -\frac{A+B}{2} + \frac{A-B}{2}\sqrt{-3} \quad \text{and} \quad -\frac{A+B}{2} - \frac{A-B}{2}\sqrt{-3}$$

$$\text{where } A = \left( -\frac{b}{2} + \sqrt{\frac{b^2}{4} + \frac{a^3}{27}} \right)^{1/3}$$

$$B = \left( -\frac{b}{2} - \sqrt{\frac{b^2}{4} + \frac{a^3}{27}} \right)^{1/3}$$

To calculate the value of  $w_B$  at which the ratio  $(\sigma_{rf})_{iH}/(\sigma_{rf})_i$  becomes a maximum or a minimum. We take the case of air at  $P = 0.5$  torr,  $E = \frac{400-300}{10}$  volts/cm where 400 volts is the striking voltage and 300 volts is the combined anode and cathode fall and the distance between cathode and anode is 10 cm. So  $E/P = 20$  volts/cm. torr; from Von Engel (1957) for

air for  $E/P = 20$  volts/cm torr

$$T_e = 2.5 \text{ eV}$$

$$v_r = 8.414 \times 10^7 \text{ cm/s.}$$

$$d = L^2/P^2 v_r^2 \quad \text{and } L = 1/15 \text{ Von Engel (1957)}$$

$$\text{So } \alpha = 2.511 \times 10^{-18}$$

$$\delta_c = v_r P/L = 6.31 \times 10^8.$$

$$\omega = 10 \text{ MC/s}$$

and the values of  $P$ ,  $q$  and  $r$  have been calculated

$$P = 6.246 \times 10^{17} \quad q = 5.045 \times 10^{34}, \quad r = -26.3 \times 10^{51}.$$

$$a = -7.96 \times 10^{34} \quad b = -18.6 \times 10^{51},$$

$$A = 2.598 \times 10^{17} \quad B = 1.022 \times 10^{17}$$

$$\omega_B = 6 \times 10^8 \quad H_{\max} = 25 \text{ gauss}$$

and it can be shown  $\frac{d^2}{d\omega^2} [(\sigma_{rf})_{iH}/(\sigma_{rf})_i]$  is positive and variation of  $\sigma_{rH}$  with  $H$  will show a minimum at a certain value of  $H$ .

### DISCUSSION

It is thus possible to calculate analytically the value of the magnetic field at which the radio frequency conductivity (imaginary part) becomes a minimum and such calculations can be carried out for different gases for different pressure and frequency of the exciting radio frequency field. The effect of the magnetic field is to increase the axial electric field and

at the same time reduce the charge particle density along the axis, but the rate of increase of the axial electric field predominates the loss of <sup>electron</sup> density at the axis for higher values of magnetic field and so the radio frequency conductivity increases at higher magnetic field values.

R E F E R E N C E S

Sen, S.N. and Ghosh, A.K., Ind. J. ur. Pure & Appl. Phys.  
4, 70, 1966.

Gupta, R.N. and Mandal, S.K., Ind. J. Phys., 41, 251, 1967.

Gilardini, A., Nuovo Cimento Supplement. 13, 9, 1959.

Sen, S.N. and Gupta, R.N., Ind. J. Pure & Appl. Phys.  
7, 117, 1969.

Ghosal, S.K., Nandi, G.P. and Sen, S.N., International  
J. Electronics, (G.B) 41, 509, 1976.

Von Engel, A., Ionised Gases (Clarendon Press, Oxford,  
1959.

Beckman, L., Proc. Phys. Soc. (Lond) 61, 515, 1948.

Sn, S.N. and Gupta, R.N., Jour. Phys. Appl. Phys. (G.B)  
4, 510, 1971.

CHAPTER IVC

PROPAGATION OF MICROWAVES THROUGH A PLASMA  
FILLED WAVE-GUIDE - A POSSIBLE DIAGNOSTIC METHOD

## CHAPTER - IV

PART CPROPAGATION OF MICROWAVES THROUGH A PLASMA FILLED  
WAVE GUIDE - A POSSIBLE DIAGNOSTIC METHOD.INTRODUCTION

The method of measurement of plasma parameters such as the charged particle density and the collision frequency of electrons with neutral atoms by propagating a beam of microwaves through the plasma under investigation is a standard diagnostic technique. The method consists in measuring the attenuation constant  $\alpha$  and the phase constant  $\beta$  of the propagating microwave signal which can be mathematically related with the collision frequency and charged particle density in a plasma. Our object is to show in this work that a variation of the above method of propagation of microwave through a wave guide which has been filled with the plasma can yield some additional information regarding the radio frequency conductivity and dielectric constant of the plasma.

THEORETICAL ANALYSIS

We consider a rectangular wave guide of length  $x_0$  width  $z_0$  and height  $y_0$  the origin of the coordinates being  $x = y = z = 0$  and the wave is propagating along the  $x$  axis. We shall further assume that the wave guide is infinitely long and no reflection from the adjoining sides is taking place. We shall first deduce

the electric and magnetic field configuration within the wave guide for the transverse electric mode and applying the boundary conditions deduce the cut off frequency for both the cases namely (I) when the guide is filled with air as dielectric (II) when a plasma is the dielectric. From Maxwell's equation we have with  $\sigma$ ,  $\mu$  and  $\epsilon$  as the conductivity, permeability and dielectric constant

$$\frac{\partial H_z''}{\partial y} - \frac{\partial H_y''}{\partial z} = (\sigma + j\omega\epsilon) E_x''$$

$$\frac{\partial H_x''}{\partial z} - \frac{\partial H_z''}{\partial x} = (\sigma + j\omega\epsilon) E_y''$$

$$\frac{\partial H_y''}{\partial x} - \frac{\partial H_x''}{\partial y} = (\sigma + j\omega\epsilon) E_z''$$

$$\frac{\partial E_z''}{\partial y} - \frac{\partial E_y''}{\partial z} = -\mu j\omega H_x''$$

$$\frac{\partial E_x''}{\partial z} - \frac{\partial E_z''}{\partial x} = -\mu j\omega H_y''$$

$$\frac{\partial E_y''}{\partial x} - \frac{\partial E_x''}{\partial y} = -\mu j\omega H_z''$$

(4.15)

If  $\gamma$  is propagation constant and the direction of propagation is x axis we can write

$$H'' = H' e^{-\gamma x} \quad \text{and} \quad E'' = E' e^{-\gamma x}$$

Then from equation (4.15)

$$\begin{aligned}
 \frac{\partial H'_z}{\partial y} - \frac{\partial H'_y}{\partial z} &= (\sigma + j\omega\epsilon) E'_x \\
 \frac{\partial H'_x}{\partial z} + \gamma H'_z &= (\sigma + j\omega\epsilon) E'_y \\
 -\gamma H'_y - \frac{\partial H'_x}{\partial y} &= (\sigma + j\omega\epsilon) E'_z \\
 \frac{\partial E'_z}{\partial y} - \frac{\partial E'_y}{\partial z} &= -j\omega\mu H'_x \\
 \frac{\partial E'_x}{\partial z} + \gamma E'_z &= -j\omega\mu H'_y \\
 \gamma E'_y + \frac{\partial E'_x}{\partial y} &= j\omega\mu H'_z
 \end{aligned} \tag{4.16}$$

for T.E. wave  $E'_x = 0$

Then from equation (4.16)

$$\begin{aligned}
 \frac{\partial H'_z}{\partial y} - \frac{\partial H'_y}{\partial z} &= 0 \\
 \frac{\partial H'_x}{\partial z} + \gamma H'_z &= (\sigma + j\omega\epsilon) E'_y \\
 \gamma E'_y + \frac{\partial H'_x}{\partial z} &= -(\sigma + j\omega\epsilon) E'_z \\
 \frac{\partial E'_z}{\partial y} - \frac{\partial E'_y}{\partial z} &= -j\omega\mu H'_x \\
 \gamma E'_z &= -j\omega\mu H'_y \\
 \gamma E'_y &= -j\omega\mu H'_z
 \end{aligned} \tag{4.17}$$

utilizing these equations it can be deduced that

$$\frac{\partial^2 H'_x}{\partial y^2} + \frac{\partial^2 H'_x}{\partial z^2} = - [\gamma^2 - (\sigma + j\omega\epsilon) j\omega\mu] H'_x \quad (4.18)$$

when there is no plasma,  $\sigma = 0 \ll \omega\epsilon$

$$\text{so, } \frac{\partial^2 H'_x}{\partial y^2} + \frac{\partial^2 H'_x}{\partial z^2} = - (\gamma^2 + \omega^2\mu\epsilon) H'_x \quad (4.19)$$

By the principle of separation of variables the equation can be solved and we get

$$H'_x = A \cos(\sqrt{A_1} y) \cos(\sqrt{A_2} z) \quad (4.20)$$

$$\text{where } A_1 + A_2 = \gamma^2 + \omega^2\mu\epsilon \quad (4.21)$$

and A is a constant.

Then it can be shown that

$$H'_y = A \frac{\gamma}{\gamma^2 + \omega^2\mu\epsilon} \sqrt{A_1} \sin(\sqrt{A_1} y) \cos(\sqrt{A_2} z) \quad (4.22)$$

$$H'_z = A \frac{\gamma}{\gamma^2 + \omega^2\mu\epsilon} \sqrt{A_2} \cos(\sqrt{A_1} y) \sin(\sqrt{A_2} z) \quad (4.23)$$

$$E'_y = A \frac{j\omega\mu}{\gamma^2 + \omega^2\mu\epsilon} \sqrt{A_2} \cos(\sqrt{A_1} y) \sin(\sqrt{A_2} z) \quad (4.24)$$

$$E'_z = -\frac{A j\omega\mu}{\gamma^2 + \omega^2\mu\epsilon} \sqrt{A_1} \sin(\sqrt{A_1} y) \cos(\sqrt{A_2} z) \quad (4.25)$$

Applying the boundary conditions

$E'_z = 0$  at  $y = 0$  and at  $y = y_0$ , we get

$$\sqrt{A_1} y_0 = m\pi \quad \text{or, } A_1 = \frac{m^2 \pi^2}{y_0^2} \quad (4.26)$$

and  $E'_y = 0$  at  $z = 0$  and  $z = z_0$

$$\sqrt{A_2} z_0 = n\pi \quad \text{or } A_2 = \frac{n^2 \pi^2}{z_0^2} \quad (4.27)$$

from (4.21), (4.26) and (4.27) we get  $\gamma^2 = \left(\frac{m\pi}{y_0}\right)^2 + \left(\frac{n\pi}{z_0}\right)^2 - \omega^2 \mu \epsilon$

$$\gamma = \alpha + j\beta = \sqrt{\left(\frac{m\pi}{y_0}\right)^2 + \left(\frac{n\pi}{z_0}\right)^2 - \omega^2 \mu \epsilon}$$

If  $\frac{m^2 \pi^2}{y_0^2} + \frac{n^2 \pi^2}{z_0^2} > \omega^2 \mu \epsilon$ ,  $\alpha$  is finite,  $\beta = 0$   
no propagation

If  $\frac{m^2 \pi^2}{y_0^2} + \frac{n^2 \pi^2}{z_0^2} < \omega^2 \mu \epsilon$ ,  $\alpha = 0, \beta$  is finite  
there is propagation

The critical frequency at which attenuation stops and transmission begins is

$$\omega_c = \sqrt{\left[\left(\frac{m\pi}{y_0}\right)^2 + \left(\frac{n\pi}{z_0}\right)^2\right]} / \mu \epsilon \quad (4.28)$$

When the wave guide is filled with plasma we have,

$$\frac{\partial^2 H'_x}{\partial y^2} + \frac{\partial^2 H'_x}{\partial z^2} = - \left\{ \gamma^2 - (\sigma + j\omega\epsilon) j\omega\mu \right\} H'_x \quad (4.29)$$

where  $\sigma$  is the plasma conductivity  $\epsilon_p$  is the dielectric constant of the plasma, it being assumed  $\mu$  is not much different for a plasma than it is for air. In the same manner as before deducing the values of two tangential electric components and applying the boundary conditions we get

$$\gamma = \alpha + j\beta = \sqrt{\left[ \frac{m^2 \pi^2}{y_0^2} + \frac{n^2 \pi^2}{z_0^2} + j\omega\mu\sigma - \omega^2\mu\epsilon_p \right]} \quad (4.30)$$

$$\text{If } \frac{m^2 \pi^2}{y_0^2} + \frac{n^2 \pi^2}{z_0^2} > (\omega^2\mu\epsilon_p - j\omega\mu\sigma)$$

$\alpha$  will be finite.

$$\text{If } \frac{m^2 \pi^2}{y_0^2} + \frac{n^2 \pi^2}{z_0^2} < (\omega^2\mu\epsilon_p - j\omega\mu\sigma)$$

then  $\beta$  will be finite and cut off will occur when

$$\omega_{cp}^2 \mu \epsilon_p - j\omega\mu\sigma = \frac{m^2 \pi^2}{y_0^2} + \frac{n^2 \pi^2}{z_0^2} \quad (4.31)$$

where  $\omega_{cp}$  is the cut off frequency when plasma is present.

In absence of plasma

$$\omega_C^2 \mu \epsilon = \frac{m^2 \pi^2}{y_0^2} + \frac{n^2 \pi^2}{z_0^2} \quad \text{form (4.28)}$$

$$\text{So, } \omega_{cp}^2 \mu \epsilon_p - J\omega\mu\sigma = \omega_C^2 \mu \epsilon$$

$$\omega_{cp}^2 \frac{\epsilon_p}{\epsilon} - \omega_C^2 = J\omega\sigma/\epsilon \quad (4.32)$$

when there is no plasma  $\epsilon_p = \epsilon$  and  $\sigma = 0$

$$\text{So, } \omega_{cp}^2 = \omega_C^2 \quad (4.33)$$

We have further from (4.30)

$$\alpha^2 - \beta^2 + 2\alpha J\beta = \frac{m^2 \pi^2}{y_0^2} + \frac{n^2 \pi^2}{z_0^2} + J\omega\mu\sigma - \omega^2 \mu \epsilon_p$$

$$\text{and } \sigma = \sigma_r - J\sigma_i \quad (4.34)$$

where  $\sigma_r$  is the real part of conductivity and  $\sigma_i$  is the imaginary part and  $\epsilon_p = \epsilon' - J\epsilon''$  and the symbols have the same significance as in the case of  $\sigma$ ; then from equation

(4.30)

$$\begin{aligned} \alpha^2 - \beta^2 + 2\alpha J\beta &= \frac{m^2 \pi^2}{y_0^2} + \frac{n^2 \pi^2}{z_0^2} + J\omega\mu(\sigma_r - J\sigma_i) \\ &\quad - \omega^2 \mu (\epsilon' - J\epsilon'') \\ &= \frac{m^2 \pi^2}{y_0^2} + \frac{n^2 \pi^2}{z_0^2} + J\omega\mu\sigma_r + \omega\mu\sigma_i - \omega^2 \mu \epsilon' + J\omega^2 \mu \epsilon'' \end{aligned}$$

$$\text{then } \alpha^2 - \beta^2 = \frac{m^2 \pi^2}{y_0^2} + \frac{n^2 \pi^2}{z_0^2} + \omega \mu \sigma_i - \omega^2 \mu \epsilon' \quad (4.35)$$

$$\text{and } 2\alpha\beta = \omega \mu \sigma_r + \omega^2 \mu \epsilon'' \quad (4.36)$$

We have further [equation 4.32]

$$\omega_{cp}^2 \frac{\epsilon' - J\epsilon''}{\epsilon} - \omega_c^2 = \frac{J\omega}{\epsilon} (\sigma_r - J\sigma_i)$$

$$\omega_{cp}^2 \frac{\epsilon'}{\epsilon} - J\omega_{cp}^2 \frac{\epsilon''}{\epsilon} = \omega_c^2 + \frac{J\omega\sigma_r}{\epsilon} + \frac{\omega\sigma_i}{\epsilon}$$

$$\omega_{cp}^2 \frac{\epsilon'}{\epsilon} = \omega_c^2 + \frac{\omega\sigma_i}{\epsilon}$$

(4.37)

$$\text{and } \omega_{cp}^2 \epsilon'' = \omega\sigma_r$$

$$\text{So, } \epsilon'' = \frac{\omega}{\omega_{cp}^2} \sigma_r \quad (4.38)$$

From the relation (4.36) and (4.38)

$$\begin{aligned} 2\alpha\beta &= \omega\mu\sigma_r + \omega^2\mu\epsilon'' \\ &= \omega\mu\sigma_r + \frac{\omega^2\mu\omega}{\omega_{cp}^2} \sigma_r \\ &= \sigma_r \left[ 1 + \frac{\omega^2}{\omega_{cp}^2} \right] \mu\omega \end{aligned} \quad (4.39)$$

$$\text{so, } \sigma_r = \frac{2\alpha\beta}{\omega\mu \left[ 1 + \frac{\omega^2}{\omega_{cp}^2} \right]}$$

$$\text{and } \epsilon'' = \frac{\omega}{\omega_{cp}^2 \omega\mu} \left[ \frac{2\alpha\beta}{1 + \frac{\omega^2}{\omega_{cp}^2}} \right]$$

$$= \frac{2\alpha\beta}{\mu[\omega^2 + \omega_{cp}^2]}$$

(4.40)

We have from eqn. (4.37)

$$\epsilon' = \epsilon \frac{\omega_c^2}{\omega_{cp}^2} + \frac{\omega\sigma_i}{\omega_{cp}^2}$$

and putting the value of  $\epsilon'$  in eqn.(4.35)

$$\omega\mu \left[ \frac{\omega_{cp}^2 - \omega^2}{\omega_{cp}^2} \right] \sigma_i = \alpha^2 - \beta^2 + \frac{\omega^2}{c^2} \cdot \frac{\omega_c^2}{\omega_{cp}^2} - \left( \frac{m^2 \pi^2}{y_0^2} + \frac{n^2 \pi^2}{z_0^2} \right)$$

$$\text{or } \sigma_i = \frac{1}{\omega\mu} \left[ \left\{ \frac{\omega_{cp}^2}{\omega_{cp}^2 - \omega^2} \right\} (\alpha^2 - \beta^2) + \frac{\omega^2}{c^2} \cdot \frac{\omega_c^2}{\omega_{cp}^2 - \omega^2} - \frac{\omega_{cp}^2}{\omega_{cp}^2 - \omega^2} \left\{ \frac{m^2 \pi^2}{y_0^2} + \frac{n^2 \pi^2}{z_0^2} \right\} \right]$$

(4.41)

and similarly it can be shown that

$$\epsilon' = \epsilon \frac{\omega_c^2}{\omega_{cp}^2} + \frac{\alpha^2 - \beta^2}{\mu(\omega_{cp}^2 - \omega^2)} + \frac{1}{\mu} \frac{1}{\omega_{cp}^2 - \omega^2} \cdot \frac{\omega^2}{c^2} \cdot \omega_c^2 / \omega_{cp}^2 - \frac{1}{\mu} \cdot \frac{1}{(\omega_{cp}^2 - \omega^2)} \left\{ \frac{m^2 \pi^2}{y_0^2} + \frac{n^2 \pi^2}{z_0^2} \right\}$$

(4.42)

DISCUSSION

Equations (4.39), (4.40), (4.41) and (4.42) show that  $\sigma_r, \epsilon'', \sigma_i, \epsilon'$  can be calculated in terms of the quantities which can be measured experimentally. The first measurement consists in determining the cut off frequency of the wave guide with air as dielectric by sending a microwave signal whose frequency can be varied. The frequency at which transmission stops and reflection begins is the cut off frequency  $\omega_c$ . The same procedure is applied when the plasma is formed within the wave guide which provides us with the value of the cut off frequency  $\omega_{cp}$ . The second part of the experiment consists in setting up a microwave interferometer with one branch consisting of a calibrated attenuator and a calibrated phase shifter while the other branch propagates the microwave signal the frequency of which is larger than the cut off frequency  $\omega_{cp}$ . By the standard microwave technique  $\alpha$  and  $\beta$  can be obtained. Thus by measuring  $\omega_c, \omega_{cp}, \beta$  and  $\alpha$  and applying equations (4.39), (4.40), (4.41) and (4.42) we can obtain  $\sigma_r, \epsilon'', \sigma_i$  and  $\epsilon'$  respectively. Now

$$\sigma_r = \frac{ne^2}{m} \cdot \frac{\gamma_c}{\gamma_c^2 + \omega^2}$$

$$\sigma_i = \frac{ne^2}{m} \cdot \frac{\omega}{\gamma_c^2 + \omega^2}$$

and

From those two relations  $n$  and  $\gamma_c$  can be obtained where  $n$  is the charged particle density and  $\gamma_c$  is the electron atom

collision frequency. Further

$$\epsilon' = 1 - \frac{4\pi n e^2}{m(\omega^2 + \nu_c^2)}$$

$$\epsilon'' = \frac{4\pi n e^2}{m} \cdot \frac{\nu_c}{\omega} \cdot \frac{1}{\nu_c^2 + \omega^2}$$

From the last two equations  $\nu_c$  and  $n$  can be determined as well and compared with the values calculated from  $\sigma_r$  and  $\sigma_i$ .

Thus this method enables us to obtain the four quantities  $\sigma_r$ ,  $\sigma_i$ ,  $\epsilon'$  and  $\epsilon''$  and is an improvement upon the standard microwave technique of plasma diagnostic.

CHAPTER IVD

CRITICAL FREQUENCY FOR MICROWAVE PROPAGATION  
IN A RAREFIED MAGNETISED PLASMA

## CHAPTER - IV

PART DCRITICAL FREQUENCY FOR MICROWAVE PROPAGATION  
IN A RAREFIED MAGNETISED PLASMAINTRODUCTION

It is well known that the dielectric constant of a plasma when collision of electrons with neutral atoms and molecules is not taken into consideration is given by

$$\epsilon = 1 - \frac{\omega_p^2}{\omega^2} \quad (4.43)$$

where,  $\omega_p = \frac{4\pi ne^2}{m}$  is the electron plasma oscillation frequency and ' $\omega$ ' is the frequency of incident microwave and hence the refractive index  $\mu$  is given by

$$\mu = \left[ 1 - \frac{\omega_p^2}{\omega^2} \right]^{1/2} \quad (4.44)$$

If  $\omega_p < \omega$ ,  $\mu$  is real and micro waves propagate through the plasma and if  $\omega_p > \omega$ , then  $\mu$  is imaginary and hence there will be no propagation. The critical freq.  $\omega_c = \omega_p$  and if  $\omega_c$  can be determined then as  $\omega_p = \left( \frac{4\pi ne^2}{m} \right)^{1/2}$  the electron or ion density 'n' can be obtained. The method therefore consists the sending a microwave beam of variable frequency

through the plasma and noting the frequency at which transmission stops and reflection begins. This is a standard method of determining the charged particle density in plasma and is the same method adopted in case of ionosphere surrounding.

However, it is known that in case of ionosphere, the effect of earth's magnetic field has to be taken into consideration and for thermonuclear reaction, a plasma has to be confined by a magnetic field. Hence in both the cases the effect of magnetic field has to be taken into consideration in calculating the critical frequency of microwave propagation. In the following section the dielectric constant of the plasma has therefore been calculated taking into consideration the effect of collision of charged particles with neutral atoms and molecules.

### THEORETICAL TREATMENT

#### Effect of magnetic field on the dielectric const. of plasma medium:

Let us consider the plasma is confined within the tube, as shown in Fig. (4.2) under the influence of r.f. electric field, along x-axis. Let a uniform magnetic field of strength 'H' be applied along z-direction, which is also shown.

Under this consideration, the equation of motion of electron inside the plasma is given by

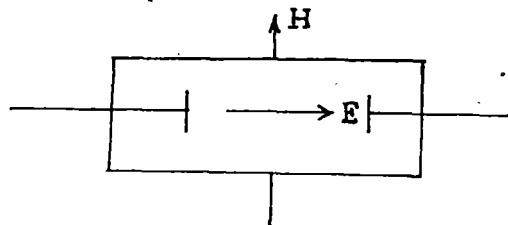


Fig. 4.2

$$m \frac{dv_x}{dt} + m \nu_c v_x + H e v_y = e E_0 e^{j\omega t} \quad , \quad \text{along x-axis and} \quad (4.45)$$

$$m \frac{dv_y}{dt} + m \nu_c v_y - H e v_x = 0 \quad , \quad \text{along y-axis} \quad (4.46)$$

where,  $v_x$  and  $v_y$  stand for the component of velocity of electron along x and y - direction and  $\nu_c$  stands for the collision frequency.

Eqns. (4.45) and (4.46) may be modified in the following form as

$$\frac{dv_x}{dt} + \nu_c v_x + \omega_H v_y = \left( \frac{e}{m} \right) E_0 e^{j\omega t} \quad (4.47)$$

$$\text{and} \quad \frac{dv_y}{dt} + \nu_c v_y - \omega_H v_x = 0 \quad (4.48)$$

$$\left( \text{where, } \omega_H = \frac{eH}{m} \right)$$

Let us consider the trial solution, given by

$$v_x = A e^{j\omega t} \quad \text{and} \quad v_y = B e^{j\omega t}$$

$$\therefore \frac{dv_x}{dt} = A j \omega e^{j\omega t}$$

(A & B stand for amplitude)

$$\text{and} \quad \frac{dv_y}{dt} = B j \omega e^{j\omega t}$$

Substituting above value in eqn. (4.48) we have,

$$Bj\omega e^{j\omega t} + \gamma_c B e^{j\omega t} - \omega_H A e^{j\omega t} = 0$$

$$\text{or, } B = \frac{A \omega_H}{\gamma_c + j\omega}$$

(4.49)

Again, substituting in eqn. (4.47), we have,

$$Aj\omega e^{j\omega t} + \gamma_c A e^{j\omega t} + \omega_H B e^{j\omega t} = \frac{e}{m} E_0 e^{j\omega t}$$

Now, substituting the value of B from eqn. (4.49),

we have,

$$\left( Aj\omega + \gamma_c A + \omega_H \frac{A \omega_H}{\gamma_c + j\omega} \right) e^{j\omega t} = \frac{e}{m} E_0 e^{j\omega t}$$

$e^{j\omega t} \neq 0$ , Hence we have

$$A = \frac{(e/m) E_0}{\gamma_c + j\omega + \frac{\omega_H^2}{\gamma_c + j\omega}}$$

Now, substituting the value of 'A' in the exp. of

' $v_x$ ', we have,

$$v_x = \frac{(e/m) E_0 e^{j\omega t}}{\gamma_c + j\omega + \frac{\omega_H^2}{\gamma_c + j\omega}} \quad (4.50)$$

The conduction current, will be given by

$$i_c = nev_x = \frac{(ne^2/m) E_0 e^{j\omega t}}{\sigma_c + j\omega + \frac{\omega_H^2}{\sigma_c + j\omega}} \quad (4.51)$$

Again, let us calculate the displacement current

' $i_d$ ' is given by

$$i_d = \frac{1}{4\pi} j\omega E_0 e^{j\omega t} \quad (4.52)$$

Again, from Maxwell's eqn.

$$\nabla \times \vec{H} = \frac{4\pi}{c} (i_c + i_d) \quad (4.53)$$

Now, substituting the value of ' $i_c$ ' and  $i_d$  in above eqn. (8), we have,

$$\begin{aligned} \nabla \times \vec{H} &= \frac{4\pi}{c} \left[ \frac{(ne^2/m) E_0 e^{j\omega t}}{\sigma_c + j\omega + \frac{\omega_H^2}{\sigma_c + j\omega}} + \frac{j\omega E_0 e^{j\omega t}}{4\pi} \right] \\ &= \frac{4\pi}{c} \left[ \frac{(ne^2/m)}{\sigma_c + j\omega + \frac{\omega_H^2}{\sigma_c + j\omega}} + \frac{j\omega}{4\pi} \right] E_0 e^{j\omega t} \quad (4.54) \end{aligned}$$

$$\text{Again, } \nabla \times \vec{H} = E_0 e^{j\omega t} \cdot \frac{4\pi}{C} \frac{j\omega\epsilon}{4\pi} \quad (4.55)$$

Where,  $\epsilon$  stands for dielectric const.

Comparing eqn.(4.54) and(4.55), we have

$$\frac{4\pi}{C} E_0 e^{j\omega t} \frac{j\omega\epsilon}{4\pi} = \frac{4\pi}{C} \left[ \frac{(ne^2/m)}{\gamma_c + j\omega + \frac{\omega_H^2}{\gamma_c + j\omega}} + \frac{j\omega}{4\pi} \right] E_0 e^{j\omega t}$$

$$\text{So, } j\omega\epsilon = 4\pi \left[ \frac{(ne^2/m)}{\gamma_c + j\omega + \frac{\omega_H^2}{\gamma_c + j\omega}} + \frac{j\omega}{4\pi} \right] \quad (4.56)$$

It is clear from above expression that  $\epsilon$  contains both real and imaginary part.

Let us consider,  $\epsilon = (\epsilon' - j\epsilon'')$ . Under this consideration, eqn. (4.56) becomes

$$j\omega(\epsilon' - j\epsilon'') = 4\pi \left[ \frac{(ne^2/m)}{\gamma_c + j\omega + \frac{\omega_H^2}{\gamma_c + j\omega}} + \frac{j\omega}{4\pi} \right]$$

$$\text{or, } j\omega\epsilon' + \omega\epsilon'' = 4\pi A \quad (4.57)$$

$$\begin{aligned}
\text{where, } A &= \frac{ne^2/m}{\nu_c + j\omega + \frac{\omega_H^2}{\nu_c + j\omega}} + \frac{j\omega}{4\pi} \\
&= \frac{(ne^2/m)}{\nu_c + j\omega + \frac{\omega_H^2(\nu_c - j\omega)}{\nu_c^2 + \omega^2}} + \frac{j\omega}{4\pi} \\
&= \frac{(ne^2/m)}{\nu_c + \frac{\omega_H^2 \nu_c}{\nu_c^2 + \omega^2} + j\omega - j \frac{\omega_H^2 \omega}{\nu_c^2 + \omega^2}} + \frac{j\omega}{4\pi} \\
&= \frac{\frac{ne^2}{m} \cdot \left[ \left\{ \nu_c + \frac{\omega_H^2 \nu_c}{\nu_c^2 + \omega^2} \right\} - j \left\{ \omega - \frac{\omega_H^2 \omega}{\nu_c^2 + \omega^2} \right\} \right]}{\left( \nu_c + \frac{\omega_H^2 \nu_c}{\nu_c^2 + \omega^2} \right)^2 + \left( \omega - \frac{\omega_H^2 \omega}{\nu_c^2 + \omega^2} \right)^2} + \frac{j\omega}{4\pi} \\
&= \frac{(ne^2/m) \left( \nu_c + \frac{\omega_H^2 \nu_c}{\nu_c^2 + \omega^2} \right)}{\left( \nu_c + \frac{\omega_H^2 \nu_c}{\nu_c^2 + \omega^2} \right)^2 + \left( \omega - \frac{\omega_H^2 \omega}{\nu_c^2 + \omega^2} \right)^2} \\
&\quad + j \left[ \frac{\omega}{4\pi} - \frac{(ne^2/m) \left( \omega - \frac{\omega_H^2 \omega}{\nu_c^2 + \omega^2} \right)}{\left( \nu_c + \frac{\omega_H^2 \nu_c}{\nu_c^2 + \omega^2} \right)^2 + \left( \omega - \frac{\omega_H^2 \omega}{\nu_c^2 + \omega^2} \right)^2} \right]
\end{aligned}$$

Now, substituting the value of 'A' from eqn. (4.58) in eqn. (4.57) and equating the real and imaginary part of both side we have,

$$(\epsilon')_H = 4\pi \left[ \frac{1}{4\pi} - \frac{(ne^2/m) \left( \omega - \frac{\omega \omega_H^2}{\omega_C^2 + \omega^2} \right)}{\omega \left\{ \left( \omega_C + \frac{\omega_H^2 \omega_C}{\omega_C^2 + \omega^2} \right)^2 + \left( \omega - \frac{\omega_H^2 \omega}{\omega_C^2 + \omega^2} \right)^2 \right\}} \right] \quad (4.59)$$

$$\text{and } (\epsilon'')_H = \frac{4\pi(ne^2/m) \left( \omega_C + \frac{\omega_H^2 \omega_C}{\omega_C^2 + \omega^2} \right)}{\omega \left\{ \left( \omega_C + \frac{\omega_H^2 \omega_C}{\omega_C^2 + \omega^2} \right)^2 + \left( \omega - \frac{\omega_H^2 \omega}{\omega_C^2 + \omega^2} \right)^2 \right\}} \quad (4.60)$$

Above two eqn. gives us the expression of  $(\epsilon')$  and  $(\epsilon'')$  under the influence of external magnetic field 'H'.

Special case:

Now considering  $\omega_H = \frac{eH}{m} = 0$  (in the absence of external mag. field), we have

$$\epsilon'' = \frac{4\pi ne^2}{m\omega} \times \frac{\omega_C}{\omega_C^2 + \omega^2} = \frac{\omega_p^2 \omega_C}{\omega(\omega_C^2 + \omega^2)} \quad (4.61)$$

$$\text{and } \epsilon' = 1 - \frac{4\pi(ne^2/m)\omega}{\omega(\gamma_c^2 + \omega^2)} = 1 - \frac{\omega_p^2}{\gamma_c^2 + \omega^2} \quad (4.62)$$

Above two expressions are the expressions of  $\epsilon'$  and  $\epsilon''$  in the absence of magnetic field.

Now, at very low pressure, when  $\gamma_c$  (= collision frequency) may be neglected, eqn. (4.59) becomes

$$(\epsilon')_H = 1 - \frac{\omega_p^2(\omega^2 - \omega_H^2)\omega^2}{\omega^2(\omega^2 - \omega_H^2)^2} = 1 - \frac{\omega_p^2}{\omega^2 - \omega_H^2} \quad (4.63)$$

Now, let us define the critical frequency ' $\omega_c$ ' such that at  $\omega = \omega_c$ ,  $(\epsilon')_H = 0$

$$\text{i.e., } \omega_c^2 - \omega_H^2 = \omega_p^2$$

$$\text{or, } \omega_c^2 = \omega_p^2 + \omega_H^2$$

(4.64)

From eqn. (4.64), ' $\omega_c$ ' has been calculated for different values of magnetic field varying from 1 to 100 g and the value of ' $\omega_p$ ' has been taken to be equal to  $\omega_p = \sqrt{\frac{4\pi ne^2}{m}}$  and for  $n = 10^{10}$ ,  $\omega_p = 9 \times 10^8$ . The calculated values are given in Table (4.1). The values of ' $\omega_c$ ' with different magnetic field  $\omega_c$  is given in table 4.1.

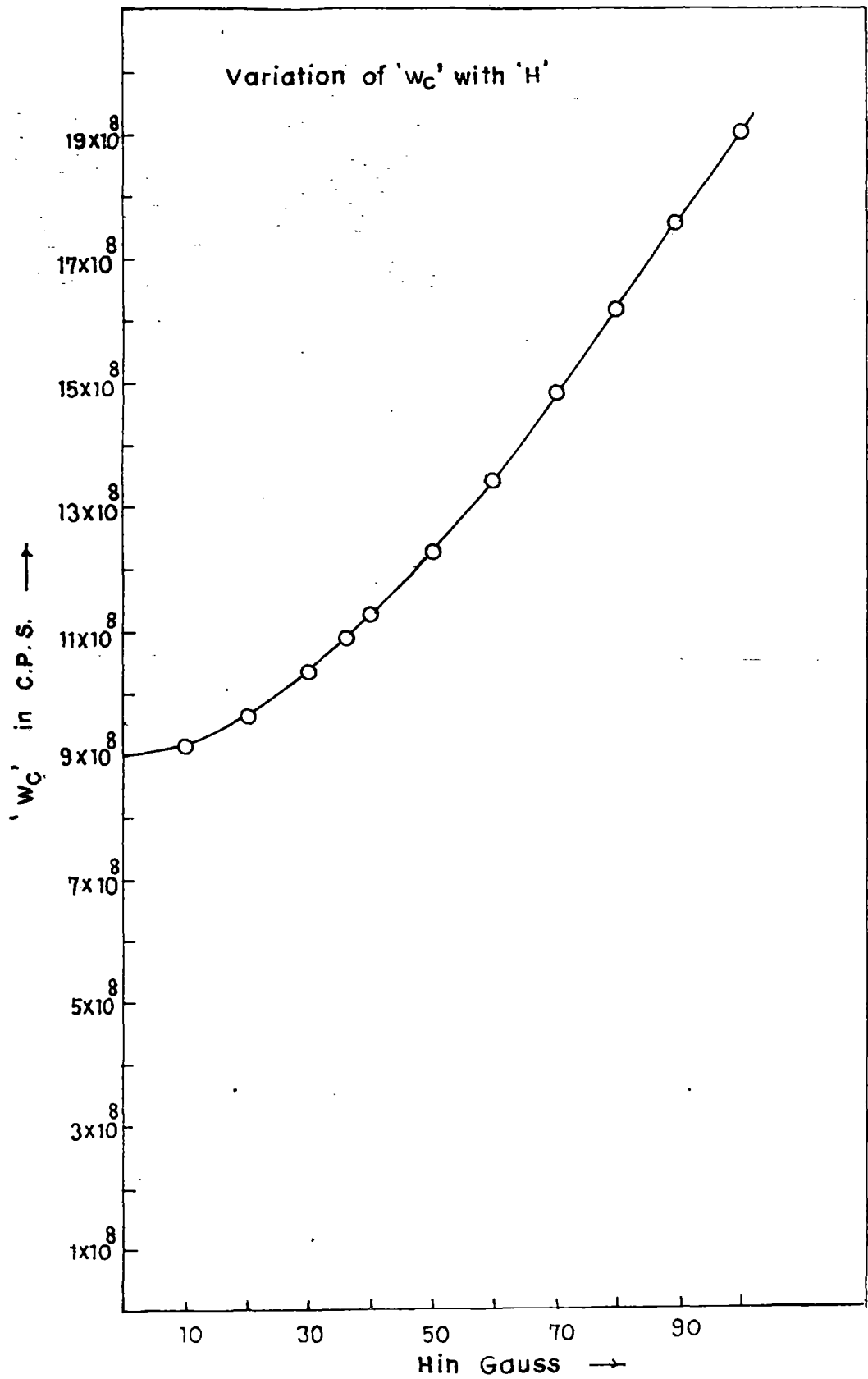


Fig. 4.3

Table - (4.1)

$$\omega_p = 9 \times 10^8 \text{ cycles/sec}$$

Magnetic field in Gauss	$\omega_H$ in C.P.S.	$\omega_c$ in C.P.S.
10	$1.67 \times 10^8$	$9.15 \times 10^8$
20	$3.34 \times 10^8$	$9.59 \times 10^8$
30	$5.01 \times 10^8$	$10.3 \times 10^8$
40	$6.68 \times 10^8$	$11.20 \times 10^8$
50	$8.35 \times 10^8$	$12.27 \times 10^8$
60	$10.02 \times 10^8$	$13.46 \times 10^8$
70	$11.69 \times 10^8$	$14.75 \times 10^8$
80	$13.36 \times 10^8$	$16.10 \times 10^8$
90	$15.03 \times 10^8$	$17.51 \times 10^8$
100	$16.7 \times 10^8$	$18.97 \times 10^8$

Value 'H' for which  $(\epsilon')_H$  &  $(\epsilon'')_H$  will attain it's maximum value

From eqn. (4.59), the value of  $\epsilon'$  has been calculated for its maximum value with the variation of mag. field in the following manner.

For this, let

$$4\pi \left( \frac{ne^2}{m} \right) = K' \quad (\text{Const. w.r. to } \omega_H)$$

Under this consideration, expression of  $(\epsilon')_H$  becomes

$$(\epsilon')_H = 1 - K' \frac{(\nu_C^2 + \omega^2 - \omega_H^2)(\nu_C^2 + \omega^2)}{\nu_C^2 (\nu_C^2 + \omega^2 + \omega_H^2)^2 + \omega^2 (\nu_C^2 + \omega^2 - \omega_H^2)^2}$$

Differentiating above equation with respect to 'H', we have

$$\frac{d(\epsilon')_H}{d\omega_H} = \frac{K' (\nu_C^2 + \omega^2) 2\omega_H}{\nu_C^2 (\nu_C^2 + \omega^2 + \omega_H^2)^2 + \omega^2 (\nu_C^2 + \omega^2 - \omega_H^2)^2}$$

$$\frac{K' (\nu_C^2 + \omega^2 - \omega_H^2)(\nu_C^2 + \omega^2) [4\nu_C^2 \omega_H (\nu_C^2 + \omega^2 + \omega_H^2) - 4\omega^2 \omega_H^2 (\nu_C^2 + \omega^2 - \omega_H^2)]}{\nu_C^2 (\nu_C^2 + \omega^2 + \omega_H^2)^2 + \omega^2 (\nu_C^2 + \omega^2 - \omega_H^2)^2}$$

Now  $\frac{d(\epsilon')_H}{d\omega_H} = 0$  gives

$$2\nu_C^2 (\nu_C^2 + \omega^2 + \omega_H^2)^2 + 2\omega^2 (\nu_C^2 + \omega^2 - \omega_H^2)^2$$

$$= 4\nu_C^2 (\nu_C^2 + \omega^2 + \omega_H^2)(\nu_C^2 + \omega^2 - \omega_H^2) - 4\omega^2 (\nu_C^2 + \omega^2 - \omega_H^2)^2$$

Now, substituting  $\nu_C^2 + \omega^2 = p^2$  in above equation

we have  $2\nu_C^2 (p^2 + \omega_H^2)^2 + 2\omega^2 (p^2 - \omega_H^2)^2 = 4\nu_C^2 (p^2 + \omega_H^2)(p^2 - \omega_H^2) - 4\omega^2 (p^2 - \omega_H^2)^2$

$$\text{or, } (\nu_C^2 + \omega^2 + 4\nu_C^2 + 4\omega^2)\omega_H^4 + (2p^2\nu_C^2 - 2p^2\omega^2 - 8\omega^2 p^2)\omega_H^2$$

$$+ (\nu_C^2 p^4 + \omega^2 p^4 - 4\nu_C^2 p^4 + 4\omega^2 p^4) = 0$$

$$\text{or, } 5(\nu_C^2 + \omega^2)\omega_H^4 + 2p^2(\nu_C^2 - 5\omega^2)\omega_H^2 + (5\omega^2 p^4 - 3\nu_C^2 p^4) = 0$$

$$\text{or, } 5p^2\omega_H^4 + 2p^2(\nu_C^2 - 5\omega^2)\omega_H^2 + (5\omega^2 p^4 - 3\nu_C^2 p^4) = 0$$

$$\text{or, } \omega_H^2 = \frac{-2p^2(\rho_c^2 + 5\omega^2) \pm \sqrt{4p^4(\rho_c^2 - 5\omega^2) - 4 \cdot 5p^2(5\omega^2 p^4 - 3\rho_c^2 p^4)}}{10p^2}$$

$$\text{or, } \omega_H^2 = \frac{-(\rho_c^2 - 5\omega^2) \pm \sqrt{(\rho_c^2 - 5\omega^2)^2 - 5(\rho_c^2 + \omega^2)(5\omega^2 - 3\rho_c^2)}}{5}$$

$$\text{or, } \omega_H^2 = \frac{(-\rho_c^2 + 5\omega^2) + \sqrt{16\rho_c^4 - 20\rho_c^2\omega^2}}{5}$$

(Considering only positive sign)

$$\text{or, } \omega_H = \frac{\sqrt{(-\rho_c^2 + 5\omega^2) + 2(4\rho_c^4 - 5\rho_c^2\omega^2)^{1/2}}}{\sqrt{5}}$$

(4.65)

The corresponding value of 'H', under the influence of which,  $(\epsilon')_H$  will be maximum given by

$$H = \frac{m}{e} \sqrt{\frac{(-\rho_c^2 + 5\omega^2) + 2(4\rho_c^4 - 5\rho_c^2\omega^2)^{1/2}}{5}}$$

(4.66)

At low pressure (neglecting  $\rho_c$ ), the value of ' $\omega_H$ ' in which  $(\epsilon')_H$  is maximum will be given by

$$\omega_H = \sqrt{\frac{5\omega^2}{5}} = \omega$$

(4.67)

Again, from eqn. (4.60), the value of the magnetic field for which  $(\epsilon'')_H$  becomes maximum has also been calculated in following.

Now,

$$(\epsilon'')_H = \frac{4\pi(ne^2/m)\nu_C \left(1 + \frac{\omega_H^2}{\nu_C^2 + \omega^2}\right)}{\omega \left\{ \nu_C^2 \left(1 + \frac{\omega_H^2}{\nu_C^2 + \omega^2}\right)^2 + \omega^2 \left(1 - \frac{\omega_H^2}{\nu_C^2 + \omega^2}\right)^2 \right\}}$$

Let us assume,  $\frac{4\pi(ne^2/m)\nu_C}{\omega} = K$  [constant with respect to  $\omega_H$ ]

Under this consideration, above eqn. becomes

$$(\epsilon'')_H = \frac{K(\nu_C^2 + \omega^2 + \omega_H^2)(\nu_C^2 + \omega^2)}{\nu_C^2(\nu_C^2 + \omega^2 + \omega_H^2)^2 + \omega^2(\nu_C^2 + \omega^2 - \omega_H^2)^2}$$

Now, differentiating both side of above equation with respect to ' $\omega_H$ ', we have,

$$\frac{d(\epsilon'')_H}{d\omega_H} = \frac{K(\nu_C^2 + \omega^2) \cdot 2\omega_H}{\nu_C^2(\nu_C^2 + \omega^2 + \omega_H^2)^2 + \omega^2(\nu_C^2 + \omega^2 - \omega_H^2)^2}$$

$$= \frac{K(\nu_C^2 + \omega^2 + \omega_H^2)(\nu_C^2 + \omega^2) \left[ \nu_C^2 4\omega_H(\nu_C^2 + \omega^2 + \omega_H^2) - 4\omega^2\omega_H(\nu_C^2 + \omega^2 - \omega_H^2) \right]}{\left\{ \nu_C^2(\nu_C^2 + \omega^2 + \omega_H^2)^2 + \omega^2(\nu_C^2 + \omega^2 - \omega_H^2)^2 \right\}^2}$$

Now,  $\frac{d(\epsilon'')}{d\omega_H} = 0$  gives,

$$\begin{aligned} 2\omega_C^2 (\omega_C^2 + \omega^2 + \omega_H^2)^2 + 2\omega^2 (\omega_C^2 + \omega^2 - \omega_H^2)^2 \\ = 4\omega_C^2 (\omega_C^2 + \omega^2 + \omega_H^2)^2 - 4\omega^2 (\omega_C^2 + \omega^2 + \omega_H^2)(\omega_C^2 + \omega^2 - \omega_H^2) \end{aligned}$$

Let us assume,  $\omega_C^2 + \omega^2 = p^2$

The above eqn. becomes

$$2\omega^2 (p^2 - \omega_H^2)^2 = 2\omega_C^2 (p^2 + \omega_H^2)^2 - 4\omega^2 (p^2 + \omega_H^2)(p^2 - \omega_H^2)$$

$$\text{or, } (2\omega_C^2 + 2\omega^2)\omega_H^4 + 4p^2(\omega_C^2 + \omega^2)\omega_H^2 + 2p^4(\omega_C^2 - 3\omega^2) = 0$$

$$\text{or, } \frac{1}{p^2}\omega_H^4 + 2\omega_H^2 + (\omega_C^2 - 3\omega^2) = 0$$

$$\text{so, } \omega_H^2 = \frac{-2 \pm \sqrt{4 - 4\frac{1}{p^2}(\omega_C^2 - 3\omega^2)}}{(2/p^2)}$$

$$= -p^2 \pm \sqrt{p^4 - p^2(\omega_C^2 - 3\omega^2)}$$

Substituting the value for  $p^2 = (\omega_C^2 + \omega^2)$  in above expression, we have

$$\omega_H^2 = -(\omega_C^2 + \omega^2) + \sqrt{(\omega_C^2 + \omega^2)^2 - (\omega_C^2 + \omega^2)(\omega_C^2 - 3\omega^2)}$$

(Negative sign is not considered)

$$= -(\omega_C^2 + \omega^2) + \sqrt{4\omega^4 + 4\omega_C^2\omega^2}$$

$$\text{so, } \omega_H = \pm \sqrt{-(\omega_C^2 + \omega^2) + 2\omega^2 \left(1 + \frac{\omega_C^2}{\omega^2}\right)^{1/2}}$$

(4.68)

Neglecting negative sign in above expression we have the magnitude of magnetic field in which  $(\epsilon'')_H$  will be maximum is

$$H = \frac{m}{e} \sqrt{-(\nu_c^2 + \omega^2) + 2\omega^2 \left(1 + \frac{\nu_c^2}{\omega^2}\right)^{1/2}} \quad (4.69)$$

Now, at low pressure, (neglecting  $\nu_c$ ) the expression of ' $\omega_H$ ' under which the value of  $(\epsilon'')_H$  will be extremum is given by

$$\omega_H^2 = -\omega^2 + \sqrt{4\omega^4} \quad \left[ \text{from eqn. (4.68)} \right]$$

$$\text{i.e. } \omega_H = \omega \quad (4.70)$$

### DISCUSSION

From above mathematical treatment, following interesting result will be obtained.

From eqn. (4.67) and (4.68), it is seen that, in the absence of collision (i.e. at low pressure when the collision between particles inside plasma is neglected),  $(\epsilon')_H$  and also  $(\epsilon'')_H$  will be maximum at the frequency  $\omega = \omega_H$ . This result can be explained because in presence of magnetic field, the charged particles will be driven due to the Lorentz force to the wall of the discharge tube and the plasma will become almost equivalent to a neutral gas and hence will have higher dielectric

constant than the neutral gas.

From the nature of the curve in Fig. (4.3) it is seen that ' $\omega_c$ ' increases with 'H' at first slowly and then rapidly. Consequently, for high magnetic field, high frequency micro waves are to be utilized.

The most interesting point is evident from eqn. (4.64) is  $\omega_c^2 = \omega_p^2 + \omega_H^2$ . It suggests that as if the ion-plasma frequency has been increased from ' $\omega_p$ ' to  $\omega_p^2 + \omega_H^2$ . The same result can be obtained independently if we consider the effect of magnetic field on electron plasma oscillation. The theoretical calculation is given in following.

Electron Plasma oscillation in the presence of magnetic field:

Let the plasma be confined inside the tube clearly shown in following. Let us suppose that the wave oscillation takes place along x-axis and the magnetic field is acted along Z-axis.

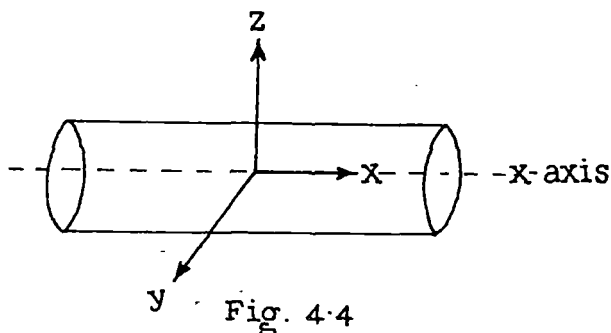


Fig. 4.4

Under this consideration, the equation of motion of electron becomes

$$m \frac{dv_x}{dt} = -e[E + Bv_y] \quad (4.70)$$

and 
$$m \frac{dv_y}{dt} = eBv_x \quad (4.71)$$

Let us suppose that, the velocity of propagation of wave along x-direction is in the form

$$v_x = v_{x0} e^{-j(\omega t - Kx)} \quad (4.72)$$

and along y-axis, it becomes

$$v_y = v_{y0} e^{j(Kx - \omega t)} \quad \text{where} \quad K = \frac{2\pi}{\lambda}$$

$$\frac{dv_x}{dt} = -j\omega v_x \quad \text{and} \quad \frac{dv_y}{dt} = -j\omega v_y$$

Substituting  $\frac{dv_y}{dt}$  in equation (4.71), we have

$$m(-j\omega)v_y = eBv_x \quad (4.73)$$

$$\text{so, } v_y = -\frac{eB}{m} \cdot \frac{1}{j\omega} v_x$$

Again, putting  $\frac{dv_x}{dt}$  and ' $v_y$ ' from above in equation (4.70), we have

$$m(-j\omega)v_x = -e \left[ E - \frac{eB^2}{mj\omega} v_x \right]$$

$$\text{or, } mj\omega v_x + \frac{e^2 B^2}{m} \cdot \frac{1}{j\omega} v_x = eE$$

$$\text{or, } v_x = \frac{eE}{mj\omega + (e^2 B^2 / mj\omega)}$$

$$\text{or, } v_x = \frac{eE \cdot mj\omega}{j^2 m^2 \omega^2 (1 - \frac{e^2 B^2}{m^2 \omega^2})}$$

$$\text{So, } v_x = \frac{eE}{mj\omega (1 - \frac{\omega_H^2}{\omega^2})} \quad \left[ \because \omega_H^2 = \frac{e^2 B^2}{m^2} \right]$$

$\omega_H$  is the cyclotron frequency

Now, if an elementary volume of unit cross section is considered along x-direction and if ' $n_0$ ' stands for the number of particles per unit volume of plasma, then number of particles entering inside this volume per sec. is  $n_0 v_x$  where,  $v_x$  is the velocity of particles along x-direction.

No. of particles leaving from it per sec. is

$$n_0 (v_x + \frac{dv_x}{dx} dx)$$

Remaining particle inside it is given by  $-n_0 \frac{dv_x}{dx} dx$

per unit volume, it becomes  $-n_0 \frac{dv_x}{dx}$

If ' $n$ ' stands for the increase of particle per unit volume inside it at any instant, then

$$\frac{\partial n}{\partial t} = -n_0 \frac{\partial v_x}{\partial x}$$

$$\text{or, } \frac{\partial n}{\partial t} + n_0 \frac{\partial v_x}{\partial x} = 0$$

(4.74)

If it is assumed,  $n = n_0 \exp j(kx - \omega t)$

then  $\frac{\partial n}{\partial t} = -j\omega n$

and  $\frac{\partial v_x}{\partial x} = jk v_x$ , when  $v_x = v_0 e^{j(kx - \omega t)}$

Substituting above value in eqn.(4.74), we have

$$-j\omega n = -n_0 jk v_x$$

$$\text{So, } n = n_0 \frac{k}{\omega} v_x \quad (4.75)$$

Due to this increase of particles per unit volume, the electric field which will be produced, satisfy the following Poisson equation given by

$$\nabla \cdot \vec{E} = -4\pi n e$$

In one dimension, it becomes

$$\frac{dE}{dx} = -4\pi e \cdot n_0 \frac{k}{\omega} \cdot v_x \quad (\text{Substituting the value of 'n' from eqn.(4.75)}) \quad (4.76)$$

Considering,  $E = E_0 e^{j(kx - \omega t)}$ , we have

$$\frac{dE}{dx} = jkE \quad (4.77)$$

Putting the value of  $\frac{dE}{dx}$  from (4.77) and ' $v_x$ ' from [4.72 in eqn. 4.76], we have

$$jKE = -4\pi en_0 \frac{k}{\omega} \cdot \frac{eE}{mj\omega(1 - \frac{\omega_H^2}{\omega^2})}$$

$$\text{or, } m\omega^2(1 - \frac{\omega_H^2}{\omega^2}) = \frac{4\pi n_0 e}{m} = \omega_p^2$$

' $\omega_p$ ' stands for natural plasma frequency.

$$\text{So, } \omega^2 - \omega_H^2 = \omega_p^2$$

$$\text{or, } \omega^2 = \omega_H^2 + \omega_p^2$$

$$\text{or, } \omega = \sqrt{\omega_H^2 + \omega_p^2}$$

Hence, electron plasma frequency in the presence of magnetic field will be identical with critical frequency. ' $\omega_c$ ' in which the dielectric constant of plasma medium is zero in the presence of magnetic field at very low pressure.

The above results which are discussed above can be utilized in calculating charge particle density in a magnetised plasma both in the case of ionosphere as well as in the case of thermonuclear plasma confined by magnetic field.

CHAPTER V

LOW DENSITY PLASMA IN A MAGNETIC FIELD

## CHAPTER V

## LOW DENSITY PLASMA IN A MAGNETIC FIELD

When a magnetic field acts upon a low density plasma as in the case of glow discharge, various changes such as increase of equivalent pressure, decrease in length of cathode dark space, a change in radial ion density in the positive column and marked changes in the voltage current characteristics of the discharge take place. Theoretical interpretation of the phenomena has been provided by Townsend (1938) and by Allis and Allen (1937) who have investigated the motion of electrons in the presence of electric field, a magnetic field and a concentration gradient. Most of the experimental works have been done in longitudinal magnetic field. The effect of a transverse magnetic field on the positive column as regards the electron temperature, electric field and electron density has been calculated by Beckman (1948) on a theoretical basis and the calculations agree fairly well with the experimental results obtained in the case of hydrogen, nitrogen, neon and helium. The general effects of a transverse magnetic field have been investigated by McBee and Daw (1955) on an unconfined glow discharge in air within the pressure range of 0.3 to 10 torr and discharge current from 0.05 to 2.5 Ampere with the magnetic field varying from zero to 7000 gauss. They found with probe measurements that the anode and cathode fall first decrease and then increase, along with this the positive

column and the anode region become more luminous. The variation of discharge current in a transverse magnetic field (0 to 3000 Gauss) has been studied by Sen and Gupta (1971) in the positive column of a glow discharge in air, carbondioxide, hydrogen, helium and neon within the pressure range of 80 to 200m torr. The current increases with the magnetic field and shows a maximum at a particular value of the magnetic field which is the same for all the gases and independent of pressure for the same initial discharge current. Utilizing Beckman's expression (1948) for the axial electric field and the radial electron density in presence of a transverse magnetic field a detailed mathematical theory was advanced which could explain the results satisfactorily. Besides the change in these parameters, magnetic field in a low density plasma will produce Hall effect and also affect the process of diffusion.

A method has been suggested by Sen, Ghosh and Ghosh (1983) for evaluation of electron temperature in a glow discharge by measurement of diffusion voltage. In presence of magnetic field, however, the voltage which is measured between the two probes one at the axis and other away from the axis will be affected both by the diffusion process and the Hall voltage developed between the probes. Hence to calculate the electron temperature in a transverse magnetic field by the methods suggested by Sen, Ghosh and Ghosh (1983) the two processes are to be separated and only the diffusion voltage has to be taken into consideration in calculating the electron temperature from

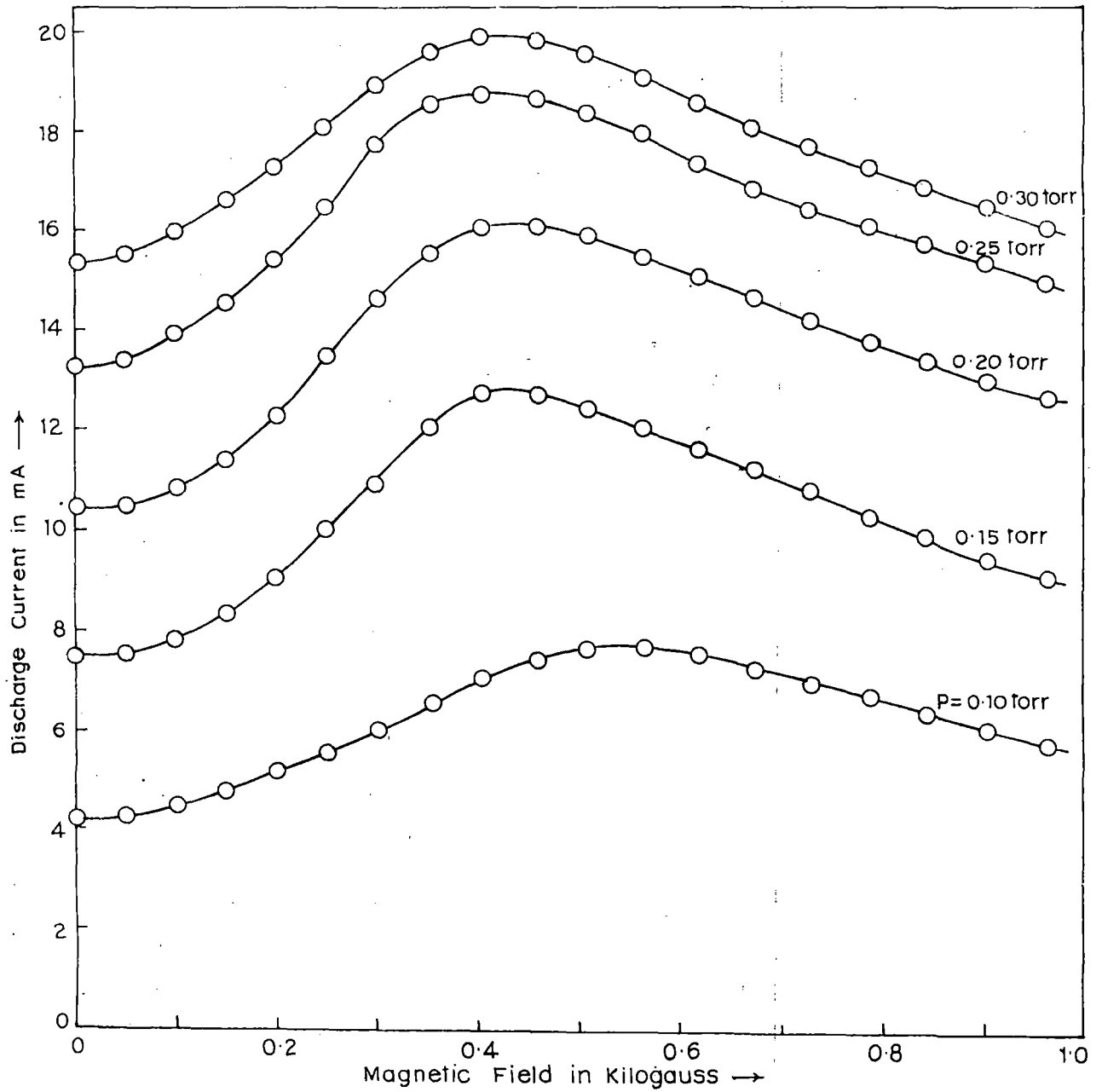


Fig. 5-d.

the expression (Sen, Ghosh and Ghosh, 1983)

$$\frac{kT_{eH}}{e} = \frac{V_{RH}}{\log[J_0(2.405 \frac{r}{R}) \exp(-aH)]} \quad (5.1)$$

where, in presence of magnetic field,  $T_{eH}$  is the electron temperature and  $V_{RH}$  is the diffusion voltage measured between the probes and

$$a = \frac{eEr c_i^{1/2}}{2kT_e P} \quad \text{and} \quad c_i = \left( \frac{e}{m} \cdot \frac{L}{v_r} \right)^2$$

$E$  is the axial voltage drop per cm of the discharge.  $L$  is the mean free path at 1 torr,  $v_r$  is the random velocity of electrons and  $r$  is the distance between the probes.

#### Results and discussion

In the first part of the work, the variation of discharge current in air at different pressures where a transverse magnetic field is present has been measured. The results are presented in Fig. 5a for pressures 0.10, 0.20, 0.25 and 0.30 torr with magnetic field varying from zero to 900 gauss. It is observed that the current gradually rises (Table 5-IV, Fig. 5a) and attains a maximum value near about the magnetic field of 400 gauss for all the pressures and then gradually decreases. Similar results have been previously obtained by Sen and Gupta (1971) in case of air and other gases. The results were explained by assuming the effect of magnetic field on the axial electric field and

radial electron density distribution and it was shown that the magnetic field at which the discharge current became a maximum was given by

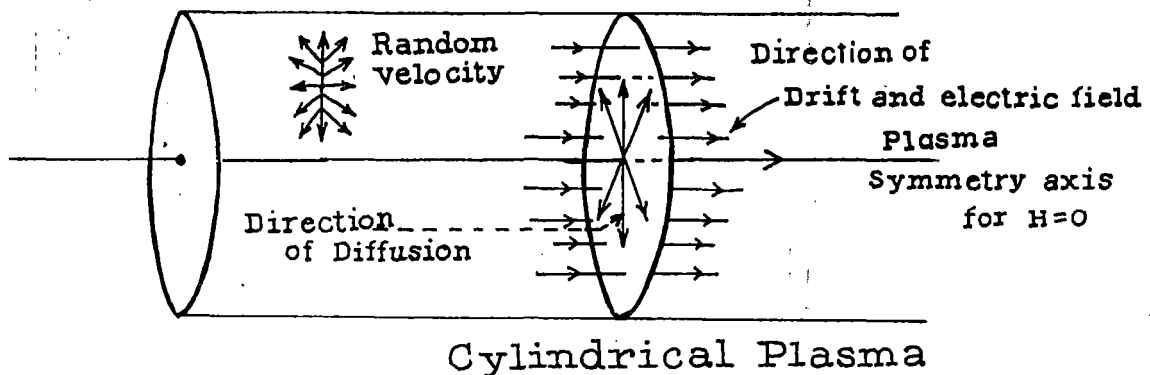
$$H_{\max} = 12.41 \times 10^{-2} (T_e/k)^{1/2} \quad (5.2)$$

where  $T_e$  is the electron temperature and  $k$  is the Boltzmann constant. The value of the magnetic field as calculated from equation 5.2 was in very good agreement with observed experimental results. Since the main object of this investigation is to study the effect of diffusion of charged particles in the magnetic field in a low density plasma the whole physical process occurring in a magnetised plasma has been reconsidered.

It is observed from the present experimental work that the current through the glow discharge plasma changes in presence of transverse magnetic field. Also the process of diffusion changes in a transverse magnetic field. Since the drift current and diffusion are basically controlled by the random velocity of electrons and ions in a plasma, there must be a change in the random and drift velocity of electrons and ions under the action of transverse magnetic field. We can, however, neglect the change in drift and random velocity of ions because of their large mass and hence low contribution to the flow rate either in case of current or in case of diffusion. Since the flow of electrons towards the direction of drift and towards the direction of diffusion comes from the same plasma space, there must be an increase in the electron

flow rate in the direction of diffusion if there is a decrease in the direction of drift velocity and vice versa.

If this really happens within the plasma space under the influence of transverse magnetic field, the change in the mean flow rate of electrons  $v_{DH}$  towards the direction of diffusion per unit  $v_{DH}$  per unit magnetic field must be same as the change in the current density,  $j_H$ , at the place of diffusion per unit current density,  $j_H$ , per unit magnetic field. The mean flow rate towards diffusion is the flow rate averaged over the entire cross section at any place within the cylindrical plasma column.



The velocity of diffusion  $v_{DH}$  in a transverse magnetic field,  $H$ , is given by

$$v_{DH} = D_H \frac{1}{n_H} \frac{dn_H}{dr} \quad (5.3a)$$

where  $D_H$ ,  $n_H$  and  $(dn_H/dr)$  are the diffusion constant, concentration of electrons and concentration gradient along radial direction respectively and all in presence of transverse magnetic field. Thus the mean flow rate  $U_{DH}$  is given by,

$$U_{DH} = \frac{\int_0^R v_{DH} n_H dr}{\int_0^R dr} = \frac{1}{R} D_H n_H \quad (5.3b)$$

Hence according to the assumption,

$$\frac{1}{U_{DH}} \frac{dU_{DH}}{dH} = \frac{1}{J_H} \frac{dJ_H}{dH} \quad (5.4a)$$

$$\text{or } \frac{D_H \frac{dn_H}{dH} + n_H \frac{dD_H}{dH}}{D_H n_H} = \frac{n_H \frac{dv_H}{dH} + v_H \frac{dn_H}{dH}}{n_H v_H}$$

where  $v_H$  is the drift velocity of electrons.

Thus we have,

$$\frac{1}{D_H} \frac{dD_H}{dH} = \frac{1}{v_H} \frac{dv_H}{dH} \quad (5.4b)$$

But the contribution of diffusion term i.e., the left hand term of equation 5.4a, receives the contribution of electrons from either of the random stream of electrons. One of the random stream moves in the direction of drift while the other moves opposite to the direction of drift. But these two streams moving by the random velocity of electrons, have almost same concentration. Slight difference may arise due to drift velocity which is usually small compared to random velocity and hence the difference in concentration between the two oppositely moving streams may be neglected. Thus only half of the electron concentration moving along drift contributes to the drift current while twice of that concentration contributes to diffusion. So only half of the contribution of the diffusion term should be taken into consideration. Thus we have,

$$\frac{1}{2} \frac{1}{D_H} \frac{dD_H}{dH} = \frac{1}{v_H} \frac{dv_H}{dH} \quad (5.5)$$

However, these two terms in 5.5 cannot be exactly equal because some of the particles which are moving parallel to the magnetic field will not be affected but they will still contribute to the process of diffusion. So we assume that

$$\frac{1}{2} \frac{1}{D_H} \frac{dD_H}{dH} - \frac{1}{v_H} \frac{dv_H}{dH} = b \quad (5.6)$$

where  $b$  will be a constant at a particular pressure. Now

$$D_H = \frac{D_0}{1 + \omega_H^2 \tau^2}$$

for low density plasma, where  $\omega_H$  is the electron cyclotron frequency and  $\tau$  is the collision time between an electron and atom. So,

$$\omega_H^2 \tau^2 = \left( \frac{eH}{m} \cdot \frac{\lambda_e}{v_r} \right)^2 = \left( \frac{e}{m} \cdot \frac{L}{v_r} \right)^2 \frac{H^2}{P^2}$$

Where  $L$  is the mean free path of the electron in the gas at a pressure of one torr and  $P$  is the pressure. So putting

$$\left( \frac{e}{m} \cdot \frac{L}{v_r} \right)^2 = C_1$$

we have,  $D_H = \frac{D_0}{1 + C_1 H^2/P^2}$  (5.7)

So from equation 5.6 and 5.7, we get

$$\frac{1}{v_H} \frac{d v_H}{d H} + b = \frac{C_1 H / P^2}{1 + C_1 H^2 / P^2} \quad (5.8)$$

We have neglected the sign because in this discussion we are concerned only with the values of the terms. Now equation 5.8 depicts the exact situation, such that the left hand contribution due to change in current added to the constant  $b$  exactly equals the right hand contribution due to change in flow by diffusion. From 5.8, integrating from zero to  $H$ , we get

$$v_H = v_0 (1 + C_1 H^2 / p^2)^{1/2} e^{-bH} \quad (5.9)$$

The concentration of charged particles also suffers change in presence of magnetic field and if  $n_0$  and  $\lambda_0$  are the electron density and mean free path in absence and  $n_H$ ,  $\lambda_H$  are the corresponding quantities in presence of magnetic field, then

$$n_0 \lambda_0 = n_H \lambda_H$$

considering that the number within a mean free path does not change.

$$\text{Now, } \lambda_H = \lambda_0 / (1 + C_1 H^2 / p^2)^{1/2}$$

[Blevin and Haydon  
(1958)]

$$\text{so, } n_H = n_0 (1 + C_1 H^2 / p^2)^{1/2} \quad (5.10)$$

Hence the current density in presence of magnetic field is

$$J_H = n_H e v_H = n_0 e v_0 (1 + C_1 H^2 / p^2)^{1/2} e^{-bH}$$

$$\text{or } I_H = I_0 (1 + C_1 H^2 / p^2)^{1/2} e^{-bH} \quad (5.11)$$

To find the variation in discharge current in the magnetic field, we put

$$\frac{dI_H}{dH} = 0, \quad \frac{bC_1}{p^2} H^2 - \frac{2C_1}{p^2} H + b = 0$$

$$So, H = \frac{1 \pm \sqrt{1 - \frac{b^2 p^2}{C_1}}}{b} \quad (5.12)$$

As will be shown subsequently that  $b^2 p^2 / C_1$  is considerably less than one. So we get two values of H at which the discharge current either becomes a maximum or minimum.

$$H' = \frac{2}{b} - \frac{b p^2}{2C_1} \quad (5.13a)$$

$$\text{and } H'' = \frac{b p^2}{2C_1} \quad (5.13b)$$

The procedure for calculating the values of b and  $C_1$  from experimental data at different pressures are given in Appendix. From the values of b and  $C_1$ , the values of  $H'$  and  $H''$  have been calculated and entered in Table 5-I.

Table 5-I

Pressure in torr	b	C <sub>1</sub>	H' in gauss	H'' in gauss	H <sub>max</sub> (expt.) in gauss
0.10	5.46 x 10 <sup>-3</sup>	7.11x10 <sup>-7</sup>	327.90	38.40	405
0.20	4.95x10 <sup>-3</sup>	2.32x10 <sup>-6</sup>	361.30	42.70	410
0.25	5.52x10 <sup>-3</sup>	4.20x10 <sup>-6</sup>	321.20	41.07	402
0.30	6.19x10 <sup>-3</sup>	6.90x10 <sup>-6</sup>	282.70	40.37	400

It is thus seen that the values calculated from 5.13a are in agreement with the values obtained from experimental results to a certain extent; which may be due to the fact that the values of C<sub>1</sub> have been calculated on quantities whose values are to a certain extent uncertain. Further it has been shown by Sen and Das (1973) that the relation  $\lambda_H = \lambda_0 / (1 + C_1 H^2 / p^2)^{1/2}$  is valid over a certain range of (H/P) values.

Electron temperature in magnetic field:

Since electrons and ions in a transverse magnetic field tend to be separated by Lorentz force, self diffusion will gradually predominate at higher values of H and so far transverse magnetic field H, the self diffusion co-efficient D is considered.

$$\text{So we have, } D_0 = \frac{1}{3} \lambda_r v_r$$

where  $\lambda_r$  is the mean free path and  $v_r$  is the random velocity.

$$\text{Then } D_H = \frac{1}{3} \lambda_{rH} v_{rH}$$

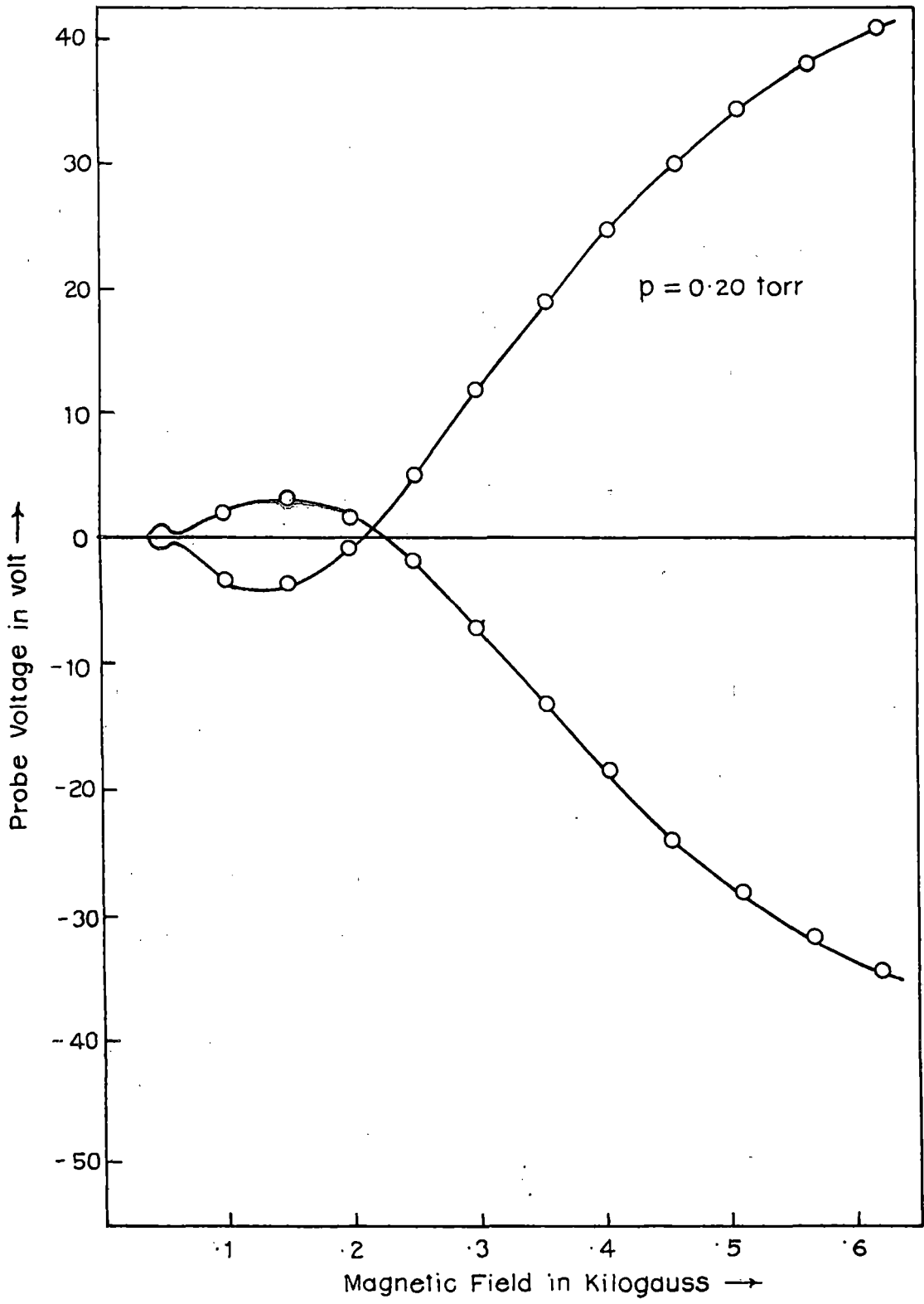


Fig. 5b

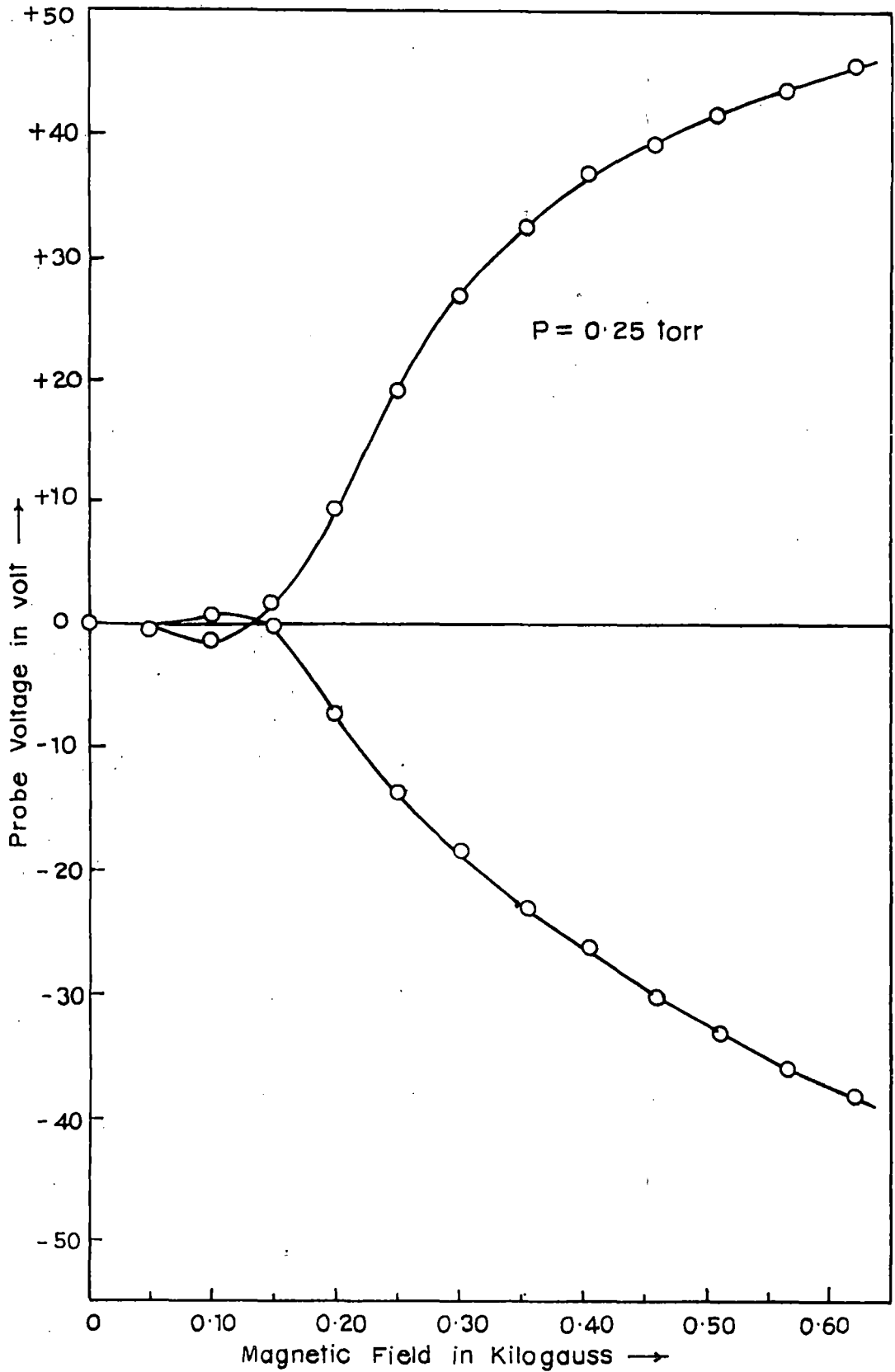


Fig. 5-C.

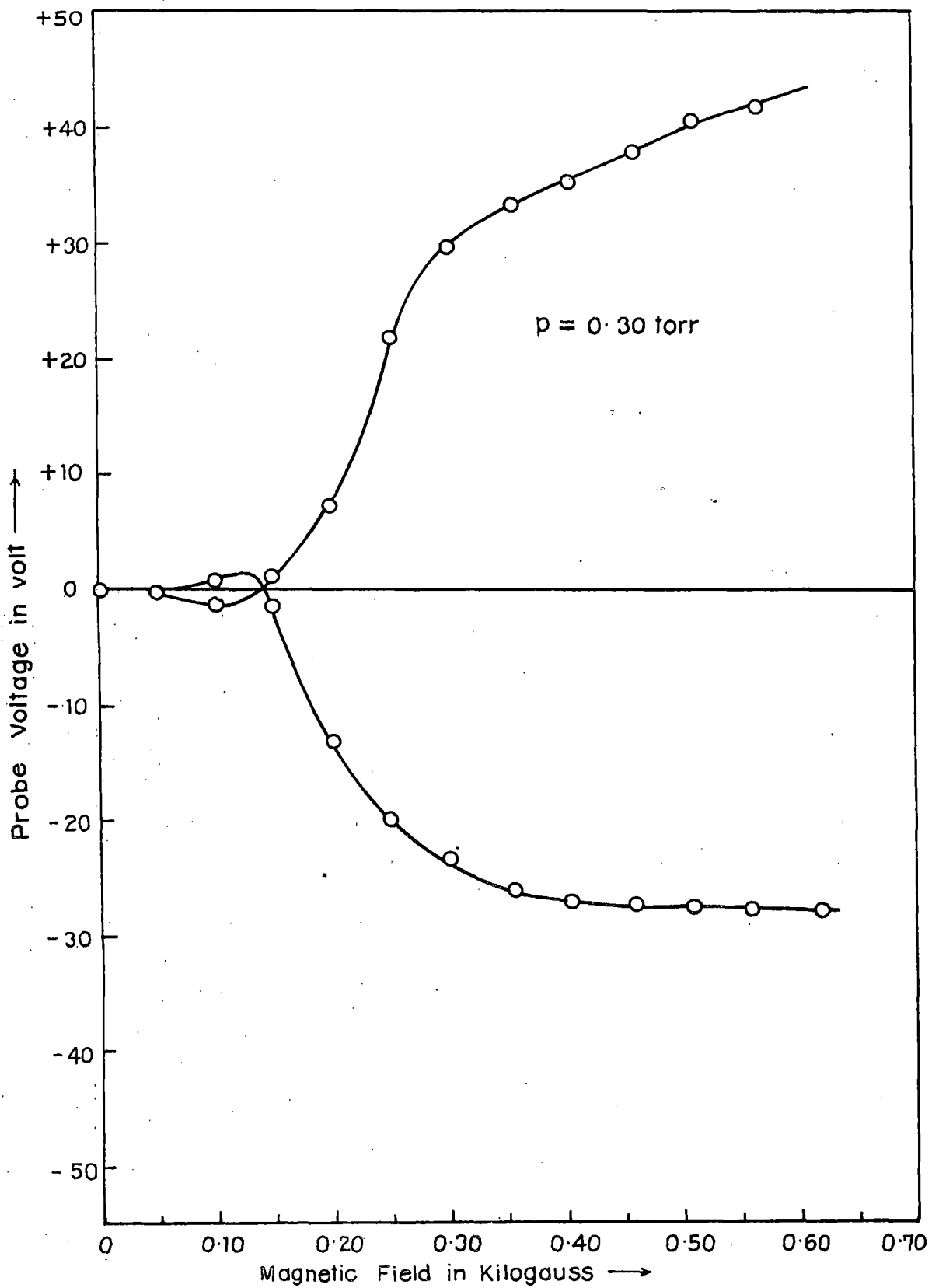


Fig. 5-d.

$$\text{so } \frac{D_H}{D_0} = \frac{\lambda_{rH} \cdot v_{rH}}{\lambda_r \cdot v_r}$$

Putting expression for  $\lambda_{rH}$  and  $D_H$ , we get  $v_{rH} = \frac{v_r}{(1 + C_1 H^2/P^2)^{1/2}}$

$$\text{but } \frac{1}{2} m v_{rH}^2 = k T_{eH} = \frac{1}{2} m v_r^2 / (1 + C_1 \frac{H^2}{P^2}) = \frac{k T_{e0}}{(1 + C_1 \frac{H^2}{P^2})}$$

Thus when electron self diffusion predominates, then

$$T_{eH} = T_{e0} / (1 + C_1 \frac{H^2}{P^2}) \quad (5.14)$$

In the 2nd part of the experiment the voltage developed across the two probes one along the axis and other parallel to the axis but away from the axis and adjacent to the wall of the discharge tube has been measured (Table 5-V) over a transverse magnetic field varying from 0.05 to 0.62 kilogauss for pressures 0.20, 0.25 and 0.30 torr. The representative curves are shown in figure 5b, 5c, 5d. In each case it is found that the voltage becomes negative for small values of magnetic field and then becomes positive and rapidly increases with the increase of transverse magnetic field applied in a certain direction. When the field is reversed, the voltage across the probes changes in sign but not in nature, i.e., the voltage across the probes

becomes positive for small values of magnetic field and then becomes negative and the negative voltage rapidly increases with magnetic field.

The behaviour of probe voltage should be like that because the transverse magnetic field produces Hall voltage across the probes as a result of charge separation caused by the Lorentz force, but charge separation is opposed [Simon (1955), Longmire (1956), Kaufman (1958)] by the inherent tendency of the plasma which tries to remain electrically neutral by increasing the diffusion in a direction reverse to the direction in which charges moves by Lorentz force.

So when direction of magnetic field is reversed, the sign of probe voltage should change, since the probes remain in the previous geometrical position. The value of probe voltage should have remained same in spite of reversing the magnetic field, but due to the difference in the asymmetry of charge distribution introduced by the reversal of magnetic field with respect to the position of the probes, the value of probe voltage in the two cases have small difference. Thus these two voltages simultaneously appear across the probes and hence voltage measured between the probes is neither a true Hall voltage, nor a true diffusion voltage but a difference between the two voltages is measured between the probes.

So an analytical expression for diffusion voltage and Hall voltage in a transverse magnetic field applied to a plasma,

will help us know the expression for the voltage that appears between the probes.

Computation of diffusion voltage in a transverse magnetic field:

We have deduced in the previous section

$$n_H = n_o \left( 1 + C_1 \frac{H^2}{p^2} \right)^{1/2}$$

$$\text{So, } \frac{dn_H}{n_H} = \frac{C_1 H/p^2}{1 + C_1 \frac{H^2}{p^2}} dH + \frac{dn_o}{n_o} \quad (5.15)$$

The velocity of diffusion in a transverse magnetic field may be written as

$$v_{DH} = \frac{D_H}{n_H} \frac{dn_H}{dr}$$

If the electric field caused by diffusion along the radial vector of the cylindrical discharge tube be  $E_H$  and  $\mu_H$  is the mobility, then

$$v_{DH} = \mu_H E_H$$

$$\text{So, } E_H dr = \frac{D_H}{\mu_H} \frac{dn_H}{n_H} = \frac{kT_{eH}}{e} \cdot \frac{dn_H}{n_H} = \frac{kT_{e0}/e}{1 + C_1 \frac{H^2}{p^2}} \cdot \frac{dn_H}{n_H}$$

So, diffusion voltage between the probes is given by,

$$\int_0^R E_H dr = -V_{DH} = \frac{kT_{e0}}{e} \int_0^R \frac{C_1 H/p^2}{(1 + C_1 \frac{H^2}{p^2})^2} dH + \frac{1}{1 + C_1 \frac{H^2}{p^2}} \int_0^R \frac{kT_{e0}}{e} \frac{dn_o}{n_o}$$

Putting the expression for  $d\eta_H/\eta_H$  from 5.15

$$\text{at } r = 0, \log J_0 = 0$$

and at  $r \approx R$ , i.e., when the other probe away from the axis is placed close to the wall of the discharge tube, where a sheath of immobile negative charges is formed, and since the electron temperature measures the kinetic energy of the electrons and as the charges are immobile,

$$T_{e0} = 0 \quad \text{at } r = R$$

So under this placement of probes, the 2nd term in 5.16 vanishes. So we have

$$-V_{DH} = \frac{kT_{e0}}{e} \cdot \frac{C_1 H^2 / p^2}{1 + C_1 H^2 / p^2} \quad (5.17)$$

Thus 5.17 gives the expression for diffusion voltage in a transverse magnetic field applied to a discharge plasma.

Computation of Hall voltage in case of plasma:

From the equation of motion of charged particles in a magnetic field, we have in a steady state,

$$\left. \begin{aligned} sV_x &= - \frac{e\gamma/m}{1 + \omega_H^2 \gamma^2} (E_x - \omega_H \gamma E_y) \\ sV_y &= - \frac{e\gamma/m}{1 + \omega_H^2 \gamma^2} (E_y + \omega_H \gamma E_x) \end{aligned} \right\} \quad (5.18)$$

If discharge current flows along x-axis, and a magnetic field is applied along z-axis, there will be no current along y-axis in case of a confined plasma.

So,  $\delta V_y = 0$ , which gives

$$E_y = -\omega_H \tau E_x \quad (5.19)$$

where  $E_x$  is the electric field applied along x-axis and  $E_y$  is the field developed to resist any flow of current along y-axis.

So Hall voltage that will appear between the probes whose surfaces are along y-axis and placed at a distance  $d$  from each other, will be given by

$$V_H = -\omega_H \tau E_x d \quad (5.20)$$

$\omega_H = eH/m$  is the cyclotron frequency, and  $\tau$  is the time of collision of electron with the atom and  $E_x$  is the electric field in which the probes are immersed.

But the electrodes in the discharge tube, which are smaller than the diameter of the discharge tube and which are used to provide electric field in the discharge tube, cannot produce uniform electric field from the axis to the periphery of the tube. Rather the field is considerably reduced outside imaginary cylinder enclosed by the electrodes, and on the wall inside the sheath of immobile charges the electric field is practically reduced to zero in the direction of discharge. So

one should use mean electric field  $E_x$  in equation 5.20 in place of  $E_x$ . If electric field on the axis is  $E_x$  and that on the wall is zero, the mean electric field is given by

$$\bar{E}_x = \frac{1}{2} E_x \quad (5.21)$$

But 
$$E_x = \frac{E_{xH}}{\left(1 + C_1 \frac{H^2}{p^2}\right)^{1/2}}$$

where  $E_{xH}$  is the true electric field that is present in presence of magnetic field and hence is measurable experimentally when magnetic field is present. Thus we have

$$V_H = -\frac{1}{2} \sqrt{C_1} \frac{H}{p} \cdot \frac{E_{xH}}{\left(1 + C_1 \frac{H^2}{p^2}\right)^{1/2}} \cdot d \quad (5.22)$$

Thus according to our assumption, the probe voltage is given by

$$V_{PH} = + \left[ \frac{kT_{e0}}{e} \cdot \frac{C_1 H^2 / p^2}{1 + C_1 \frac{H^2}{p^2}} - \frac{1}{2} \sqrt{C_1} \frac{H}{p} \cdot \frac{E_{xH}}{\left(1 + C_1 \frac{H^2}{p^2}\right)^{1/2}} \cdot d \right] \quad (5.23a)$$

$$V_{PH} = + \left[ \frac{kT_{eH}}{e} \cdot C_1 H^2 / p^2 - \frac{1}{2} \sqrt{C_1} \frac{H}{p} \cdot \frac{E_{xH}}{\left(1 + C_1 \frac{H^2}{p^2}\right)^{1/2}} \cdot d \right] \quad (5.23b)$$

The expression is expected to give correct probe voltage from a value of transverse magnetic field at which self diffusion of electrons predominates over the ambipolar diffusion and if all the parameters are experimentally measured in a set up for discharge current, pressure and magnetic field. In the present experiment, we have measured  $E_{xH}$  and  $C_1$  but not  $T_{eH}$ . Equation 5.23a and 5.23b both become identities for  $H = 0$ . So except for  $H = 0$ , we can measure  $T_{eH}$  with the experimental set up described with the help of equation 5.23b. However, we can solve for  $T_{e0}$ , using equation 5.23a and then calculate the values of  $V_{PH}$  for the other values of  $H$ .

Putting  $d = 1.2$  cm for probe separation and other values from table 5-II for  $H = 200$  gauss (for the mean value of  $H$  from 0 to 400 gauss) we get  $kT_{e0}/e = 77.66$  volt with the help of equation 5.23a.

Then we calculate other values of  $V_{PH}$  from 0 to 400 gauss using the values from table 5-II and enter the results of calculation in table 5-III along with the experimental values of  $V_{PH}$  and is shown in Fig. 5e.

We thus observe that the nature of variation of the probe voltage when both the diffusion and Hall voltage are taken into consideration is the same as observed experimentally. The quantitative agreement is highly satisfactory for values of magnetic field greater than 150 gauss. The discrepancy observed for low values of magnetic field may be due to the Bohm diffusion process where  $D_H$  is proportional to  $1/H$  instead of  $1/H^2$ .

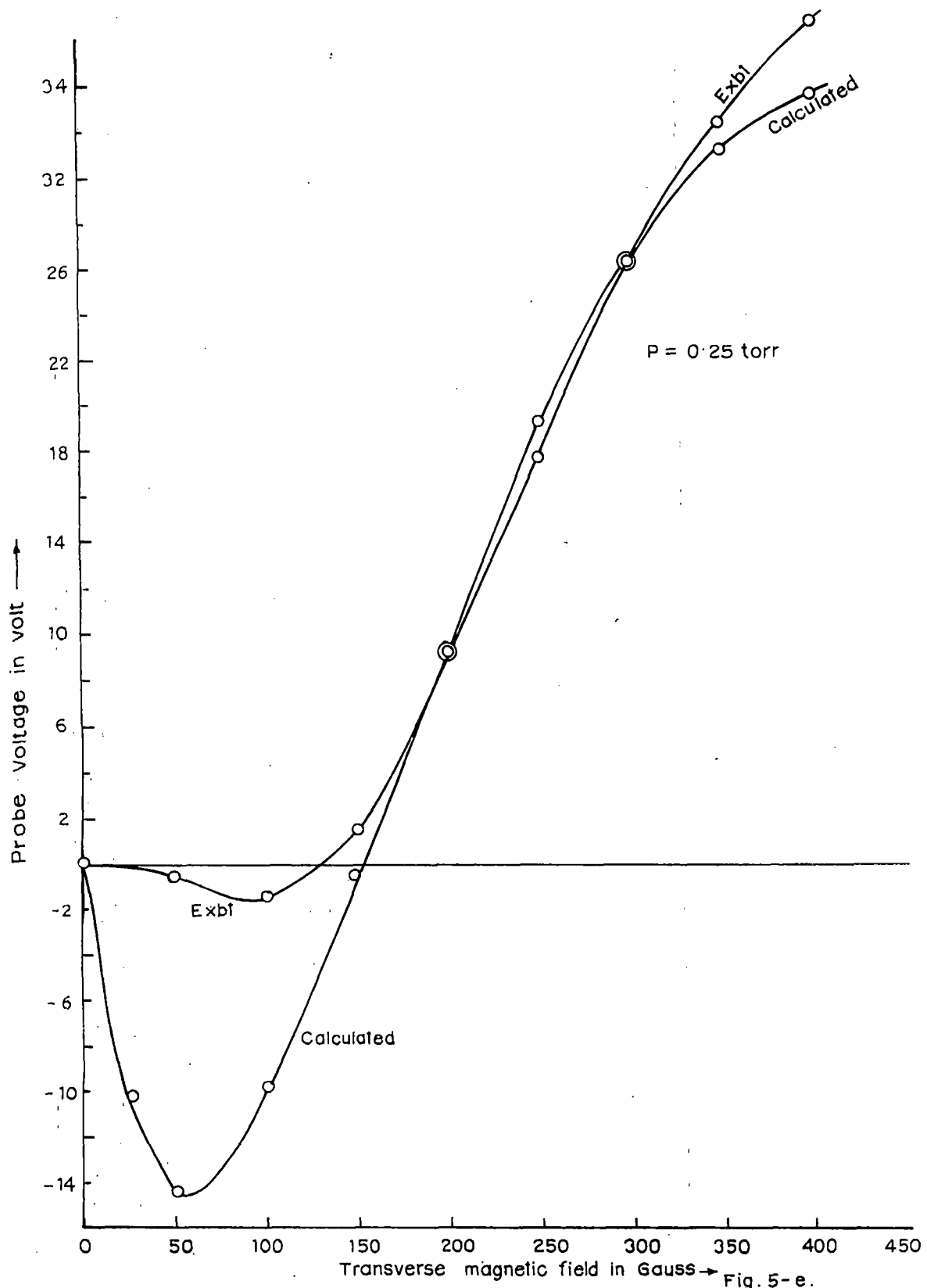


Fig. 5-e.

Table 5 - II

$$C_1 = 4.2 \times 10^{-6} \text{ torr}^2/\text{gauss}^2 \text{ and } p = 0.25 \text{ torr}$$

in uss	0	25	50	100	150	200	250	300	350	400
mA	13.25	13.30	13.35	13.80	14.55	15.45	16.50	17.85	18.45	18.75
H in lt/cm	111.7	111.5	111.3	107.0	100.6	92.9	83.9	72.4	67.3	64.7
obe ltage in lt (expt.)	0	-0.30	-0.50	-1.50	1.50	9.25	19.25	26.75	32.25	36.50

Table 5-III

p = 0.25 torr (Air)

Magnetic field in Gauss	0	25	50	100	150	200	250	300	350	400
Probe voltage in volt (expt.)	0	-0.30	-0.50	-1.5	1.5	9.25	19.25	26.75	32.25	36.5
Probe voltage in volt (calculated)	0	-10.34	-14.48	-9.75	-0.39	9.25	17.64	26.75	31.00	33.54

Appendix A

$$\text{Let } x_H = \frac{I_H}{I_0} = \left(1 + C_1 \frac{H^2}{p^2}\right) e^{-bH}$$

$$\frac{x_{H_1} e^{bH_1}}{x_{H_2} e^{bH_2}} = \frac{H_1^2}{H_2^2} = \frac{1}{4}$$

if we take  $H_2 = 2H_1$   
for  $P_1 = P_2 = P$

$$\text{Let, } e^{bH_1} = y$$

$$\text{Hence, } \frac{x_{H_1} y^{-1}}{x_{H_2} y^{-1}} = \frac{1}{4}$$

Solving the equation for  $y$ , we have two values of  $y$  given by

$$y_1 = \frac{2x_{H_1} - \sqrt{4x_{H_1}^2 - 3x_{H_2}}}{x_{H_2}}$$

and

$$y_2 = \frac{2x_{H_1} + \sqrt{4x_{H_1}^2 - 3x_{H_2}}}{x_{H_2}}$$

$$\text{Hence, } b = \frac{\ln y_1}{H_1 \ln e} \quad \text{or} \quad b = \frac{\ln y_2}{H_1 \ln e}$$

$$\text{Again, } x_{H_1} e^{bH_1} = 1 + C_1 \frac{H^2}{p^2} = x_{H_1} y$$

$$C_1 = \frac{x_{H_1} y_1 - 1}{H_1^2 / p^2} \quad \text{or} \quad C_1 = \frac{x_{H_1} y_2 - 1}{H_1^2 / p^2}$$

Appendix B

For  $p = 0.20$  torr

$$b = 4.95 \times 10^{-3} \quad \text{and} \quad C_1 = 2.32 \times 10^{-6}$$

$$\therefore \frac{b^2 p^2}{C_1} = \frac{4.95^2 \times 10^{-6} \times 4 \times 10^{-2}}{2.32 \times 10^{-6}} = 0.4224$$

$$\text{So, } \frac{b^2 p^2}{C_1} < 1$$

Table 5-IV (Air)

Current through magnet in Amp	Discharge current in mAmp for pressure p in torr (when transverse magnetic field is applied)				
	p = 0.10 torr	p = 0.15 torr	p = 0.20 torr	p = 0.25 torr	p = 0.30 torr
0	4.15	7.50	10.45	13.25	15.35
.05	4.25	7.55	10.50	13.40	15.55
.10	4.45	7.85	10.85	13.90	16.00
.15	4.75	8.35	11.40	14.55	16.65
.20	5.15	9.05	12.30	15.45	17.35
.25	5.55	10.05	13.45	16.50	18.10
.30	6.00	10.95	14.65	17.80	18.95
.35	6.55	12.10	15.55	18.55	19.60
.40	7.05	12.75	16.05	18.75	19.90
.45	7.45	12.75	16.10	18.70	19.80
.50	7.65	12.45	15.90	18.40	19.55
.55	7.70	12.10	15.50	18.00	19.05
.60	7.55	11.65	15.10	17.40	18.55
.65	7.25	11.25	14.70	16.90	18.10
.70	6.95	10.80	14.25	16.50	17.70
.75	6.75	10.30	13.80	16.15	17.30
.80	6.40	9.90	13.45	15.80	16.90
.85	6.05	9.45	13.05	15.40	16.50
.90	5.80	9.10	12.75	15.00	16.10

Table 5 - V (Air)

Current through the magnet in p	Probe Voltage in Volt for pressures p in torr					
	p = 0.20 torr		p = 0.25 torr		p = 0.30 torr	
	Magnet Field Forward	Magnetic Field reversed	Magnet Field Forward	Magnetic Field Reversed	Magnetic Field Forward	Magnetic Filed Reversed
	0	0	0	0	0	0
05	-0.2	+0.1	-0.5	+0.1	-0.4	+0.1
10	-3.4	+2.0	-1.4	+0.6	-1.4	+0.8
15	-3.7	+3.2	+1.6	-0.4	+1.0	-1.5
20	-0.7	+1.7	+9.1	-7.2	+7.7	-13.0
25	+5.0	-1.7	+19.2	-13.5	+21.2	-19.9
30	+11.7	-7.2	+26.7	-18.6	+29.5	-23.5
35	+19.0	-13.0	+32.5	-22.8	+33.1	-26.0
40	+24.8	-18.5	+36.7	-26.1	+35.5	-27.0
45	+30.0	-24.0	+39.5	-29.9	+38.0	-27.3
50	+34.5	-28.0	+41.6	-33.0	+40.1	-27.3
55	+38.0	-31.7	+43.6	-36.0	+42.0	-27.5
60	+40.9	-34.4	+45.7	-37.5	+43.8	-27.8

R E F E R E N C E S

1. Allies W.P. and Allen H.W. , Phys. Rev., 52, 710, 1937.
2. Beckman L, Proc. Phys. Soc., 61, 515, 1948.
3. Blevin H.A. and Haydon S.C., Am. J. Phys., 11, 18, 1958.
4. Bohm D, "The characteristics of electrical discharge in Magnetic field" Edited by Geuthrie A and Wakerling R.K., MacGraw Hill Book Co., 1949.
5. Kaufman A.N., Phys. Rev., 109, 1, 1958.
6. Langmuir C.L. and Rosenbluth M.N., Phys. Rev. 103, 507, 1956.
7. Mc Bee W.D. and Daw W.G., Commun. Electron, 72, 229, 1953.
8. Sen S.N. and Gupta R.N, J. Phys. D (Appl. Phys.), 4, 510, 1971.
9. Sen S.N., Ghosh S.K. and Ghosh B, Ind. J. Pure and Appl. Phys., 21, 613, 1983.
10. Simon A, Phys. Rev., 98, 315, 1955.
11. Townsend J.S., Phil. Mag., 25, 259. 1938

CHAPTER VI

CURRENT GENERATION PROCESS, HIGH CURRENT  
DENSITY AND CATHODE PHENOMENA IN AN ARC PLASMA

## CHAPTER VI

CURRENT GENERATION PROCESS, HIGH CURRENT DENSITY  
AND CATHODE PHENOMENA IN AN ARC PLASMA

## INTRODUCTION

It is known that many attempts both theoretical and experimental have been made to explain the high current density and low cathode fall in arcs. It has been generally observed that low boiling point metals have very high cathode current density and the cathode fall of the potential is of the order of least ionization potential of the gas in which the arc burns. Theoretical investigation of the phenomena has been provided by Thomson and Thomson (1933) and by Loeb (1952). Two theories have been advanced namely thermionic emission and field emission to explain the observed experimental results. The most accepted mechanism for the production of large electron current at the cathode is thermionic emission. Because of the high velocity of electrons the space charge region is taken to be due to positive ions and utilizing the space charge equation of Childs and Langmuir and assuming that the cathode drop region to be of the order of one mean free path of the electron or even less the observed cathode current density which varies from a few hundred to a few thousand amperes can be qualitatively explained. Further extension of the theory gives the value of electric field at the cathode and for most of the metals this

comes out to be of the order of  $10^5$  volts/cm to  $10^6$  volts/cm. The possibility of such high field strengths has led some workers [Compton (1923) Langmuir (1923)] to suggest that the necessary electrons are produced by field emission. A modification of the field emission theory was suggested by Druyvestyn (1936) where the field is presumed to be produced in an extremely thin layer of relatively high resistance by a layer of positive ions on the outer surface. Ramberg (1932) however deduced from his experimental results that arcs of Cu, Hg, Ag and Au are of the field emission type and those of C, Ca, Mn are thermionic in nature. However, it is noted that the current due to field emission is far less than the arc current, being of the order of  $10^{-6}$  to  $10^{-7}$  amp/sq.cm. However it has been suggested that since the effect of the electric field is to lower the effective value of the work function, both field and thermionic emission may work together.

The nature of the electrode regions in the arc is poorly understood inspite of extensive research carried out over the decades. This lack of understanding is a consequence of the complexities prevailing in these regions caused by the interaction of electrical, magnetic, thermal and fluid dynamic effects which are difficult to assess and sometimes impossible to control. It is also doubtful whether velocity distribution of plasma particles (electrons, ions and neutrals) close to the electrodes is Maxwellian in nature. Finkelnburg and Maecker (1956) and Ecker (1961) have given a comprehensive review of

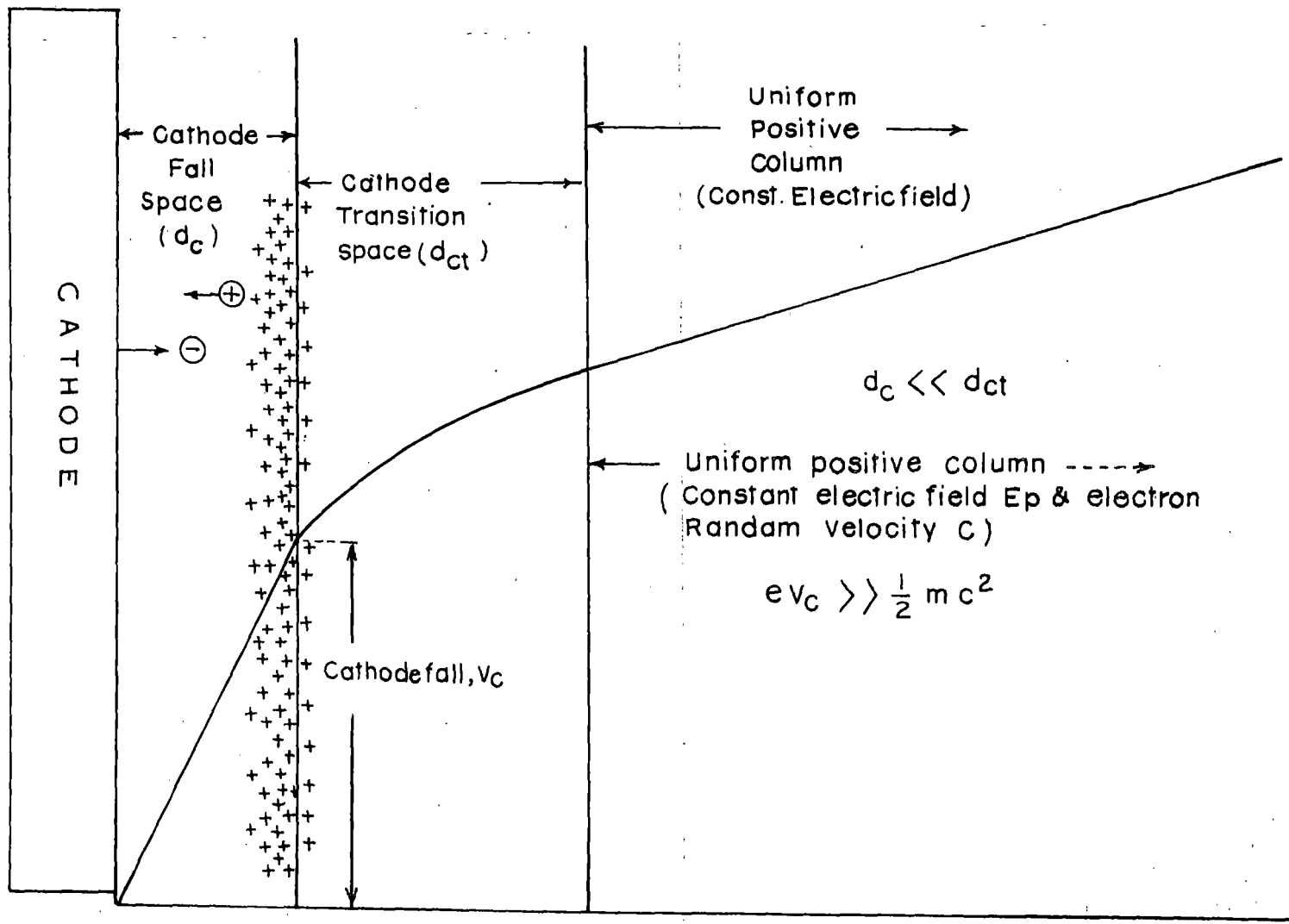


Fig. 6-I: Cathode to positive column of an arc.

the experimental results in arcs.

In the present work we have been able to show that all arcs are basically thermionic in nature irrespective of the melting point of the cathode material. Also it has been shown that the space charge layer forming the boundary of the cathode fall space is only at a distance of a mean free path from the cathode surface and ionization of vapour inside the cathode fall space is the main factor for the high current in the arc. A generalised theory has been developed for the high current density and the cathode fall and experiments have been performed to verify the deductions of the theory with observed experimental results.

#### ANALYTICAL EVALUATION OF THE PROCESS

Fig. 6.1 gives a magnified representation of the cathode, cathode fall space  $d_c$ , cathode transition space  $d_{ct}$  and the positive column of the arc. The cathode transition space is the distance between the cathode fall surface and the beginning of the positive column.

Following assumptions have been made in this theory:

- 1) Each of the thermally emitted electrons while coming across the cathode fall space attains a kinetic energy  $eV_c$  at the boundary of the fall space when electron velocity is given by

$$v_c = \left( \frac{2eV_c}{m} \right)^{1/2}$$

where  $v_c$  is the emerging velocity of the electrons and  $V_c$  is the cathode fall.

- 2) Each such electron when it enters into the cathode transition space ionises one atom within a very short distance from the boundary of the cathode fall space.
- 3) The excess energy after ionisation over that of the random energy  $\frac{1}{2} mC^2$  of the electrons in the uniform positive column is spent by collision until it reaches the uniform position column and attains the random energy of the electrons in the uniform positive column where  $C$  is the random velocity of the electron in the positive column.
- 4) When equilibrium is established, the boundary of the cathode fall space and the positive charge distribution across the fall space boundary remain statistically stationary, so long the external parameters like pressure, and arc current remain unaltered.
- 5) The field required for the emission of electrons in the fall space is supplied by the positive charge layer across the fall space boundary which also shields the cathode from the rest of the arc.
- 6) The cathode fall space boundary is at a distance of a mean free path from the cathode surface. So the span of cathode fall space is of the order of a mean free path.
- 7) The span of the cathode transition space  $d_{ct}$ , i.e., the distance from the fall space boundary to the beginning of uniform positive column is much greater than the span of cathode fall space ( $d_c$ )

$$\text{So, } d_c \ll d_{ct}$$

8) By suddenly stopping the arc by some external means like magnetic field, it has been observed that about 2% of the power consumed by the running arc is still flowing in the circuit through the arc giving only violet and ultraviolet radiation between the electrodes so long the electrode is hot. So we assume that a running arc produces considerable ultraviolet radiation in the fall space which is absorbed by the metal vapour in one or two steps. Also due to the collision between on coming vapour and positive ions in the fall space all vapours are ionised and the energy spent by  $I_c V_c$  in the fall space is uniformly sprayed through the area of emission of vapour around a small area at the centre where the discharge is taking place. Thus a cumulative ionisation process goes on until all vapours are ionised in the fall space and an uniform energy distribution in the fall space is established.

9) Thus if such process as in (8) is truly taking place, then the positive ion current will gradually increase as we proceed towards the cathode and will definitely be maximum on the cathode surface. Here we must mention the work of Lee and Greenwood (1964) where they found for a 200A carbon arc, a positive ion current to vary from zero at the column end to 15% of the total current at the cathode surface end.

10) Each electron is supposed to be uniformly retarded while moving through the cathode transition space.

11) Ionisation potential  $V_i$  may correspond to any of the components of the working fluid in the arc. By component we mean the gas or gases already present, metal vapour or any new gas formed at the cathode by any chemical reaction.  $V_i$  is mostly expected to be the lowest of the  $V_i$ -s and may be a higher one also in some cases due to the nature of the gases.

12) In fact ionisation by electrons leaving the cathode fall boundary takes place after several mean free paths and the velocity of the ionising electron is supposed to drop to a velocity  $v_D$  which must be associated to the characteristics of the fluid in the transition space. So we supposed this velocity to be the geometric mean of the two extreme velocities, e.g.  $v_c$  and  $C$ , so  $v_D$  is given by  $v_D = (v_c C)^{\frac{1}{2}}$ .

13) Span of cathode emission area and span of cathode fall space change in the same way with pressure such that the ratio of these two is independent of pressure and is constant so long cathode temperature remains at a particular value.

14) Due to high field in the fall space, the thermal emission, here, is Schottky emission.

Theoretical deduction:

Since uniform retardation  $f$  is considered in the transition space, so we have

$$f = \frac{v_c^2 - C^2}{2dct} \quad (6.1)$$

where  $v_c$  is the velocity of the electron, as it emerges from the cathode fall space and  $C$  is the random velocity of the electrons in the positive column. Time taken for this change in velocity will be

$$t = \frac{v_c - C}{f} = \frac{2d_{ct}}{v_c + C} \quad \dots (6.2) \quad \left[ \text{from eqn. (6.1)} \right]$$

when equilibrium in the arc is established, if  $n_T$  is the net number of electrons coming out from fall space in one sec. through unit area, then total number of electrons coming out through an area  $S$  of fall space and in time  $t$  will be

$$n_T \frac{2d_{ct}}{v_c + C} S$$

For low energy electrons the ionisation efficiency is given by

$$\alpha = ap (V - V_i)$$

when "a" is the number of ion-pairs produced by collision per volt per meter per mm. of Hg pressure. Hence number of positive ions generated by collision in the cathode transition space by these electrons will be

$$n_T \frac{2d_{ct}}{v_c + C} \cdot s \cdot a \cdot p (V_{ct} - V_i) d_{ct}$$

$V_{ct}$  is the voltage at a distance  $d_{ct}$  after the fall space,  $V_i$  is the ionisation potential of the gas or vapour in the transition space. Hence number of positive ions per unit volume becomes

$$n_T \frac{2ap}{v_c + C} (V_{ct} - V_i) d_{ct}$$

In place of  $d_{ct}$  if we consider a distance  $x$  then charge density at a distance  $x$  is given by

$$\rho_x = n_T e \frac{2ap}{v_c + c} (V_x - V_i) x \quad (6.3)$$

But  $v_x^2 = v_c^2 - 2fx$ ,  $v_x$  is the velocity at a distance  $x$ .

$$\text{So, } v_x^2 = v_c^2 - \frac{v_c^2 - c^2}{d_{ct}} x$$

replacing each of the velocities by equivalent voltages.

We get,

$$V_x = V_c - \frac{V_c - \frac{mc^2}{2e}}{d_{ct}} x, [e \text{ is the electronic charge}]$$

$$\text{So, } \rho_x = n_T e \frac{2ap}{v_c + c} \left[ V_c - V_i - \left( V_c - \frac{mc^2}{2e} \right) \frac{x}{d_{ct}} \right] x \quad (6.4)$$

$$\text{By Poisson's equation } \frac{d^2V}{dx^2} = - \rho / \epsilon_0 \quad (\text{in MKS unit})$$

and boundary conditions are,

$$\text{at } x = 0 \quad V = 0, (dV/dx) = 0$$

$$\text{at } x = d_c \quad V = V_c, (dV/dx) = Ec$$

Thus we get,

$$- \frac{dV}{dx} = \frac{n_T e}{\epsilon_0} \cdot \frac{2ap}{v_c + c} \left[ (V_c - V_i) \frac{x^2}{2} - \left( V_c - \frac{mc^2}{2e} \right) \frac{x^3}{3d_{ct}} \right] + C_1$$

So putting boundary conditions, we have

$$\left| -\frac{dV}{dx} \right| = E_C = \frac{n_T e}{\epsilon_0} \cdot \frac{2ap}{v_C + c} \cdot \frac{d_C^2}{2} \left[ (V_C - V_i) - \left( V_C - \frac{mc^2}{2e} \right) \frac{2d_C}{3d_{ct}} \right] \quad (6.5)$$

$$\text{and } V_C = \frac{n_T e}{\epsilon_0} \cdot \frac{2ap}{v_C + c} \cdot \frac{d_C^3}{6} \left[ (V_C - V_i) - \left( V_C - \frac{mc^2}{2e} \right) \frac{d_C}{2d_{ct}} \right] \quad (6.6)$$

Ignoring the difference in  $\frac{2d_C}{3d_{ct}}$  and  $\frac{d_C}{2d_{ct}}$  in (6.5) and (6.6) we

$$\text{have,} \quad E_C \approx \frac{3V_C}{d_C} \quad (6.7)$$

Now we assume that each electron coming out from cathode fall space ionises one neutral atom within a short distance  $l$  from the cathode fall space boundary, so we can write with  $K$  as a loss factor

$$ap(V_C - V_C K \frac{l}{\lambda} - V_i) l = 1 \quad (6.8)$$

where  $V_C K \frac{l}{\lambda}$  is the net energy lost by collisions upto an instant just before ionisation takes place.

Thus  $K$ , here, is not a true loss factor but a loss factor which includes the gain in energy by the electron between two consecutive collisions and loss by collision. Eqn. (6.8) gives

$$l = \frac{(V_C - V_i) \pm \sqrt{(V_C - V_i)^2 - \frac{4V_C K}{aL_1}}}{2p \frac{V_C K}{L_1}} \left[ \lambda = \frac{L_1}{p} \right]$$

where  $L_1$  is the mean free path of the electron at 1 torr. But under the stated condition  $l$  cannot have two values in the transition region since  $V_C < 2V_i$ . Hence equating the discriminant to zero, we get,

$$K = \frac{aL_1(V_C - V_i)^2}{4V_C} \quad (6.9a)$$

$$l = \frac{V_C - V_i}{2p \frac{V_C K}{L_1}} = \frac{2}{ap(V_C - V_i)} \quad (6.9b)$$

Again we consider, when an atom is ionised by an electron through collision, the rest of the energy is lost by collision until equilibrium random velocity  $C$  in the uniform positive column is attained by the electron. So we can write by excluding the energy of one atom ionisation,

$$e(V_C - V_i) K \cdot \frac{d_{ct} - d_c}{\lambda} = \frac{1}{2} m (v_D^2 - C^2) \quad (6.10)$$

But  $v_C > v_D \gg C$  because  $E/p$  in the uniform positive column of an arc for high  $p$ , is given by

$$E/p < 1 \text{ Volt/cm. torr}$$

Again  $\lambda \approx d_c$  and  $d_c \ll d_{ct}$

$$\text{So, } \frac{d_c}{d_{ct}} = \frac{2eK(V_c - V_i)}{m v_D^2} = \frac{aL_1 e}{2m v_D^2} \cdot \frac{(V_c - V_i)^3}{V_c} \quad (6.11)$$

Thus we have, from eqn. (6.6)

$$V_c = \frac{n_T e}{\epsilon_0} \cdot \frac{ap}{3 v_c} \cdot d_c^3 \cdot (V_c - V_i) \left[ 1 - \frac{aL_1 e}{4m v_D^2} (V_c - V_i)^2 \right]$$

and a mean value of  $C$  for  $0.5 < E/p < 1$  is taken to be  $0.6 \times 10^4$  m/sec and a mean value of  $V_c$  is taken to be 18 V.

Thus

$$v_c = \sqrt{\frac{2 \times 1.6 \times 10^{-19} \times 18}{9.1 \times 10^{-31}}} \text{ m/s} = 2.52 \times 10^6 \text{ m/s}$$

$$\text{and } v_D = \sqrt{v_c C} = \sqrt{1.51 \times 10^{10}} \text{ m/s}$$

$$\text{Hence } \frac{aL_1}{4m v_D^2} = 5.32 \times 10^{-3} \text{ (in MKS unit)}$$

where  $a = 26$  ion pair /V/m/m.m. of Hg (Air)

$L_1 = 7 \times 10^{-5}$  meter m.m. of Hg (Air)

$m = 9.1 \times 10^{-31}$  Kg (electron)

So we have,

$$V_c = \frac{n_T e}{\epsilon_0} \cdot \frac{ap}{3 v_c} \cdot d_c^3 (V_c - V_i) \left[ 1 - 5.32 \times 10^{-3} (V_c - V_i)^2 \right] \quad (6.12)$$

upto this we have dealt with  $n_T$ , the net no. of electrons emitted from fall space. Now we want to get the value of the ratio  $n_T/n_e$  where  $n_e$  is the directly generated electron from the cathode. Let  $\alpha_c$  be the area of cathode spot from where the electron is basically emitted under the influence of heat and field, which may be called a thermal emission though cathode surface at the actual spot is highly different from the surface of the metal. Actually, the surface at the spot is a mixture of vapour and partially molten metal in case of low melting point metals. And in case of refractory metals like carbon the surface is a mixture of carbon particles and Co,  $Co_2$  for air as a working fluid. Some refractory metals like W, when operated at a low cathode temperature, the emission area may be a solid surface, partly. Thus this is not the surface of a pure thermionic emitter.

Let  $A_0$  be the total area, excluding the  $\alpha_c$  at the centre of  $A_0$ , from where vapourisation of metal (cathode) takes place.

$$A_0 \gg \alpha_c$$

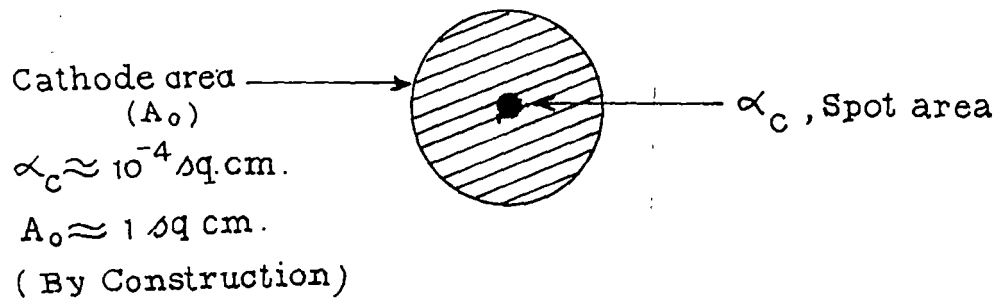
Let us assume the power  $I_c V_c$  is spent uniformly from every part of the area  $A_0$ .

$$\text{Let } P = I_c V_c \text{ joule/Sec} = I_c V_c \times 10^7 \text{ ergs/sec}$$

Let  $W_e$  is the energy spent exclusively for electron emission, i.e., excluding any energy spent against vapourisation and the

ionisation of the vapour, and  $W_m$  is the total energy spent for vapourisation followed by ionisation of the vapour. So, as we have assumed the energy spent is uniformly distributed over the area  $A_o$ , we can write

Actual position on the cathode



$$\frac{W_e}{\alpha_c} = \frac{W_m}{A_o} \quad (6.13)$$

and  $W_e + W_m = P$  is the total power consumed on the cathode

$$W_e = \frac{\alpha_c}{\alpha_c + A_o} (W_e + W_m) \approx \frac{P \alpha_c}{A_o} \quad (6.14a)$$

and

$$W_m = \frac{A_o}{\alpha_c + A_o} P \approx P \quad (6.14b)$$

Electron emission energy is given by

$$E_e = \phi \times 9.63 \times 10^{11} \text{ ergs/mole} \quad (6.15)$$

where  $\phi$  is the work function of the metal. Metal vapourisation energy is given by

$$E_v = LM \times 4.2 \times 10^7 \text{ ergs/mole}$$

L is the latent heat per gm.

M is the molecular weight

Metal vapour ionisation energy is given by

$$E_i = V_i \times 9.63 \times 10^{11} \text{ ergs/mole}$$

$V_i$  is the ionisation potential of the vapour atom. Hence the metal vapourisation followed by ionisation requires an energy given by

$$E_m = E_v + E_i = (LM + 2.29 \times 10^4 V_i) 4.2 \times 10^7 \text{ ergs/mole} \quad (6.16)$$

Hence number of electrons emitted is given by

$$N_e = \frac{W_e}{E_e} = \frac{(P \alpha_c / A_0) \text{ ergs/sec}}{\phi \times 9.63 \times 10^{11} \text{ ergs/mole}} = \frac{\alpha_c P}{A_0 \phi \times 9.63 \times 10^{11}} \text{ mole/sec.}$$

$$\text{So } N_e = \frac{\alpha_c P N}{A_0 \phi \times 9.63 \times 10^{11}} \text{ no./sec.} = \frac{\alpha_c P}{A_0 \phi} \times 6.25 \times 10^{11} \text{ no./sec.} \quad (6.17)$$

where N is the Avogadro's number. And vapour ion produced is given by

$$\begin{aligned} N_m &= \frac{W_m}{E_m} = \frac{P \text{ (ergs/sec)}}{(LM + 2.29 \times 10^4 V_i) \times 4.2 \times 10^7 \text{ ergs/mole}} \\ &= \frac{P}{(LM + 2.29 \times 10^4 V_i) \times 4.2 \times 10^7} \text{ mole/sec.} \\ &= \frac{PN}{(LM + 2.29 \times 10^4 V_i) \times 4.2 \times 10^7} \text{ no./sec.} \end{aligned}$$

$$\text{So, } N_m = \frac{P \times 1.43 \times 10^{16}}{LM + 2.29 \times 10^4 V_i} \text{ no./sec.} \quad (6.18)$$

Hence total number of electrons emitted per sec.,

$$N_T = N_m + N_e \approx N_m$$

Hence total number per unit area is given by

$$n_T = \frac{N_T}{A_0} = \frac{N_m}{A_0} = \frac{P \times 1.43 \times 10^{16}}{A_0 (LM + 2.29 \times 10^4 V_i)} \text{ no./sec./area} \quad (6.19)$$

And number of electrons emitted directly from metal per unit area per sec. is given by

$$n_e = \frac{N_e}{A_0} = \frac{\alpha_c P}{A_0^2 \phi} \times 6.25 \times 10^{11} \text{ no./sec./area} \quad (6.20)$$

$$\text{So, } \frac{n_T}{n_e} = \frac{(A_0 \phi / \alpha_c) \times 2.29 \times 10^4}{LM + 2.29 \times 10^4 V_i} \quad (6.21)$$

$$\text{Now let, } \frac{(A_0 \phi / \alpha_c) \times 2.29 \times 10^4}{LM + 2.29 \times 10^4 V_i} = \beta_c \quad (6.22)$$

$$\text{So, } n_T = \beta_c n_e \quad (6.23)$$

Thus now using (6.23) in (6.12) we get

$$V_C = \frac{n_e e}{\epsilon_0} \beta_C \frac{ap}{3V_C} d_C^3 (V_C - V_i) \left[ 1 - 5.32 \times 10^{-3} (V_C - V_i)^2 \right] \quad (6.24)$$

But  $n_e$  is the directly emitted electron from metal by the action of temperature  $T_C$  and field  $E_C$ . So due to Schottky effect we can write

$$n_e = n_0 \exp\left(\frac{0.44}{T_C} \sqrt{E_C}\right) \quad (\text{in MKS unit})$$

Thus we have,

$$V_C = \frac{n_0 e}{\epsilon_0} \beta_C \frac{ap}{3V_C} d_C^3 (V_C - V_i) \exp\left(\frac{0.44}{T_C} \sqrt{E_C}\right) \left[ 1 - 5.32 \times 10^{-3} (V_C - V_i)^2 \right] \quad (6.25)$$

Thus  $n_0 e = J_0$  is the directly emitted current density on the cathode spot where discharge takes place. So now using eqn. (6.7), and  $d_C \approx \lambda = \frac{L_1}{p}$  we get

$$E_C = \frac{3V_C}{d_C} = \frac{3V_C}{\lambda} = \frac{3pV_C}{L_1} \quad (6.26)$$

and hence, with  $v_c = \left( \frac{2eV_c}{m} \right)^{1/2}$  we have

$$\frac{pV_c^{3/2}}{(V_c - V_i) [1 - 5.32 \times 10^{-3} (V_c - V_i)^2]} = \left[ \frac{j_0 \beta_c d_c a L_1^2}{3\epsilon_0 \sqrt{\frac{2e}{m}}} \right] \text{Exp} \left[ \frac{0.44}{T_c} \sqrt{\frac{3}{L_1}} \sqrt{V_{cP}} \right] \quad (6.27)$$

Now  $\alpha_c$  and  $d_c$  both are controlled by pressure. So we assume  $d_c$  and  $\alpha_c$  varies in the same way with change in pressure. So  $d_c/\alpha_c$  is constant and  $j_0$  is constant, so long  $T_c$  remains same. So we can take

$$\frac{j_0 \beta_c d_c L_1^2 a}{3\epsilon_0 (2e/m)^{1/2}} \quad \text{a constant which depends only}$$

on cathode Temperature  $T_c$  and nature of the cathode. So taking,

$$A = \frac{j_0 \beta_c d_c L_1^2 a}{3\epsilon_0 (2e/m)^{1/2}}$$

$$\text{and } \frac{0.44}{T_c} \sqrt{\frac{3}{L_1}} \log_{10} e = b$$

We have,

$$\log \left[ \frac{pV_c^{3/2}}{(V_c - V_i) [1 - 5.32 \times 10^{-3} (V_c - V_i)^2]} \right] = \log_{10} A + b \sqrt{V_{cP}} \quad (6.28)$$

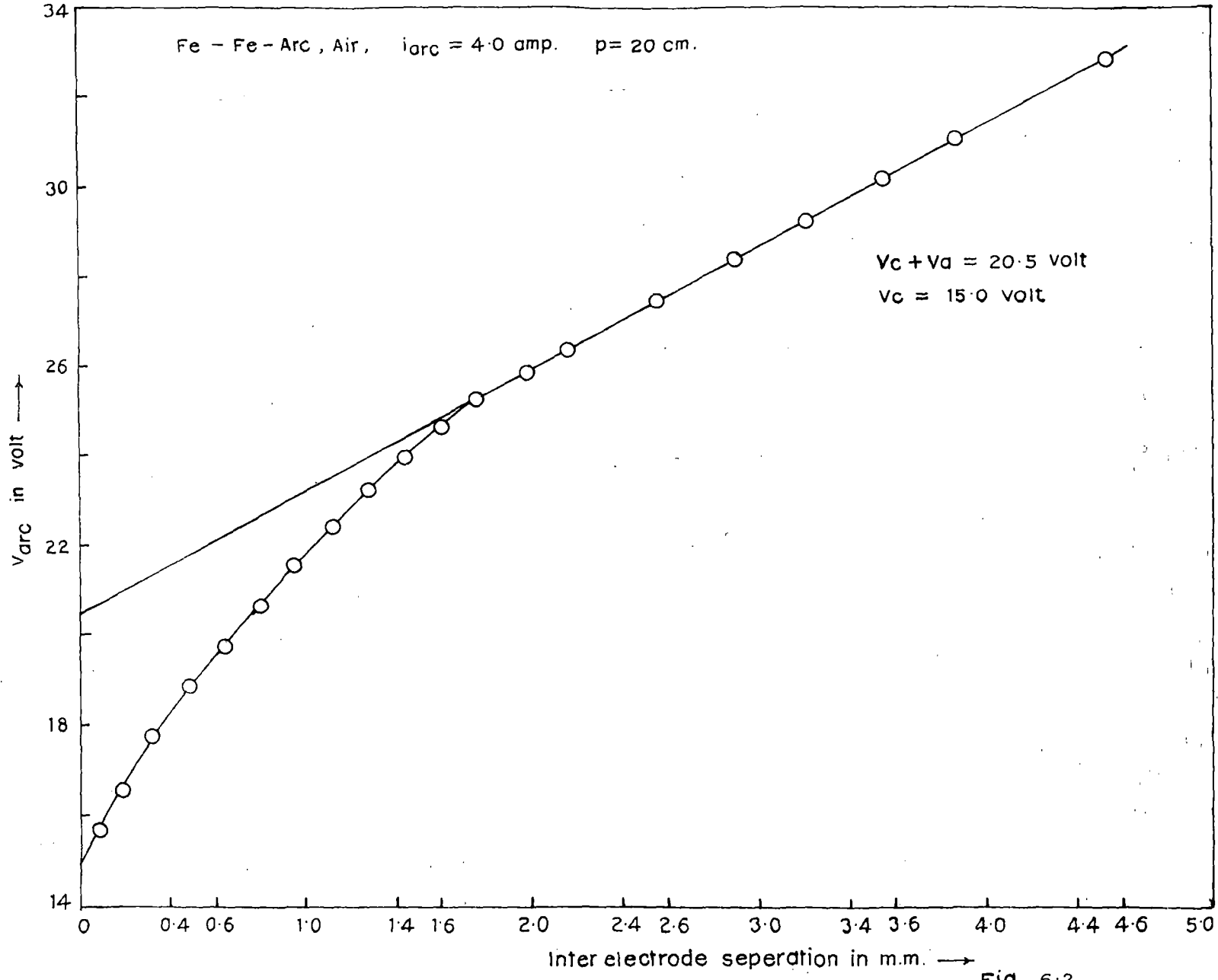


Fig. 6.2.

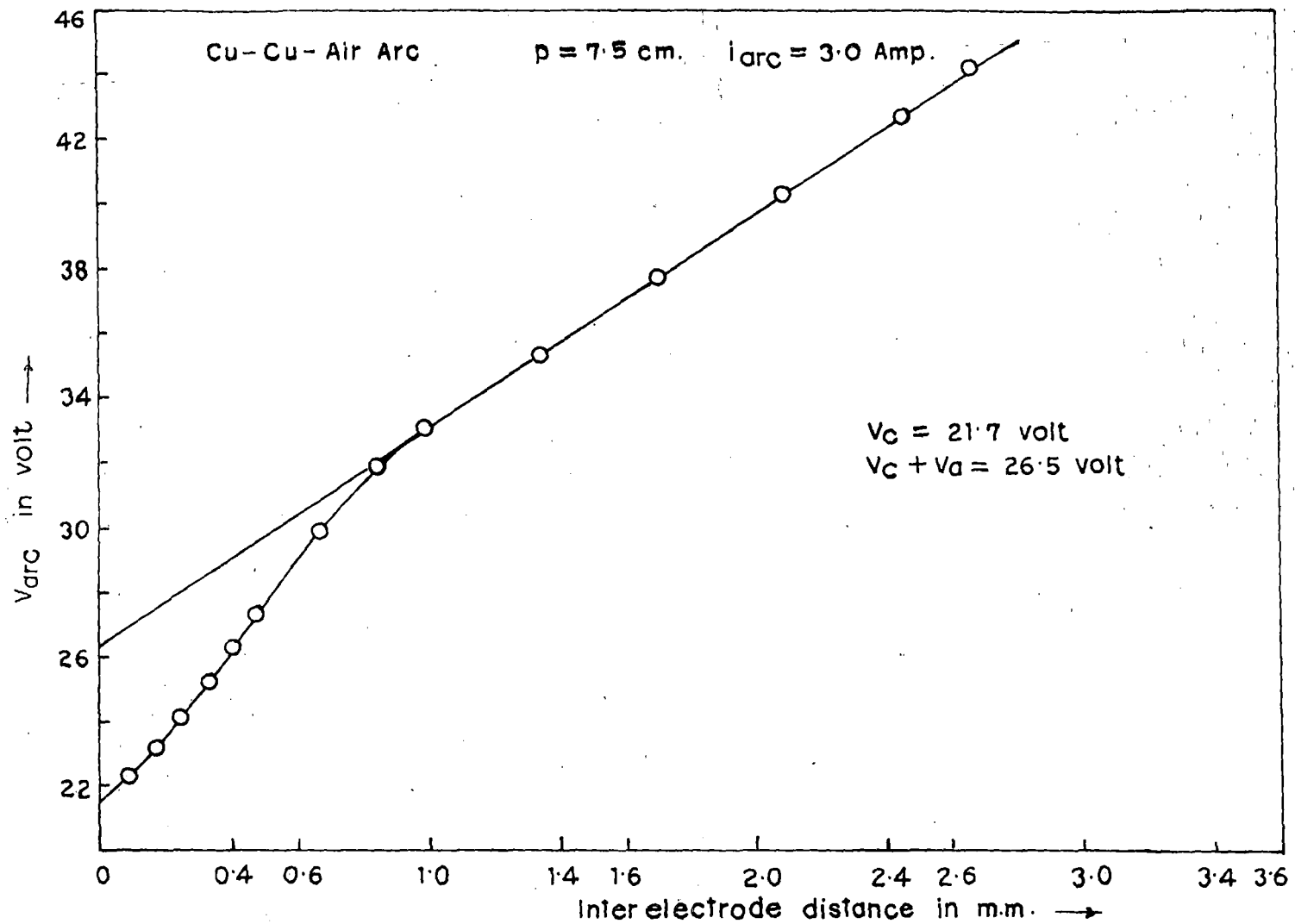


Fig. 6.3.

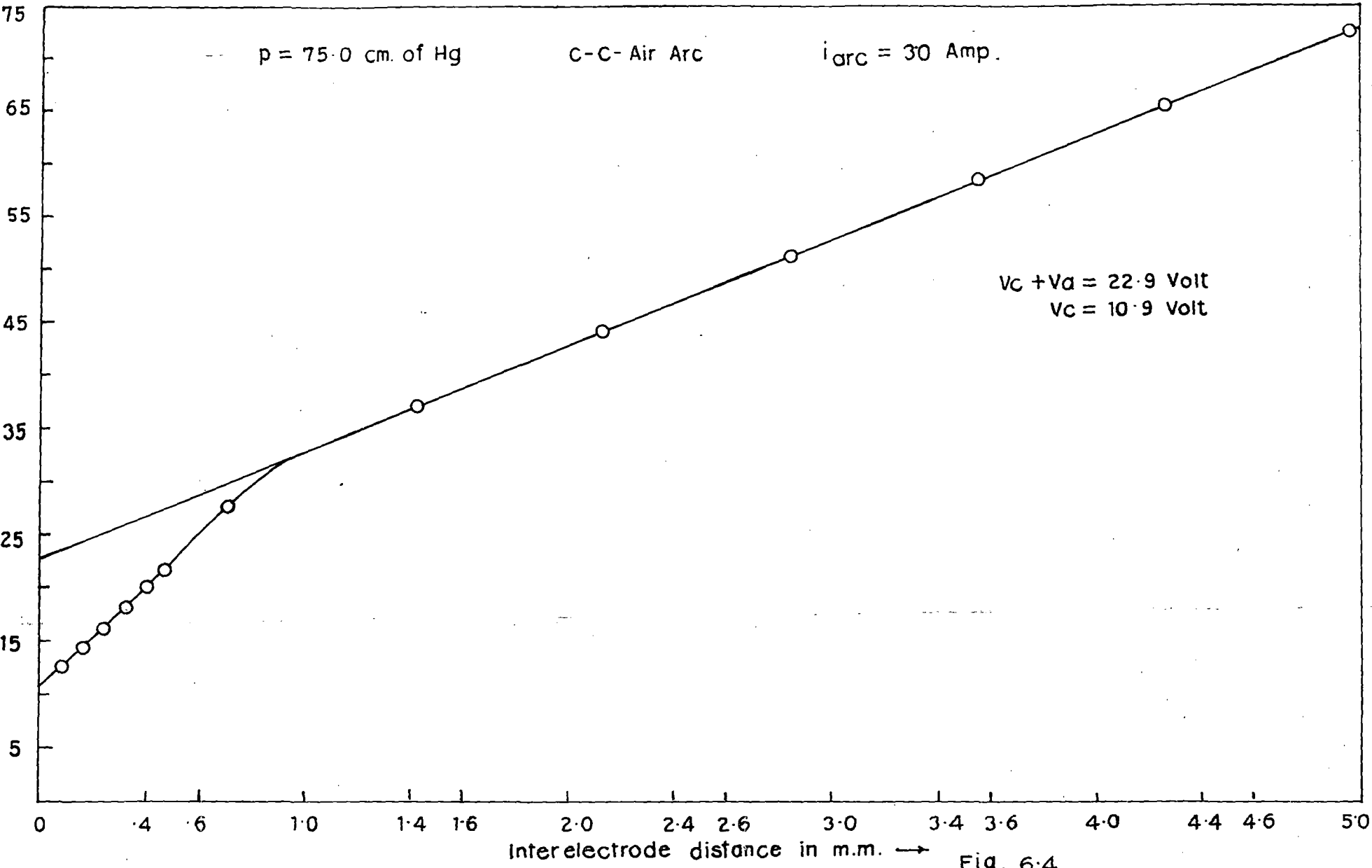


Fig. 6.4.

So from equation (6.28) we can conclude that if

$$\log_{10} \left[ \frac{pV_c^{3/2}}{(V_c - V_i) \{ 1 - 5.32 \times 10^{-3} (V_c - V_i)^2 \}} \right]$$

is plotted against

$\sqrt{V_c p}$ , the curve should be a straight line if the assumptions are valid.

#### EXPERIMENTAL ARRANGEMENT AND RESULTS

It is evident from equation (6.28) that to verify the theoretical deduction with the experimental results we have to measure the cathode fall for a wide range of pressure. The arcs investigated in the present work are Cu-Cu, C-C and Fe-Fe arc in air. The arc is struck in a chamber (Fig. 2.7) which can be gradually evacuated. The pressure inside was maintained by a rotary pump and two needle valves one connected at the input and the other at the output. The distance between the two electrodes could be varied and the experiment consists in measuring the arc voltage for various cathode anode separation distances. The variation of arc voltage with separation distance was plotted and the value of the cathode fall was obtained by the standard method as was done previously (Sen, Gantait and Jana, 1988). Three representative curves Fig. 6.2, 6.3 and 6.4 in the present case are shown. The electrode separation was measured with the help of a linear scale and a large circular scale and it was possible to measure a minimum distance of

separation of 0.004 mm. and the arc drop was measured with a digital meter. The results were obtained for three types of arc mentioned above with pressure variation from 50.0 mm to 750 mm. The pressure was measured with a mercury manometer with one end sealed. To prevent fluctuation of the arc current a constant current device was utilized. The results for Cu-Cu, C-C and Fe-Fe arc in air are shown in table 6.1, 6.2 and 6.3.

Table 6.1

$i_{\text{arc}} = 3.0 \text{ amp,}$  Cu-Cu-Air-Arc

P in mm Hg	$V_c + V_a$ in volt	$V_c$ in volt	$V_a$ in volt
50	24.0	21.1	2.9
75	26.5	21.7	4.8
100	29.4	21.4	8.0
125	29.6	20.7	8.9
150	28.5	19.6	8.9
175	26.5	19.0	7.5
200	25.1	18.6	6.5
225	24.4	18.3	6.1
250	23.9	18.0	5.9
350	22.5	17.1	5.4
450	21.5	16.4	5.1
550	20.8	15.8	5.0
650	20.4	15.4	5.0
750	20.0	15.0	5.0

Table 6.2

C-C-Air-Arc

 $i_{\text{arc}} = 3.0 \text{ Amp}$ 

p in mmHg	Experimental value			Value from extrapolated graph	
	$V_c + V_a$ in volt	$V_c$ in volt	$V_a$ in volt	$V_c$ in volt	$V_a$ in volt
50	27.4	13.2	14.2	13.2	14.2
75	29.6	14.0	15.6	14.0	15.6
100	33.5	15.0	18.5	15.0	18.5
125	35.6	15.4	20.2	15.4	20.2
150	35.6	14.6	21.0	15.3	21.0
175	29.7	12.3	17.4	14.9	21.5
200	25.3	9.3	16.0	14.6	21.6
225	29.4	11.4	18.0	14.1	21.5
250	33.7	13.7	20.0	13.7	21.1
275	33.8	13.4	20.4	13.4	20.6
300	33.1	13.1	20.0	13.1	20.0
350	31.0	12.8	18.2	12.8	18.2
450	27.8	12.0	15.8	12.0	15.8
550	25.7	11.5	14.2	11.5	14.2
650	24.1	11.2	12.9	11.2	12.9
750	22.9	10.9	12.0	10.9	12.0

Table 6.3

Fe-Fe-Air Arc

 $i_{\text{arc}} = 4.0 \text{ Amp}$ 

P in cmHg	$V_c + V_a$ in volt	$V_c$ in volt	$V_a$ in volt
5.0	15.7	10.4	5.3
7.5	16.9	11.7	5.2
10.0	18.0	12.8	5.2
12.5	19.0	13.7	5.3
15.0	19.8	14.4	5.4
17.5	20.25	14.75	5.5
20.0	20.50	15.0	5.5
22.5	20.2	14.75	5.45
25.0	19.65	14.35	5.30
27.5	18.85	13.80	5.05
30.0	18.20	13.40	4.80
35.0	17.35	12.95	4.40
40.0	16.85	12.70	4.15
45.0	16.6	12.60	4.00

Table 6.4

Fe-Fe-Air-Arc

$$i_{\text{arc}} = 4.0 \text{ Amp}$$

$$V_i = 7.9 \text{ volt (Fe} \rightarrow \text{Fe}^+)$$

$$R = \frac{pV_c^{3/2}}{(V_c - V_i)\{1 - 5.32 \times 10^{-3}(V_c - V_i)^2\}}$$

$$T_c = 2400^\circ\text{K}$$

$$L_1 = 7 \times 10^{-5} \text{ meter mm. of Hg.}$$

$p$ in mm of Hg	$V_c$ in volt	$\sqrt{V_c}$	$(V_c - V_i)$ in volt	$[1 - 5.33 \times 10^{-3} \sqrt{V_c p} \times (V_c - V_i)^2]$	$\sqrt{V_c p}$	$\text{Log}_{10} R$	$R$ (in MKS)
50	10.4	3.22	2.5	0.9668	22.80	2.84	692.8
75	11.7	3.42	3.8	0.9232	29.62	2.93	855.5
100	12.8	3.58	4.9	0.8723	35.78	3.03	1072.1
125	13.7	3.70	5.8	0.8210	41.38	3.12	1330.7
150	14.4	3.79	6.5	0.7752	46.48	3.21	1624.7
175	14.75	3.84	6.85	0.7504	50.81	3.29	1928.3
200	15.0	3.87	7.1	0.7318	54.77	3.35	2234.5
225	14.75	3.84	6.85	0.7504	57.61	3.39	2479.3
250	14.35	3.79	6.45	0.7787	59.90	3.43	2707.1
275	13.80	3.71	5.90	0.8148	61.60	3.47	2928.8
300	13.40	3.66	5.50	0.8391	63.40	3.50	3188.1
350	12.95	3.60	5.05	0.8643	67.32	3.57	3738.4
400	12.70	3.56	4.8	0.8774	71.30	3.63	4294.1
450	12.60	3.55	4.7	0.8825	75.30	3.69	4852.9

Table 6.5

Cu-Cu-Air-Arc

 $i_{\text{arc}} = 3.0$  Amp $T_c = 2200^\circ\text{K}$  $V_i = 12.1$  volt ( $\text{O}_2 \rightarrow \text{O}_2^-$ ) $L_1 = 7.0 \times 10^{-5}$  metre mm. of Hg.

$$R = \frac{p V_c^{3/2}}{(V_c - V_i) \{ 1 - 5.32 \times 10^{-3} (V_c - V_i)^2 \}}$$

$p$ in mm of Hg	$V_c$ in volt	$\sqrt{V_c}$	$(V_c - V_i)$ in volt	$[1 - 5.32 \times 10^{-3} \times (V_c - V_i)^2]$	$\sqrt{V_c} p \log_{10} R$	$R$
50	21.1	4.59	9.0	0.5690	32.48 2.98	945.6
75	21.7	4.66	9.6	0.5097	40.34 3.19	1550.0
100	21.4	4.63	9.3	0.5399	46.26 3.30	1973.0
125	20.7	4.55	8.6	0.6065	50.87 3.35	2257.0
150	19.6	4.43	7.5	0.7008	54.22 3.39	2478.0
175	19.0	4.36	6.9	0.7467	57.66 3.45	2814.0
200	18.6	4.31	6.5	0.7752	60.99 3.50	3182.0
225	18.3	4.28	6.2	0.7955	64.17 3.55	3573.0
250	18.0	4.24	5.9	0.8148	67.08 3.60	3969.0
350	17.1	4.14	5.0	0.8670	77.36 3.76	5716.0
450	16.4	4.05	4.3	0.9016	85.91 3.89	7710.0
550	15.8	3.97	3.7	0.9272	93.22 4.00	10056.0
650	15.4	3.92	3.3	0.9421	100.1 4.10	12622.0
750	15.0	3.87	2.9	0.9553	106.1 4.20	15715.0

Table 6.6

C-C-Air-Arc

$$i_{\text{arc}} = 3.0 \text{ Amp}$$

$$T_c = 3500^\circ\text{K}$$

$$V_i = 9.2 \text{ volt (Cyanogen } C_2N_2)$$

$$L_1 = 7 \times 10^{-5} \text{ meter mm of Hg}$$

$$R = \frac{pV_c^{3/2}}{(V_c - V_i) \{ 1 - 5.32 \times 10^{-3} (V_c - V_i)^2 \}}$$

$$L_1 = 7.0 \times 10^{-5} \text{ meter mm. of Hg}$$

$p$ in mm of Hg	$V_c$ in volt	$\sqrt{V_c}$	$(V_c - V_i)$	$[1 - 5.32 \times 10^{-3} \times (V_c - V_i)^2]$	$\sqrt{V_c} p$	$\log_{10} R$	$R$
50	13.2	3.63	4.0	0.915	25.69	2.82	654.6
75	14.0	3.74	4.8	0.877	32.40	2.97	932.9
100	15.0	3.87	5.8	0.821	38.73	3.11	1291.1
125	15.4	3.92	6.2	0.795	43.87	3.19	1530.9
150	15.3	3.91	6.1	0.802	47.91	3.26	1834.2
175	14.9	3.86	5.7	0.827	51.06	3.33	2135.2
200	14.6	3.82	5.4	0.845	54.04	3.39	2444.5
225	14.1	3.75	4.9	0.872	56.32	3.44	2784.3
250	13.7	3.70	4.5	0.892	58.52	3.50	3157.1
275	13.4	3.66	4.2	0.906	60.70	3.55	3544.4
300	13.1	3.62	3.9	0.919	62.69	3.60	3969.4
350	12.8	3.58	3.6	0.931	66.93	3.68	4785.3
450	12.0	3.46	2.8	0.958	73.48	3.84	6965.4
550	11.5	3.39	2.3	0.972	79.53	3.98	9591.1
650	11.2	3.35	2.0	0.979	85.32	4.10	12455.6
750	10.9	3.30	1.7	0.985	90.42	4.21	16110.8

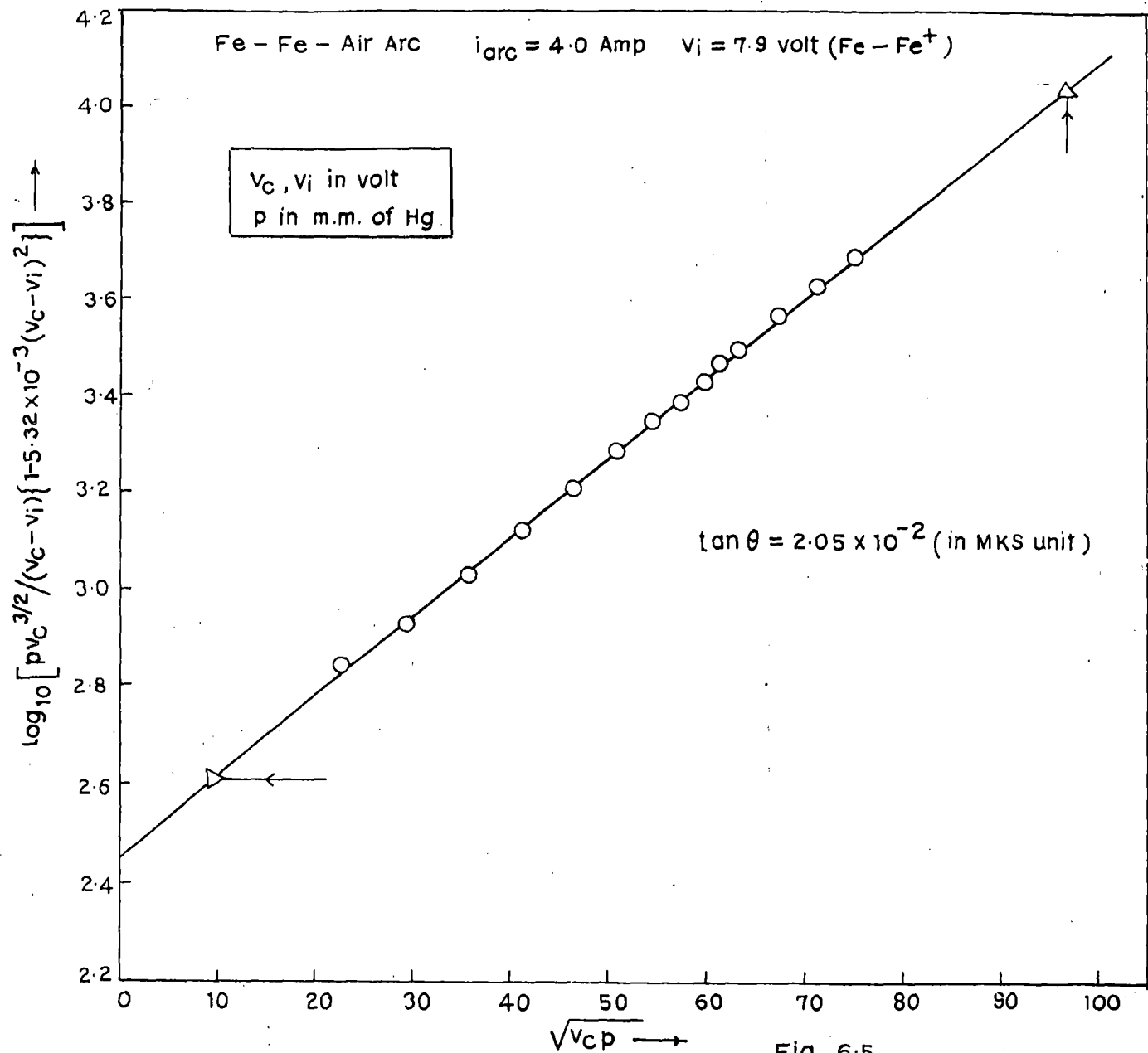


Fig. 6.5.

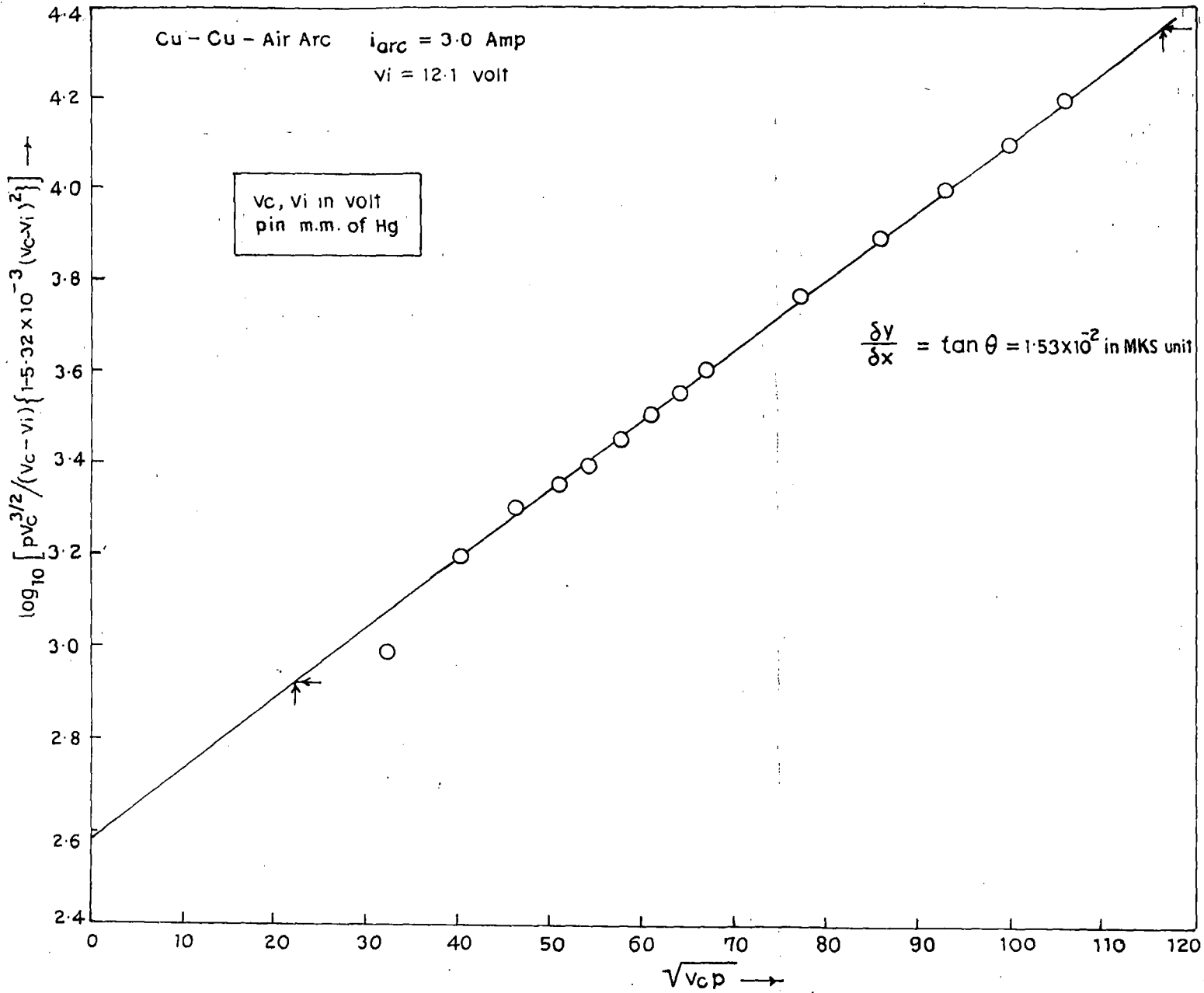


Fig. 6.6.

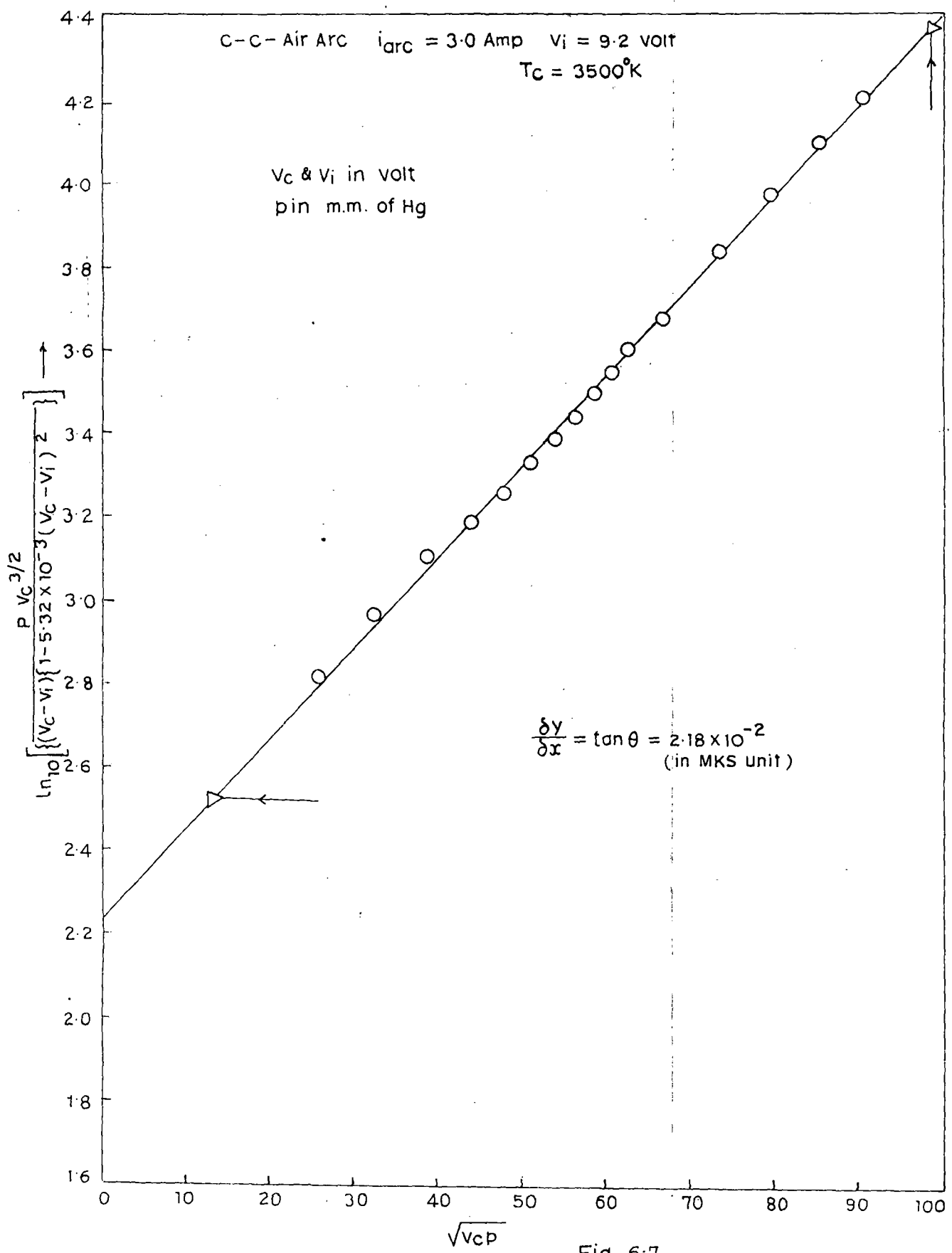


Fig. 6-7.

## DISCUSSION

From the values of  $V_c$  and the corresponding pressure the values of  $\sqrt{V_c p}$  and that of  $\log_{10} \frac{p V_c^{3/2}}{(V_c - V_i) \{1 - 5.32 \times 10^{-3} (V_c - V_i)^2\}}$  have been calculated where the value of  $V_i$  has been taken from the literature (Cobine, 1958) for Cu-Cu, C-C and Fe-Fe arcs and the results are entered in Table 6.5, 6.6 and 6.7. The figures (6.5), (6.6) and (6.7) show that when

$$\log_{10} \frac{p V_c^{3/2}}{(V_c - V_i) \{1 - 5.32 \times 10^{-3} (V_c - V_i)^2\}}$$

is plotted against  $\sqrt{V_c p}$  the curves are straight lines as predicted by equation (6.28) which shows that the assumptions in the deduction of the theory are valid. Further from the slope of the curves the value of  $b$  has been calculated,

$$\text{where } b = \frac{0.44}{T_c} \sqrt{\frac{3}{L_1}} \log_{10} e \quad \left[ \text{in MKS} \right]$$

and taking the value of  $T_c$  and  $L_1$  from literature (Von Engel, 1965) the calculated and experimental values of  $b$  are entered in Table 6.7. The agreement for the three arcs is quite satisfactory considering the uncertainty in the values of  $T_c$  and  $L_1$ .

Table 6.7

Metal	Value of b in MKS units (theoretical)	Value of b in MKS units (experimental)
Cu	$1.82 \times 10^{-2}$	$1.53 \times 10^{-2}$
Fe	$1.65 \times 10^{-2}$	$2.07 \times 10^{-2}$
C	$1.01 \times 10^{-2}$	$2.18 \times 10^{-2}$

Calculation of  $\beta_c$

From our deduction 
$$\beta_c = \frac{(A_0 \phi / \alpha_c) 2.29 \times 10^4}{LM + 2.29 \times 10^4 V_i}$$

We have taken  $A_0 = 1$  sq. cm. and  $\alpha_c = 10^{-4}$  sq. cm. [Cobine (1958)] and because of lack of data for variation of  $\alpha_c$  with pressure we have taken the value of  $\alpha_c$  at  $p = 760$  mm of Hg. so that  $(A_0 / \alpha_c) \approx 10^4$ . The value of  $L$ ,  $M$ ,  $\phi$ ,  $V_i$  and  $T_c$  have been obtained from literature and Cobine (1958) and are shown in table 6.8.

Table 6.8

Metal	Cu	Fe	C
L Cal/gm	730	1071.4	7000
M(Mole) in gm	63.5	56.0	12.0
$\phi$ in volts	4.45	4.44	8.0
$V_i$ in volts	7.7	7.9	11.3
$T_c$ in $^{\circ}$ K	2200	2400	3500
$\beta_c$	$4.58 \times 10^3$	$4.22 \times 10^3$	$5.34 \times 10^3$

$$\text{From the relation } A = \frac{j_0 \beta_c d_c L_1^2 a}{3 \epsilon_0 \sqrt{2e/m}}$$

where  $a = 26$  ion pairs/v/m/mm of Hg, at  $p = 1$  torr.  $L_1 =$

$7 \times 10^{-5}$  m [at  $2200^\circ\text{C} (= T_c)$  by Sulhertand's formula],

$\epsilon_0 = 1.11 \times 10^{-10}$  F/meter,  $e/m = 1.7593 \times 10^{11}$  coulombs/kg

the value of  $\beta_c$  for the three arcs are obtained from Table

6.8 and the intercept of the curves along the X axis in

Fig. 6.5, 6.6 and 6.7 gives the value of  $\log_{10} A$  and hence that of A.

Hence the values of  $J_0$  have been calculated and entered in table 6.9.

Table 6.9

Metal	$\log_{10} A$	A	$j_0 \beta_c$	$j_0$ in MKS unit	$j_0$ in CGS unit
Cu	2.75	562.3	$9.45 \times 10^{12}$	$2.06 \times 10^9$	$2.06 \times 10^5$
Fe	2.45	281.8	$4.73 \times 10^{12}$	$1.12 \times 10^9$	$1.12 \times 10^5$
C	2.24	173.8	$2.92 \times 10^{12}$	$5.46 \times 10^8$	$5.46 \times 10^4$

$$\text{Further } J = J_0 \exp (b \sqrt{V_c p})$$

At  $p = 1$  atom.

$$b \sqrt{V_c p} \text{ (for Cu)} = 1.63$$

$$\text{So } J = 1.057 \times 10^6 \text{ A/cm}^2$$

$$\text{for Fe, } b \sqrt{V_c p} = 2.02$$

$$\text{So } J = 8.5 \times 10^5 \text{ A/cm}^2$$

$$\text{for C, } b \sqrt{V_c p} = 2.08$$

$$\text{So, } J = 4.368 \times 10^5 \text{ A/cm}^2$$

From the comparison of experimental results with theoretical deduction we can conclude that the agreement is quite satisfactory and the values of the cathode current density, is in good agreement with published experimental data (Hirsh and Oskam 1978). As mentioned by Cobine (1958) the determinations of the cathode current density are subject to considerable uncertainty because it is extremely difficult to estimate the exact active area of the cathode spot. The results thus indicate that in the metals studied in this investigation thermionic emission plays a dominant role. We have not considered the effect of field emission in this discussion but as is generally believed both the effects may be simultaneously active.

R E F E R E N C E S

- J.J. Thomson and G.P. Thomson, *Conduction of Electricity through gases*. Cambridge Univ. Press, 1933.
- L.B. Loeb, *Brit. J. Appl. Phys.*, 3, 341, 1952.
- K.T. Compton, *Phys. Rev.*, 21, 266, 1923.
- L. Langmuir, *Gen. Elec. Rev.*, 26, 735, 1923.
- M.J. Druyvesteyn, *Nature*, 137, 580, 1936.
- W. Ramberg, *Ann. D. Physik*, 12, 319, 1932.
- W. Finkelburg, and T. Peters, *Encyclo. Phys.* 22, 254, 1956.
- G. Ecker, *Ergibnisse exakten, Nature Wissensch* 33, 1, 1961.
- Lee and Green Wood, 1964.
- S.N. Sen, M. Gantait and D.C. Jana, *Ind. J. Phys.* 62B, 78, 1988.
- Von Engel, *Ionised Gases*, 2nd Edition Clarendon Press, Oxford, 1965.
- J.D. Cobine, *Gaseous Conductors*, Dover Publications, Inc. New York, 1958.
- Hirsh, M.L. and Oskam, H.J., *Gaseous Electronic*, Vol. I, Academic Press, New York, 1978.

CHAPTER VII

LOW FREQUENCY OSCILLATION IN ARC PLASMA

## CHAPTER VII

## LOW FREQUENCY OSCILLATIONS IN ARC PLASMA

## 1. INTRODUCTION

There occur various types of oscillations and waves in a plasma. In order to detect such oscillations in a mercury arc plasma and also to see whether such an arc can be utilized for the generation of steady electromagnetic oscillations, an experiment was set up as shown in figure 2.12. It is known that the negative resistance of a vacuum tube was used for generation of electromagnetic oscillations as in the case of dynatron oscillators. A gas diode produces an arc discharge that has a negative resistance and in the early days of radio such arc oscillators were frequently used as transmitters of radio waves. Since the mercury arc has a negative resistance that is the current decreases with the increase of voltage it was presumed that a suitable circuit connected with a mercury arc can be utilized for the generation of steady electrical oscillations. Hence the present work was undertaken.

## 2. Experimental arrangement

The mercury arc used in the experiment is an arc tube made of pyrex of 41 cm. length, 26.5 cm. anode cathode spacing, 2.2 cm. inner diameter and 2.5 cm. outer diameter. Such arcs have been used in the laboratory recently (Sen et al 1990). The arc was excited between two mercury pool electrodes

(fitted with two tungsten wires for external electrical connection) by a 250 volt D.C. generator with a rheostat to control the current. The whole arc assembly was kept inside transformer oil which was cooled by circulating cold water through copper tube in the form of a coil and placed inside the oil. The mean temperature of the oil was  $55^{\circ}\text{C}$  throughout the experiment. The temperature of the oil has an important bearing on the oscillation. To maintain the pressure constant in the tube dry air which acts as a buffer gas was introduced by a variable microleak needle valve fitted in the vacuum arrangement. The pressure was measured by a calibrated pirani gauge. A circuit consisting of an inductance  $L$  ( $100 \mu\text{H}$ ) and a capacity ( $4 \mu\text{F}$ ) and a variable resistance  $R$  is connected in parallel with the arc. A secondary coil loosely coupled with the inductance  $L$  and tuned by the variable capacity provides the output which is connected to an oscilloscope (Dumont type 766 H/F). In addition, there is connected a digital frequency meter to measure accurately the frequency of the generated oscillation (Fig. 2.12). The object is to study the variation of frequency and amplitude of generated oscillation, if any, with arc current, pressure and external magnetic field. For measurement in a transverse magnetic field a portion of the positive column of the arc was placed between the pole pieces of an electromagnet which was run by a stabilized D.C. power supply (Type EM .20) and the magnetic field calibrated by a gauss meter (Model G14). The arc current was varied from 1 to



Vertical span = 26 cm  
Vertical gain = 0.5 mV/cm  
Wave amplitude = 1.3 mV, frequency = 3.46 Kc/s  
Arc current = 2.1 Amp  
Pressure = 0.05 Torr

Vertical wave span on CRO = 3.0 cm  
Vertical gain = 0.5 mV/cm  
Wave amplitude = 1.5 mV  
Mag fld = 76 Gauss  
Arc current = 2.1 Amp  
Pressure = 0.05 Torr

Vertical span = 2.7 cm  
Vertical gain = 0.1 mV/cm  
Wave Amplitude = 0.27 mV, frequency = 4.87 Kc/s  
Arc current = 2.2 Amp  
Pressure = 0.005 Torr

2.5 amp the pressure from .005 to .1 torr and the magnetic field from zero to 120 gauss.

### 3. Experimental results

#### General observation

- (a) There is a maximum value of the arc current beyond which there is no oscillation.
- (b) There is a minimum current below which the arc can continue without showing oscillation but the arc is extinguished if oscillations tend to build up.
- (c) Cooling is essential if stable oscillations are desired.
- (d) For a particular value of C there is a maximum value of L beyond which no oscillations can build up. But below this maximum value of L, frequency is found to be independent of L.
- (e) The generation of oscillation and its stability takes time. So one has to wait before final tuning of the oscillatory circuit and recording of data.

#### Quantitative observations:

Sinusoidal oscillations have been observed and photographed with the help of the oscilloscope with the attached camera when the arc current, pressure inside the tube and external magnetic field have been varied within certain limits. Some of the photographs are presented. Quantitative measurements of frequency and amplitude of the generated oscillation have

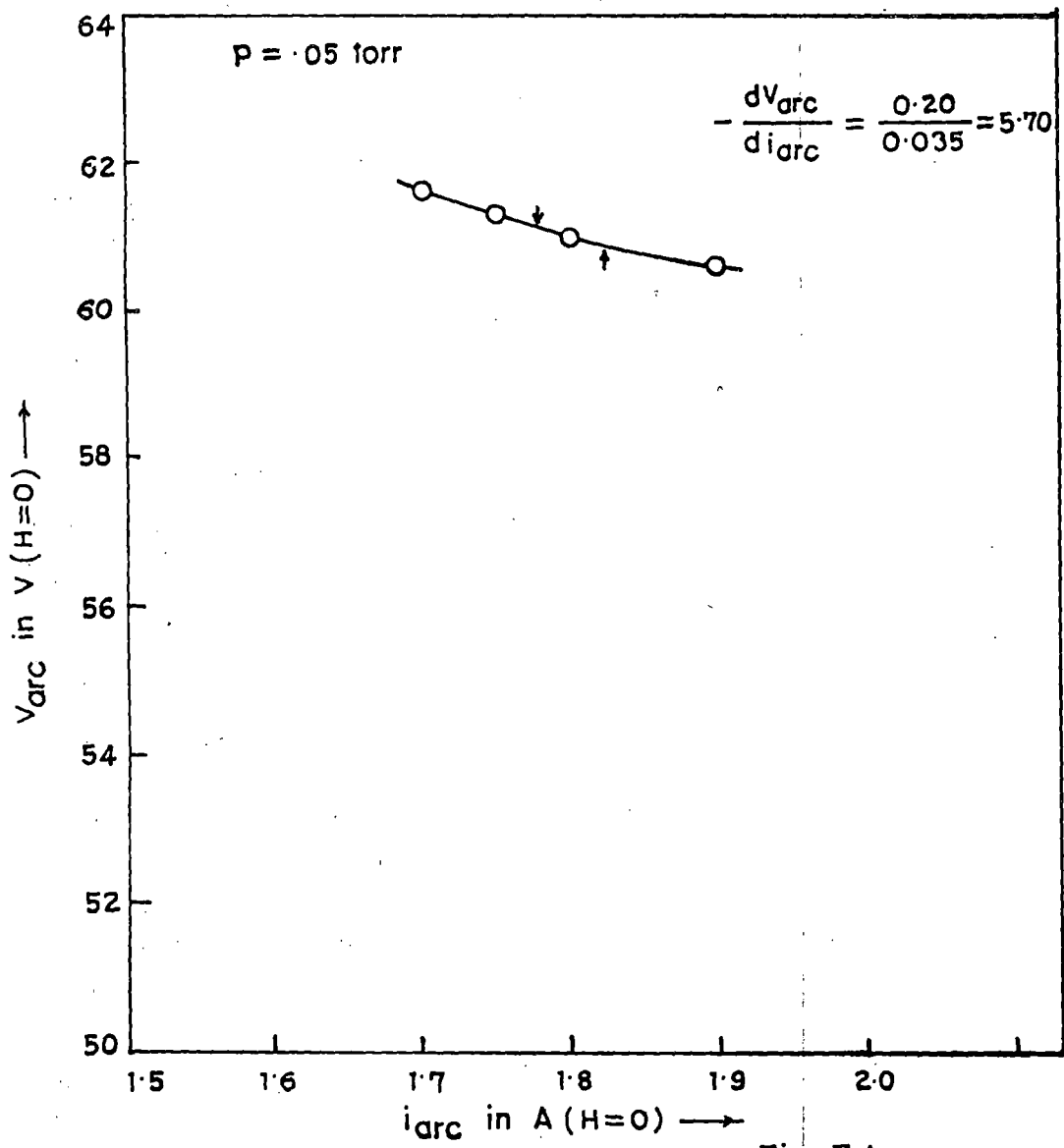


Fig. 7-1.

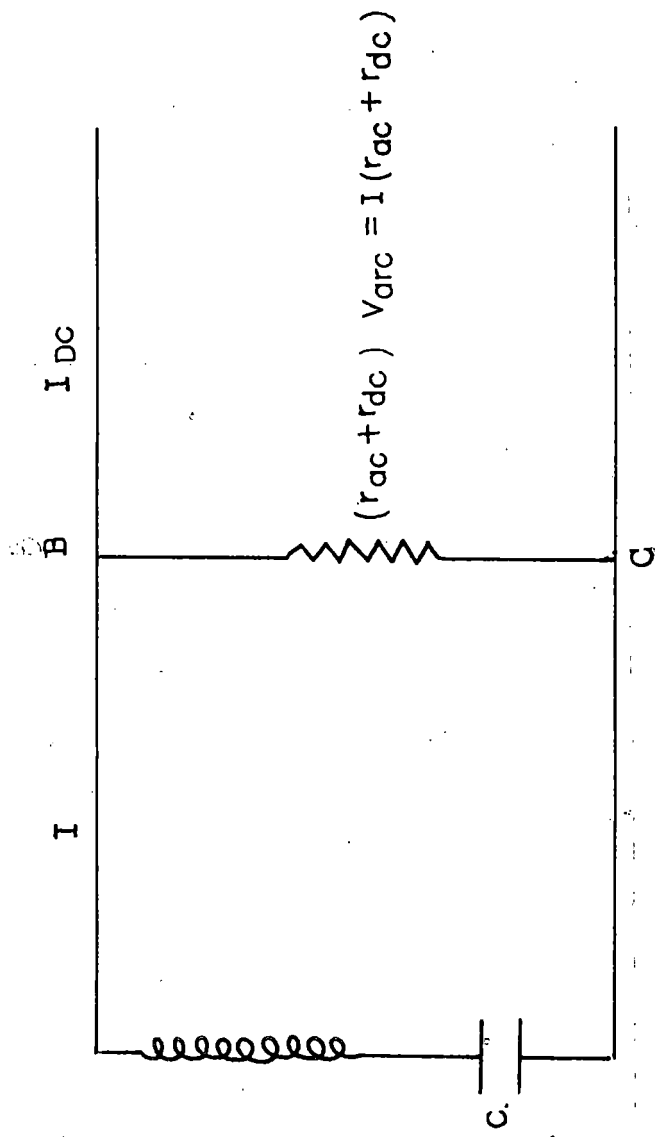


Fig. 7.2.

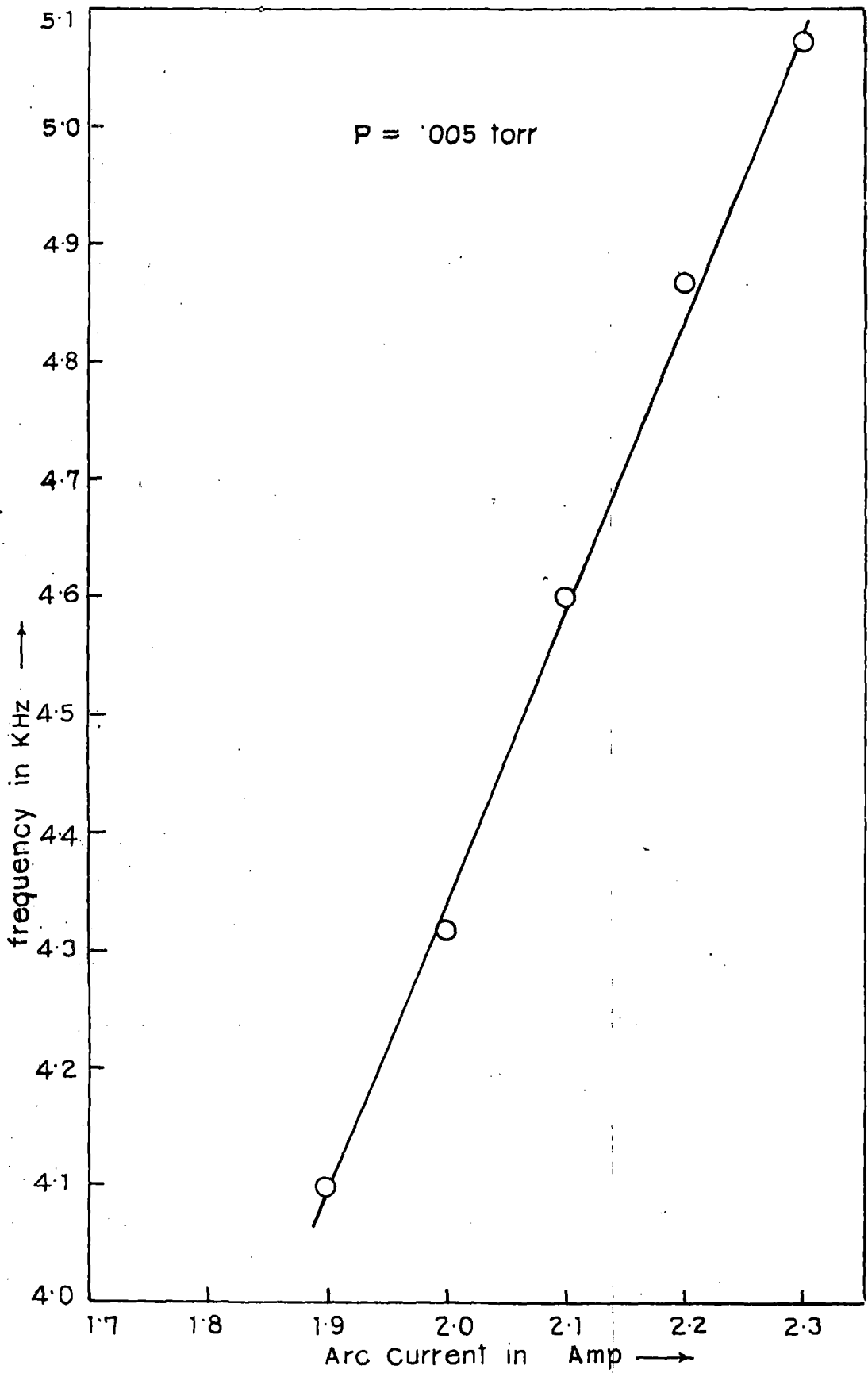


Fig. 7.3.

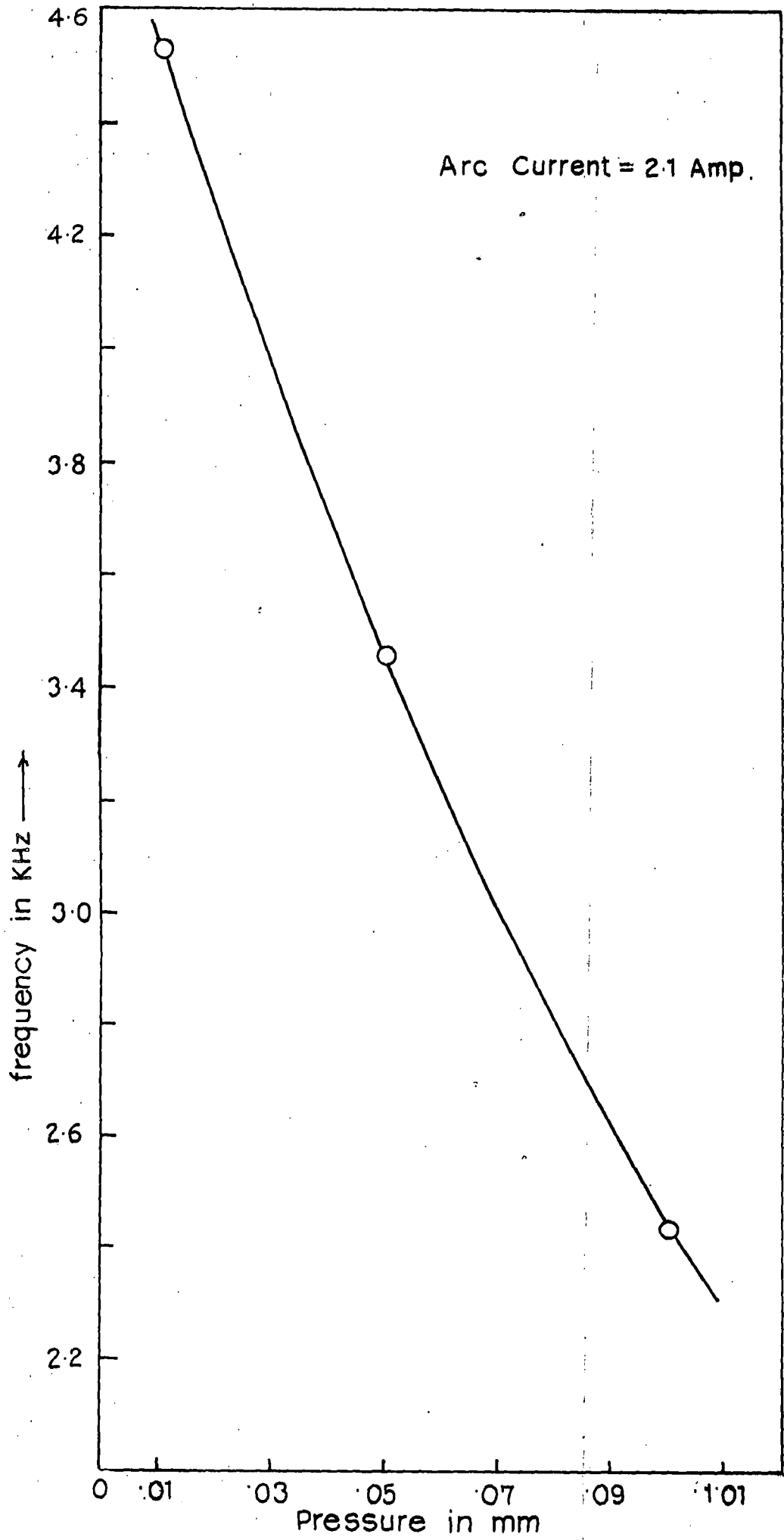
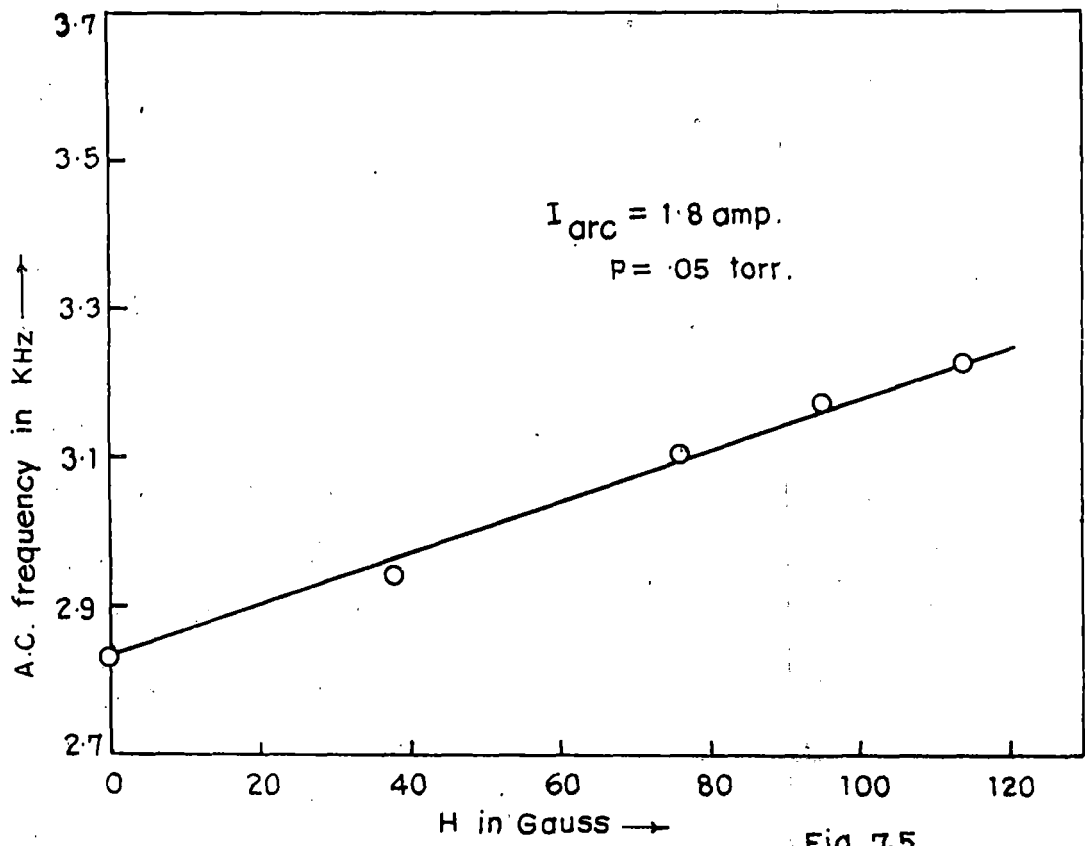


Fig. 7-4.



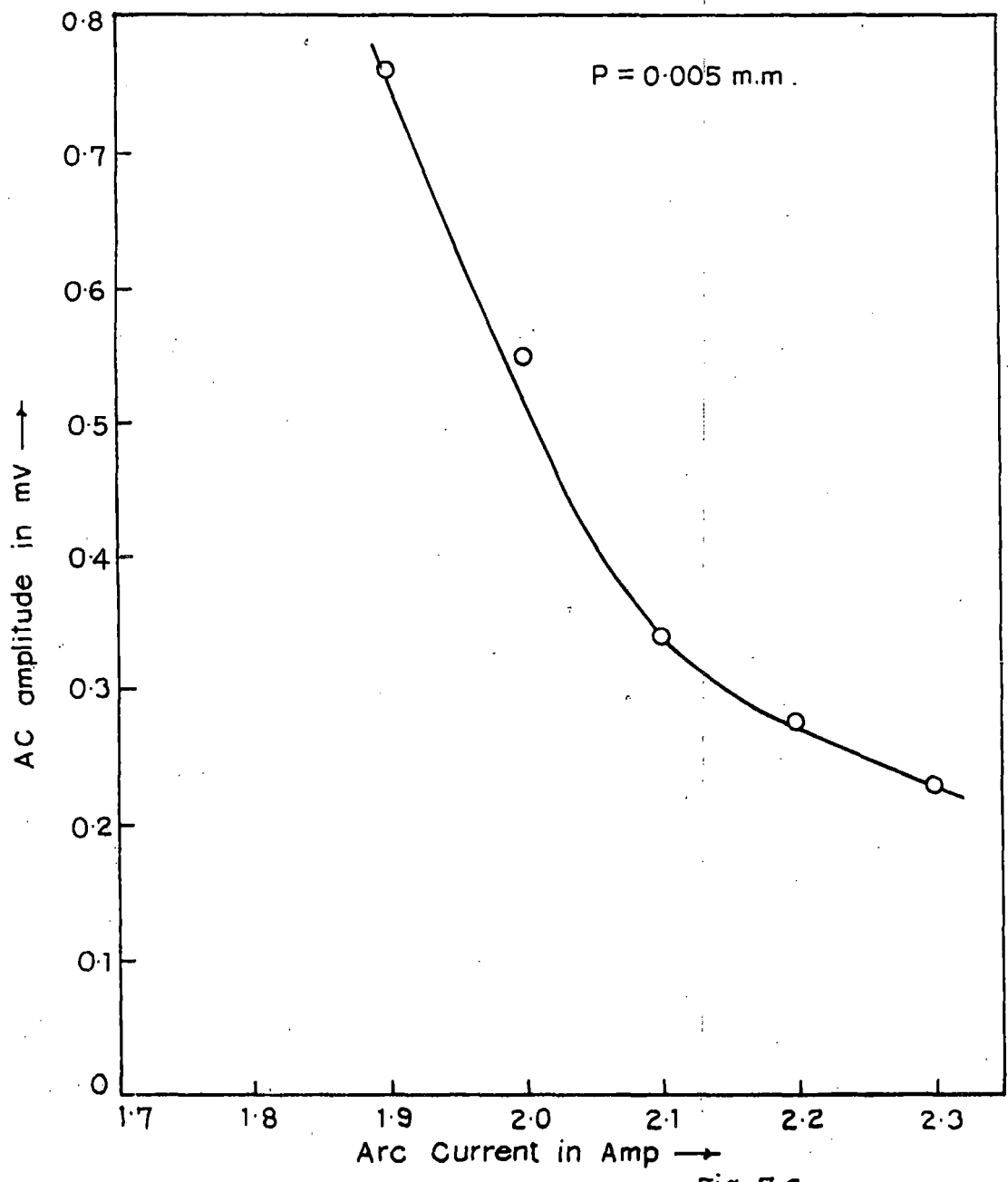


Fig. 7.6.

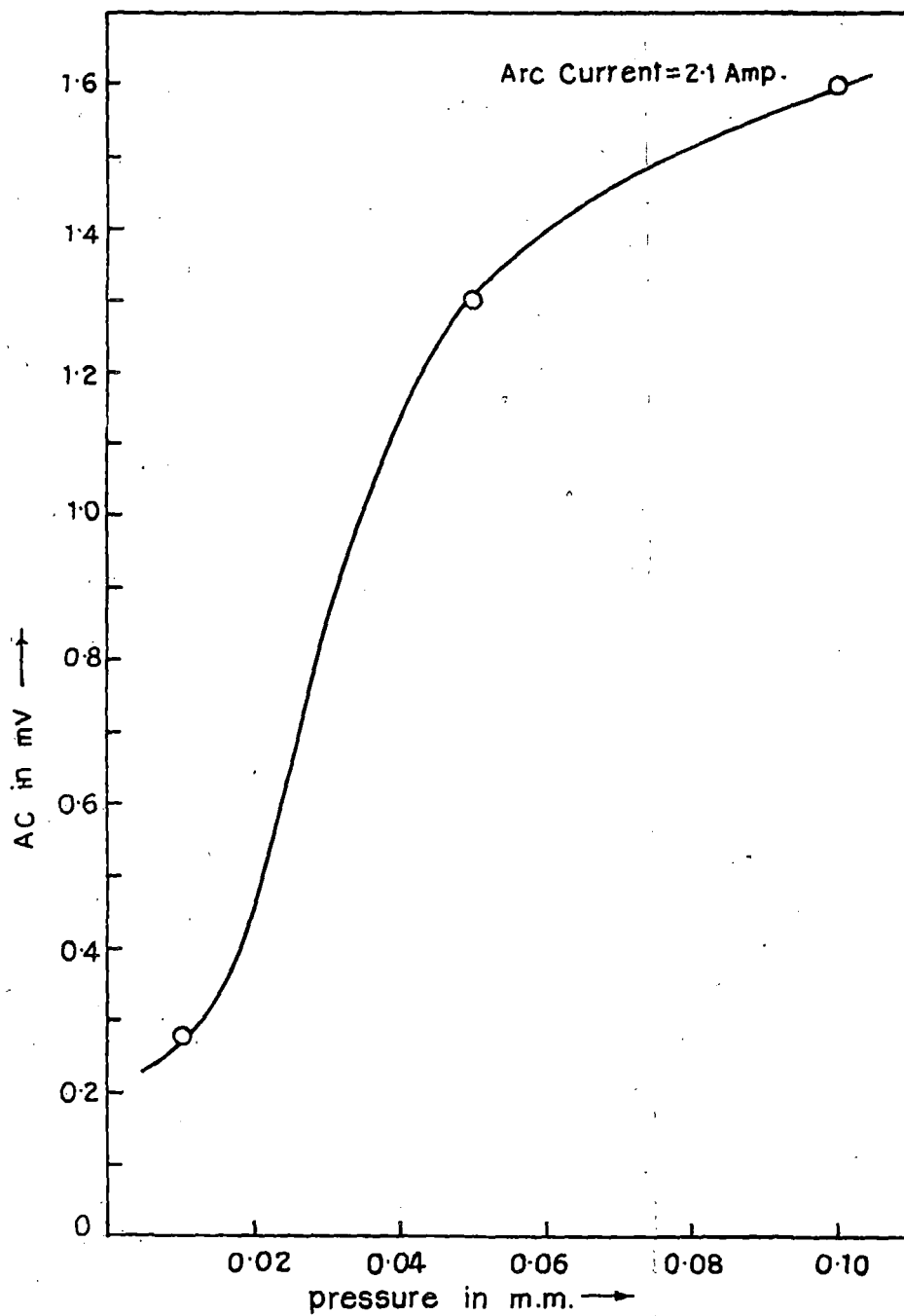


Fig. 7.7.

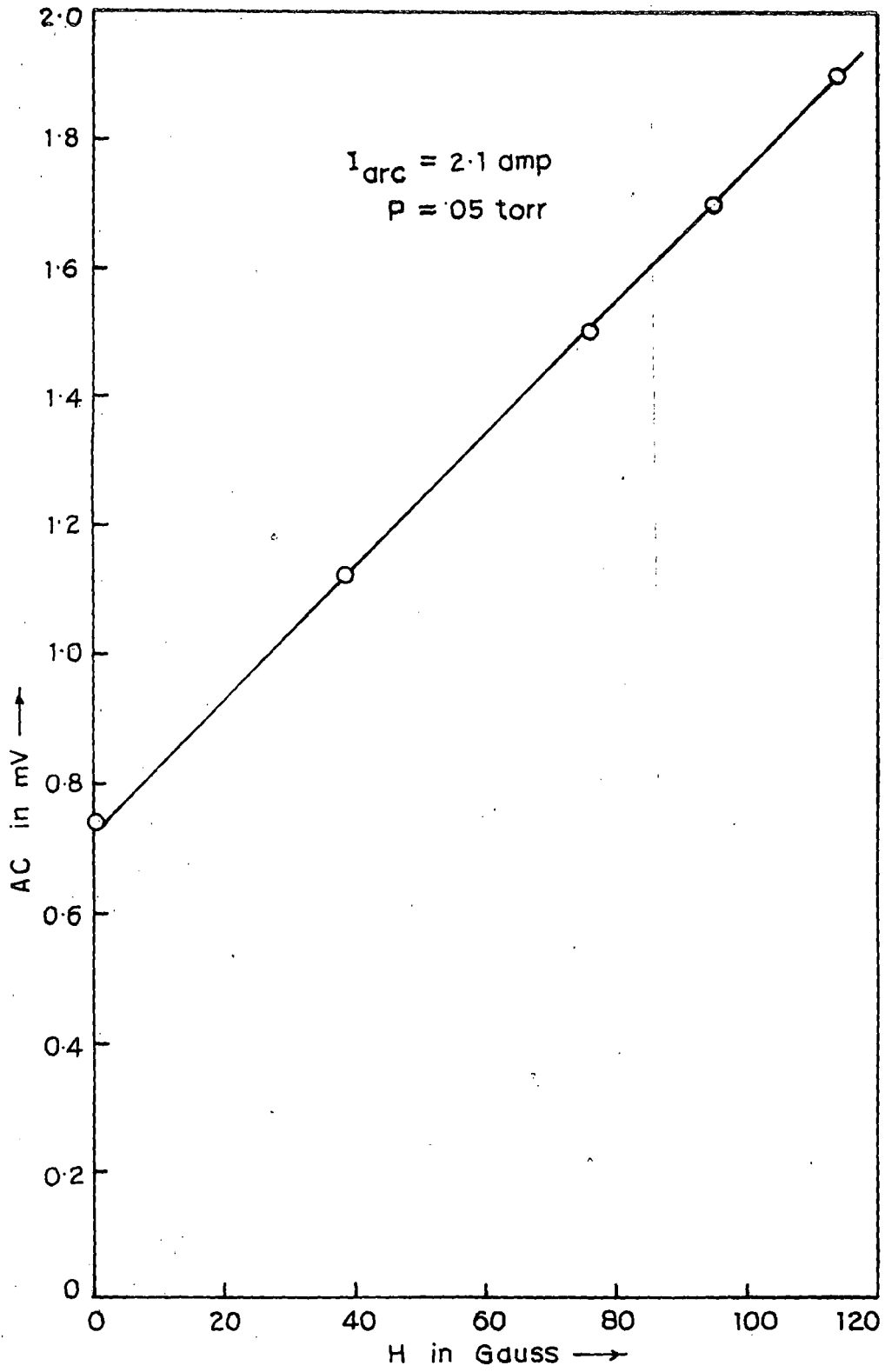


Fig. 7.8.

been made. The results are reproduced in Figs. (7.3 to 7.8). From the nature of the curves the following deductions have been made.

Fig. 7.3 The generated frequency varies from 4.1 Kc/s to 5.075 Kc/s for variation of arc current from 1.9 to 2.3 amp. at a pressure of .005 torr and the variation is linear. Similar results are obtained at other pressures also.

Fig. 7.4. The generated frequency is 4.54 KHz at  $P = .01$  torr and then decreases rapidly with the increase of pressure upto 0.1 torr at an arc current of 2.1 amp. Similar variation of frequency with pressure was observed for other arc currents as well.

Fig. 7.5. The generated frequency increases with the increase of the magnetic field linearly for arc current  $I = 1.8$  amp. Similar variation is observed at other arc currents also.

Fig. 7.6. Shows that output voltage decreases with the increase of arc current at a pressure of .005 torr.

Fig. 7.7. shows that the output voltage increases with the increase of pressure.

Fig. 7.8 shows that the output voltage increases linearly with increase of magnetic field at  $P = .05$  torr and arc current 2.1 amp. The same behaviour is observed for  $P = .005$  torr and arc current 1.75 amp.

#### 4. Discussion

As we started with our initial objective we wanted to generate oscillations employing the negative characteristics of

current voltage relation in a mercury arc just as in the case of dynatron oscillation. Two types of oscillations are possible in such a system (a) damped sinusoidal oscillation, (b) sinusoidal oscillation with constant amplitude. In the photographs produced it is evident that oscillations are purely sinusoidal with constant amplitude and even if there is a small amount of damping it cannot be detected; in that case we shall assume the oscillations to be sinusoidal with constant amplitude. The equation comprising the arc and the external oscillatory circuit is

$$L \frac{di}{dt} + Ri + \left( \frac{1}{C} \int i dt + e \right) = 0 \quad (7.1)$$

where L and C are the external inductance and capacity, R includes the d.c. resistance of the arc together with any external resistance and e is the voltage across the arc, then from eqn. (7.1)

$$L \frac{d^2 i}{dt^2} + R \frac{di}{dt} + \frac{de}{dt} + \frac{i}{C} = 0$$

or

$$L \frac{d^2 i}{dt^2} + \frac{i}{C} + \left( R + \frac{de}{di} \right) \frac{di}{dt} = 0$$

In an arc  $\left( \frac{de}{di} \right)$  is negative and from the variation of arc voltage with arc current it is found that  $\left( \frac{de}{di} \right)$  is of the order of 4.5 ohms varying from 4 to 6.3 ohms for arc current varying from 1.9 to 2.3 amp whereas the d.c. resistance of the arc varies from 24.92 to 19.41  $\Omega$  over the same range of arc current, so even if the external resistance  $R_0$  is made zero the condition that

$R + \frac{de}{di}$  should be zero is not satisfied. Consequently according to the theory of generation of such oscillations they should be heavily damped whereas in actual practice sinusoidal oscillations with constant amplitude are observed (Refer to Photographs). Further the frequency of such damped oscillations is given by  $f = \frac{1}{2\pi} \sqrt{\frac{1}{LC} - \frac{R^2}{4L^2}}$  and it is found by putting the values of  $R = 16.74 \Omega$  and  $L = 100 \mu H$  that  $\frac{1}{LC} \ll \frac{R^2}{4L^2}$  and the frequency becomes imaginary. Consequently the oscillations observed are not damped oscillations neither they can be regarded as generated due to negative resistance of the mercury arc, because the frequency of such generated oscillations is given by

$$f = \frac{1}{2\pi\sqrt{LC}}$$

and if we put the values of  $L$  and  $C$ , it is of the order of 8 Kc/s whereas the frequency range obtained here lies between 2.2 Kc/s to 5.2 Kc/s depending upon the value of arc current, pressure and magnetic field. Further according to the theory of dynatron oscillation the frequency generated is exclusively a function of the values of external capacity and inductance and should not be a function of the arc current or pressure in the arc and it was therefore concluded that the recorded oscillations are not the dynatron type of oscillations but the source is within the arc tube itself. Also by varying the external inductance from a value of  $40 \mu H$  to  $100 \mu H$ , the

frequency of the detected oscillations remains the same. Hence the oscillations cannot be due to dynatron oscillations. We also considered the possibility that the arc may have some inductance due to the fact that the arc current may create a magnetic field and the magnetic energy can be linked with the equivalent inductance of the arc. The energy associated with the magnetic field is  $\frac{\mu H^2}{8\pi}$  where  $\mu$  is the permeability of the plasma and  $H$  is the magnetic field due to the flow of the arc current and if  $L$  is the equivalent inductance of the arc then

$$\frac{\mu H^2}{8\pi} \frac{4}{3} \pi R^3 = \frac{1}{2} LI^2$$

and  $H = \frac{2I}{R}$

where  $I$  is the arc current.

where  $R$  is the radius of the arc tube or  $L = \frac{4}{3} \mu R$ . It is assumed that  $\mu$  for a plasma is unity then the inductance of an arc is of the order of  $10^{-9}$  henry or  $10^{-3}$  microhenry whereas the external inductance in the circuit is 100 microhenry and consequently the arc inductance will have no effect on the generated frequency. Hence the detected oscillations must have its origin in the arc itself.

To further investigate whether the oscillations observed are electron plasma oscillations it is noted that electron plasma frequency is of the order of  $9 \times 10^3 \sqrt{n}$  where  $n$  is the electron or ion density and assuming  $n$  in the arc to be of the

order of  $10^{12}$  (Sen, Gantait and Acharyya, 1989) the electron plasma frequency is of the order of 9000 Mc/s. On the other hand the ion plasma frequency in case of mercury is of the order of 1.5 Mc/s, but since the frequency of the observed oscillation is of the order of 2 to 6 Kc/s, we can conclude that these oscillations are neither electron plasma nor ion plasma oscillations.

Assuming for the present that such an oscillation exists within the arc and to study the variation of frequency of the output oscillations with arc current, pressure and magnetic field let us refer to fig. (7.2) as equivalent circuit, we assume that through the arc both the d.c. and a.c. currents are flowing where the instantaneous voltage across the arc is

$$I(r_{ac} + r_{dc}) = V_{arc} \quad (7.2)$$

$$r_{dc} = \frac{V_{DC} - V_C - V_d}{I_{dc}} \quad \text{and} \quad r_{ac} = \frac{\partial V_{DC}}{\partial I_{DC}}$$

where  $I_{dc}$  is the d.c. current through the arc and  $V_{dc}$  is the d.c. voltage drop across the arc and  $V_C$  and  $V_A$  are the cathode and anode fall respectively. If  $V_L$  and  $V_{CC}$  are the voltages across L and C then the voltage between B and C  $\left[ \text{refer to fig. (7.2)} \right]$  is  $V_L + V_{CC}$  and considering from the arc side the voltage between B and C is

$$V_{arc} - (V_L + V_{CC})$$

$$\text{then } V_L + V_{cc} = V_{arc} - (V_L + V_{cc}) \quad (7.3)$$

Then from equations (7.2) and (7.3)

$$I(r_{dc} + r_{ac}) = 2I \left[ \frac{1}{j\omega C} + j\omega L \right]$$

$$r_{ac} + r_{dc} = 2 \sqrt{\omega^2 L^2 + \frac{1}{\omega^2 C^2}}$$

$$\text{or, } 4\omega^4 L^2 C^2 - (r_{ac} + r_{dc})^2 C^2 \omega^2 + 4 = 0$$

$$\text{or, } \omega^2 = \frac{(r_{ac} + r_{dc})^2 C^2 \pm \sqrt{(r_{ac} + r_{dc})^4 C^4 - 64L^2 C^2}}{8L^2 C^2}$$

The values of  $r_{ac}$  have been calculated from the characteristic curves showing the variation of arc voltage against arc current. It is found from actual measurement of the values of  $I_{ac}$  and  $r_{dc}$

$$\text{that } (r_{ac} + r_{dc})^4 C^4 > 64L^2 C^2$$

$$\text{so } \omega^2 \approx \frac{4}{(r_{ac} + r_{dc})^2 C^2} \quad (7.4a)$$

$$\text{Or, } \omega^2 = \frac{(r_{ac} + r_{dc})^2}{4L^2} - \frac{4}{(r_{ac} + r_{dc})^2 C^2} \quad (7.4b)$$

But in the present case, as we have mentioned, the frequency does not change with inductance  $L$ , so we have not considered the equation (7.4b).

$$\text{From eqn. (7.4a) } f = \frac{1}{\pi(r_{ac} + r_{dc})C} = \frac{79.62}{(r_{ac} + r_{dc})} \text{ Kc/s} \quad (7.5)$$

as C in the tank circuit is  $4 \mu\text{F}$ .

where f is the frequency of oscillation in kilo cycles/sec.

From the variation of arc voltage with arc current the values of  $r_{ac} = \partial V_{DC} / \partial I_{DC}$  have been calculated for a pressure of .005 torr and arc current varying from 1.9 to 2.3 amp. The values of  $r_{dc}$  have been calculated from the relation  $r_{dc} = \frac{V_{DC} - V_c - V_a}{I_{DC}}$

and for mercury  $V_c + V_a$  has been taken to be 10 volts (Von Engel 1965). The results are entered in table 7a.

Table 7a  
p = 0.005 torr

$I_{arc}$ in amp.	2.3	2.2	2.1	2.0	1.9
$-r_{ac}$	4.0	4.4	4.9	5.5	6.3
$r_{dc}$	19.41	20.48	21.64	22.95	24.92
$r_{ac} + r_{dc}$	15.41	16.08	16.74	17.45	18.62
f Kc/s (calculated)	5.17	4.95	4.76	4.56	4.28
f Kc/s (Experimental)	5.09	4.85	4.60	4.35	4.10
DC arc drop (volts)	54.65	55.05	55.45	55.90	56.40

Thus the value of frequency calculated from equation (7.5) gives values very close to those observed and shows the variation with arc current which is also consistent with experimental results. However, values calculated from equation (7.5) are

higher than those observed. Further if

$$(r_{ac} + r_{dc})^4 C^4 - 64L^2 C^2 = 0$$

$$r_{ac} + r_{dc} = 2\sqrt{2L/C}$$

and putting  $L = 100 \mu\text{H}$  and  $C = 4 \mu\text{F}$

$$r_{ac} + r_{dc} = 14.142 \Omega$$

So this is the minimum value of  $r_{ac} + r_{dc}$  for which  $I_{dc} = 2.8$  amp. So 2.8 amp. is the maximum current upto which oscillations can be obtained. Further  $(r_{ac} + r_{dc})$  increases with pressure and so frequency will decrease with pressure (Fig. 7.4).

Variation of frequency of generated oscillation with magnetic field.

It is observed that when the magnetic field is applied the arc current diminishes and the arc voltage increases as has been observed earlier by Sen and Das (1973) starting with the initial arc current of 1.8 amp at which the frequencies of generated oscillations have been measured the measured values of arc current and arc voltages are entered in table (7.2).

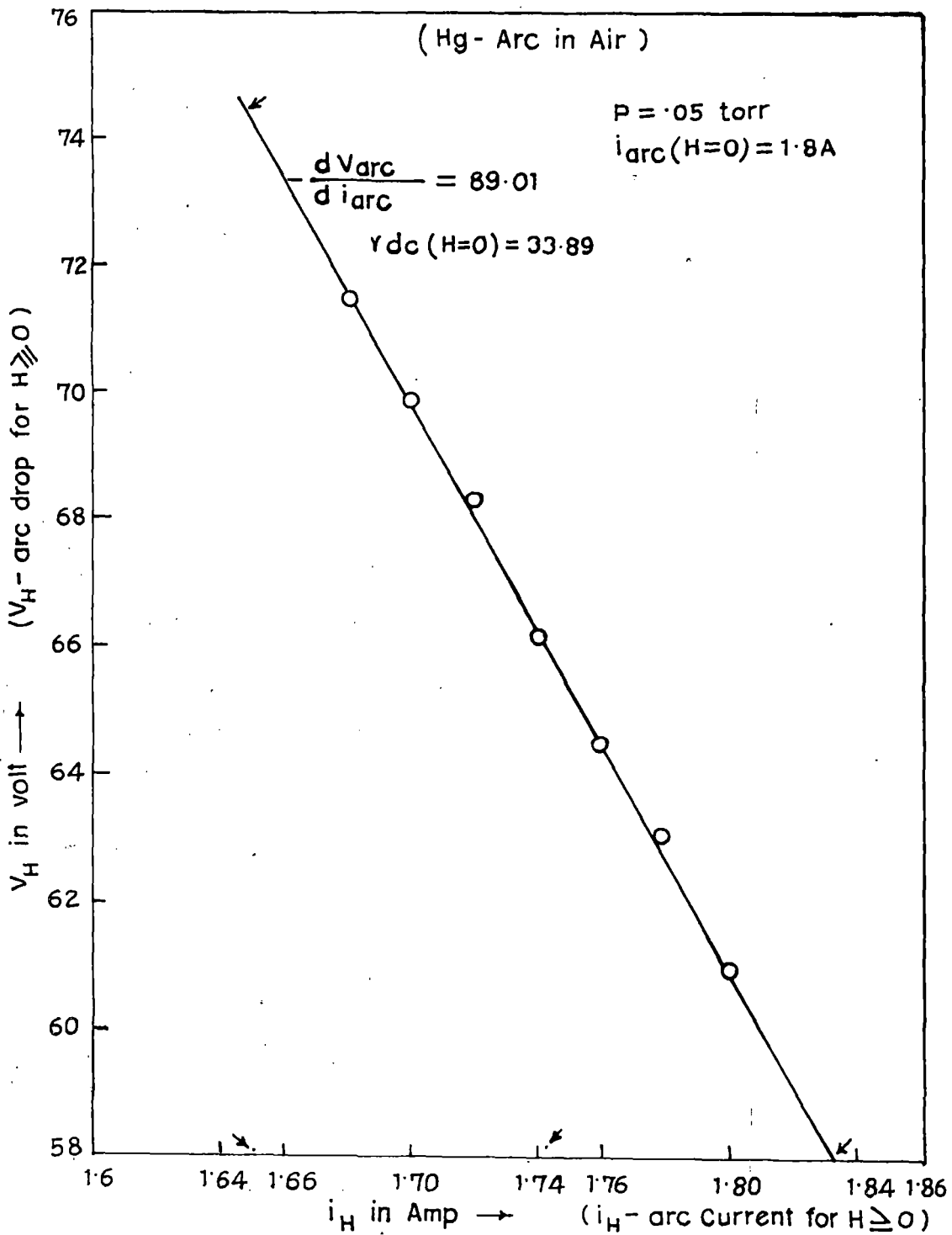


Fig. 7.9.

Table 7.2

Pressure = 0.05 torr; initial arc current 1.8 A.

H in G	0	19	38	57	76	95	114
I amp.	1.8	1.78	1.76	1.74	1.72	1.70	1.68
V <sub>arc</sub> in volts	61	63.1	64.5	66.2	68.3	69.9	71.5

The results are plotted in Fig. (7.9) showing the variation of arc voltage against arc current in presence of magnetic field from which it is observed that  $r_{ac} = \partial V_{arc} / \partial i_{arc} = -89.01 \Omega$  and is a constant. The values of  $r_{ac}$  can be calculated from the values of  $V_{arc}$  and  $I_{arc}$  as entered in table (7.2) for values of magnetic field used in the experiment. The results are entered in table (7.3).

Table 7.3

H in gauss	0	19	38	57	76	95	114
$r_{dc} \Omega$	33.89	35.45	36.65	38.05	39.71	41.12	42.56
$r_{ac} \Omega$	-89.01	-89.01	-89.01	-89.01	-89.01	-89.01	-89.01
$(r_{ac} + r_{dc}) \Omega$	-55.12	-53.56	-52.36	-50.96	-49.30	-47.89	-46.45
fKc/s (Calculated)	1.44	1.49	1.52	1.56	1.62	1.66	1.71
1.95 x f Kc/s (Calculated)	2.81	—	2.96	—	3.16	3.24	3.33
f Kc/s (expt.)	2.83	—	2.94	—	3.10	3.17	3.22

The values of the frequency of oscillation have been calculated from the relation

$$f = \frac{1}{\pi(r_{ac} + r_{dc})C} \quad \text{where } C = 4 \mu\text{F}$$

$$= \frac{79.62 \text{ Kc/s}}{(r_{ac} + r_{dc})}$$

The calculated values of frequency are entered in the fifth row of Table (7.3).

As the calculated frequencies are almost half of the observed frequencies it was thought worthwhile to calculate  $(r_{ac} + r_{dc})$  in an alternative way. For this purpose the output

voltage across the arc was measured around a small variation of the arc current (1.8 amp) from 1.7 to 1.9 A in absence of the magnetic field. The characteristic curve is plotted in Fig. (7.1) and the results are entered in table (7.4) at a pressure of .05 torr.

Table 7.4

p = 0.05 torr, H = 0 Gauss

$I_{\text{arc}}$ amp	1.7	1.75	1.8	1.9
$V_{\text{arc}}$ volts	61.6	61.3	61.0	60.6
$r_{\text{dc}}$	-	-	33.89	-
$-r_{\text{ac}}$	-	-	5.70	-
$r_{\text{dc}} + r_{\text{ac}}$	-	-	28.19	-

From the slope of (V-I) characteristic curve the value of  $r_{\text{ac}}$  is -5.70 and hence  $(r_{\text{ac}} + r_{\text{dc}}) = 28.19$  in absence of magnetic field and from  $I_{\text{H arc}} = \frac{V_{\text{H arc}}}{r_{\text{ac}} + r_{\text{dc}}}$ ;  $(r_{\text{ac}} + r_{\text{dc}}) = 55.12$  for  $H \rightarrow 0$  and those should be equivalent.

$$\text{So } \frac{[(r_{\text{ac}})_{\text{H}} + (r_{\text{dc}})_{\text{H}}]_{\text{H} \rightarrow 0}}{[r_{\text{ac}} + r_{\text{dc}}]_{\text{H} = 0}} = \frac{55.12}{28.19} = 1.95$$

and hence the calculated frequencies in the fifth row of table 7.3 should be each multiplied by the factor 1.95. The calculated frequencies thus obtained are entered in the sixth row of table (7.3) which are in close agreement with observed frequencies as entered in the seventh row of table (7.3)

Amplitude of oscillation:

The output voltage at the secondary of the circuit (shown in Fig. 7.1) has been measured for different values of arc current, pressure and magnetic field Fig. 7.6, 7.7 and 7.8. The total current that flows through the arc at resonance is

$$I = \frac{V_{\text{arc}}}{r_{\text{ac}} + r_{\text{dc}}}$$

and this includes both the arc current and the a.c. current due to generation of electromagnetic oscillation. Taking the value of  $V_{\text{arc}} = (V_{\text{DC}} - V_{\text{C}} - V_{\text{A}})$  where  $V_{\text{A}}$  and  $V_{\text{C}}$  are the values for the anode and cathode fall respectively and those of  $r_{\text{ac}}$  and  $r_{\text{dc}}$  from Table 7.1 the values of  $I = I_{\text{dc}} + I_{\text{ac}}$  have been entered in the second column of table 7.5. Deducing the values of arc current from the total current  $I$ , the values of the fluctuating current  $I_{\text{ac}}$  have been calculated and entered in column (3) table 7.5. The a.c. voltage developed across the arc is

$$I_{\text{ac}} (r_{\text{ac}} + r_{\text{dc}}) = V_{\text{ac}}$$

the values of  $V_{ac}$  are entered in the fourth column in table 7.5. Then  $V_{ac}$  is  $2(V_L + V_{cc})$  where  $V_L$  is the voltage drop across the inductance  $L$  and  $V_{cc}$  is the voltage drop across the condenser  $C$  and assuming  $V_L = V_{cc}$ ,  $V_{ac} = 4 V_L$ . The values of  $V_L$  are entered in the fifth column of table 7.5 for  $p = 0.005$  torr.

Table 7.5  
 $P = 0.005$  torr

$I_{dc}$ arc current amp.	$I = I_{ac} + I_{dc}$ amp	$I_{ac}$ amp.	$V_{ac}$ volts	$V_L$ volts
2.3	2.897	.597	9.2	2.3
2.2	2.802	.602	9.681	2.42
2.1	2.716	.616	10.31	2.58
2.0	2.630	.630	10.99	2.75

The output voltages have been measured at the output of the secondary circuit and consequently the quantitative agreement cannot be expected. However, qualitative agreement is quite satisfactory. The output voltage decreases with the increase of the arc current.

However, when the magnetic field is gradually increased at an initial arc current of 1.8 amp it is found that the output voltage of generated oscillations increases with the magnetic

field. To make a quantitative estimate we have calculated the total current  $I = (I_{ac} + I_{dc})$  for various values of the magnetic field from the data entered in table 7.2 for  $V_{arc}$  and values of  $(r_{ac} + r_{dc}) \times 1.95$  from table 7.3. The calculated data are entered in table 7.6.

Table 7.6

Mag. field in gauss	$I_{ac} + I_{dc}$ amp.	$I_{dc}$ amp	$I_{ac}$ amp.	$V_{ac}$ volts	$V_L$ volts
0	2.102	1.8	.302	8.762	2.19
19	2.239	1.78	.459	12.91	3.23
38	2.341	1.76	.581	16.01	4.00
57	2.469	1.74	.729	19.55	4.89
76	2.632	1.72	.812	23.66	5.91
95	2.773	1.70	1.073	27.05	6.76
114	2.925	1.68	1.445	35.32	8.88

Since a fraction of this output voltage across the arc will appear across the primary of the inductance the output voltage measured across the secondary will be proportional to this voltage and the results in the last column of table 7.6 show that the output voltage increases almost linearly with the magnetic field as is observed experimentally. No attempt has been made to compare the theoretical and experimental results quantitatively.

As regards the origin of these low frequency oscillations it has been discussed above that these oscillations can neither be electron plasma oscillation nor can they be due to ion plasma oscillations. Further the experimental results indicate that they cannot be due to dynatron oscillation either, we are thus led to assume that since air is used here as a quenching gas the oxygen present can attach electrons and thereby negative ions are formed [Sen and Sathya (1980)] and as the percentage of background air pressure is very small the density of negative ions should be very small. On this assumption we get the frequency of oscillation of these negative oxygen ions is  $5.353 \times 10^2 \sqrt{n}$  and equating this with the observed frequency of 5 KC/s, we get a probable value of negative oxygen ion density to be of the order of  $10^2$ .

It is difficult to pin point the exact source to which these oscillations are due. However, by assuming its existence and making some simple assumptions it has been shown that the observed and calculated frequencies of emitted electro magnetic waves are very nearly consistent with regard to variation of current, pressure and magnetic field. The general trend of variation of amplitude with variation of these parameters, is also consistent with that observed experimentally.

We can thus conclude that the object with which the present experiment was set up could not be achieved due to the fact that the combined value of  $r_{dc}$ ,  $r_{ac}$  in combination

with any resistance could not be made equal to zero which is essential for production of dynatron oscillation. This however, can be achieved by a proper design of the mercury arc. Instead a new type of oscillation with very low frequency has been detected in the process.

R E F E R E N C E S

Sen S.N, Acharya C, Gantait M and Bhattacharjee B,  
Int. J. Electronics, 68, 421, 1990.

Sen S.N. and Das R.P., Int. J. Electronics, 34, 527, 1973.

Sen S.N. and Sadhya S.K., Int. J. Electronics, 49, 235, 1980.

Sen S.N., Gantait N and Acharya C, Ind. Jour. Pure and  
Appl. Phys., 27, 220, 1989.

Von Engel A, Ionised gases 2nd edn., Oxford University  
Press, Oxford, 1965.

CHAPTER VIIIA

EVALUATION OF PLASMA MAGNETISATION COEFFICIENT

## CHAPTER - VIII

PART - A

## EVALUATION OF PLASMA MAGNETISATION CO-EFFICIENT

## INTRODUCTION

Townsend and Gill (1938) calculated the effect of magnetic field on the breakdown potential of a gas under radio frequency excitation and showed that the mobility  $\mu_H$  of electrons in the direction of electric field is reduced with increase in transverse magnetic field H and is given by

$$\mu_H = \frac{\mu_0}{1 + \omega_H^2 \gamma^2} = \frac{\mu_0}{1 + c_1 \frac{H^2}{p^2}} \quad (8.1)$$

And the co-efficient of diffusion  $D_H$  is reduced with the increase of transverse magnetic field H and is given by

$$D_H = \frac{D_0}{1 + c_1 \frac{H^2}{p^2}} \quad (8.2)$$

where  $\gamma$  is the time between two successive collisions and  $\omega_H$  is the cyclotron frequency and are given by

$$\gamma = \frac{\lambda}{v_r}, \quad \omega_H = \frac{eH}{m} \quad \text{and} \quad \lambda = \frac{L_1}{p}$$

where  $\lambda$  and  $v_r$  are mean free path and random velocity respectively and  $L_1$  is the mean free path at one torr.

$$c_1 = \left( \frac{e}{m} \cdot \frac{L_1}{v_r} \right)^2 \quad (8.3)$$

Blevin and Haydon (1958) arrived at a new expression for equivalent pressure by calculation of electron mass energy and drift velocity in a magnetic field and the equivalent pressure  $P_H$  in presence of magnetic field  $H$  is given by,

$$P_H = P_0 \left( 1 + C_1 \frac{H^2}{p^2} \right)^{1/2} \quad (8.4)$$

Brown (1956, 1959) has shown that effective diffusion length  $\Lambda_H$  appropriate to infinite parallel plates in presence of magnetic field is given by

$$\Lambda_H = \Lambda_0 \left( 1 + C_1 \frac{H^2}{p^2} \right)^{1/2} \quad (8.5)$$

It has also been shown by Sen and Gupta (1971) that the axial electric field  $E_H$  increases in presence of transverse magnetic field and is given by

$$E_H = E_0 \left( 1 + C_1 \frac{H^2}{p^2} \right)^{1/2} \quad (8.6)$$

Sen and Gupta (1971) also showed that the electron temperature  $T_{eH}$  in presence of transverse magnetic field is given by

$$T_{eH} = T_{e0} \left( 1 + C_1 \frac{H^2}{p^2} \right)^{1/2} \quad (8.7)$$

Sen and Das (1973) pointed out that the mean free path  $\lambda_H$  in presence of transverse magnetic field is given by

$$\lambda_H = \lambda_0 / \left( 1 + C_1 \frac{H^2}{p^2} \right)^{1/2} \quad (8.8)$$

Sen and Gupta (1964) found from their measurement of electron mobility in glow discharge plasma in presence of transverse magnetic field that the constant  $C_1$ , presently called "Plasma magnetisation co-efficient", gradually falls with the rise of transverse magnetic field. Sadhya and Sen (1980) and Sen, Ghosh and Ghosh (1983) pointed out that the relation

$$T_{eH} = T_{e0} \left( 1 + C_1 \frac{H^2}{P^2} \right)^{1/2} \text{ holds good only for low values of } H/P.$$

Thus it was clear from experimental evidence that the constant  $C_1$  changes with  $(H/P)$ . Hence it was felt by us that the nature of the constant  $C_1$  is required to be investigated for its functional dependence on the transverse magnetic field applied to the plasma. Thus an attempt has been made to evaluate  $C_1$ , which should be extremely useful to explain the discrepancy in case of so many experimental results connected with  $C_1$ .

#### Theoretical evaluation of $C_1$

$C_1$  in a transverse magnetic field is given by

$$C_1 = \left( \frac{e}{m} \cdot \frac{L_1}{v_r} \right)^2 \quad (8.3)$$

But  $L_1$ , the mean free path, should change with transverse magnetic field due to the motion of electrons on the arcs of circles in presence of transverse magnetic field and should be given in the same way as mean free path at any other pressure is expressed in terms of magnetic field. So mean free path  $L_1$

in presence of transverse magnetic field is given by

$$L_1 = \frac{L_{10}}{\left(1 + C_1 \frac{H^2}{p^2}\right)^{1/2}} \quad (8.9)$$

$$\text{Again } T_{eH} = T_{e0} \left(1 + C_1 \frac{H^2}{p^2}\right)^{1/2} \quad (8.7)$$

$$\text{Hence, } \frac{1}{2} m v_{rH}^2 = k T_{eH} = \frac{1}{2} v_{r0}^2 \times \left(1 + C_1 \frac{H^2}{p^2}\right)^{1/2}$$

$$\text{So, } v_{rH} = v_{r0} \left(1 + C_1 \frac{H^2}{p^2}\right)^{1/4} \quad (8.10)$$

where  $v_{rH}$  and  $v_{r0}$  are the random velocities in presence and absence of magnetic field.

$$C_1^{1/2} = \frac{e}{m} \cdot \frac{L_{1H}}{v_{rH}} = \frac{e}{m} \cdot \frac{L_{10}}{v_{r0}} \times \frac{1}{\left(1 + C_1 \frac{H^2}{p^2}\right)^{3/4}}$$

$$\text{Let, } \frac{e}{m} \frac{L_{10}}{v_{r0}} = C_{10}^{1/2}$$

$$\text{Thus, } C_1 = \frac{C_{10}}{\left(1 + C_1 \frac{H^2}{p^2}\right)^{3/2}} \quad (8.11)$$

Now, in the expression  $1 + C_1 \frac{H^2}{p^2}$  [8.1 to 8.8] we are to replace  $p$  by  $P_H / \left(1 + C_1 \frac{H^2}{p^2}\right)^{1/2}$  because the pressure that is measured by external means is not  $p$  but  $P_H$ . Since for the pressure inside the plasma,  $p_H$  is in equilibrium with the rest of the system. Thus  $P_H$  and the pressure outside the plasma in

the rest of the system must be same, otherwise there will be a constant outward flow of the gas until equilibrium is established. Thus we may assume that  $P_H$  and the pressure externally measured are identical in magnitude. So  $(1 + C_1 \frac{H^2}{p^2})$  should be given by

$$1 + C_1 \frac{H^2}{p^2} \equiv \left[ 1 + C_1 \frac{H^2}{P_H^2} \left( 1 + C_1 \frac{H^2}{p^2} \right) \right] \quad (8.12)$$

where  $P$  is the pressure for  $H = 0$  and  $P_H$  is the pressure for  $H \neq 0$ . Thus with 8.11 and 8.12 we have

$$\begin{aligned} 1 + C_1 \frac{H^2}{p^2} &= 1 + \frac{C_{10}}{\left( 1 + C_1 \frac{H^2}{p^2} \right)^{3/2}} \cdot \frac{H^2}{P_H^2} \left( 1 + C_1 \frac{H^2}{p^2} \right) \\ &= 1 + \frac{C_{10}}{\left( 1 + C_1 \frac{H^2}{p^2} \right)^{1/2}} \frac{H^2}{P_H^2} \end{aligned}$$

Now for first order approximation we take,  $C_1$  in the denominator to be approximately equal to  $C_{10}$  and hence we have

$$1 + C_1 \frac{H^2}{p^2} = 1 + \frac{C_{10}}{\left( 1 + C_{10} \frac{H^2}{p^2} \right)^{1/2}} \frac{H^2}{P_H^2}$$

Where  $P_H$  is the externally measured pressure. Thus, on comparison, we have plasma magnetisation co-efficient given by

$$C_1 = \frac{C_{10}}{\left( 1 + C_{10} \frac{H^2}{p^2} \right)^{1/2}} \quad (8.13)$$

Thus  $\log C_1$  vs  $\log (1 + C_{10} \frac{H^2}{p^2})$  should be a straight line.

Sen and Gupta (1964) presented values of  $C_1$  for different values of transverse magnetic field applied to plasma column. They obtained the values of  $C_1$  from the measurement of electron mobility in plasma in presence of magnetic field  $H$ . From graphical plotting of a mean extrapolated graph of  $C_1$  vs  $H$ , we have collected the values of  $C_1$  for different values of  $H$  and also  $C_{10}$  for  $H = 0$ . The values of  $C_1$ ,  $\log_{10} C_1$ ,  $\log_{10}(1 + C_{10} \frac{H^2}{p^2})$  for different values of  $H$  entered in table 8a for a pressure of 0.01 torr.

Table 8a

( $P = 0.01$  torr)

H in Gauss	0	38	76	114	150	182	216	250
$C_1$ in $\frac{\text{torr}^2}{\text{Gauss}^2} \times 10^7$	12	2.6	0.9	0.55	0.40	0.34	0.25	0.23
$\log_{10}(C_1 \times 10^7)$	1.08	0.42	-0.05	-0.26	-0.40	-0.47	-0.60	-0.64
$1 + C_{10} \frac{H^2}{p^2}$	1	18.28	70.36	157	271	398	560	751
$\log_{10}(1 + C_{10} \frac{H^2}{p^2})$	0	1.26	1.85	2.20	2.43	2.60	2.75	2.88

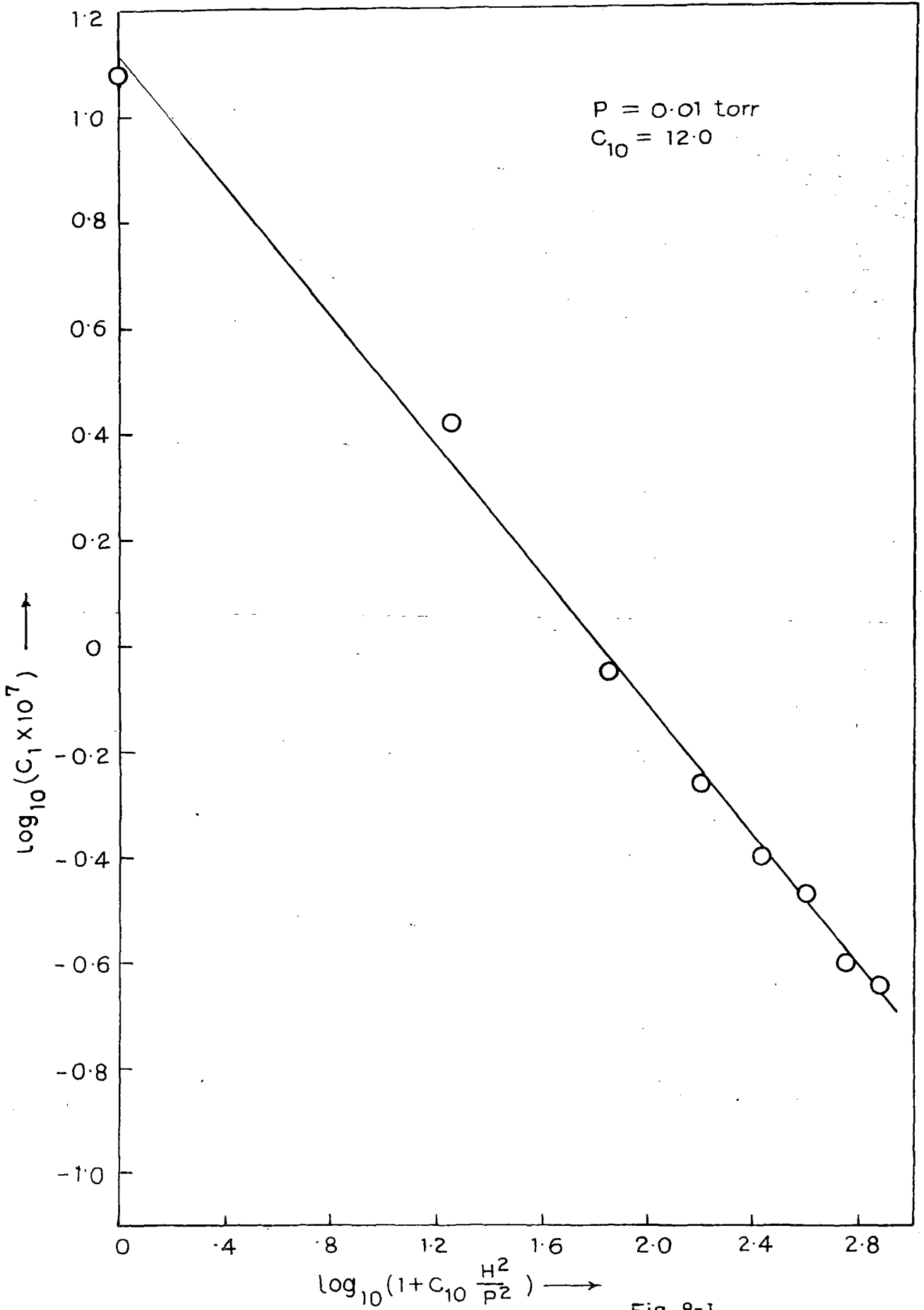


Fig. 8-1

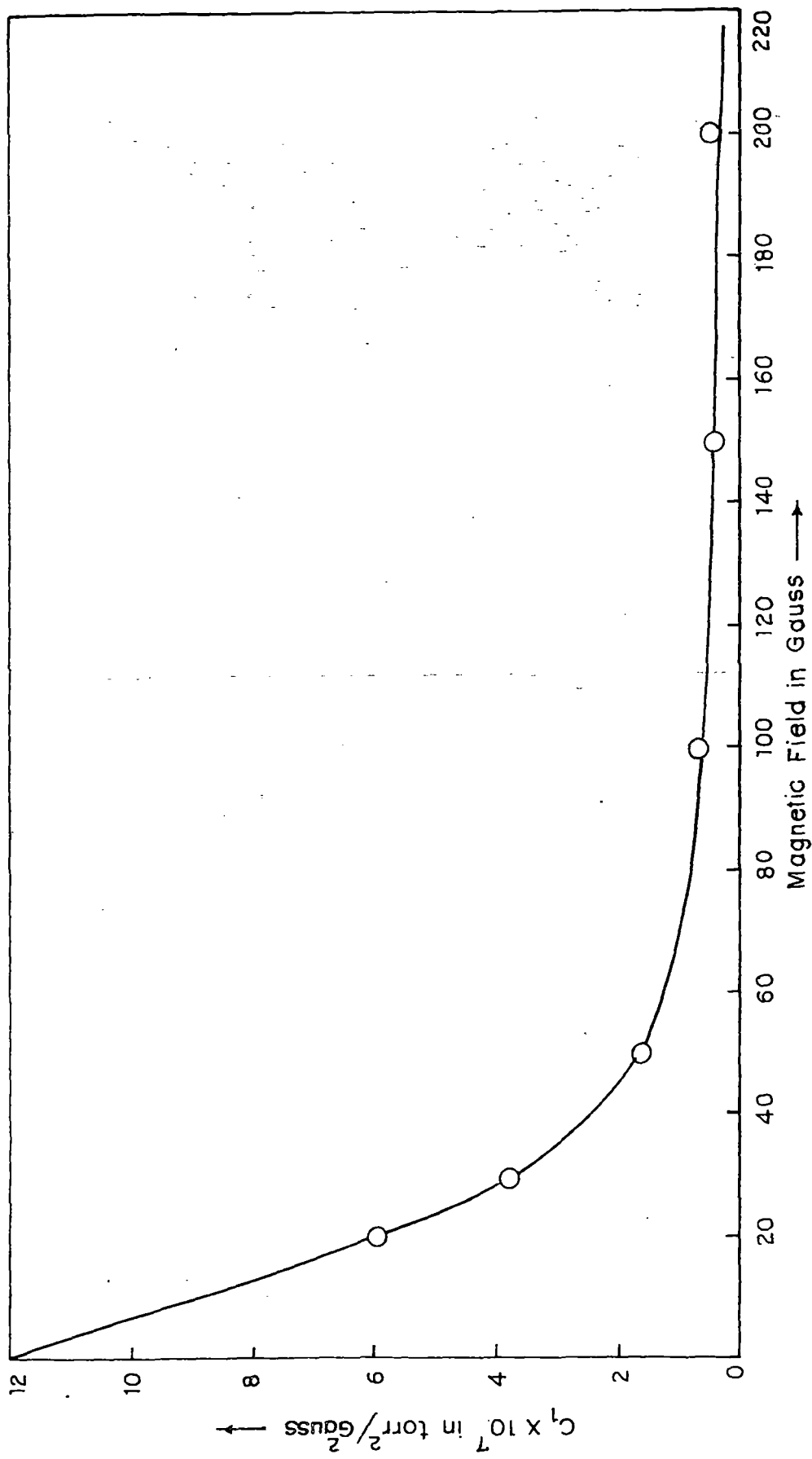


Fig. 8-II

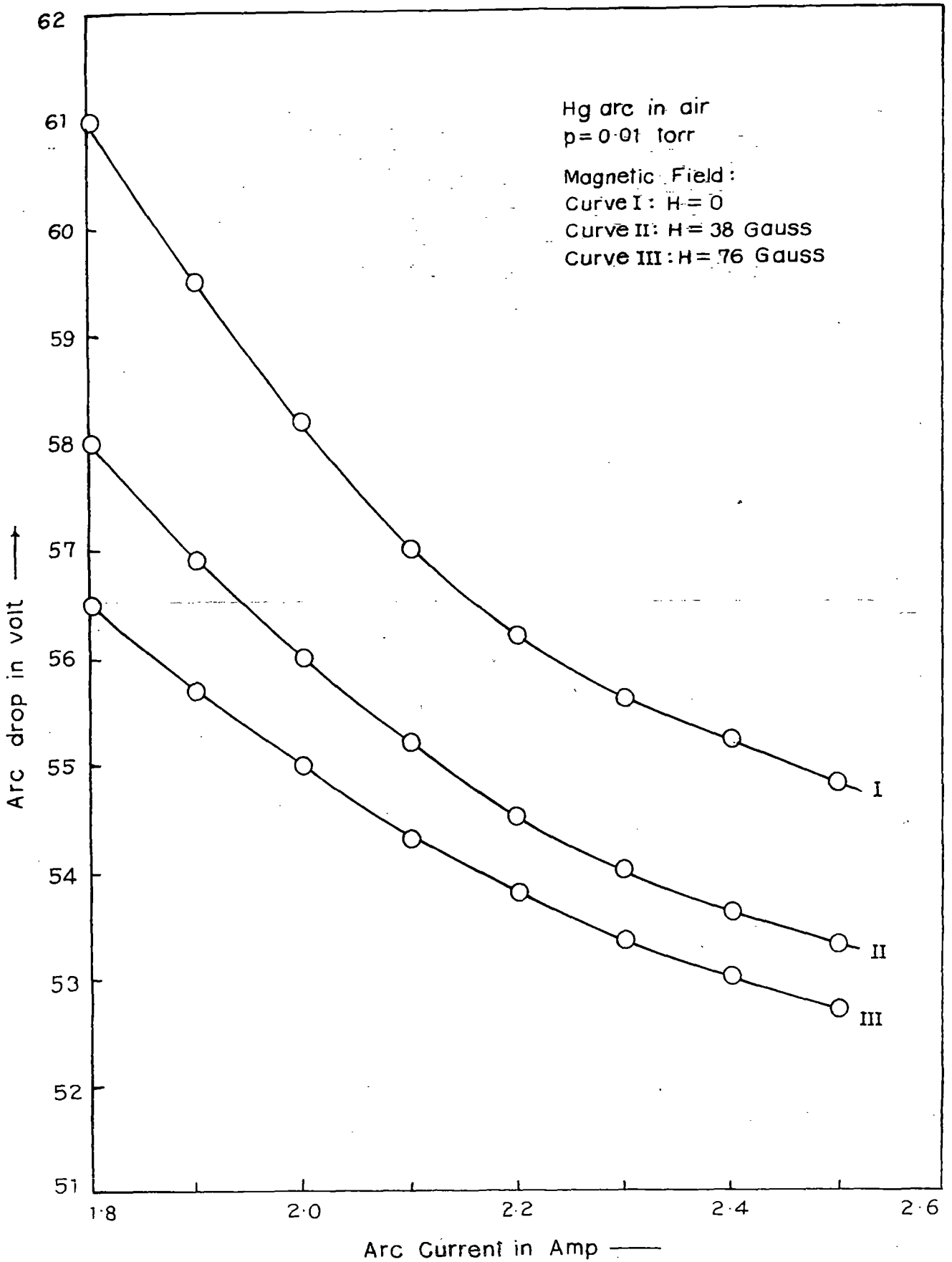


Fig. 8-III

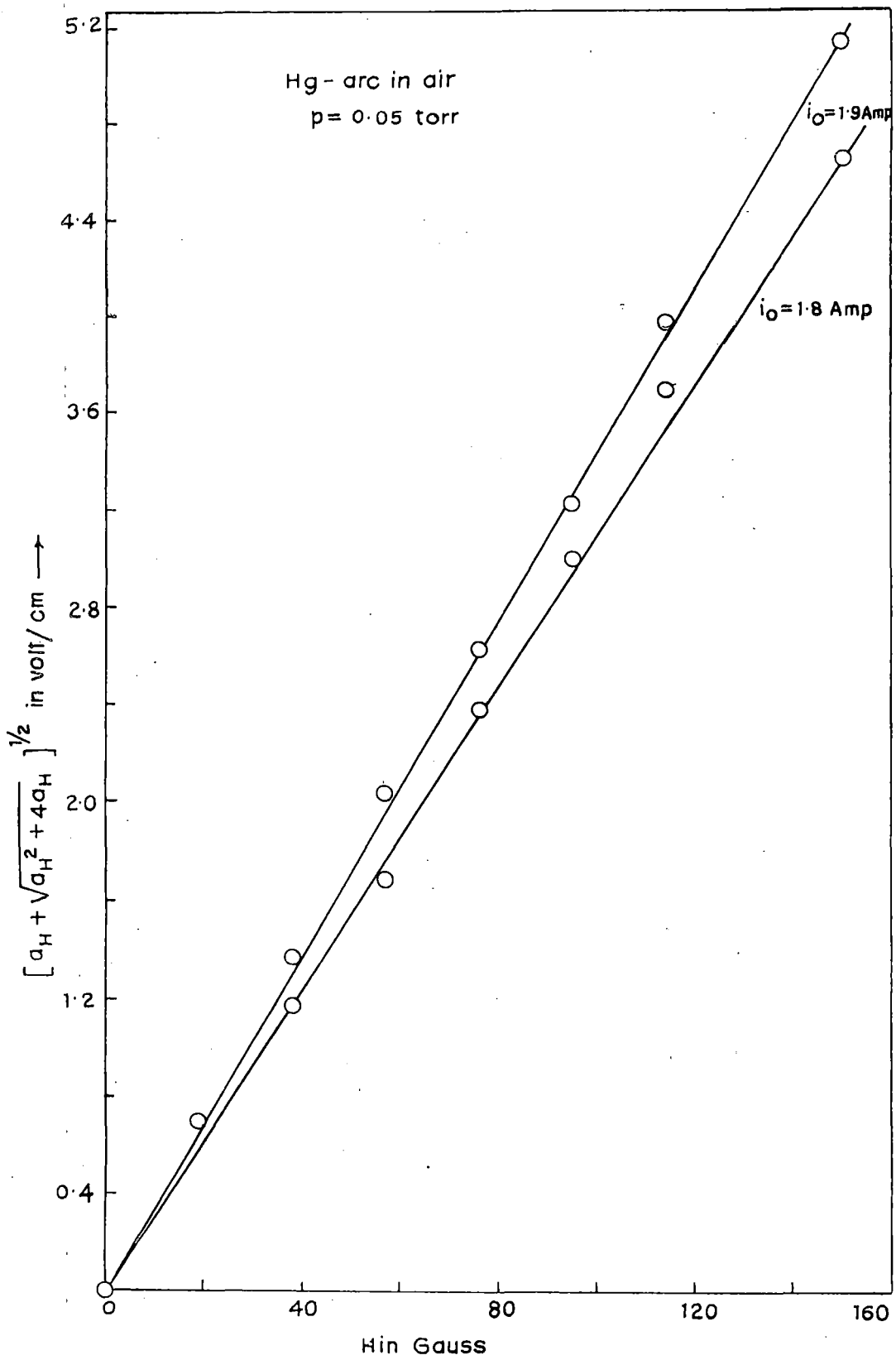


Fig. 8-IV

The graph of  $\log_{10}(C_1 \times 10^7)$  vs  $\log_{10}(1 + C_{10} \frac{H^2}{p^2})$  is shown in Fig. 8-I, and Fig. 8-II shows the graph of the values of  $C_1$  vs  $H$  as obtained from the works of Sen and Gupta (1964).

### Discussion

The expression 8.13 may fail for very high values of  $H/p$  when we may take,

$$C_1 = \frac{C_{10}}{C_1^{1/2} \frac{H}{p}}, \text{ i.e. } C_1 = \frac{C_{10}^{2/3}}{(H/p)^{2/3}} \quad (8.14)$$

The theory may also fail for extremely low values of pressure when the relation 8.8 is no longer valid.  $C_1$  may also be a function of current as reported by Sen and Das (1973) and as is also found in our present work as described in Part B of this chapter, vide, Fig. 8-IV. and  $C_1$  should never be zero for low  $H/p$  and for whatever large current. The value of  $C_1$  as presented by Sen and Das (1973) in case of a mercury arc for different discharge current, it is found that  $C_1$  steadily tends towards zero with rise of discharge current. But in the present case,  $C_1 = \left( \frac{e}{m} \cdot \frac{L_1}{V_r} \right)^2$  should not be zero with rise of current at any moderate value of  $(H/p)$ . Though  $C_{10}$  may be a function of discharge current due to rise of gas temperature with discharge current. Because gas temperature in turn may influence  $(L_{10}/V_{r0})$ . The results produced in Part B of this chapter really shows the change in  $C_{10}$  with discharge current.

The slope of the curve in Fig.8-I is found to be about -0.62 which according to the theory is required to be -0.50 but may be considered to be in close agreement because there may be a small error in the measurement of  $C_{10}$ .

In this connection, it may be pointed out that the evaluation of  $C_1$  was carried out by Sen and Jana (1977) in longitudinal magnetic field applied to glow discharge plasma.  $C_1/C_{10}$  was calculated and measured, but the calculated results was in close agreement to their experimental results only for low values of magnetic fields.

Finally, it may be pointed out that the value of  $C_1$  given by Mc Daniel (1964) is of the order of  $10^{-6}$  and that given by Sen and Das (1973) is also of the order of  $10^{-6}$  & so is  $C_1$  for mercury. Thus it may be assumed that  $C_1$  for arc should be of the order  $10^{-6}$  for moderate values of  $H/P$  as is found in the results presented by us in the Part B of this chapter.

## CHAPTER VIII B

STUDY OF MAGNETIC FIELD DEPENDENCE OF TRADITIONALLY  
USED PLASMA MAGNETISATION COEFFICIENT AND OF CROSS  
SECTIONAL AREA OF AN ARC

PART B

Study of magnetic field dependence of traditionally used plasma magnetisation co-efficient and of cross-sectional area of an arc.

In order to verify the newly evolved magnetic field dependence of the traditionally used plasma magnetisation co-efficient, as derived in Part A of this chapter, we have adopted a simple experimental method which can apply both to an arc as well as a glow discharge plasma. In the present case we have performed the experiment on a cylindrical arc discharge plasma, a part of whose column was kept immersed in the transverse magnetic field. The selection of an arc in this case is due to the fact that it has a standard equation representing its characteristics, vide, Ayreton relation, and also in the present case, identical theoretical conclusions have been obtained from two entirely different equations, of which one is an equation which is in general applicable to any of the discharge plasma and the other is the Ayreton relation. And hence we have been able to show that the effective cross-sectional area undergoes change with magnetic field. Experimental set up is identical, except for the tank circuit part, to that described in connection with the experiment on plasma oscillation depicted in Chapter VII. Though for the present purpose we have recorded discharge currents, voltages and axial electric field for different values of transverse magnetic field.

Theoretical deductions and experimental results:

In case of a discharge plasma, either an arc or a glow, we have a commonly applicable equation, such as

$$V_0 = iR + V \quad (8.15)$$

where  $V_0$  is the constant supply voltage and  $R$  is the constant limiter resistance and  $i$ ,  $V$  are the discharge current and discharge voltage drop respectively. Just under the stated external circuit condition, if we apply a transverse magnetic field to a part of a column of a discharge plasma, the discharge current and discharge drop voltage will undergo respective changes, even though the supply voltage and limiter resistance remain unchanged. Thus representing  $i$  by  $i_H$  and  $V$  by  $V_H$  in presence of magnetic field, we have

$$R di_H + dV_H = 0$$

$$\text{i.e. } \frac{dV_H}{di_H} = -R = \text{Constant} \quad (8.16)$$

Now the same conclusion can be obtained from Ayreton relation (1902), vide,

$$V = a + \frac{b}{i} \quad (8.17)$$

where  $a$  &  $b$  are constants. Now, in presence of transverse magnetic field, the nature of arc characteristics should not

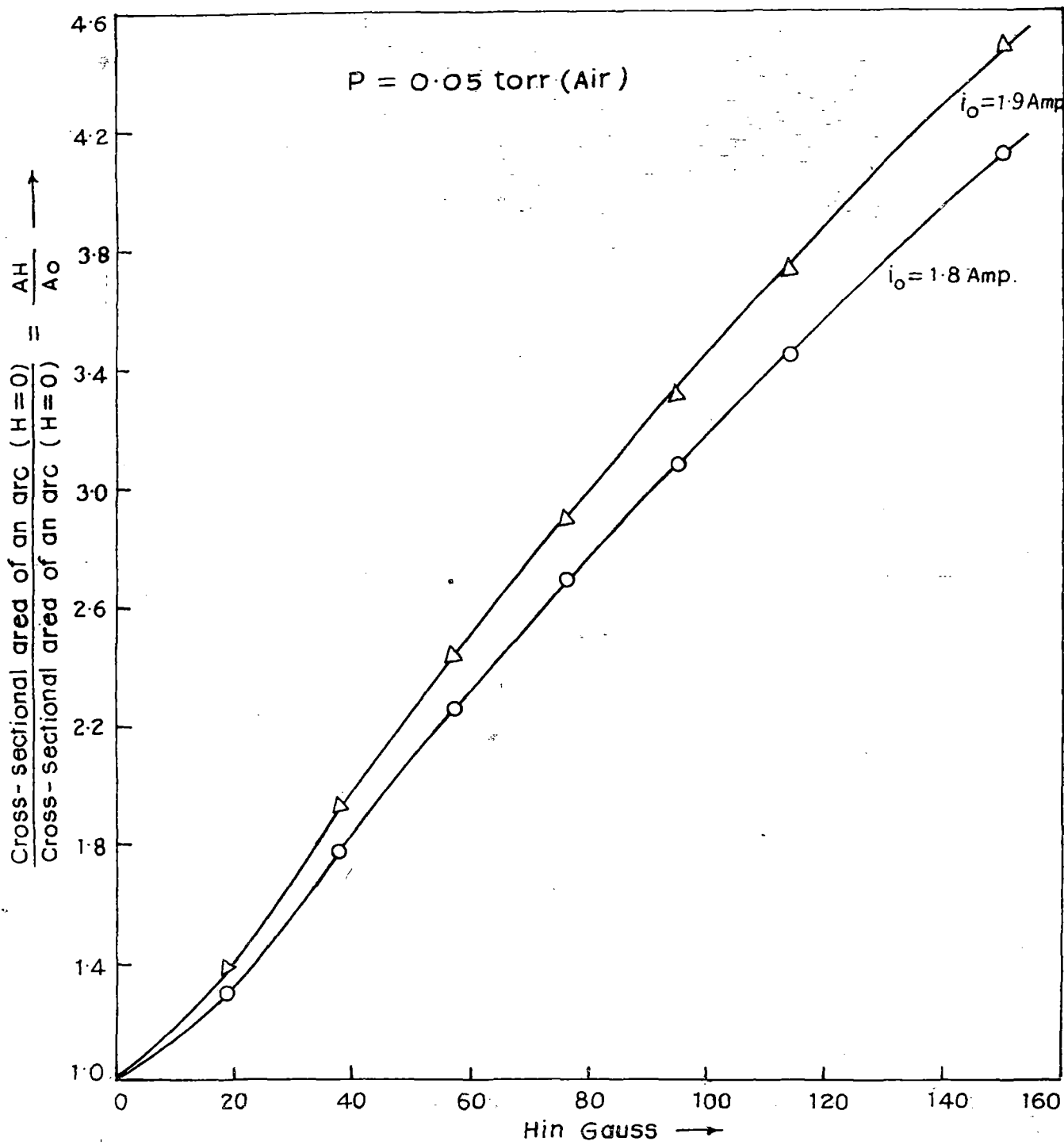


Fig. 8-V

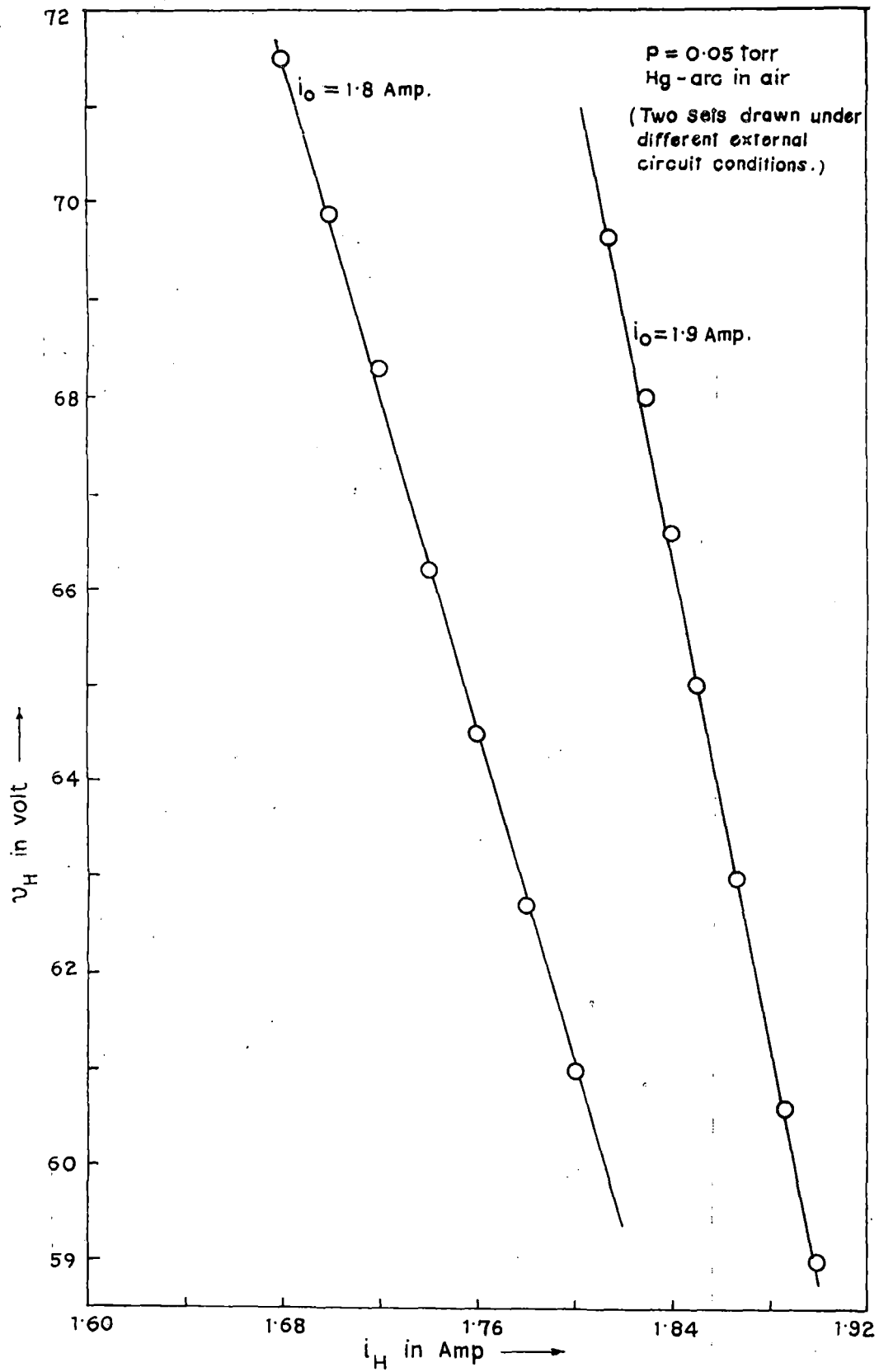


Fig. 8-VI

suffer any basic change. This fact is revealed when characteristics curves are drawn in presence of transverse magnetic field, as is shown in Fig. 8-III. Thus in presence of transverse magnetic field  $H$  Ayreton relation can be written as,

$$V_H = a + \frac{b}{i_H} \quad (8.18)$$

Thus for unaltered supply voltage and limiter resistance, we have

$$\lim_{\substack{i_H \rightarrow i_0 \\ \text{as } H \rightarrow 0}} \frac{V_H - V_0}{i_H - i_0} = - \lim_{\substack{i_H \rightarrow i_0 \\ \text{as } H \rightarrow 0}} \frac{b}{i_H^2 i_0} \quad (8.19)$$

where  $v_0$  and  $i_0$  correspond to the respective values in absence of magnetic field. Hence

$$\frac{dV_H}{di_H} = - \frac{b}{i_0^2} = \text{constant} \quad (8.20)$$

Thus we see  $v_H$  vs  $i_H$  when plotted will give straight lines if  $V_0$  and  $R$  are unaltered, as is shown in Fig. 8-VI. Thus,

$$|di_H| = \frac{l}{R} |dV_H| = \frac{l}{R} l dE_H$$

where  $l$  is the length of the column immersed in the transverse magnetic field and  $dE_H$  is the change in axial electric field. So

$$di_H = A_0 \sigma_0 dE_H \quad (8.21)$$

$$\text{taking } R = \frac{l}{\sigma_0 A_0}$$

where  $\sigma_0$  and  $A_0$  represent conductivity and cross-sectional area.

$A_0 \sigma_0$  of the resistance  $R$  must correspond also to that of the plasma, since  $i_0 = A_0 \sigma_0 E_0$  and  $i_H = A_H \sigma_H E_H$  are representing currents through the plasma in absence and in presence of magnetic field. Under this condition, 8.21 also indicates,  $A_H \sigma_H$  for the plasma must remain unchanged in presence of magnetic field. Hence

$$A_H \sigma_H = A_0 \sigma_0$$

$$\text{So, } A_H = A_0 \frac{\sigma_0}{\sigma_H} = A_0 \frac{n_0}{n_H} \cdot \frac{\lambda_0}{\lambda_H} \cdot \frac{v_{rH}}{v_{r0}} \quad (8.22)$$

where  $v_{r0}$  &  $v_{rH}$  are the random velocities in absence and in presence of magnetic field.

Thus using eq<sup>n</sup> (8.8) & (8.10) and also using

$$n_H = n_0 e^{-aH} \quad (\text{Sen and Das, 1973})$$

We get,

$$A_H = A_0 \left(1 + C_1 \frac{H^2}{p^2}\right)^{3/4} e^{aH} \quad (8.23)$$

#### Plasma magnetisation co-efficient

From 8.6, we have,

$$E_H = E_0 \left(1 + C_1 \frac{H^2}{p^2}\right)^{1/2}$$

and from 8.13,  $C_1 = \frac{C_{10}}{(1 + C_{10} \frac{H^2}{p^2})^{1/2}}$

Thus we get, 
$$\left[ \frac{E_H^2 - E_0^2}{E_0^2} \right]^2 = \frac{(C_{10} \frac{H^2}{p^2})^2}{1 + C_{10} \frac{H^2}{p^2}} = b_H \text{ (say)}$$

Hence, we have

$$\sqrt{C_{10}} \frac{H}{p} = \left[ \frac{b_H + \sqrt{b_H^2 + 4b_H}}{2} \right]^{1/2} \quad (8.24)$$

Negative sign in front of the discriminant is dropped because  $C_{10}$  and hence  $C_1$  cannot be negative. Thus, if the assumptions are correct then the plot of  $\frac{H}{p}$  vs  $\left[ \frac{b_H + \sqrt{b_H^2 + 4b_H}}{2} \right]^{1/2}$  must be a straight line, the slope of which will give  $\sqrt{C_{10}}$ .

Now, in the present case, since  $p$  is kept constant throughout, we have plotted  $H$  vs  $\left[ \frac{b_H + \sqrt{b_H^2 + 4b_H}}{2} \right]^{1/2}$  and is shown in Fig. 8-IV. The nature of change ( $A_H/A_0$ ) is shown in Fig. 8-V, as calculated with the help of measured values of  $C_1$  for required magnetic fields.

"a" in the expression 8.23 is given by,

$$a = \frac{e E C_1^{1/2} r}{2(k T_e) p} \quad (\text{Sen and Das, 1973})$$

$e$  is the electronic charge,  $E$  is the axial electric field,  $r$  is the distance from the axis of the cylindrical plasma,  $kT_e$  is the electron energy, and  $P$  is the pressure.

$$kT_{e0} = 6 \text{ eV at } i_0 = 1.8 \text{ Amp}$$

$$\text{and } kT_{e0} = 5 \text{ eV at } i_0 = 1.9 \text{ Amp}$$

obtained by extrapolation of the data given by Ghosal, Nandi and Sen (1979).

Since we consider the total cross-sectional area in (8.23) we take the mean over the total radius. Hence we have,

$$a = \frac{e E C_1^{1/2} R}{4 (kT_e) P}$$

where  $R$  is the tube radius.

$$\text{Thus using 8.4, 8.6, 8.7 and 8.13, } a_H = \frac{a_0}{\sqrt{\left(1 + C_{10} \frac{H^2}{P^2}\right)^{1/2} + C_{10} \frac{H^2}{P^2}}}$$

where  $a_H$  and  $a_0$  are values of  $a$  in presence and absence of magnetic field and  $a_0$  is given by,

$$a_0 = \frac{e E_0 C_{10}^{1/2} R}{4 (kT_{e0}) P_0}$$

For  $i_0 = 1.8$  Amp at  $p = 0.05$  torr and  $R = 1.8 \times 10^{-2}$  m  
and  $E_0 = 1.84 \times 10^2$  V/meter  $kT_{e0} = 6 \times 1.6 \times 10^{-19}$  Jule

$$a = 4.31 \times 10^{-3} \text{ per Gauss}$$

and for  $i_0 = 1.9$  Amp at  $p = 0.05$  torr and  $R = 1.8 \times 10^{-2}$  m

$E_0 = 1.76 \times 10^2$  V/meter  $kT_{e0} = 5 \times 1.6 \times 10^{-19}$  Jule

$$a_0 = 5.45 \times 10^{-3} \text{ per Gauss}$$

We have the values of  $\left[ \frac{b_H + \sqrt{b_H^2 + 4b_H}}{2} \right]^{1/2}$  for different values of  $H$  and have entered in the sixth column of table 8b and 8c. And the values of  $A_H/A_0$  for different values of  $H$  have been entered in the fourth and seventh column of table 8d.

Table 8b

Length of the magnetised column =  $l=5$  cm

pressure = 0.05 torr

Initial arc current (Hg-Arc) = 1.8 Ampere

Magnetic Field in Gauss H	Discharge current in Amp. $i_H$	Arc drop in Volt $V_H$	Drop across Magnetised part of the column in volt $V_H$	Electric Field in Volt/cm $E_H = \frac{V_H}{l}$	$\left[ \frac{b_H + (b_H^2 + 4b_H)^{1/2}}{2} \right]^{1/2}$ in volt cm	$C_{10}$ in torr <sup>2</sup> /Gauss <sup>2</sup>
0	1.8	61	9.2	1.84	0	
19	1.78	62.7	10.9	2.18	0.70	
38	1.76	64.5	12.7	2.54	1.18	$2.44 \times 10^{-6}$
57	1.74	66.2	14.4	2.88	1.69	
76	1.72	68.3	16.5	3.30	2.39	
95	1.70	69.9	18.1	3.62	3.01	
114	1.68	71.5	19.7	3.94	3.71	
150	1.655	73.55	21.75	4.35	4.68	

Table 8c

Length of the magnetised column =  $l = 5.0$  cm

pressure = 0.05 torr. Initial arc current (Hg arc) = 1.9 Amp

Magnetic Field in Gauss H	Discharge current in Amp. $i_H$	Arc drop in Volt $V_H$	Drop across Magnetised part of the column in volt $V_H$	Electric Field in Volt/cm $E_H = \frac{V_H}{l}$	$\left[ \frac{b_H + (b_H^2 + 4b_H)}{2} \right]^{1/2}$ in Volt/cm	$C_{10}$ in torr <sup>2</sup> /Gauss <sup>2</sup>
0	1.9	59.0	8.80	1.76	0	
19	1.886	60.6	10.40	2.08	0.70	
38	1.867	63.0	12.80	2.56	1.37	$2.9756 \times 10^{-6}$
57	1.85	65.0	14.80	2.96	2.04	
76	1.84	66.6	16.40	3.28	2.64	
95	1.83	68.0	17.80	3.56	3.24	
114	1.81	69.65	19.45	3.89	4.00	
150	1.796	71.9	21.71	4.34	5.17	

Table 8d

Mercury arc in air,  $p = 0.05$  torr

Magnetic field in Gauss H	Initial arc current = 1.8 Amp			Initial arc current = 1.9 Amp		
	$C_1$ in $\frac{\text{torr}^2}{\text{Gauss}^2} \times 10^6$	$a_H$ in $(\text{Gauss})^{-1} \times 10^4$	$\frac{A_H}{A_0}$	$C_1$ in $\frac{\text{torr}^2}{\text{Gauss}^2} \times 10^6$	$a_H$ in $(\text{Gauss})^{-1} \times 10^4$	$\frac{A_H}{A_0}$
0	2.4414	43.10	1.0	2.9756	54.5	1.0
19	2.1047	35.04	1.300	2.4797	42.58	1.377
38	1.5751	25.06	1.771	1.8034	29.62	1.925
57	1.1968	18.90	2.250	1.3464	22.06	2.427
76	0.9463	15.02	2.690	1.0589	17.52	2.889
95	0.7800	12.46	3.074	0.8675	14.49	3.306
114	0.6598	10.64	3.443	0.7329	12.33	3.729
150	0.5097	8.34	4.113	0.5646	9.63	4.481

The ratio ( $A_H/A_0$ ) shows that discharge current gradually takes larger cross-sectional area for its passage with the rise of magnetic field strength. So, as soon as  $A_H$  exceeds the discharge tube cross-section, higher power will be consumed at the wall of the discharge tube. The higher power will be lost to the tube wall by collision and will be neutralized due to immobile charges at the wall. And hence wall temperature will rise and the plasma should become increasingly luminous with the increase of magnetic field, which is really observed by us and by many other authors [Sen Das & Gupta (1972)]. And the compression in plasma because of obstruction to expansion may finally lead to a modification of the present theory at very high values of magnetic field and at comparatively low values of tube cross-section.

R E F E R E N C E S

- Ayrton H, "The electric Arc", The electrician Series, D. Van Nostrand Co. Inc. New York, pp 120, 130, 1902.
- Beckman I, Proc. Phys. Soc., 61, 515, 1948.
- Blevin H.A. and Haydon H.C., Aust. J. Phys., 11, 18, 1958.
- Brown S.C., Hand book of Physics (Berlin: Springer Verlag)1956,  
Ibid, Basic Data in Plasma Physics, (New York, Technology Press, MIT & John Wiley, 1959.
- Ghosal S.K., Nandi G.P. and Sen S.N., Int. J. Electronics, 47, 415, 1979.
- Mc Daniel E.W., "Collision Phenomena in ionized gases, John Wiley and Sons Inc., 1964.
- Sadhya S.K. and Sen S.N., J. Phys. D (GB), 13, 1275, 1980.
- Sen S.N., Das R.P. and Gupta R.N., Jour. Phys. D, Appl. Phys., 5, 1260, 1972.
- Sen S.N. and Das R.P., Int. J. Electronics, 34, 527, 1973.
- Sen S.N. and Gupta R.N., J. Phys. D, 4, 510, 1971.
- Ibid, Ind. J. Phys., 38, 383, 1964.
- Sen et al , Ind. J. Pure and Appl. Phys., 21, 613
- Sen S.N. and Jana D.C., J. Phys. Soc. Japan, 43, 1729, 1977.
- Townsend J.J. and Gill E.W.B, Phil. Mag., 26, 290, 1938.

CHAPTER IX

SUMMARY AND CONCLUSION

## SUMMARY AND CONCLUSION

In the present work some of the physical properties of glow discharge and arc plasma have been experimentally investigated and theoretical analysis of the observed results has been presented. It is expected that the conclusions drawn from the investigation will extend our knowledge regarding the process of initiation and maintenance of the low density and high density plasma.

A. Energy loss mechanism in a collision dominated plasma:

The loss of energy of the electrons due to collision with neutral atoms and molecules in a collision dominated plasma has been theoretically investigated. It is shown that as the loss factor  $K$  is dependent upon  $(E/P)$ , the reduced field, it is essential to take into consideration the variation of  $K$  in calculating the current through the plasma. The theoretical expression for the plasma current thus deduced agrees very well with observed experimental results. Further the values of the plasma parameters such as electron density drift and random velocity of the electron calculated from theoretical expressions combined with experimental results in air, hydrogen and nitrogen agree quite well with literature values.

B. Some new methods suggested for measurement of plasma parameters:

- i) Measurement of plasma current and capacitative current in a radio frequency gas discharge:

By introducing a variable choke in parallel with the discharge tube and noting the resonant current in the main as well as in the parallel circuit containing choke, the plasma current as well as the capacitative current can be separated and measured. A mathematical formulation of the theory of measurement has been presented.

- ii) Radio frequency conductivity of an ionised gas in a transverse magnetic field:

The variation of the imaginary part of the radio frequency conductivity of an ionised gas in a transverse magnetic field has been calculated by taking into consideration the variation of the axial electric field in presence of transverse magnetic field. The analysis shows that the rf conductivity becomes a minimum at a certain value of the magnetic field, which is solely dependent upon the pressure. Some numerical calculation of the magnetic field for the minimum radio frequency conductivity for certain values of pressure has been presented.

iii) Propagation of microwaves through a plasma filled wave guide - a possible diagnostic method;

Propagation of microwaves through a plasma filled wave guide has been considered starting from the basic electromagnetic equations of Maxwell. The cut-off frequencies  $\omega_c$  and  $\omega_{cp}$ , without and with plasma,  $\alpha$  and  $\beta$  where  $\alpha$  is the attenuation constant per unit length and  $\beta$  is the phase constant per unit length have been shown to be implicitly related with  $\sigma_r$  and  $\sigma_i$ , the real and imaginary conductivity, and  $\epsilon'$  and  $\epsilon''$ , the real and imaginary dielectric constants of the plasma. From these measurement the electron density and collision frequency of electrons with neutral atoms can be calculated.

iv) Critical frequency for microwave propagation in a rarefied magnetised plasma;

In this section a detailed theoretical investigation has been presented to find how the critical frequency for microwave propagation in a plasma is affected in presence of magnetic field; the values of  $\epsilon'$ , the real part, and  $\epsilon''$ , the imaginary part of the dielectric constant have been calculated in presence of transverse magnetic field from which the numerical values of cut off frequency for a variation of magnetic field from 10 to 100 gauss have been obtained for an assumed value of electron plasma frequency. It is observed that the cut-off frequency increases with the increase of the magnetic field.

An interesting result obtained is that  $\omega_c^2 = \omega_p^2 + \omega_H^2$  which suggests that, as if, the electron plasma frequency has increased from  $\omega_p$  to  $(\omega_p^2 + \omega_H^2)^{1/2}$  - a result which can be obtained when we consider the effect of magnetic field on electron plasma oscillation.

### C. Low density plasma in a magnetic field:

In this chapter a low density plasma has been subjected to a varying transverse magnetic field and with the help of two probes one along the axis and the other along the periphery, the radial voltage developed has been measured for three values pressures. It is suggested that the voltage thus developed is the resultant of two voltages, namely the diffusion voltage in presence of magnetic field and the Hall voltage. A detailed mathematical analysis has been carried out in which the values of both these voltages have been calculated separately and an expression for the resultant voltage obtained. The experimental results are in excellent agreement with the theoretical calculation specially for values of magnetic field greater than 150 gauss. It is suggested that the discrepancy observed for low values of magnetic field may be due to dependence of diffusion co-efficient on  $1/H$  instead of on  $1/H^2$ . It is pointed out that in all Hall voltage measurement in plasma the contribution of diffusion voltage in presence of magnetic field should be taken into consideration.

D. Current generation process, high current density and cathode phenomena in an arc plasma;

A detailed mathematical theory has been presented regarding the mechanism of current emission phenomena, the high current density in metallic arcs. The mathematical analysis is based upon some reasonable assumptions and it has been shown that all arcs are basically thermionic in nature irrespective of the melting point of the cathode material. A generalised theory has been developed for calculating the current density and the cathode fall, and the experimental part consists in measuring cathode fall with wide variation of pressure. The experimental results are in excellent agreement with theoretical calculations. The results clarify the nature of much of the complex physical processes occurring near and at the cathode surface of the arc and it is concluded that in the arcs studied in this investigation thermionic processes have a dominant role to play.

E. Low frequency oscillation in an arc plasma:

Low frequency oscillations in the range of 2 KC/S to 6 KC/S have been detected in a mercury arc plasma. Besides the frequency of oscillation the output voltage has also been measured for variation of arc current from 1.7 to 2.3 ampere for three values of pressure and for a transverse magnetic field varying upto 114 Gauss. A theoretical treatment of the

plasma has been presented which can satisfactorily explain the experimental results. The possible origin of these low frequency oscillations has been discussed.

#### F. Evaluation of plasma magnetisation co-efficient:

In this chapter an analytical derivation of the expression  $C_1 = \left( \frac{e}{m} \cdot \frac{L}{v_r} \right)^2$  which has been defined as 'plasma magnetisation co-efficient' has been derived. From the theoretical treatment it has been deduced that  $C_1$  is a function of  $H/P$ , the reduced magnetic field. Previous and present experimental results are in accordance with the theoretical deduction. The effective cross-sectional area of an arc, in presence of magnetic field has also been discussed.

SCIENCE LIBRARY  
UNIVERSITY OF TORONTO  
1954